

AD-A186 607

DTIC FILE COPY Bulletin 52
(Part 1 of 5 Parts)

②

THE SHOCK AND VIBRATION BULLETIN

Part 1
Welcome, Keynote Address,
Invited Papers, Rotor Dynamics and Machinery Vibration

MAY 1982

A Publication of
THE SHOCK AND VIBRATION
INFORMATION CENTER
Naval Research Laboratory, Washington, D.C.

DTIC
ELECTE
NOV 19 1987
S D
Q&D

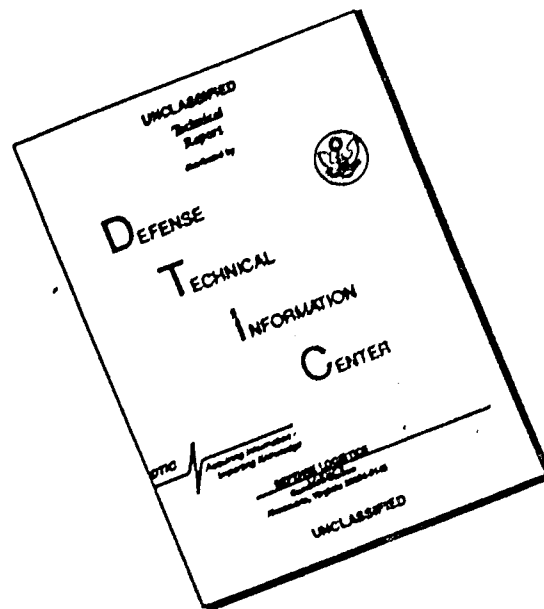


Office of
The Under Secretary of Defense
for Research and Engineering

Approved for public release; distribution unlimited.

87 10 28 032

DISCLAIMER NOTICE



THIS DOCUMENT IS BEST QUALITY AVAILABLE. THE COPY FURNISHED TO DTIC CONTAINED A SIGNIFICANT NUMBER OF PAGES WHICH DO NOT REPRODUCE LEGIBLY.

**BLANK PAGES
IN THIS
DOCUMENT
WERE NOT
FILMED**

SYMPOSIUM MANAGEMENT

THE SHOCK AND VIBRATION INFORMATION CENTER

Henry C. Pusey, Director

Rudolph H. Volin

J. Gordan Showalter

Jessica Hileman

Elizabeth A. McLaughlin

Bulletin Production

**Publications Branch, Technical Information Division,
Naval Research Laboratory**

Bulletin 52
(Part 1 of 5 Parts)

THE SHOCK AND VIBRATION BULLETIN

MAY 1982

**A Publication of
THE SHOCK AND VIBRATION
INFORMATION CENTER
Naval Research Laboratory, Washington, D.C.**

Accession For	
NTIS CRA&I	<input checked="checked" type="checkbox"/>
DTIC TAB	<input type="checkbox"/>
Unannounced	<input type="checkbox"/>
Justification	
By	
Distribution/	
Availability Codes	
Dist	Avail and/or Special
A-1	

The 52nd Symposium on Shock and Vibration was held at the Monteleone Hotel, New Orleans, LA on October 26-28, 1981. The Defense Nuclear Agency, Washington, D.C. and the U.S. Army Waterways Experiment Station, Vicksburg, MS were Co-Hosts.



**Office of
The Under Secretary of Defense
for Research and Engineering**

CONTENTS

PAPERS APPEARING IN PART 1

Welcome

WELCOME	1
Colonel Tilford Creel, Commander/Director, U.S. Army Waterways Experiment Station, Vicksburg, MS	

Keynote Address

KEYNOTE ADDRESS	3
Marvin Atkins, Director, Offensive and Space Systems, Office of the Under Secretary of Defense Research Engineering, Department of Defense, Washington, DC	

Invited Papers

EQUIPMENT SURVIVABILITY ON THE INTEGRATED BATTLEFIELD	5
Charles N. Davidson, Technical Director, U.S. Army Nuclear and Chemical Agency, Springfield, VA	
NAVAL OPERATIONS IN A NUCLEAR ENVIRONMENT	11
Captain Donald Alderson, U.S.N., Acting Chief, Tactical Nuclear Weapons Project Office (PM-23) Department of the Navy, Washington, DC	
SURVIVABILITY REQUIREMENTS FOR FUTURE AIR FORCE SYSTEMS	13
Henry F. Cooper, Deputy for Strategic and Space Systems, Assistant Secretary of the Air Force (Research, Development and Logistics), Washington, DC	
NUCLEAR HARDNESS VALIDATION TESTING	17
Edward Conrad, Deputy Director (Science and Technology), Defense Nuclear Agency, Washington, DC	
ELIAS KLEIN MEMORIAL LECTURE — THE CHANGING DIMENSIONS OF QUALIFICATION TESTING	35
H. Norman Abramson, Vice-President, Engineering Sciences, Southwest Research Institute, San Antonio, TX	
REQUIRED DEVELOPMENTS IN STRUCTURAL DYNAMICS	49
Ben K. Wada, Jet Propulsion Laboratory, Pasadena, CA	
EFFECT OF SEALS ON ROTOR SYSTEMS	55
David P. Fleming, NASA, Lewis Research Center, Cleveland, OH	
MACHINERY VIBRATION EVALUATION TECHNIQUES	67
R. L. Eshleman, The Vibration Institute, Clarendon Hills, IL	
SHAFT VIBRATION MEASUREMENT AND ANALYSIS TECHNIQUES	81
Donald E. Bently, President, Bently Nevada Corporation, Minden, NV	

Rotor Dynamics and Machinery Vibration

SPIN TEST VIBRATIONS OF PENDULOUSLY-SUPPORTED DISC/CYLINDER ROTORS	95
F. H. Wolff and A. J. Molnar, Westinghouse Research and Development Center, Pittsburgh, PA	
MODAL ANALYSIS AS A TOOL IN THE EVALUATION OF A TURBINE WHEEL FAILURE	101
A. L. Moffa and R. L. Leon, Franklin Research Center, Philadelphia, PA	
CONTRIBUTION TO THE DYNAMIC BEHAVIOUR OF FLEXIBLE MECHANISMS	125
E. Imam, J. Der Hagopian and M. Lalanne, Institut National des Sciences Appliquées, Villeurbanne, France	
SELF-EXCITED VIBRATION OF A NONLINEAR SYSTEM WITH RANDOM PARAMETERS	135
R. A. Ibrahim, Texas Tech University, Lubbock, TX	

PAPERS APPEARING IN PART 2

Invited Papers

Space Shuttle Loads and Dynamics

SPACE SHUTTLE MAIN ENGINE (SSME) POGO TESTING AND RESULTS

J. R. Fenwick, Rockwell International, Rocketdyne Division, Canoga Park, CA and
J. H. Jones and R. E. Jewell, NASA, Marshall Space Flight Center, Huntsville, AL

SPACE SHUTTLE SOLID ROCKET BOOSTER WATER ENTRY CAVITY COLLAPSE LOADS

R. T. Keefe and E. A. Rawls, Chrysler Corporation, Slidell, LA and
D. A. Kross, NASA, Marshall Space Flight Center, Huntsville, AL

SPACE SHUTTLE SOLID ROCKET BOOSTER REENTRY AND DECELERATOR SYSTEM LOADS AND DYNAMICS

R. Moog, Martin Marietta/Denver Division, Denver, CO and D. Kross, NASA,
Marshall Space Flight Center, Huntsville, AL

INVESTIGATION OF SIDE FORCE OSCILLATIONS DURING STATIC FIRING OF THE SPACE SHUTTLE SOLID ROCKET MOTOR

M. A. Behring, Thiokol Corporation/Wasatch Division, Brigham City, UT

Space Shuttle Data Systems

DEVELOPMENT OF AN AUTOMATED PROCESSING AND SCREENING SYSTEM FOR THE SPACE SHUTTLE ORBITER FLIGHT TEST DATA

D. K. McCutchen, NASA, Johnson Space Center, Houston, TX, J. F. Brose, Lockheed Engineering and
Management Services Company, Inc., Houston, TX and W. E. Palm, McDonnell Douglas Corp., Houston, TX

DEVELOPMENT OF A VIBROACOUSTIC DATA BASE MANAGEMENT AND PREDICTION SYSTEM FOR PAYLOADS

F. J. On, NASA, Goddard Space Flight Center, Greenbelt, MD and
W. Hendricks, Lockheed Missiles and Space Company, Sunnyvale, CA

AUTOMATION OF VIBROACOUSTIC DATA BANK FOR RANDOM VIBRATION CRITERIA DEVELOPMENT

R. C. Ferebee, NASA, Marshall Space Flight Center, Huntsville, AL

THE DEVELOPMENT AND VERIFICATION OF SHUTTLE ORBITER RANDOM VIBRATION TEST REQUIREMENTS

M. C. Coody, NASA, Johnson Space Center, Houston, TX, H. K. Pratt, Rockwell International Corporation,
Downey, CA and D. E. Newbrough, Management and Technical Services Corporation, Houston, TX

SPACE SHUTTLE ORBITER ACOUSTIC FATIGUE CERTIFICATION TESTING

R. A. Stevens, Rockwell International, Downey, CA

Space Shuttle Thermal Protection Systems

STRUCTURAL CHARACTERISTICS OF THE SHUTTLE ORBITER CERAMIC THERMAL PROTECTION SYSTEM

P. A. Cooper, NASA, Langley Research Center, Hampton, VA

SHUTTLE TILE ENVIRONMENTS AND LOADS

R. J. Muraca, NASA, Langley Research Center, Hampton, VA

DYNAMIC AND STATIC MODELING OF THE SHUTTLE ORBITER'S THERMAL PROTECTION SYSTEM

J. M. Housner, G. L. Giles and M. Vallas, NASA, Langley Research Center, Hampton, VA

BUFFET LOADS ON SHUTTLE THERMAL-PROTECTION-SYSTEM TILES

C. F. Coe, NASA, Ames Research Center, Moffett Field, CA

UNSTEADY ENVIRONMENTS AND RESPONSES OF THE SHUTTLE COMBINED LOADS ORBITER TEST

P. H. Schuetz, Rockwell International, Downey, CA and
L. D. Pinson and H. T. Thornton, Jr., NASA, Langley Research Center, Hampton, VA

Space Shuttle Main Engine Dynamics

VIBRATION MATURITY OF THE SPACE SHUTTLE MAIN ENGINES

E. W. Larson and E. Mogil, Rockwell International/Rocketdyne Division, Canoga Park, CA

STRUCTURAL RESPONSE OF THE SSME FUEL FEEDLINE TO UNSTEADY SHOCK OSCILLATIONS

E. W. Larson, G. H. Ratekin and G. M. O'Connor, Rockwell International/Rocketdyne Division, Canoga Park, CA

PAPERS APPEARING IN PART 3

Environmental Testing and Simulation

DIGITAL CONTROL OF A SHAKER TO A SPECIFIED SHOCK SPECTRUM

J. F. Unruh, Southwest Research Institute, San Antonio, TX

GUNFIRE VIBRATION SIMULATION ON A DIGITAL VIBRATION CONTROL SYSTEM

J. Cies, Hewlett-Packard Company, Paramus, NJ

MEASUREMENT OF ALL COMPONENTS OF STRAIN BY A 3-D FIBER OPTIC STRAIN GAGE

S. Edelman and C. M. Davis, Jr., Dynamic Systems, Inc., McLean, VA

REGISTRATION OF THREE SOIL STRESS GAGES AT 0 THROUGH 28 MPa (4000 psi)

C. R. Welch, U.S. Army Engineer Waterways Experiment Station, Corps of Engineers, Vicksburg, MS

**CABLE PROTECTION FOR GROUND SHOCK INSTRUMENTATION IN SEVERE ENVIRONMENTS —
RESULTS OF AN EVALUATION TEST**

C. R. Welch, U.S. Army Engineer Waterways Experiment Station, Corps of Engineers, Vicksburg, MS

STRUCTURAL RESPONSE OF HEPA FILTERS TO SHOCK WAVES

P. R. Smith, New Mexico State University, Las Cruces, NM and W. S. Gregory, Los Alamos National Laboratory, Los Alamos, NM

**A TECHNIQUE COMBINING HEATING AND IMPACT FOR TESTING REENTRY VEHICLE IMPACT
FUZES AT HIGH VELOCITIES**

R. A. Benham, Sandia National Laboratories, Albuquerque, NM

USE OF A DROPPED WEIGHT TO SIMULATE A NUCLEAR SURFACE BURST

C. R. Welch and S. A. Kiger, U.S. Army Engineer Waterways Experiment Station, Corps of Engineers, Vicksburg, MS

ANALYSIS AND TESTING OF A NONLINEAR MISSILE AND CANISTER SYSTEM

R. G. Benson, A. C. Deerhake and G. C. McKinnis, General Dynamics/Convair Division, San Diego, CA

BIO-DYNAMIC RESPONSE OF HUMAN HEAD DURING WHOLE-BODY VIBRATION CONDITIONS

B. K. N. Rao, Birmingham Polytechnic, Perry Barr, England

Flight Environments

YC-15 EXTERNALLY BLOWN FLAP NOISE

Capt. L. G. Peck, Flight Dynamics Laboratory, Air Force Wright Aeronautical Laboratories, Wright-Patterson AFB, OH

DETERMINATION OF THE DYNAMIC ENVIRONMENT OF THE F/FB-111 TAIL POD ASSEMBLY

J. Chinn and P. Bolds, Air Force Wright Aeronautical Laboratories, Wright-Patterson AFB, OH

AN ASSESSMENT OF THE A-10's CAPABILITY TO OPERATE ON ROUGH SURFACES

T. G. Gerardi and D. L. Morris, Air Force Wright Aeronautical Laboratories, Wright-Patterson AFB, OH

SUBCRITICAL FLUTTER TESTING USING THE FEEDBACK SYSTEM APPROACH

C. D. Turner, North Carolina State University, Raleigh, NC

TOMAHAWK CRUISE MISSILE FLIGHT ENVIRONMENTAL MEASUREMENT PROGRAM

E. S. Rosenbaum and F. L. Gloyna, General Dynamics/Convair Division, San Diego, CA

TEST PROGRAM TO DEVELOP VIBROACOUSTICS TEST CRITERIA FOR THE GALILEO BUS

D. L. Kern and C. D. Hayes, Jet Propulsion Laboratory, California Institute of Technology, Pasadena, CA

SLV-3 FLIGHT VIBRATION ENVIRONMENT

S. A. Palaniswami, G. Muthuraman and P. Balachandran, Aerospace Structures Division,
Vikram Sarabhai Space Centre, Trivandrum, India

PAPERS APPEARING IN PART 4

Fatigue and Random Loading

FATIGUE LIFE PREDICTION FOR VARIOUS RANDOM STRESS PEAK DISTRIBUTIONS

R. G. Lambert, General Electric Company, Aircraft Equipment Division, Utica, NY

FATIGUE LIFE EVALUATION, STOCHASTIC LOADING AND MODIFIED LIFE CURVES

M. El Menoufy, H. H. E. Leipholz and T. H. Topper, University of Waterloo, Waterloo, Ontario, Canada

THE EFFECTS OF ENDURANCE LIMIT AND CREST FACTOR ON TIME TO FAILURE UNDER RANDOM LOADING

A. J. Curtis and S. M. Moite, Hughes Aircraft Company, Culver City, CA

SINGLE POINT RANDOM MODAL TEST TECHNOLOGY APPLICATION TO FAILURE DETECTION

W. M. West, Jr., NASA, Johnson Space Center, Houston, TX

FORCED VIBRATIONS OF A LARGE DAMPED MECHANICAL SYSTEM

D. W. Nicholson, Naval Surface Weapons Center, White Oak, Silver Spring, MD

INDIRECT FOURIER TRANSFORM (IFT) AND SHOCK RESPONSE - A DETAILED PRESENTATION OF BASIC THEORY

C. T. Morrow, Encinitas, CA

Control, Isolation and Damping

ACTIVE VIBRATION CONTROL OF LARGE FLEXIBLE STRUCTURES

T. T. Soong and J. C. H. Chang, State University of New York at Buffalo, Buffalo, NY

FORCE OPTIMIZED RECOIL CONTROL SYSTEM

P. E. Townsend, U.S. Army Armament Research and Development Command, Dover, NJ,
R. J. Radkiewics, U.S. Army Armament Research and Development Command, Rock Island, IL and
R. F. Gartner, Honeywell, Inc., Edina, MN

PERFORMANCE ANALYSIS OF HIGH-SPEED HYDRAULIC SUSPENSION SYSTEMS IN MULTIPLE WHEELED LAND TRANSPORTERS

P. Woods, Martin Marietta Corporation, Denver, CO

NONLINEAR ANALYSIS OF PNEUMATIC FORCE GENERATORS USED FOR VIBRATION CONTROL

S. Sankar, Concordia University, Montreal, Quebec, Canada, R. R. Guntur, Union College, Schenectady, NY,
and S. G. Kalumber, Electronic Associates, Inc., West Long Branch, NJ

REDUCTION OF HYDRAULIC LINE OSCILLATING PRESSURES INDUCED BY PUMP CAVITATION

G. Druhak, P. Marino and M. Bernstein, Grumman Aerospace Corporation, Bethpage, NY

RUBBER ISOLATORS FOR THE ADATS MISSILE

J. Frottier, Oerlikon-Buehler Werkzeugmaschinenfabrik, Zurich, CH and
C. F. O'Hearne, Martin Marietta Orlando Aerospace, Orlando, FL

TIME AND TEMPERATURE EFFECTS ON CUSHIONS

G. S. Mustin, Naval Sea Systems Command, Washington, DC

EXTRANEUS EFFECTS IN DAMPING MEASUREMENT

R. J. Hooker, University of Queensland, Queensland, Australia and
S. Prasertan, Prince of Songkla University, Hat-yai, Thailand

DYNAMIC ANALYSIS OF A LARGE STRUCTURE WITH ARTIFICIAL DAMPING

Q. L. Tian, D. K. Liu, Y. P. Li and D. F. Wang, Institute of Mechanics,
The Chinese Academy of Sciences, Beijing, China

AN EXPERIMENTAL STUDY OF THE NONLINEAR BEHAVIOUR OF A STRANDED CABLE AND DRY FRICTION DAMPER

C. S. Chang and Q. Tian, Institute of Mechanics, The Chinese Academy of Sciences, Beijing, China

RESPONSE OF PNEUMATIC ISOLATOR TO STANDARD PULSE SHAPES
M. S. Hundal, The University of Vermont, Burlington, VT

PAPERS APPEARING IN PART 5

Mathematical Modeling

DAMPED STRUCTURE DESIGN USING FINITE ELEMENT ANALYSIS
M. F. Kluesener and M. L. Drake, University of Dayton Research Institute, Dayton, OH

DETERMINATION OF NORMAL MODES FROM MEASURED COMPLEX MODES
S. R. Ibrahim, Old Dominion University, Norfolk, VA

THE EFFECT OF JOINT PROPERTIES ON THE VIBRATIONS OF TIMOSHENKO FRAMES
I. Yaghmai, Sharif University of Technology, Tehran, Iran and
D. A. Frohrib, University of Minnesota, Minneapolis, MN

SOIL STRUCTURE INTERACTION AND SOIL MODELS
J. M. Ferritto, Naval Civil Engineering Laboratory, Port Hueneme, CA

FINITE ELEMENTS FOR INITIAL VALUE PROBLEMS IN DYNAMICS
T. E. Simkins, U.S. Army Armament Research and Development Command, Watervliet, NY

Structural Dynamics

A PROCEDURE FOR DESIGNING OVERDAMPED LUMPED PARAMETER SYSTEMS
D. J. Inman, State University of New York at Buffalo, Buffalo, NY and
A. N. Andry, Jr., Lockheed California Company, Burbank, CA

ON THE OPTIMAL LOCATION OF VIBRATION SUPPORTS
B. P. Wang and W. D. Pilkey, University of Virginia, Charlottesville, VA

DYNAMIC BUCKLING OF PINNED COLUMNS
J. M. Ready, David W. Taylor Naval Ship Research and Development Center, Bethesda, MD

LARGE DEFLECTION RANDOM RESPONSE OF SYMMETRIC LAMINATED COMPOSITE PLATES
K. R. Wentz and D. B. Paul, Air Force Wright Aeronautical Laboratories, Wright-Patterson AFB, OH and
C. Mei, Old Dominion University, Norfolk, VA

DYNAMIC CHARACTERISTICS OF A NON-UNIFORM TORPEDO-LIKE HULL STRUCTURE
A. Harari, Naval Underwater Systems Center, Newport, RI

VIBRATION AND ACOUSTIC RADIATION FROM POINT EXCITED SPHERICAL SHELLS
E. H. Wong, Naval Ocean Systems Center, San Diego, CA and
S. I. Hayek, The Pennsylvania State University, University Park, PA

DAMPING OF SHALLOW-BURIED STRUCTURES DUE TO SOIL-STRUCTURE INTERACTION
F. S. Wong and P. Weidlinger, Weidlinger Associates, Menlo Park, CA and New York, NY

**TITLES AND AUTHORS OF PAPERS PRESENTED IN THE
SHORT DISCUSSION TOPICS SESSION**

NOTE: These papers were only presented at the Symposium. They are not published in the Bulletin and are only listed here as a convenience.

TRANSFER FUNCTION ANALYSIS OF LARGE STRUCTURES
H. J. Weaver, Lawrence Livermore National Laboratory, Livermore, CA

SHOCK HARDENED STRUCTURAL ATTACHMENTS FOR HONEYCOMB BULKHEADS
P. W. Buermann, Gibbs & Cox, Inc., New York, NY

DISCOVERING THE THIRD (AND SECOND) DIMENSION
B. Meeker, Pacific Missile Test Center, Point Mugu, CA

A MICROPROCESSOR BASED ADAPTIVE ISOLATION AND DAMPING OF A VIBRATING STRUCTURE
A. S. R. Murty, Indian Institute of Technology, Kharagpur, India

HARMONIC RESPONSE OF A STRUCTURE INCLUDING A DRY FRICTION DAMPER
J. Der Hagopian and M. LaLanne, Institut National des Sciences Appliquees, Villeurbanne, France

RATIONALE FOR VIBRATION TESTING IN MIL-STD-810D (DRAFT)
H. J. Caruso, Westinghouse Electric Corporation, Baltimore, MD

VIBRATION ISOLATION OF SENSITIVE IUS COMPONENTS REQUIRING THERMAL CONDUCTION
F. W. Spann, Boeing Aerospace Company, Seattle, WA

FINITE ELEMENT ANALYSIS OF SHOCK AND VIBRATION FIXTURES
L. G. Smith, Hughes Aircraft Company, Fullerton, CA

A UNIQUE METHOD FOR VIBRATION TESTING FAR BELOW THE NORMAL AMBIENT NOISE LEVEL OF ELECTRODYNAMIC SHAKERS
H. D. Camp, Jr., U.S. Army; ERADCOM, Fort Monmouth, NJ

BOLTS AND FASTENER TIGHTENING TO BROCHURE IDEALNESS THROUGH VIBRATION SIGNATURES
A. S. R. Murty, Indian Institute of Technology, Kharagpur, India

COST EFFECTIVE METHODS OF INCREASING DATA RECORDING CAPACITY
M. Dowling, Franklin Research Center, Philadelphia, PA

PIEZOELECTRIC FORCE GAUGE WITH HIGH SENSITIVITY
R. R. Bouche, Bouche Laboratories, Sun Valley, CA

PYROTECHNIC SHOCK ENVIRONMENTS MEASURED ON INERTIAL UPPER STAGE (IUS)
C. J. Beck, Jr., Boeing Aerospace Company, Seattle, WA

USE OF BAND-SELECTABLE HANNING SMOOTHING TO IMPROVE TRANSIENT WAVEFORM REPRODUCTION ON SHAKERS
D. O. Smallwood and D. L. Gregory, Sandia National Laboratories, Albuquerque, NM

SHAKER SHOCK TEST DATA - BASED ON OPTIMIZED PRE AND POST PULSES
R. T. Fandrich, Harris Corporation, Melbourne, FL

PROGRESS ON THE EDESS MACHINES
F. J. Szama, Naval Surface Weapons Center, Silver Spring, MD

MULTI-AXIS RANDOM VIBRATION TESTER FOR AVIONICS
D. Everett, Pacific Missile Test Center, Point Mugu, CA and G. Greanias, UCLA, Los Angeles, CA

ACOUSTIC FACILITY FOR CRUISE MISSILE TESTING
O. H. Moore, Jr., General Dynamics/Convair, San Diego, CA

EFFECT OF FRICTION AND MISTUNING ON THE RESPONSE OF A BLADED DISK DISCRETE MODEL
A. Muszynska, University of Dayton and Bently Nevada Corp., Minden, NV

CURRENT DEVELOPMENTS IN HUMAN VIBRATION RESEARCH
J. C. Guignard, Naval Biodynamics Laboratory, New Orleans, LA

SESSION CHAIRMEN AND COCHAIRMEN
52nd Shock and Vibration Symposium
October 27-29, 1981, New Orleans, LA

<u>Date</u>	<u>Session Title</u>	<u>Chairmen</u>	<u>Cochairmen</u>
Tuesday, 27 Oct. A.M.	Opening Session	Dr. Eugene Sevin, Defense Nuclear Agency, Washington, DC	Mr. Henry C. Pusey, Shock and Vibration Information Center, Naval Research Laboratory, Washington, DC
Tuesday, 27 Oct. P.M.	Rotor Dynamics and Machinery Vibration	Mr. Samuel Feldman, NKF Engineering Associates, Inc., Vienna, VA	Mr. Paul Maedel, Westinghouse Electric Corporation, Philadelphia, PA
Tuesday, 27 Oct. P.M.	Environmental Testing and Simulation	Mr. David O. Smallwood, Sandia National Laboratories, Albuquerque, NM	Mr. Leo Ingram, Waterways Experiment Station, Vicksburg, MS
Tuesday, 27 Oct. P.M.	Space Shuttle Loads and Dynamics	Mr. Donald C. Wade, NASA, Johnson Space Center, Houston, TX	Dr. Vernon Neubert, Pennsylvania State University, University Park, PA
Wednesday, 28 Oct. A.M.	Fatigue and Random Loading	Dr. George Morosow, Martin Marietta Corporation, Denver, CO	Dr. Grant Gerhart, U.S. Army Tank Automotive R&D Command, Warren, MI
Wednesday, 28 Oct. A.M.	Space Shuttle Data Systems	Mr. Don K. McCutchen, NASA, Johnson Space Center, Houston, TX	Mr. Jerome Pearson, Air Force Wright Aeronautical Laboratories, Wright Patterson AFB, OH
Wednesday, 28 Oct. P.M.	Control, Isolation and Damping	Mr. Ahid Nashif, Anatrol Corporation, Cincinnati, OH	Dr. John P. Henderson, Air Force Wright Aeronautical Laboratories, Wright Patterson AFB, OH
Wednesday, 28 Oct. P.M.	Space Shuttle Thermal Protection System Dynamics	Mr. Jess Jones, NASA, Marshall Space Flight Center, Huntsville, AL	Mr. Lloyd Brooks, U.S. Army Missile Command, Redstone Arsenal, AL
Thursday, 29 Oct. A.M.	Mathematical Modeling	Dr. Richard Skop, Naval Research Laboratory, Washington, DC	Dr. David I. G. Jones, Air Force Wright Aeronautical Laboratories, Wright Patterson AFB, OH
Thursday, 29 Oct. A.M.	Flight Environments	Mr. John Wafford, Aeronautical Systems Division, Wright Patterson AFB, OH	Mr. Brent Meeker, Pacific Missile Test Center, Point Mugu, CA
Thursday, 29 Oct. P.M.	Structural Dynamics	Dr. James Richardson, U.S. Army Missile Command, Huntsville, AL	Dr. Nicholas Baskas, Office of Naval Research, Arlington, VA
Thursday, 29 Oct. P.M.	Short Discussion Topics	Mr. John Favour, The Boeing Company, Seattle, WA	Mr. Joseph Gaudet, Sanders Associates, Manchester, NH

WELCOME

Colonel Tilford C. Creel
Commander and Director
U.S. Army Engineer Waterways Experiment Station
Vicksburg, Mississippi

It is my pleasure to welcome you today on behalf of the Defense Nuclear Agency and the U.S. Army Engineer Waterways Experiment Station, who are co-hosts for this 52nd Shock and Vibration Symposium.

Fifty-two (52) is also the number of years the WES has been in existence; in 1929 the Waterways Experiment Station was born and its mission was to conduct hydraulic model studies aimed at making predictions so that flooding along the Mississippi River could be controlled. In the beginning the engineering field of interest was hydraulics, which has been expanded over the years to include soils and foundations, concrete, flexible pavements, weapons effects, mobility, environmental effects, geology, terrain analysis, soil dynamics, rock mechanics, and structures. We have four laboratories to conduct our current mission. These are the Hydraulics, Geotechnical, Environmental, and the Structures Laboratories. In recent years, it has been the people in the Structures Laboratory who have had the closest association with the Defense Nuclear Agency. Our friendship traces back through the time when the DNA was the Defense Atomic Support Agency (DASA) to the time when the organization was known as the Armed Forces Special Weapons Project (AFSWP).

The initial effort, when DNA was AFSWP, began in 1951 when we were tasked to conduct an investigation to determine water wave heights and water shock loads caused by underwater explosions. At that time it was believed the way to disrupt this country would be to drop a nuclear bomb in our waterways. The resulting crater would create a large lip around the periphery which would either close up ports or dam our major streams, resulting in extensive flooding and bringing navigation to a halt. The beginning was a natural since WES had a hydraulic laboratory and a superb instrumentation group; consequently, the first research teams at WES to do work for DNA were formed from a nucleus of hydraulic engineers and instrumentation specialists. Our efforts were extended to include underwater cratering and the response of gravity dams to water shock loadings. Our first experience in a full scale nuclear test occurred in 1956-57 during Operation PLUMBBOB when we tested below ground structures to the effects of blast and shock from an aboveground burst.

We were also involved in the underwater detonations of this Operation HARDTACK series conducted in the Marshall Islands during 1958. Specifically, we analyzed structures remaining from the GREENHOUSE series of tests and measured water shock in deep and shallow water. In

these efforts we worked closely with the Naval Ordnance Laboratory, the Air Force Weapons Laboratory, and Holmes & Narver, Inc., of Los Angeles, CA. We also became involved in soil dynamics and the nucleus of engineers for this effort was from the Soils Laboratory. We were fortunate to have available talented people to address these new problems. The Director of WES in 1952 was Lt. Gen. Carroll H. Dunn, who later became the Director of DNA. We value our close association with DNA and hope it will continue.

Today we read in newspapers or hear over TV the concern of protecting missile silos to overpressures in excess of 1000's of psi. In 1955 the weapons effects community talked about getting into the very high overpressure region of 200 psi. The environment of interest has certainly become more severe to say the least, and the design of systems to resist these hostile environments is a real challenge. In our endeavors we have been not only keenly aware of the loading and response of systems but also the importance of shock and vibration effects. As an example, I remember reading a report about an aboveground reinforced concrete cubicle that was subjected to airblast generated by a nuclear detonation. The investigator stated the box successfully withstood the imposed loads — only a few hairline cracks were observed; the structure was distressed little. The he went on to say, "However, the cubicle was displaced 70 feet from its original position." I am not sure that I would have enjoyed a ride in that structure or the opportunity to learn first hand about its internal shock and vibration levels.

Most of you are aware that the Corps of Engineers conducts both military and civil work and WES conducts research in both these arenas. A healthy aspect of this dual effort is that we are able to apply technology developed for military purposes and apply it for civil purposes and vice versa. In one study, before breaching a model concrete gravity arch dam, we conducted extensive vibration tests and subjected the model to simulated earthquake motions.

We were not given permission to breach the prototype but we were able to conduct vibration tests and successfully correlated the response of the prototype and model through this technique. In this study the effect of an earthquake on such a dam was determined — a civil problem; also, the minimum amount of explosives in the reservoir at the right place to cause the dam to break was determined — a military problem.

For the past 10 years we have been conducting studies to define the freefield environment as well as tests of blasts

effects on structures, both buried and above ground, to determine their vulnerability to nuclear and conventional weapons effects. Such tests have been conducted with small charges (up to 800 lb) in test basins located near Vicksburg, with charges up to 5 tons at Fort Polk, LA; Fort Campbell, KY; and Camp Shelby, MS. We have also participated in almost every major field test sponsored by DNA.

I would like to remind you that WES is about 220 miles up river from here, and I invite you to come visit with us

when you have a chance. It has been my pleasure to welcome all of you on behalf of DNA and WES and I certainly hope that your visit will be interesting. After reviewing the list of speakers and subjects for discussion, I am sure it will be. A number of our Project Investigators are on the technical program and you will be hearing more about our efforts from them. Also, I hope you have a good time and are able to enjoy New Orleans.

KEYNOTE ADDRESS

Dr. Marvin Atkins
Director, Offensive and Space Systems, OUSDRE (S455)
Department of Defense
Washington, DC

It is a pleasure and a privilege to be able to address the Shock and Vibration Symposium. For my topic this morning, I have chosen to discuss the new strategic Forces Modernization Plan which was announced by the President on October 2nd. This is an integrated plan for improvement of all of our strategic forces — C³, Bombers, SLBM's, ICBM's and strategic defenses — which will affect the defense posture of the United States well into the next century. This plan will affect all of us here in our lives as citizens, and will directly affect many of the people in this Symposium because they will be doing important technical work which is vital in bringing this plan to fruition.

COMMUNICATIONS AND CONTROL SYSTEMS

Strategic communications and control systems are essential to the effective employment of our nuclear forces and, therefore, to the credible deterrence. Our modernization of these systems in the past has not provided systems with the requisite survivability and reliability to operate over an extended period after a Soviet attack, if that proved to be necessary. We need communications and control systems which will be as strong as the nuclear systems they support. This requires enhanced warning and attack assessment, mobile command centers that could survive an initial attack, and survivable communications links. In the near-term we will improve the survivability, performance, and coverage of radars and satellites used to warn us of a Soviet missile attack and assess its size and scope including deployment of mobile ground terminal, upgraded survivability and improved capabilities for our warning satellites, and the deployment of additional PAVE PAWS surveillance radars. We will upgrade the survivability and capability of command centers that would direct U.S. strategic forces during a nuclear war including the deployment of E-4B airborne command posts to serve the National Command Authorities in time of war, and enhancing the C-135 airborne command posts serving military commanders through the installation of upgraded satellite and very low frequency/low frequency communications and aircraft hardening against nuclear effects. We will also deploy survivability communications that link command centers with all three elements of the TRIAD.

In order to enhance our ability for long-term operation of our forces in a nuclear war environment, we will initiate a vigorous and comprehensive research and development

program leading to a communications and control system that would endure for an extended period beyond the first nuclear attack.

BOMBER FORCES

There is a general consensus on the need for new strategic bombers to replace our aging B-52 force. We therefore plan on developing a variant of the B-1 bomber, the B-1B, and will deploy 100 aircraft with the first squadron operational in 1986. We will also continue a vigorous research and development program for an Advanced Technology Bomber (ATB), incorporating "stealth" technology, for deployment in the 1990's.

Our two-bomber program is considered to be a reasonable approach to ensuring the continued viability of our strategic bomber force. The B-1B will restore our ability to penetrate Soviet air defenses during the critical period of the 1980's and will make a good cruise missile carrier and conventional bomber after the ATB is deployed and all B-52's are retired in the 1990's. The ATB will provide us with high confidence that our strategic bomber force will continue to have the ability to penetrate Soviet air defenses into the next century.

Building the B-1B now will allow time to resolve technical and operational uncertainties associated with the ATB without undue pressures to acquire this bomber as soon as possible. The B-1B will help to bolster our strategic TRIAD in the 1980's while we take steps to strengthen our land-based missiles. We cannot afford to wait until the ATB becomes available. Finally, building two bombers will stimulate competition and provide us the flexibility to adjust bomber procurement depending on future strategic needs.

In the near-term we will modify our newer B-52's (G and H models) to carry cruise missiles. The first squadron of cruise missile equipped aircraft (B-52G's) will be operational in 1982. Selected B-52's will be modernized to provide added protection against the effects of nuclear explosions (particularly electromagnetic pulse effects) and to improve their ability to survive against Soviet air defenses through installation of additional electronic countermeasures equipment. We will disperse our alert B-52's to more bases in peacetime in order to enhance their survivability. Older

B-52's (D model) will be retired in 1982 and 1983. Finally, existing KC-135 aerial tankers will be outfitted with new engines to increase airborne refueling capabilities.

SEA-BASED FORCES

Our sea-based strategic forces currently represent the most survivable element of our strategic TRIAD. We will further strengthen this force through continued construction of TRIDENT submarines at a steady rate of one per year and through development of a larger and more accurate TRIDENT II (D-5) missile.

The TRIDENT II missile, scheduled for deployment in TRIDENT submarines beginning in 1989, will have the capability of carrying more and/or larger warheads than the current TRIDENT I (C-4) missile thereby effectively utilizing the growth room in the TRIDENT submarine missile tubes. The TRIDENT II missile will nearly double the capability of each TRIDENT submarine thereby avoiding a reduction in sea-based capabilities in the 1990's when our current POSEIDON submarines reach the end of their service lives and must be retired. The TRIDENT II missile will also have much better accuracy than current sea-based missiles, thereby providing our sea-based forces with the ability to effectively attack any target in the Soviet Union, including hard targets.

In the near-term we plan to put cruise missiles on attack submarines in order to deploy a force of highly accurate nuclear warheads at sea. Deployment of these missiles will strengthen our strategic reserve and deter the use of nuclear weapons against our naval forces worldwide. In a theater role, they could also supplement the critical deployment of Ground-Launched Cruise Missiles and the PERSHING II ballistic missile in countering the massive Soviet buildup of theater nuclear forces in Europe.

ICBM MODERNIZATION

The Multiple Protective Shelter basing scheme for the MX missile will be cancelled; however, we are still faced with the problem of the current vulnerability of our MINUTEMAN and TITAN force. We will continue to develop the MX missile and will deploy at least 100 missiles in a long-term basing option in order to redress this problem.

Since the MX missile will be available in 1986, well ahead of its long-term basing, initial deployment in existing silos is the only way to avoid delaying the program. We cannot afford to put off MX with its improved accuracy, increased payload, and prompt counter-ICMB capabilities. We will therefore deploy a limited number of MX missiles, as soon as possible, in TITAN or MINUTEMAN silos that will be reconstructed by adding more steel and concrete in order to increase their hardness to nuclear effects. This interim measure would force the Soviets to develop more accurate missiles

and might well keep them from achieving a high confidence counter-MX capability until the late-1980's, by which time we will have a better system.

For long-term basing of MX we will initiate vigorous research and development programs on three options. These options are: Deep Underground Basing, deployment of MX in survivable locations deep underground; Continuous Airborne Patrol Aircraft, a survivable long-endurance aircraft that could launch MX; and Ballistic Missile Defense, active defense of land-based MX missiles. We plan to choose among these long-term basing options as soon as sufficient technical information becomes available and in any event no later than 1984.

Finally, we will deactivate all aging Titan missiles as soon as possible.

STRATEGIC DEFENSE

Due to a relatively lower priority assigned to our strategic defense systems over the past decade we have not maintained the level of credibility appropriate to our national goals. In order to take the first steps toward restoring credible strategic defensive forces the following programs will be pursued:

- In coordination with Canada, upgrade the North American air surveillance network including some combination of new over-the-horizon backscatter (OTH-B) radars and improve versions of today's ground radars.
- Replace five squadrons of aging F-106 interceptors with new F-15's.
- Buy at least six additional AWACS airborne surveillance aircraft for North American air defense to augment ground based radars in peacetime and to provide surveillance and control of interceptors in wartime.
- Continue to pursue an operational antisatellite system.
- A vigorous research and development program on ballistic missile defense for active defense of land-based missiles. This program will include technologies for space-based missile defense.
- An expanded, cost effective civil defense program will be developed in coordination with the Federal Emergency Management Agency.

In the years ahead we plan to continue our review of strategic defense to determine what additional steps may be needed to achieve a credible strategic defensive force posture.

In closing, I want to thank you again for inviting me to this Symposium, and I will look forward to the personal contributions which you will be making to the modernization of our strategic forces.

INVITED PAPERS

EQUIPMENT SURVIVABILITY ON THE INTEGRATED BATTLEFIELD

Dr. Charles N. Davidson
US Army Nuclear and Chemical Agency
Springfield, VA

Good Morning! I appreciate the opportunity to address you today on the integrated battlefield, and on the survivability of Army equipment on that battlefield. Although I recognize that the principal focus of this symposium is on shock and vibration problems, perhaps you will allow me to set the stage a little by defining the integrated battlefield; touching on the conventional, nuclear, and NBC contamination survivability programs which can drive shock and vibration survivability requirements in the Army; and indicate why these programs can no longer be considered independently. Figure 1 shows the concept of the Integrated Battlefield.

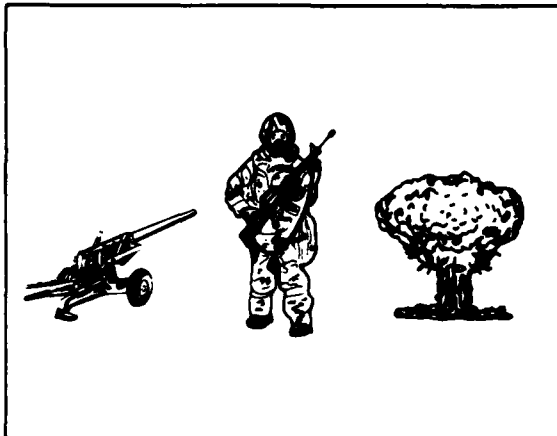


Fig. 1 — The integrated battlefield

First, let's define just what the integrated battlefield is so we'll all be talking off the same program. The Army defines this term as shown in Figure 2. Please note that nuclear and/or chemical weapons do not already have to have been employed for the integrated battlefield to exist; it is sufficient for either combatant simply to have the capability to do so. This situation results from the accepted fact that forces will not have the time or opportunity to stop and transition from one form of warfare to another. When combat begins, therefore, we must be ready to survive and fight in any and all of those environments.

THE INTEGRATED BATTLEFIELD IS A COMBAT ZONE WHERE EITHER OR BOTH COMBATANTS HAVE USED, ARE USING, OR HAVE THE CAPABILITY TO USE CONVENTIONAL, NUCLEAR, CHEMICAL, OR ELECTRONIC WARFARE WEAPONS SINGULARLY OR IN ANY COMBINATION TO ACHIEVE A MILITARY OBJECTIVE.

Fig. 2 — Integrated Battlefield

At this point, I should document the threat to show that such a battlefield is likely to exist, but I propose not to do so for several reasons. First, I don't have sufficient time; second, classification limitations here would prevent an authoritative rundown; and finally, I don't really think it's necessary. We've all been deluged with quantities of information during the last several years, from both official and unofficial sources, that, convincingly I believe, indicate that, against the Soviets, any battle will be integrated and we can expect simultaneous conventional, nuclear, and chemical fires amidst a severe EW environment. Hopefully, you will agree that this threat is real.

One more point on the integrated battlefield is important before we continue. The "IB," broad and all encompassing as it may seem, is actually a subset of an even broader concept — and Airland battle shown in Figure 3.

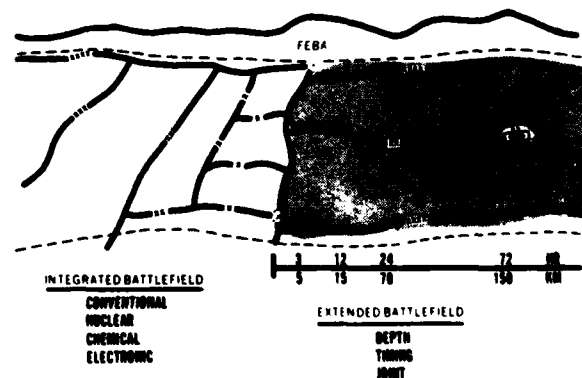


Fig. 3 — Airland battlefield concept

This concept extends the integrated battlefield deep into the enemy rear, provides, by engaging second echelon forces, time and space for forward forces to conduct their portion of the battle, and recognizes the joint Service nature of this extended battlefield.

We might summarize to this point by saying that we have defined an integrated battlefield which recognizes no time or opportunity to transition from one form of warfare to another, and which, as a consequence, requires that we ultimately consider system survivability from an integrated standpoint where synergisms may be very important.

The facts are, however, that we're not there yet and have a long way to go. We've identified the important pieces of the puzzle, know what to do with some of these pieces, but haven't yet fitted them all together (Figure 4).

Let's take a look at how the Army addresses equipment survivability today — piece by piece.

Conventional survivability (Figure 5) of course, is the business most of you are in. We assume that you will design our Army equipment to withstand the conventional environments — off-road transport, rough handling, firing shocks — and requirements documents traditionally have included criteria or specifications for doing so. Additionally, our

requirements have included criteria for surviving small arms fire and fragmentation munitions. This kind of survivability has been with us for a long time and, when people in the sixties and before discussed equipment survivability on the battlefield, they were talking about survivability on the conventional battlefield. That was fine as long as we were fighting in Korea or Vietnam, but now we have to consider a different battlefield — the integrated battlefield — with all that is implied in NBC contamination and nuclear survivability. Let's proceed, then, to look beyond conventional battlefield problems, as serious as they are, at two other programs of major concern to the Army.

The nuclear survivability program had its origins in the early 1970's. Eventually formalized by Army regulation in 1977, this piece of the survivability puzzle (Figure 6) has as its goal the research, development, testing, evaluation, logistic support, and product improvement of critical Army materiel which will survive the initial nuclear environments of the integrated battlefield. Based on the philosophy that the equipment should survive if enough of the personnel required to operate it remain combat effective, the program results in specification of thermal, airblast, initial nuclear radiation, and electromagnetic pulse criteria which are balanced to each other and to survivability of the operating crew.

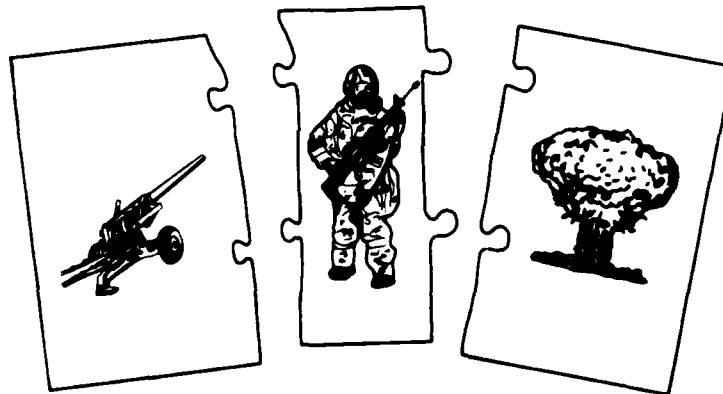


Fig. 4 — The integrated battlefield

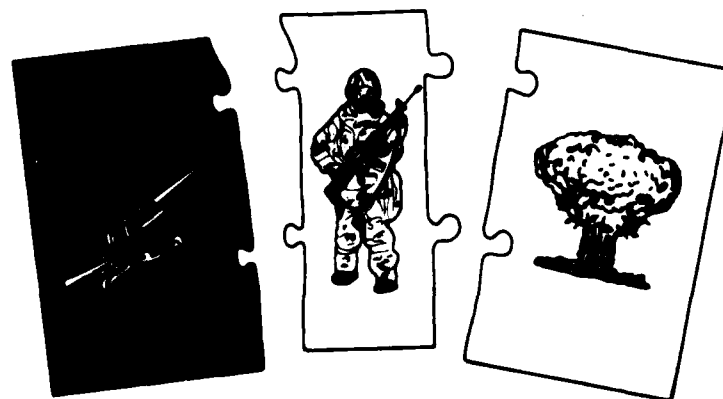


Fig. 5 — The integrated battlefield

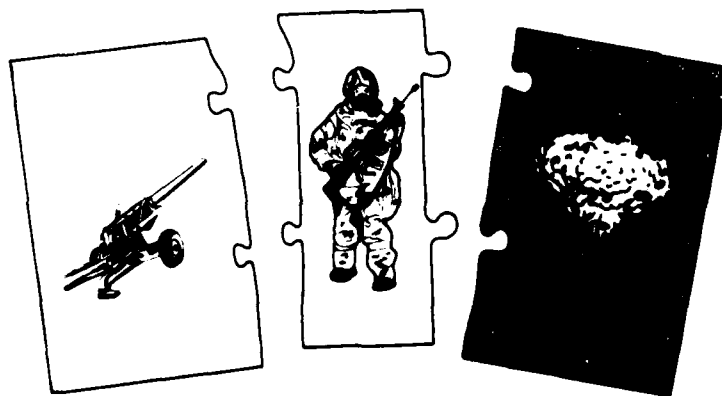


Fig. 6 — The integrated battlefield

This philosophy is not only straightforward, but has the beauty of being reasonably scenario independent. The distances from ground zero at which operating personnel become combat ineffective from nuclear effects are plotted as a function of threat weapon yield (Figure 7). The distances

accordance with the spectrum of expected threat weapon yields, usually determined by the system's planned location on the battlefield. Equipment survivability criteria are then calculated from the worst case environments corresponding to the threat constrained governing isocasualty curve (Figure 9).

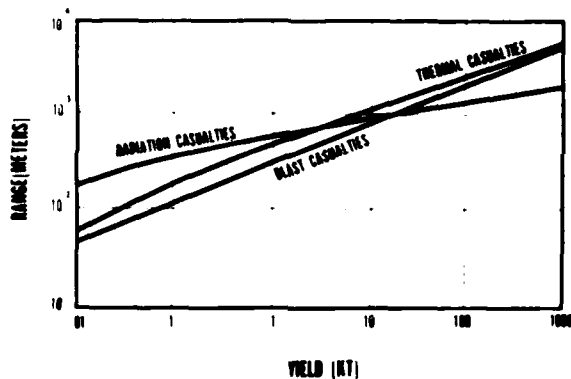


Fig. 7 — Comparison of man's vulnerability to nuclear effects

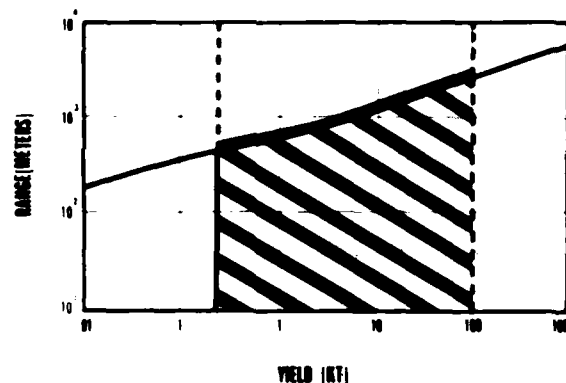


Fig. 9 — Threat constrained governing isocasualty curve

which govern or extend the farthest are determined. This governing isocasualty curve (Figure 8) is then truncated in

Airblast criteria, exemplified in Table 1 include one or more sets of eight parameters each; thermal, nuclear radiation, and EMP criteria are stated in commensurate detail. It is obvious that shock and vibration levels can be high. The equipment seeing this airblast environment could experience accelerations of several hundred "g"s.

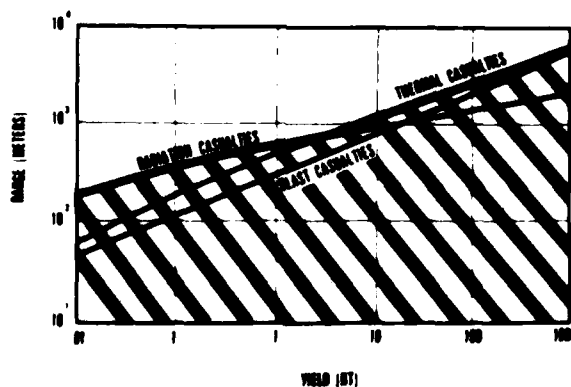


Fig. 8 — Governing isocasualty curve

Table 1 — Example Airblast Criteria

Peak Overpressure	10	PSI
Overpressure Duration	0.53	SEC
Overpressure Impulse	1.8	PSI-SEC
Peak Dynamic Pressure	2.4	PSI
Dynamic Pressure Positive Duration	0.69	SEC
Dynamic Pressure Impulse	0.68	PSI-SEC
Peak Underpressure	1.6	PSI
Arrival Time	1.1	SEC

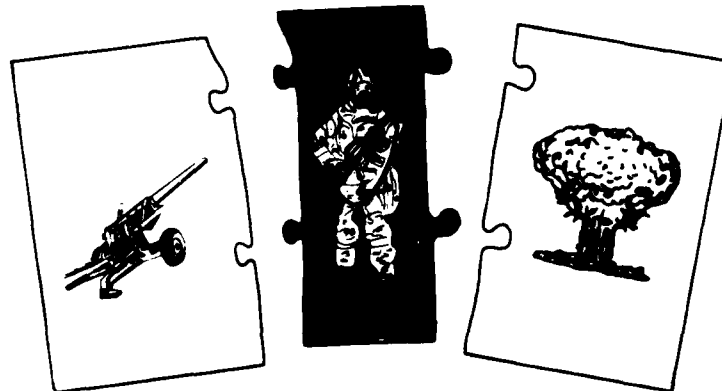


Fig. 10 — The integrated battlefield

Every materiel requirements document now written by the Army includes a statement regarding the need for nuclear survivability; if the item is critical to mission accomplishment and will not exist in sufficient quantities for timely replacement of damaged items, a full balanced set of nuclear survivability criteria will be specified. Critical systems which are high density will have high altitude EMP criteria only. Once these criteria have been specified, only the Army's Nuclear Survivability Committee, a general officer group established by Army regulation, is empowered to modify or otherwise waive the criteria. Experience shows that they have granted only two waivers in the four years of the program, and then only for clearly substantiated technological design, operational degradation, or cost considerations.

Although there are still problems with the nuclear survivability program, particularly in the areas of hardness assurance on the production line and hardness maintenance after fielding, I believe this program to be relatively well in hand. In addition to the Army regulation, other DA policy documents address the nuclear survivability of common use equipment. The Army's Training and Doctrine Command (TRADOC), which acts as the Army's combat developer and requirements writer, has issued excellent implementing regulations. Further, the Army's philosophy, methodology, and data base for developing nuclear survivability criteria have been standardized among the Australian, British, and Canadian forces as QSTAG 244, and among all NATO nations as STANAG 4145. Don't be surprised to see the same detailed nuclear survivability criteria in foreign equipment specifications as you would in US systems!

If we say that the nuclear survivability program developed in the seventies, the analogous program for equipment survivability in chemical warfare environments is emerging in the eighties. Actually, we've named this new program "NBC contamination survivability," expanding it beyond chemical contamination to include biological contamination and residual nuclear (such as fallout) contamination as well (Figure 10).

This program is still in its infancy, although the concept is established and approved to include three major elements: Decontaminability, hardness, and compatibility. We define decontaminability as shown in Figure 11. Even under a

THE ABILITY OF A SYSTEM TO BE RAPIDLY DECONTAMINATED TO REDUCE THE HAZARD TO PERSONNEL OPERATING, MAINTAINING, AND RESUPPLYING IT.

Fig. 11 — Decontaminability

"fight dirty" concept of operations, some minimal degree of equipment decontamination is required. For example, liquid chemical agents can breach the shield of the soldier's protective overgarment in time and they must be removed where they present a contact hazard. To enhance an item's decontaminability, one must, first, consider use of materials which do not absorb NBC contamination and which make easy its rapid removal with decontaminants readily available on the battlefield. Second, one must incorporate designs which reduce or prevent accumulation of NBC contamination and make those areas which are exposed readily accessible for decontamination — in other words, get rid of nooks and crannies. Third, one must employ devices and means which reduce the amount of contamination to be removed, such as positive overpressure systems for combat vehicles, packaging for supplies, and protective covers. Finally one needs to provide space and mounting brackets for installation of NBC detection, measurement, and decontamination devices, which will increase the operational effectiveness of contamination avoidance, control, and removal; and decontamination verification.

The second major element of NBC contamination survivability is hardness, which is defined in Figure 12. In general, most materiel is sufficiently resistant, or "hard," to the effects of battlefield concentrations of NBC contamination — although this cannot be assumed and must be established.

THE ABILITY OF A SYSTEM TO WITHSTAND THE DAMAGING EFFECTS OF NBC CONTAMINATION AND ANY DECONTAMINATION AGENTS AND PROCEDURES REQUIRED TO REMOVE IT.

Fig. 12 — Hardness

Invariably, the greatest damage occurs during the decontamination process. Current decontamination agents are notoriously caustic, removing paint, ruining seals and gaskets, corroding sensitive electronic components and plastics, and even causing structural damage to aircraft. As a minimum, materiel should be hardened to the extent that none of the item's essential characteristics or reliability, availability, and maintainability (RAM) requirements is adversely affected.

Decontaminability and hardness are distinct qualities. Standards for the former are expressed in terms of the residual hazard to man, and for the latter in terms of materiel damage. Nevertheless, there is a strong interrelationship. Materiel high on the decontaminability scale can reduce or eliminate the need for materiel-damaging decontaminating agents and procedures, which in turn reduces the need to harden materiel solely to withstand their deleterious effects. One thus hardens materiel to withstand the decontamination process and selects decontamination processes consonant with the materiel to be decontaminated; the two go hand-in-hand.

The third and final element of NBC contamination survivability is termed compatibility. In this context, compatibility means that the item is capable of being operated, maintained, and resupplied by personnel wearing the full NBC protective ensemble, along with any other required gear. Collective protection may be necessary to enable the crew to operate more efficiently for a critical period of time without the encumbrance of the protective ensemble, or it may be necessary to improve decontaminability by reducing the amount of contamination to be removed. But collective protection, regardless of the system selected, is not a satisfactory substitute for compatibility. Crewmen must frequently exit and enter the vehicle and weapons must be resupplied. NBC contamination will inevitably be introduced into the crew compartment, forcing assumption of a fully protected posture. Compatibility with the NBC protective ensemble is essential.

Thus, for an item to be NBC contamination survivable, it must be rapidly *decontaminable*, *hardened* to withstand NBC contamination and the decontamination process, and *compatible* for use with the full NBC protective ensemble.

Applying the above concept of NBC contamination survivability, the user must then ascertain whether it is required for his system. The rationale is clearcut: if the item is mission essential, it must be NBC contamination survivable. Unlike the rationale for nuclear survivability, neither system redundancy nor resorting to resupply provides a completely acceptable alternative. Once a unit is subject to NBC contamination, the redundant and resupplied items will become contaminated in short order.

This concept for NBC contamination survivability is not only US Army approved, but was also approved in May of this year by the Australian and United Kingdom armies and by the Canadian forces. A draft US Army regulation is currently being staffed to formalize the program at Department of the Army level, which among other things, will give oversight and criteria waiver responsibilities to the same general officer committee which oversees the nuclear survivability program. TRADOC has already published regulatory guidance in this area for its requirements document writers.

Despite these policy documents, the Army does not yet have quantitative criteria for NBC contamination survivability;

existing specifications for decontaminability, hardness, and compatibility are interim and only qualitative. We are moving to develop these quantitative criteria with all possible speed, however. As a result of an out-of-cycle fund request, a contract was let by the Army just last month for a comprehensive study to develop and recommend quantitative standards for NBC contamination survivability, suitable for Army use as criteria. Contract results are due in 11 months time; the study effort is being guided by a group chaired at the two-star level. In addition, a four-nation ABCA special working party has been established to provide Quadripartite inputs to the study during its conduct. Exactly what form these quantitative criteria will eventually take we can't yet say, of course. Perhaps decontaminability relationships will look something like Figure 13. The decontaminability standard then might state that, for a given equipment category, contamination from agent A in the crew compartment must be reducible from level X to level Z in 60 minutes using decon procedure B (level of effort 3).

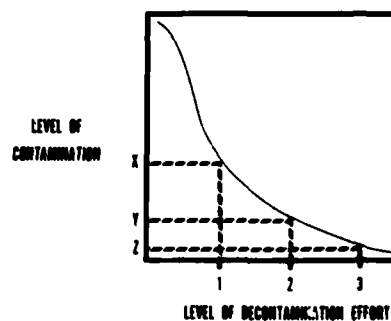


Fig. 13 - Decontaminability Standard

A hardness relationship might look like Figure 14. Since materiel is usually more susceptible to decontaminants than to the chemical contamination itself, the standard might require that RAM not be degraded below level Y after the equipment undergoes level of decontamination effort 2.

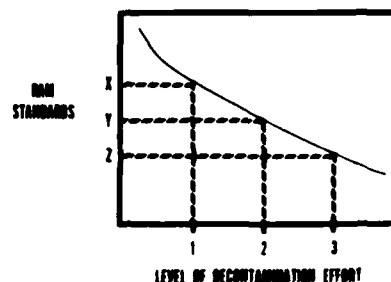


Fig. 14 - Hardness standard

And a compatibility relationship might be expressed as in Figure 15. In this case, the standard for a weapon system might require that system kill probability against enemy threats not be degraded below a certain value if the system operating crew is in mission oriented protective posture 4.

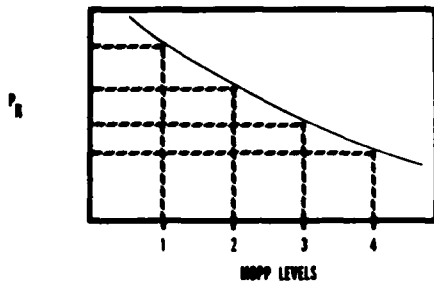


Fig. 15 -- Compatibility standard

Only time will tell exactly what form these criteria will take. What is certain, however, is that the Army will shortly latch on to another piece of the survivability puzzle by stating some form of quantitative criteria for NBC contamination survivability in requirements documentation for mission essential equipment.

Now I have briefly described three aspects of equipment survivability on the integrated battlefield. It was obvious, I'm sure, that these three programs were conceived and developed independently and at different times. Certainly they are each in a different state of maturity. But despite this historical difference, we can no longer afford to consider them independently because there are too many possible synergisms when designing equipment to survive these integrated environments. We know, for example, that increasing blast and thermal survivability concomitantly increases durability and other RAM-related characteristics. We have hard data which show that increasing the radiation shielding characteristics of tanks also significantly improves protection against conventional munitions. On the other hand, we realize that externally mounted collective protection components retrofitted to existing signal shelters are blown away at airblast levels significantly below those which the shelter itself can withstand.

We've already taken the first few steps toward integrating equipment survivability. As I mentioned earlier, one Army high level committee will oversee both the nuclear and

NBC contamination survivability programs. In addition, TRADOC's regulatory guidance on the two programs is integrated in one publication. The first system for which an attempt has been made to integrate the requirements is currently going through the experience -- with all of the anticipated growing pains. This system, the Hardened Army Tactical Shelter, has the conventional fragmentation requirement of stopping a 60 grain 500 meter/sec fragment, nuclear survivability criteria corresponding to 10 psi overpressure, the NBC contamination survivability requirements that include a collective protection overpressure system. Building these requirements into a shelter at an affordable cost and at a bearable weight is a real challenge -- but will provide information and lessons learned for integrating the equipment survivability requirements for future systems.

You, who are the developers and designers and testers of Army equipment for the integrated battlefield, will be directly charged with responsibilities for integrated survivability -- and finally putting this puzzle together (Figure 16).



Fig. 16 -- The integrated battlefield

NAVAL OPERATIONS IN A NUCLEAR ENVIRONMENT

Capt. Donald Alderson
Theater Nuclear Warfare Project Office (PM-23)
Department of the Navy
Washington, D.C.

Doctor Sevin is entirely right, we are brand new. We were chartered on 20 June 1981, and since then we have been bringing our staff on board. I would like to acquaint you with the initiatives that have recently been taken in the Naval Material Command and the way we intend to approach our responsibilities to improve the Navy's survivability posture.

The Theater Nuclear Warfare Project Office (PM-23) has a three-fold responsibility: modernize the Navy's theatre nuclear weapons stockpile, oversight management responsibilities for survivability and combat effectiveness, and rebuilding the Navy's technology base to support these two efforts.

The Charter responsibilities for survivability and combat effectiveness run along classical lines. The organization we have structured for it is a classical Naval Material Command matrix management operation. The project manager is established as a Rear Admiral's billet. I am the acting Project Manager at the present time. We plan to have 51 people in this organization in the 1983 fiscal year. We have 18 people on board now, and virtually all major positions, except for the technical director, have an incumbent.

I want to talk about several dimensions of the approach to survivability. First, and perhaps the greatest importance is for the Navy to consider those problems that will affect its combat readiness, even though we are not directly attacked — the very long range effects.

Communications black-out is a classical phenomenon with the Navy's requirement for very long haul communications in many cases; it can affect us, but we can probably compensate for it. Water waves, flash blindness, fall-out and satellite problems also affect the combat readiness of the fleet. Other local effects exist. Air blast predominates in our thinking, not to the exclusion of any other threats, but it is our biggest problem as we consider all of the local threats. This is to illustrate a point that pertains to new construction. There is a price to buy in on hardness with respect to any one threat, almost irrespective of the level selected. There is a reasonably gradual and orderly growth from one level to the next, and at that time other effects begin to predominate, and costs tend to sky-rocket. We think we know where the break-points are.

Another assessment and hardening program is the FAANTAEI program which is a cooperative program with DNA. The object is to assess the hardness of the F/A-18 and several other classes of aircraft. We have a survivability improvement program to explore functionally hardening

some communication links to EMP on 51 classes of ships; we will also explore "cheap kill" hardening from conventional weapons. We have a start next year on a C³-EMP survivability program and another new start next year on the non-EMP survivability of aircraft resulting from those effects of nuclear detonations other than EMP. These are thermal and air blast.

This is how we will approach the program. First, we will focus on the mission critical functions within the context of these several survivability parameters; then we will consider all aspects of survivability. What can active and passive defenses contribute? Are there operational procedures that mitigate the consequences? Fleet spacing is an example. We have finally answered all of those questions; then what must be done to harden platforms and equipment? Once the decision is made to harden for improved survivability, then I think our general approach will be similar to the Army's approach which Dr. Davidson described. We will establish hardening criteria, negotiate the waivers, monitor the implementation of hardening, verify effectiveness by test, (the big problem is that we do not have a final exam for our program managers), and assure attention to life cycle surveillance and hardness maintenance.

New construction is another facet of the hardness problem. There we have a chance to "get in at the keel". We can implement hardness at the platform level, and we should be able to cover all vital operational functions; it seems to be cost effective, and it should minimize validation and maintenance problems.

Major functional retrofits are still another facet of the hardness problem. The model that we will use is the back-fitting of the TOMAHAWK Cruise Missile into the DD963 class destroyers. It will be a major functional retrofit, and even though we may not be able to provide hardness assurance for the total platform, we intend to provide hardness for that single function. That is, we want to get off a planned TOMAHAWK strike irrespective of the nature of the damage to the rest of the ship, provided it is still afloat and it can provide electrical power.

It has been said that if you want to look at the US Navy in the year 2000, go down to Norfolk and look at it. A large fraction of it is there. It has been a problem getting survivability built into the Navy. Many have asked, "Why should I do it for my ship class when the rest of the Navy will be soft?" We need to focus on vital functions, consider the cost and life remaining and do what we can.

Another problem in hardening shipboard systems is they tend to be reasonably large, very concentrated and quite complex. When a ship is built, the builder provides essentially the ship, its propulsion and many of the combat systems. On the other hand, much of the vital material is government-furnished equipment; it is either "off-the-shelf" or it is procured under a totally different system: getting hardness specifications into the government-furnished equipment is a real challenge to us, and we believe it will take a long time.

We also need to do something for the existing fleet. About a half year ago CINCLANTFLT asked us what we can do if we have some warning that a nuclear attack may be imminent. Or if a nuclear attack occurs, what can we do after the fact to rapidly reconstitute our capability. We have teams out in Norfolk now doing a quick assessment. We hope to come up with damage control procedures or readiness procedures to either mitigate or help reconstitute our capability after an attack. This is principally toward these far-reaching effects.

We are setting out to do this job now, and it is challenging. The structure we must develop, however, will involve

several organizations. The Chief of Naval Operations staff is responsible for setting requirements. The platform sponsor within the Chief of Naval Operations makes the money available. The system manager who will actually build the platform, be it ship or aircraft, is also involved. PM23 is the "broker" with the nuclear expertise operating in the midst of this group of people. We have to find out how the controls are defined. Are they fiscal controls? Are they procedural controls? Is it a system such as the Army uses of a flag officer and a general officer board that must pass on waivers and accept the criteria, undefined for us as yet? Whatever it is, it must control the waiver process.

We must do better. Nuclear survivability must get into the core of all programs. And finally, we must rebuild the Navy's technology base in the nuclear weapons effects areas in the Navy's laboratory structure. Constraints exist on Program 6 funds within the Navy. We had fairly decent programs at one time, but we have a thirty percent cut in Program 6 funds. We need to use seed money in the systems development community to encourage consideration of survivability. And finally, we believe DNA can and will help us if the Navy program is well-supported.

SURVIVABILITY OF REQUIREMENTS FOR FUTURE AIR FORCE SYSTEMS

Dr. Henry F. Cooper, Jr.
Deputy for Strategic and Space Systems
Office of the Assistant Secretary of the Air Force for Research & Logistics
Washington, DC

The President's strategic package, announced on October 2, proposes the most comprehensive program for strategic force modernization since the Eisenhower years. It is composed of:

- C³I systems to assure communications with our strategic forces, even after nuclear attack,
- Modernization of our TRIAD of bombers, SLBM's, and ICBM's, and
- Improvements in Strategic Defense.

Major portions of four of these five mutually reinforcing elements of the strategic program will be implemented by the Air Force, and will be the subject of my discussion today. But, first, a word or two on the policy which motivates these proposed programs.

The intent is for these strategic improvements to greatly strengthen deterrence of nuclear war by denying the Soviets any realistic prospects, however, they may define them, of gaining an advantage by initiating the use of nuclear weapons. As noted here, deterrence remains the centerpiece of our strategic policy. However, the evolving strategic realities of the last 10-15 years have led to serious doubts of the adequacy of our concept of Mutual Assured Destruction (MAD) in providing a stable deterrent. These doubts have led to a monotone evolution of national policy over the last 10 years, as enunciated in public explanations of NSDM-242 and PD-59, toward emphasis on trans- and post-attack endurance, the ability to maintain effectiveness over a wide range of options during a protracted war, the ability to deny coercion at any stage of conflict, and the capability to administer the ultimate punishment if necessary. In other words, the trend is toward developing an apparent war fighting capability, rather than relying upon the threat of nuclear punishment for deterrence. Survivability and endurance are obviously key attributes of strategic systems responsive to this evolving policy intended to support a protracted conflict in which nuclear weapons are used.

In response to this evolving policy, the President's program stresses survivability and endurance of our strategic forces and their supporting C³I, and the ability to hold at risk targets of strategic value to the Soviet Union. I will return to this point as we discuss each of the Air Force components of the strategic package.

Over the past decade we have developed impressive C³I capabilities for peacetime use. However, we have not made these systems as survivable as we would like, nor have we provided a reliable post-attack C³I system. Thus, the President's package assigned the highest priority to improvements in our warning systems, command posts, and communications links, including the development of post-attack reconstruction capability to assure enduring C³I. These improvements are intended to ensure that we can effectively employ our nuclear forces throughout all stages of conflict, which is essential to our maintaining a credible deterrent.

Modernization plans for our warning systems include PAVE PAWS surveillance radars to detect SLBM launches, OTH-B radars and additional AWACS aircraft to detect airborne threats, satellite improvements to provide better missile warning, and mobile ground terminals to improve the survivability and endurance of satellite warning and communication systems.

We plan to upgrade the survivability and operational capability of the E-4B and EC-135 airborne command posts. Improvements include increased hardening to EMP effects and upgraded satellite and LF/VLF communication capabilities. Alternate survivable command posts, such as ground mobile command posts and deep underground posts, will also likely be considered.

Improvements in the communication links include a 500 node LF communication network to provide high confidence trans- and post-attack communication capability. This multiple-aimpoint system will be coupled with new LF/VLF mini receivers for the bombers to ensure their timely reception of execution orders. As mentioned above, mobile ground stations will also provide enduring capability. Finally, a vigorous R&D program leading to the capability to reconstitute an enduring C³I system will be undertaken. It is hard to make systems survivable in the face of highly accurate threat weapons which are capable of destroying any target that is identified and located. Thus, to assure systems that remain capable post-attack, we are compelled to think of ways of reconstituting capabilities . . . including forces, C³I, and logistics support.

As has been recognized for at least a decade, improvements in Soviet ICBM accuracy have led to the situation where our land based ICBM's are potentially vulnerable to a Soviet first strike. The Air Force's preferred response to this

threat, evolved over a like period of time, was to deploy the MX Multiple Protective Structures (MPS) system. However, after a review of basing alternatives, the President decided to reject the MPS system and to seek alternative more survivable basing modes for the MX missile. A decision was made to proceed with full scale development of the MX missile and to deploy it in either upgraded Minuteman or Titan silos until a more survivable basing mode is selected and deployed. The MX missile will provide the U.S. the capability of holding hardened Soviet systems at risk, and hopefully will motivate them to spend money to rebase their ICBM's in a more survivable basing mode. The current program calls for an intensive evaluation of three basing alternatives: (1) a Continuous Patrol Aircraft (CPA) which is intended to fly on continuous airborne alert primarily over ocean areas; (2) the development of a deceptively based Ballistic Missile Defense (BMD) which would be employed to defend the silo based MX (and Minuteman missiles); (3) deep underground tunnels which would provide survivable storage of a secure reserve force. The present program calls for a selection between these three alternatives by 1984.

The technology requirements of interest to this audience for the CPA and BMD are essentially the same as those considered previously for similar systems. On the other hand, this is the first serious study of the engineering feasibility of deep basing, and consequently, the program provides opportunities for novel developments. The deep basing concept assumes that missiles are stored at various points within an extensive tunnel complex a couple of thousand feet deep, preferably in mesas where horizontal tunnels can be drilled from the inside out, commencing at any time from immediately following the attack until perhaps a year after initiation of hostilities. Thus, there are requirements not only to survive severe shock and vibration of the direct attack, but also to provide for the continuing operational capability, in an uncertain post-attack environment, of a self-contained manned system over an extended period of time. Important technical issues requiring study also include the development of more rapid egress than can be accomplished with normal drilling procedures, and development of a means to avoid detection on drillout.

In addition to these basing modes which will be considered for deploying the MX, we expect to continue our investigation of alternate ICBM's and basing modes for future deployment. For example, smaller ICBM's, which might more conveniently be based in mobile or other deceptive ways, will be considered as a part of the Advanced Strategic Missile System (ASMS) program.

The U.S. must depend heavily on the survivability of our bombers (and sea based forces) in the 1980's while we take steps to improve the survivability of our land based missiles. Furthermore, the bomber is perhaps the most flexible and potentially enduring of our strategic forces. It can be launched and recalled, can serve as a launch platform for stand-off missiles (such as ALCM's) against fixed targets of known location, can be employed against targets of imprecise location, and can be recovered, reloaded and launched again. The President's plan calls for improvements to the B-52, purchase of 100 B-1 variants in the late 1980's, and the development of an advanced technology (Stealth) bomber (ATB) in the 1990's.

Survivability improvements of the B-52G and H force, which will be used as an ALCM launch platform into the 1990's, include EMP, blast and shock and ECM upgrades. The older B-52D's will be retired in 1982 and 1983. The 100

B-1's, the first squadron of which will be delivered by 1986, will be capable of delivering ALCM's in a stand-off mission, or of penetrating Soviet Air Defenses into the 1990's, and will have reload and multimission capabilities in protracted conflict scenarios. R&D will continue on the ATB which, under current plans, will be deployed in the 1990's.

Over 3000 ALCM's will be deployed on the B-52G's, B-52H's, and B-1's. The first squadron of B-52 ALCM carriers will be operational in 1982. KC-135's will be re-engined to increase airborne refueling capabilities.

Finally, I would note that in our efforts to ensure the capability of the bomber to play an important role in protracted war scenarios, providing enduring logistics support is a major technical and management challenge.

While there are no major new shock and vibration challenges offered by these developments of the Air Breathing leg of the TRIAD, the substantial modernization program clearly will provide the motivation for improving the quality and efficiency of the already well established technical base in this area.

We have virtually ignored strategic defensive systems for a decade. As a result, we have large gaps in radar coverage provided by the North American Air Defense Warning Network, our strategic air defense interceptors are obsolete, and our anti-satellite and ballistic missile defense programs have lagged behind those of the Soviets. The President's program takes the first steps toward restoring credible strategic defensive forces. It provides for upgrading the North American air surveillance network in coordination with Canada. The plan includes some combination of over-the-horizon backscatter (OTH-B) radars, AWACS aircraft, and improved versions of the ground radar systems that exist today. It also calls for replacing the aging five squadrons of F-106 interceptors with new F-15's. The additional AWACS aircraft will augment the ground based radars in peacetime and will provide surveillance and control for interceptors in wartime. We are also developing operational concepts by which warning and air defense capabilities can endure in a protracted conflict involving nuclear weapons.

We also plan to continue to pursue an operational anti-satellite system as a counter to the capability already demonstrated by the Soviets.

As mentioned earlier, the President's program calls for a vigorous research and development program on ballistic missile defense. The Army has the lead in pursuing alternatives that represent evolutionary improvements over BMD concepts of the past. The Air Force will, of course, integrate its programs with the Army's activities in order to assure effective coupling to BMD should that be the selection for improving the survivability of the land based ICBM's in 1984. In addition, the Air Force will be conducting research on space based lasers which might be viewed as a long term potential solution for ABM.

Finally, it is noted that civil defense is getting a boost and the Defense Department will be exploring new program alternatives in coordination with the Federal Emergency Management Agency which has the lead in the civil sector.

I would like to close my discussion with a few comments of a general nature. These thoughts will reflect not only my recent experience which has given me a broad view of Air Force strategic systems, but also my previous more

narrow background derived from my study of the survivability of strategic systems to nuclear blast and shock effects.

There is a continuing need to specify the best possible predictions of the nuclear environment and associated system response. Of particular interest are improved low-over pressure contours which might affect our estimates of aircraft safe escape; the dust environment as a function of time following a major nuclear attack which may affect the endurance and operational capabilities of various airborne systems; close-in high intensity nuclear environments important to estimates of silo hardness and deep underground system design. Of course there is the continuing requirement for improving our theoretical models for system response to nuclear effects. Given the lack of direct nuclear experience for many cases of interest and the unlikely possibility of future nuclear testing experience, there will be a continuing need to develop improved simulation test capabilities for use in the design and validation of systems. Finally, given the uncertainty inherent in this entire process, there is the need for the designer to be as creative as possible in designing to avoid surprises; that is, to design around potential but unknown problems.

Too often (in my view) the designer exercises great creativity in minimizing the cost to design to specifications that are given with great precision but which are inherently inaccurate due to uncertainties in specifying criteria. No place is this more evident than in designing systems to withstand nuclear effects where the uncertainties are often

not appreciated. Such initiatives to minimize cost have on some past systems severely constrained the ability of later designers to cope with improvements in the accuracy of the nuclear criteria, except at great expense. This classical design approach then can put us in the situation of being pennywise and pound-foolish. I would recommend that designers seriously consider innovative developments that provide growth capabilities at the margin where criteria are recognized as being very uncertain and where future research might substantially change current estimates. Similarly, it may be worth paying a little bit more for hardening technologies which provide assurance that systems can be maintained in a hard configuration. Here, specifically, I am thinking of various shielding approaches to the hardening of electronics to EMP effects whether they be aboard aircraft, satellites, or on ground equipment. It often does not cost much to design in hardness initially, but we pay dearly to retrofit.

As noted previously, there are few new requirements for shock and vibration breakthroughs. On the other hand, the several major strategic program initiatives will undoubtedly assure the continuation and enlargement of research, development and testing activities of interest in this community. We solicit your active support to improve the quality, efficiency and survivability of Air Force strategic systems.

Thank you for your kind attention.

NUCLEAR HARDNESS VALIDATION TESTING

Dr. Edward Conrad
Deputy Director (Science and Technology)
Defense Nuclear Agency
Washington, D.C. 20305

It is a real pleasure for me to be here today. Although we do many things at the Defense Nuclear Agency (DNA), I really consider the most important part of our work to be technology transfer. It is meetings such as this, where that technology transfer takes place. I am gratified that the speakers who preceded me this morning talked about what I am going to discuss. I feel it is very important that our Agency should be in tune with the needs of all of the Department of Defense. Each of the speakers you heard this morning is a close friend and colleague and I feel a strong responsibility to support them in the requirements they stipulate.

The first figure (Fig. 1) paraphrases the DNA research and development mission and identifies the organizations with which we interact. DNA is the corporation memory and the conscience of the DoD nuclear weapons effects data base and expertise. In this area, we conduct all underground nuclear tests on nuclear weapons effects and we coordinate the research among the DoD Laboratories. The Director of DNA reports to Dr. DeLauer, the Under Secretary for Research and Engineering, and also to the Chairman of the JCS since DNA manages the logistics of the nuclear stockpile as well as conducts nuclear weapons effects research.

Figure 2 shows some examples of the range of our activities. Everything you heard this morning from the previous speakers appears somewhere on this chart. Figure 3 categorizes the activities we address in terms of strategic, theater, enduring C³, biomedical and physical security. In the strategic systems our efforts include nuclear hardening survivability for land based missile systems including the EMP effects — that is the electromagnetic pulse that arises from exoatmospheric nuclear detonations. We also explore options for basing, such as secure reserve force, and consider concepts for survivability in situations such as protracted warfare. DNA is also intimately involved in the modernization in our theater nuclear forces. We provide research that supports the Office of Secretary of Defense in the High Level Group deliberations with our NATO Allies on the modernization of forces in Europe such as the long range forces, PERSHING, GLCM. We support the Navy in exploring problems of Maritime Theater Nuclear Warfare. DNA is concerned with the endurance of our command, control, and communication systems and we do research on how to provide survivability and protection to these systems. This not only includes the land lines but also satellite communications and effects on the ionosphere that occur directly by exposure to nuclear detonations. With this brief overview of the DNA activities, I will now give you examples of many of these programs in a technical discussion of the DNA efforts — especially in the areas related to the subject of this symposium — shock and vibration.

In the days of atmospheric testing, we defined many of the environments that are created by a nuclear detonation. We tried to learn as much as we could in those days about blast, ground shock, thermal radiation and nuclear radiation such as the gamma radiation and the neutrons that emanate from a nuclear weapon.

At high altitude there are ionization effects that occur in the ionosphere and at the high altitudes the rarity of the atmosphere makes the threat from the x-rays that emit from the nuclear weapon something that has to be addressed.

One example of these atmospheric effects is the STARFISH EVENT that occurred in 1962. It was a detonation that took place at 400 kilometers in altitude. The ionization occurred over a very large volume in space. This disturbance — this ionized region — was five to ten thousand kilometers in length and several thousand kilometers wide. I will return to the significance of this later on in my talk. Numerous events occur when a nuclear detonation takes place at high altitude. These are shown in Figure 4. When the radiation from this detonation strikes the upper edges of the atmosphere, it releases a charge and as this charge moves in the magnetic field of the earth, it develops an electromagnetic pulse that can move down to impinge on the surface of the earth. This is what we refer to as the EMP threat to communications and other ground systems on the surface of the earth. The x-rays from this detonation can move out to very great distances striking space objects such as satellites, reentry vehicles, or missiles. When the x-rays strike a satellite, they release a charge from the surface of the satellite and this creates a phenomenon referred to as system generated EMP (SGEMP). This effect can be highly damaging to satellites and we do investigations to learn how to characterize this effect and mitigate it.

A collection of photographs of the various testing programs DNA has conducted to simulate nuclear weapons effects is shown in Figure 5. Obviously, we no longer do atmospheric nuclear testing and so we have to provide means by underground nuclear testing or above ground simulations to learn more about these effects on our systems.

DNA conducts experiments to investigate the effects of the nuclear ionization when weapons are detonated in the atmosphere. This is shown schematically in Figure 6. We simulate this effect by the use of barium which is released at high altitudes and monitored by sending up sounding rockets in order to learn more about the chemistry that takes place in the environment. We also do transmission experiments during this test in order to evaluate the effect of these striations in producing disturbances on satellite transmission.

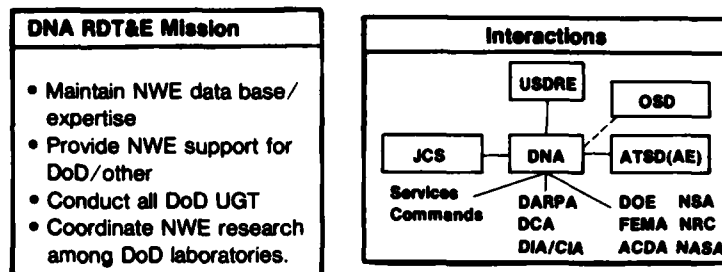


Fig. 1 — Introduction

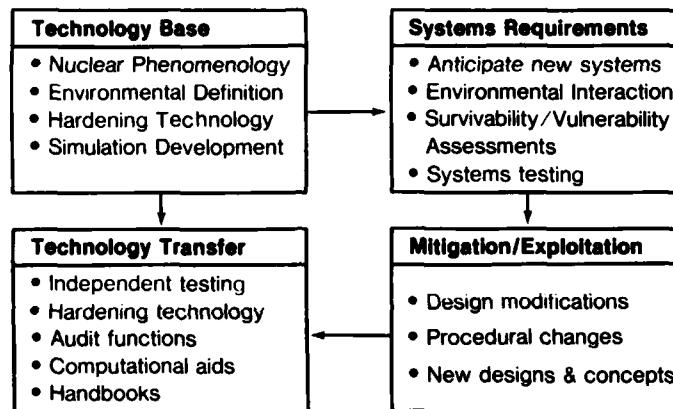


Fig. 2 — Range of DNA activities

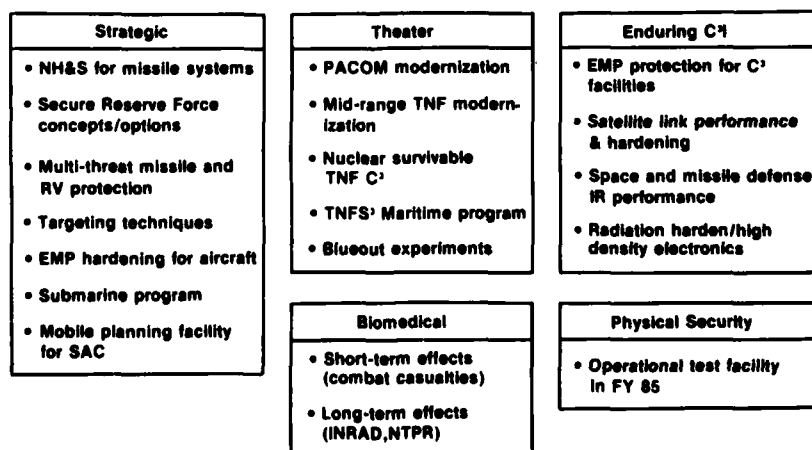


Fig. 3 — Major RDT&E activities

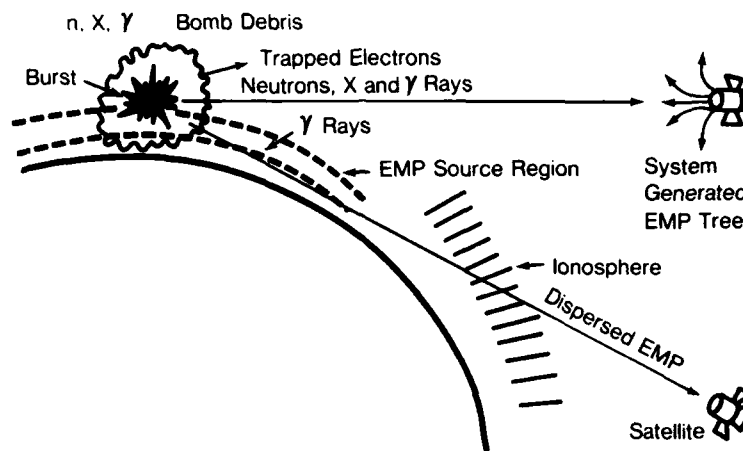


Fig. 4 — The nuclear environment

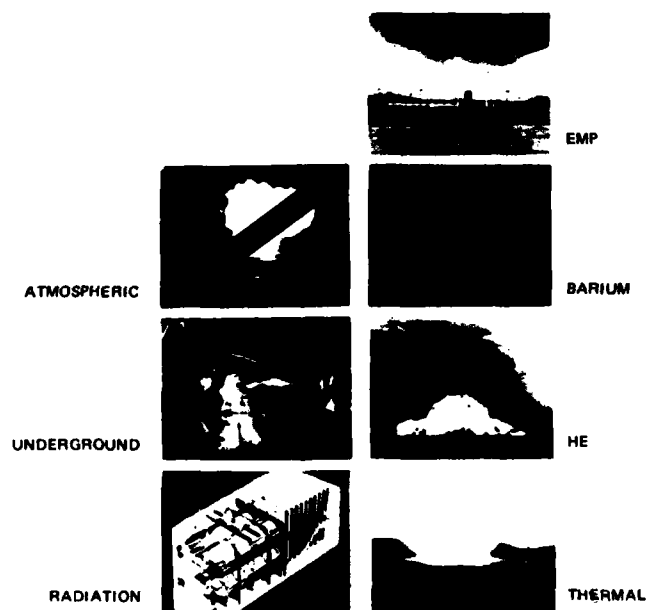


Fig. 5 — DNA testing program

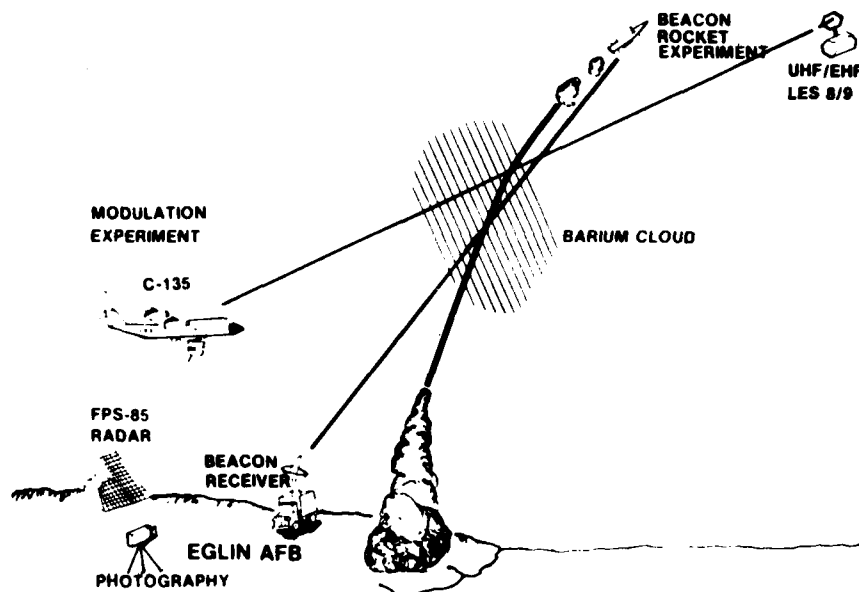


Fig. 6 — Placer experiment

As we propagate signals through it, we characterize this disturbance on our communications, and develop codes for use in simulators as described on Figure 7. In this sort of simulation we can use the transmitter receiver and the simulator on the ground to perform experiments to learn how to properly modulate and key the signals to optimize the propagation through the disturbed medium. Detonations that occur in space not only produce disruption in communication, but they also create an infrared background. Infrared is used for many applications and it is important to understand both the natural background and that created by the detonation.

In Figure 8 we see a test being performed on an aircraft to assess the effects of EMP. The object above the aircraft is an EMP simulator that develops an electrical pulse similar to that which would be seen from a nuclear detonation and which provides a threat level electrical field. By repetitive pulsing and continuous instrumentation monitoring at many points within the aircraft we can characterize what the EMP disturbance will be. One way to characterize the effects of exoatmospheric radiation on satellites which produces system generated EMP, the SGEMP effect I told you about a moment ago, is to use an underground test.

Figure 9 is a sketch of a test that was done sometime ago called HURON KING in which we examined the effects of x-rays on a satellite-like model. A vertical hole was drilled in the ground to a depth of about 1,000 feet and a nuclear device was placed at the bottom of this hole. The trick of this experiment is to let the x-rays come up this pipe and impinge on the satellite-like model and then choke the pipe off to prevent any debris from being released. You will notice the trailers that contained extensive instrumentation which recorded the satellite-like object response during the exposure. An enlarged view of the chamber that contained the satellite model is shown in Figure 10. This chamber had to be used to provide a background, in other words, an environment, to make the satellite think that it was truly in space. You will notice that there are tracks under this chamber and their purpose is illustrated in Figure 11. This is a post shot photograph of the experimental area showing what happened after

the detonation. The large crater you see occurred because after the detonation takes place, a large cavity is formed at some depth below the ground and as the earth ultimately collapses into that cavity, a crater results. As a matter of fact you can see some other craters in this photograph from previous shots. Obviously we didn't want to lose the experimental chamber and the test model and so it was pulled away from ground zero prior to time when the ground subsidence occurred. We were interested in recording the response of the model, not only during the detonation, but for some considerable time thereafter. For this reason care had to be taken to shock isolate the model within the chamber and you will hear a presentation on how this isolation was accomplished later in the meeting.

I would now like to return to a consideration of the airblast and ground shock mechanical effects and Figure 12 illustrates the nature of the problem. It is necessary to consider the combined effects of cratering, the direct induced stress wave and the airblast when evaluating ground shock. The airblast loading which induces ground shock also directly applies a dynamic overpressure to objects on the surface which is complicated by multiburst effects, reflection factors, and drag coefficients for the airburst and structural configurations being considered.

Figure 13 is an aerial photograph of a test called MISERS BLUFF that was performed to gain information on airblast and ground motion effects on a proposed siting configuration for the MX system. This test was conducted to explore what the effects would be on a basing shelter of a missile if the six nearest neighboring shelters were simultaneously targeted and introduced the complications of multiburst phenomena in airblast technology. This test was performed by the use of six one hundred and twenty ton high explosive shots and in this experiment we were able to learn how the effects from the six shots could be summed to determine the vulnerability of the central shelter. In support of MX, we have also done experiments to help in the base line design of the various shelters considered.

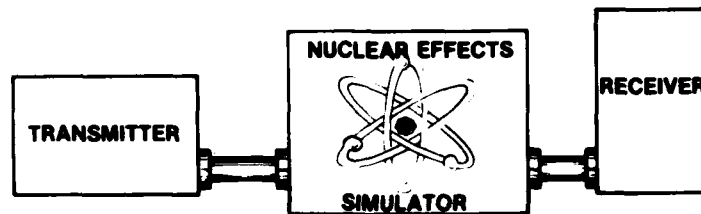


Fig. 7 - Simulator

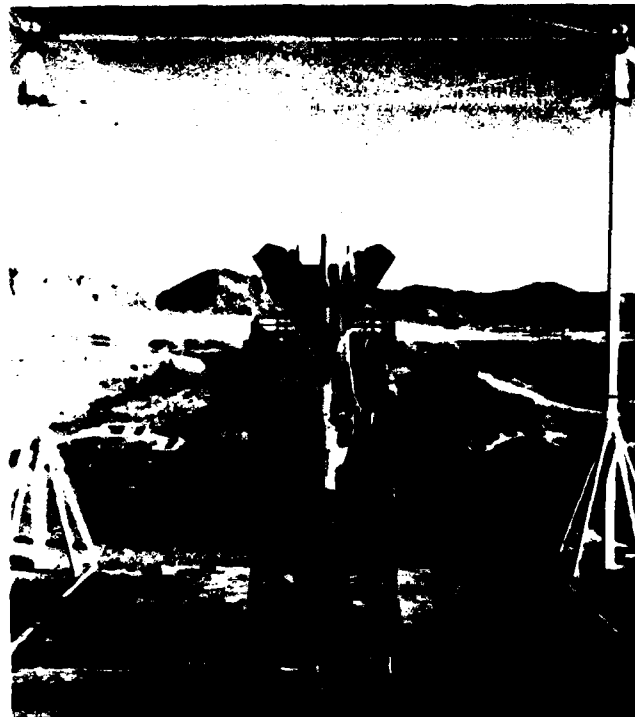
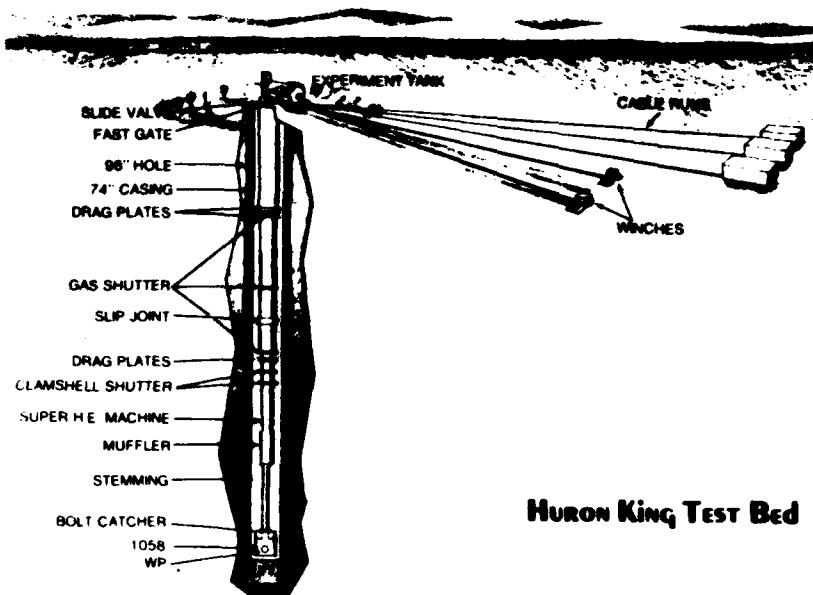


Figure 8



HURON King Test Bed

Figure 9

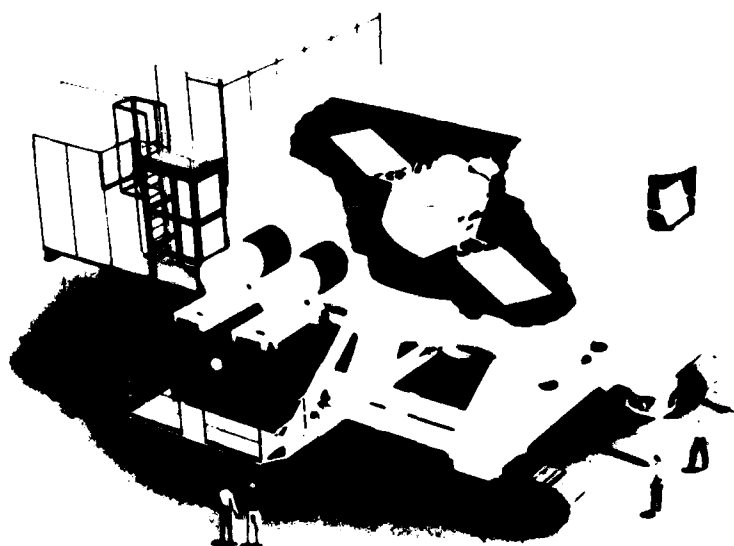


Fig. 10 — Huron King experiment configuration

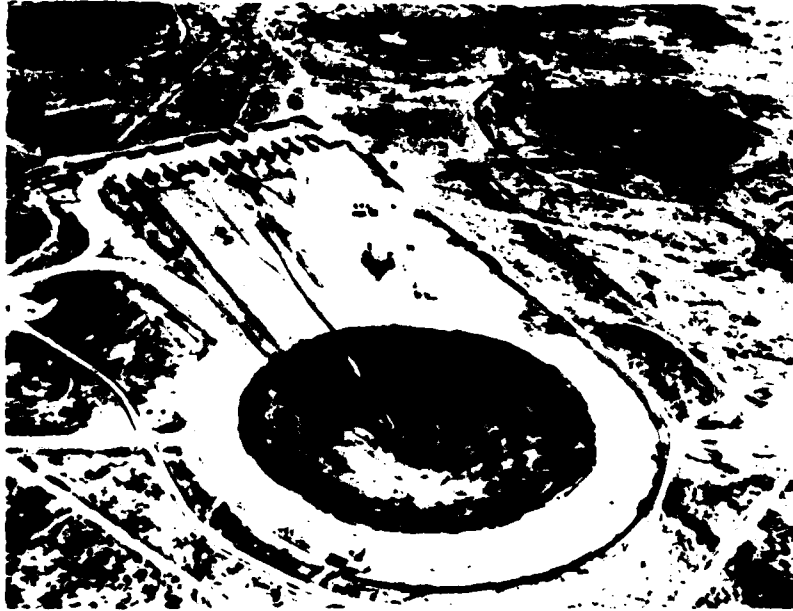


Figure 11

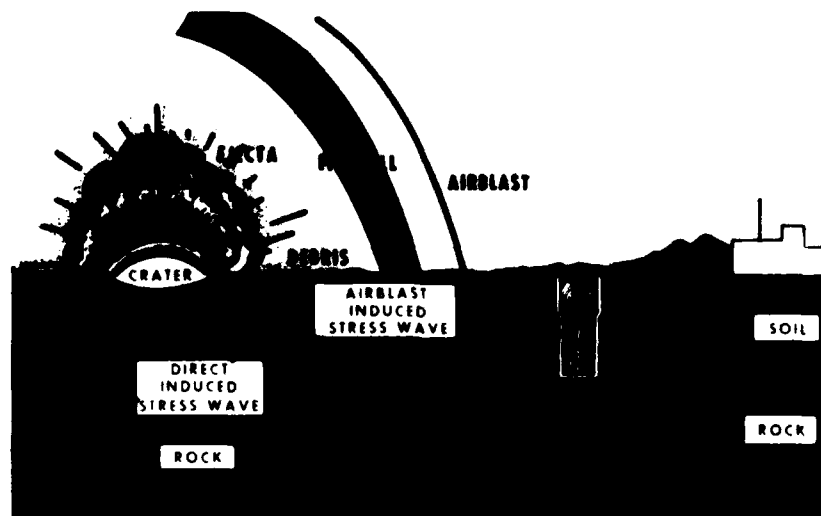


Fig. 12 -- Nature of the problem

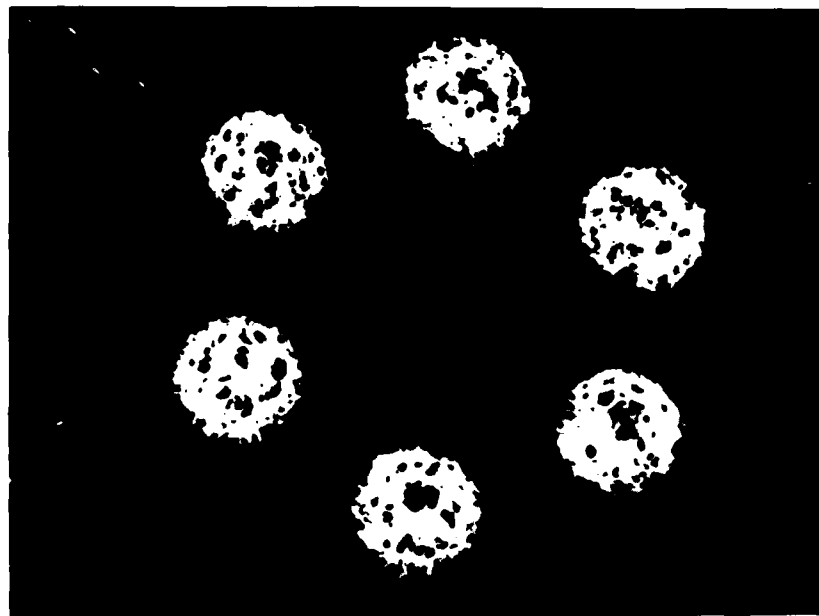


Figure 13

A model horizontal shelter in which we used a dynamic airblast simulator to assess the integrity of the door and overhead structure is shown in Figure 14. The dynamic airblast simulator is composed of a containment structure with an earth berm placed over it to improve the containment and properly shape the airblast so that physical measurements can be made to monitor the response of the shelter. Figure 15 is a photograph taken during the detonation of the HE charge. A post shot photograph of the shelter is shown in Figure 16 and illustrates that certain design changes had to be made before development could go further.

The features of the MX missile and the corresponding nuclear weapon effects threats are described in Figure 17. DNA has been working closely with the developers of the cruise missile to address such issues as blast and thermal effects on the airframe and propulsion system. We have performed experiments in which a model of the cruise missile was placed on a sled and driven past a high explosive charge to make blast measurements on the structure.

DNA is engaged in programs of cooperation with the Navy to learn more about how to harden submarines and surface vessels against the effects of underwater shock. A photograph (Figure 18) of an experiment that was done actually several years ago to learn what the effect underwater shock from a nuclear detonation would be on a submarine hull at depth. This is a one third scale model with stiffeners of a section of the submarine hull and it was tested at a depth of 2500 feet with HE. At that time, this was supposed to be a success oriented experiment and of course the hardness of this hull section had been computed with what were then contemporary analytical codes. You can see the experiment was not a resounding success. We had learned that the codes were deficient in accurately predicting the susceptibility of this section. Since that time the codes have been revised to provide a more accurate prediction of the survivability of our submarines.

A one fifth scale model of the notional submarine shown in Figure 19 is being used in a cooperative program between NAVSEA, United Kingdom, and DNA. The model is actually provided by the British. Using this model we can do underwater shock tests to learn more about the elastic response of the internal equipment to simulated nuclear loading. An illustration of the USS ARKANSAS — a nuclear propelled guided missile cruiser is at Figure 20. DNA and the Navy are preparing to do some underwater shock tests on this vessel to better characterize the mechanical response of the reactors and the cruise missile launcher in the environment of underwater detonations.

To address the effects of airblast on tactical equipment DNA periodically performs high explosive tests at the White Sands Missile Range. Figure 21 is a typical layout of such a test where the explosive charge is located at ground zero and various forms of tactical equipment, communication shelters, vehicles, weapons systems, naval deck structures, are set out at various distances and instrumented to determine their response. These tests very often have international participation. The high explosive charge in Figure 22 is being assembled at ground zero. This is typical of the recent MILL RACE and the preceding DICE THROW high explosive events. This is a stack of 628 tons of ammonium nitrate fuel oil explosive. The 628 tons is used to simulate the effect of a one kiloton nuclear detonation.

Figure 23 is a photograph of the DICE THROW event taking place. I show it to illustrate that it really does work, also to illustrate another interesting feature which appears in the photograph which is the shock wave that precedes the explosion gas cloud.

Post test photographs (Figure 24) show the blast effects on some of the equipment in the test. You also note that there are manikins lying about — those aren't real people, those are experimental manikins to learn more about the



Figure 14



Figure 15

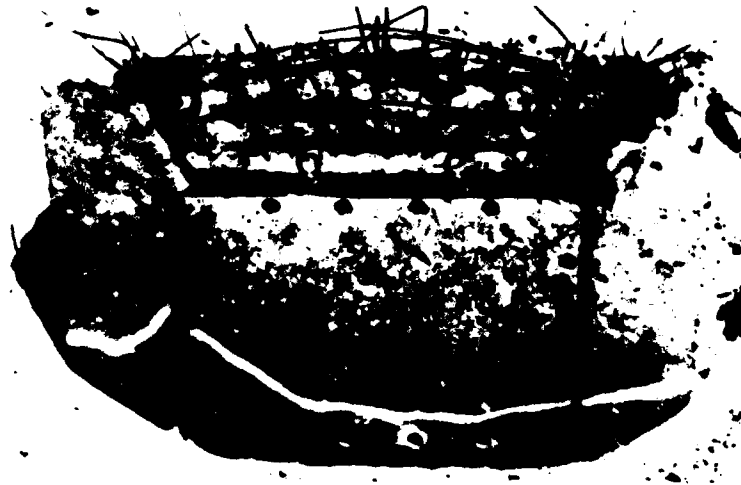
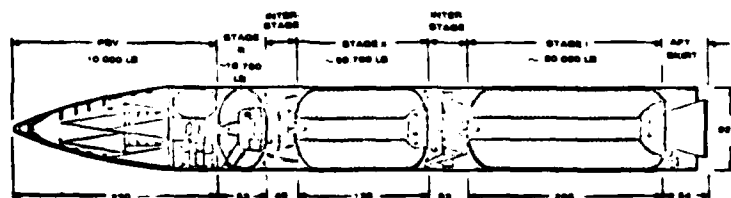


Figure 16

MX Vehicle



X-Ray Effects:

- Electronics (SGEMP/SREMP)
- Propellants
- Shroud Materials
- Booster External Protection
- Stage IV (PBV)/External Protection Interface

Thermal Effects:

- Booster External Protection

Dust/Pebbles Effects:

- Booster External Protection
- Booster Stages
- Shroud Materials

Fig. 17 - Nuclear hardness technology



Figure 18

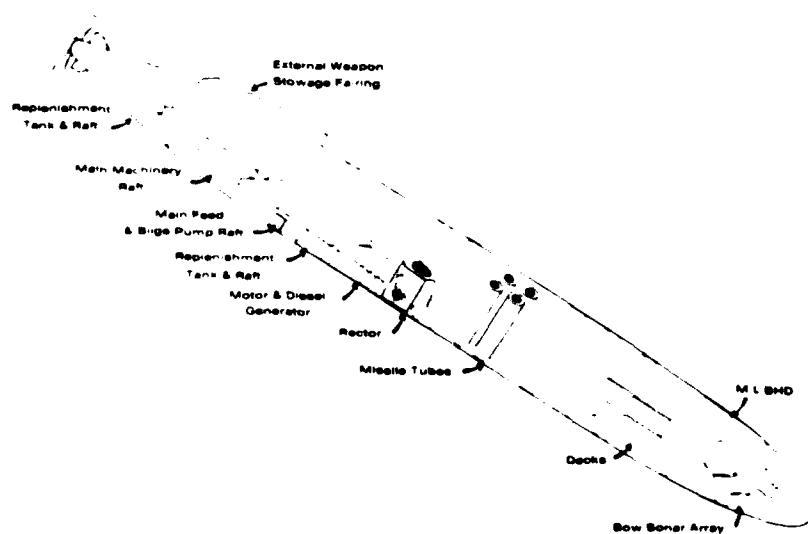


Fig 19 B-1 model

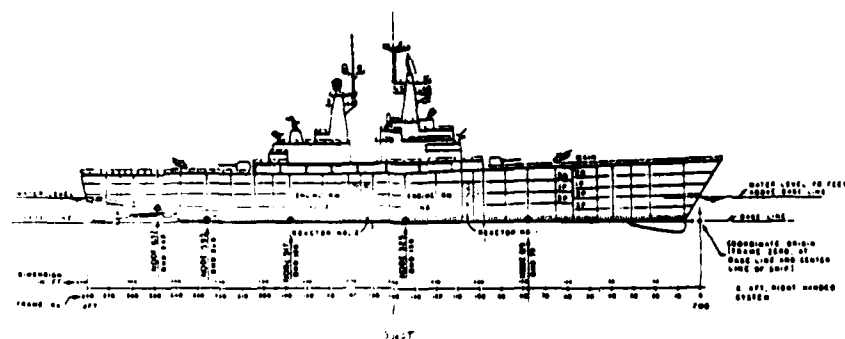


Figure 20



Fig. 21 — High explosive test bed layout

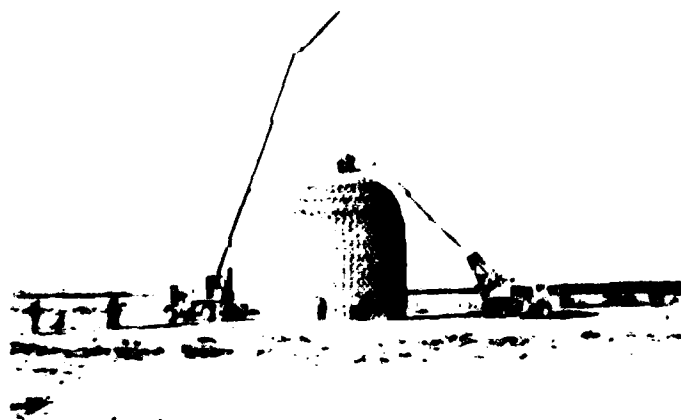


Figure 22



Figure 23



Figure 24

effects of airblast on personnel. Obviously, we are every bit as much interested in what happens to our personnel, as we are in what happens to our equipment. The Defense Nuclear Agency conducts an elaborate program of research on the nuclear effects of personnel, including the effects of radiation as well as airblast.

The previous discussion and illustrations have addressed airblast, thermal and, EMP effects but we also need to study ground shock. I would now like to address that problem. Figure 25 illustrates a high explosive simulation technique frequently referred to by the acronym HEST. It is a high explosive simulator for producing airblast loads on surface flush or shallow buried structures. It is a technique that has been used since 1963 to test operational MINUTEMAN facilities and many scaled structures. In this simulation technique the test object is placed in the earth either flush with its surface or at some distance below and layers of explosives are placed over the top of the structure. The explosive array is then covered with an earth surcharge as a containment mechanism to obtain the desired pressure time history. A photograph (Figure 26) of the experiment being assembled shows the foam which forms the cavity dimensions. The strips you see in between the foam are for the explosive charges and above this will be placed the surcharge.

An illustration of a design to simulate the direct coupling of energy to the ground is shown in Figure 27. The test is referred to as MINE THROW. The test is designed by performing calculations defining the ground motions from a nuclear burst in the hydrodynamic region. From these calculations we identify a contour of constant peaked stress selected to correspond with the contact pressure between the explosive and the ground medium to be used in the simulation. At each point along the contour, the pressure time history and the impulse is determined from the nuclear event calculation; then the explosive charge is shaped in such a way that it will reproduce as nearly as is possible the pressure history at specific impulse along the chosen contour. The charge is ignited in such a way as to attain the same arrival of the detonation wave at the contour as the ground shock from the nuclear event. Most of our previous tests have independently tried to simulate the effects of crater induced ground motion, upstream airblast induced ground motion, and local airblast. We are devising experiments in the future that will combine these effects by the combined use of simulators. This is illustrated in Figure 28.

For almost a decade we have been using the horizontal line-of-sight underground (LOS) test to do many of our experiments in both shock x-ray effects and other phenomena related to nuclear detonations. In this experimental technique we bore a tunnel into the side of a mountain for several miles.

At the end of this tunnel we placed a nuclear device and by the use of evacuated pipes for the transmission of x-rays for x-ray experiments or by side drifts to other tunnels for structures experiments, we have been able to learn an awful lot about these effects. The technique is not simple. It requires many different types of closures to protect the experimental objects so that we can properly make our measurements and recover some of the experiments. The instrumentation for some of these experiments is located in side drifts in the tunnels. In other cases, we actually run cables up to the top of the mountain to a mesa where the trailers that include the instrumentation can be parked. The complex of underground tunnels in Figure 29 is for the LOS test "DIABLO HAWK".

Over the years we have examined many different techniques for producing underground structures — means of drilling them, excavating them and means of reinforcing them as illustrated in Figure 30. We have had an ongoing program aimed at examining the integrity of these structures in an environment of nuclear produced ground motion.

Over the years it has always been appealing to consider other means of protecting our ground based strategic systems than the current use of silos. As missile accuracies increase, it becomes more and more difficult to obtain basing modes that are truly survivable to attack. I am sure you have often heard reference to what is called a secure reserve force where some assets could be protected over a long period of time to be used in a protracted conflict. One such concept considered is deep basing. In such concepts a series of missiles, launch control centers, and all ancillary equipment would be housed under a mountain or a mesa. The Defense Nuclear Agency is currently studying this concept in cooperation with the Air Force and USDRE. There are a number of critical problems which must be solved including the method of egress. If this reserve force should be housed for a number of weeks, when it is ultimately called upon there must be some means of getting it out of the mountain. Many of these concepts are to be studied in detail so that we will have a plan that is backed by experimental validation so that if the decision is ever made to deploy such a system, we will have the technology at hand to proceed.

This is a small brush of things DNA is looking at today. We feel a very strong commitment to support the Services. We are not a management organization; DNA is a service organization. We are purple suited and take a serious view of our responsibilities to all the people in the Department of Defense we work for. It is certainly my intention to keep it that way.

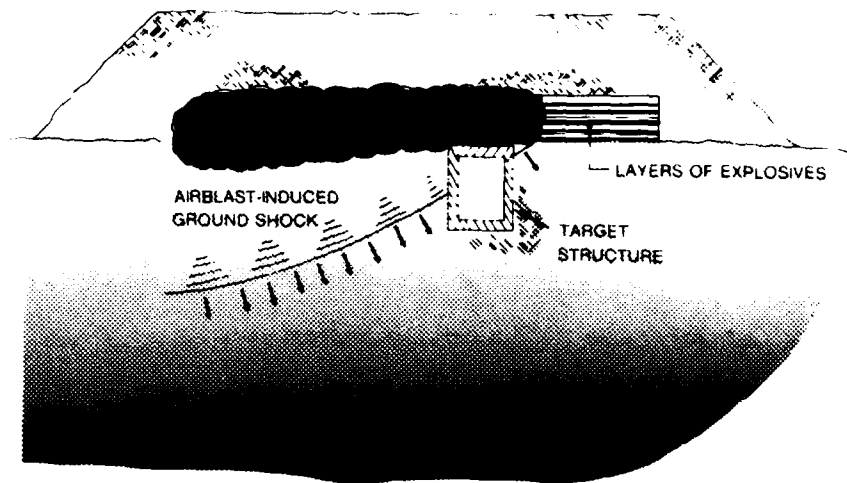


Fig. 25 — High explosive simulation technique (HEST)

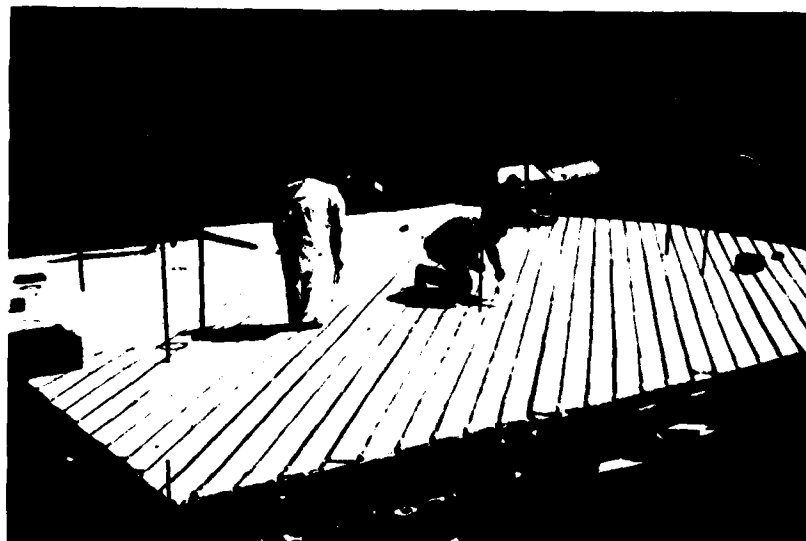


Figure 26

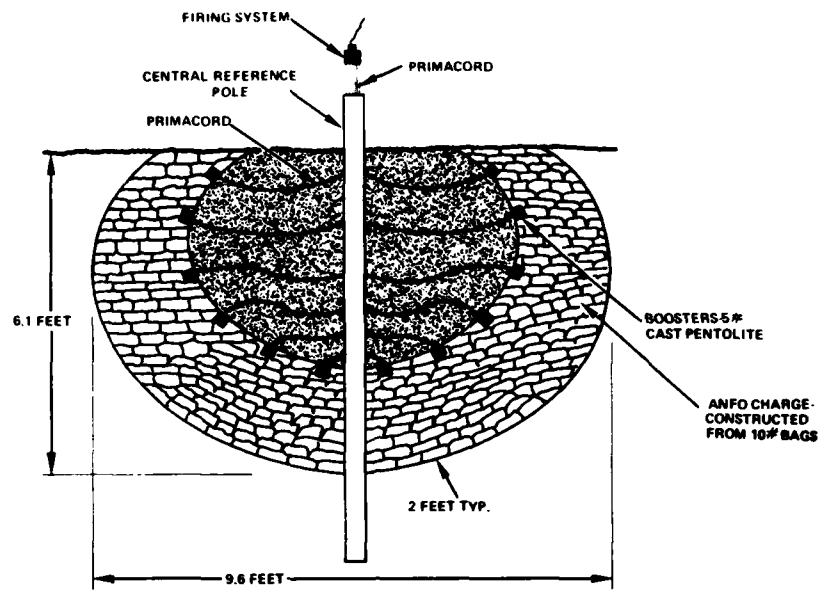


Fig. 27 - Mine throw event - conceptual design

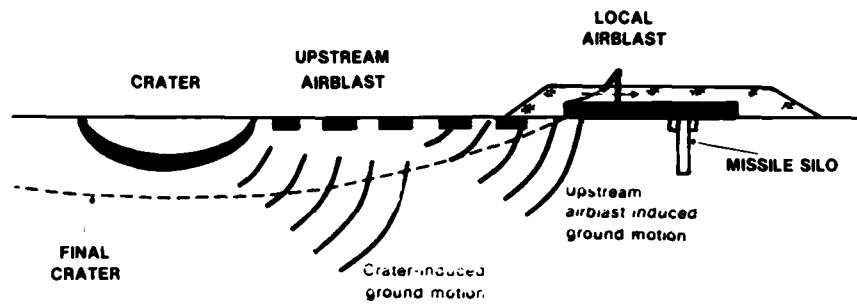


Fig. 28 - STP-3 combined effects test



Figure 29










UNLINED CYLINDER	UNLINED "CYLINDER"	UNLINED "CYLINDER"
 <p>EXCAVATION • DRILL & BLAST</p> <p>NET HARD MAT PILE DRIVER</p> <p>CYLINDER WITH SETS AND WOOD LAGGING</p>	 <p>EXCAVATION • DRILL & BLAST</p> <p>HARD MAT PILE DRIVER EARLY HLOS</p> <p>CYLINDER WITH PATTERNED GROUTED UNTENSIONED ROCK BOLTS</p>	 <p>EXCAVATION ALPINE MINER</p> <p>RECENT & CURRENT HLOS</p> <p>CYLINDER OR CYL WITH DOMED END WITH PATTERNED GROUTED & TENSIONED ROCK BOLTS</p>
 <p>EXCAVATION • DRILL & BLAST • ALPINE MINER</p> <p>RAINIER HARD TALK II HARD MAT EARLY HLOS PILE DRIVER</p> <p>RECENT & CURRENT HLOS</p> <p>CAST CONCRETE INTEGRAL LINING CYLINDER OR SPHERE</p>	 <p>EXCAVATION ALPINE MINER</p> <p>RECENT & CURRENT HLOS</p> <p>STEEL REINF CONCRETE "BUILT UP" STEEL & COMPOSITE STEEL CONCRETE LINERS WITH BACKPACKING CYLINDER OR CAPSULE</p>	 <p>EXCAVATION • CONTROLLED BLAST</p> <p>PILE DRIVER</p> <p>COMPOSITE (CONCRETE LINED WITH STEEL) INTEGRAL LINING CYLINDER</p>
 <p>EXCAVATION • DRILL & BLAST • ALPINE MINER</p> <p>HARD MAT CYLINDER MIGHTY EPIC DIABLO HAWK SPHERE</p>	 <p>EXCAVATION • DRILL & BLAST • ALPINE MINER</p> <p>HARD MAT PILE DRIVER MIGHTY EPIC DIABLO HAWK</p>	 <p>EXCAVATION • CONTROLLED BLAST (P D) • ALPINE MINER (M E D M)</p> <p>PILE DRIVER MIGHTY EPIC DIABLO HAWK</p>

Fig. 30 — Data base rock opening reinforcement

THE ELIAS KLEIN MEMORIAL LECTURE
THE CHANGING DIMENSIONS OF QUALIFICATION TESTING

H. Norman Abramson
Vice President, Engineering Sciences
SOUTHWEST RESEARCH INSTITUTE
6220 Culebra Road
San Antonio, Texas 78284

INTRODUCTION

Qualification testing is thought by many people to be a rather routine endeavor, requiring only the application of well established procedures and techniques. In actuality, however, qualification testing could hardly be more dynamic, representing as it does an interface between a multitude of vendors, customers, testing facilities, regulatory agencies, etc., each of whom is striving — but in different ways — to deliver an acceptable product at minimal incremental cost.

In the DOD field, these factors are ameliorated by the fact that the specifications are essentially determined by the government, as are the methods of testing to be employed — a stable situation, perturbed only (usually) by additional technical considerations arising during the qualification testing itself as a consequence of new design features of the product. Vendors account for the resulting additional development costs in setting product prices.

QUALIFICATION TESTING FOR THE DOD

Background

The need for a representative form of test demonstration of the capability of military hardware to meet the demands of field environments has been given serious engineering attention since World War II. [1] Even in the beginning, it was realized that various environmental parameters can influence this capability (i.e., temperature, humidity, shock, vibration, etc.), and so there has been pursued an almost continuous program of research and development aimed at establishing guidelines for conducting appropriate qualification tests, and methods for specifying these tests, for equipment manufacturers. These efforts resulted in an extensive series of Military Standards (MIL-STDs) which have been updated periodically. Several important concepts regarding test demonstrations have evolved from this general activity, two of the most significant being qualification (or proof) tests and reliability tests.

MIL-STD 810 [2] has long been a most important source of guidelines for writing environmental test specifications. A single failure during a qualification test usually constitutes grounds for rejection and subsequent redesign or other modification of the equipment. Often, such tests require time-accelerated procedures in which the environmental stress levels may be increased to compensate for reduced test durations. On the other hand, data given in MIL-STD 810 is generally recognized to be quite conservative, and therefore can lead to

unnecessary rejection of equipment that is specifically intended to be of lightweight design; this would therefore imply that qualification tests for such equipment should be developed by some procedure that includes more directly relevant data.

In the nuclear power field the situation is quite different in that the government sets only guidelines or intentions and leaves the development of actual specifications to interested professional organizations. The testing agencies (private laboratories) then develop the relevant test procedures and techniques and provide a service to vendors (whose equipment is being purchased by the A/E contractor responsible for designing and building a plant for operation by a utility company). The government is required to make final judgments as to the validity of the qualification testing that has been conducted, but often these are not rendered until many months after completion — an unstable situation. The vendors consider their products to be 'mature' and of proven reliability (under normal conditions) and have accordingly priced them to be as competitive as possible; expenses incurred subsequently for qualification of seismic environments are therefore to be minimized. Because this is a new industry, vendors (and even plant designers) sometimes have limited knowledge of dynamic environments and responses.

The purpose of this paper is to demonstrate, largely by specific cases, the changing dimensions of qualification testing in the interests of both the DOD and the nuclear power industry: In the one case the objective is "mission integrity" and is achieved principally through "generic" testing — the environment is a "stable" one. In the other case the objective is "operational reliability" and is achieved mostly through "custom" testing — the environment is an "unstable" one.

MIL-STD 781C [3] also gives standard guidelines for vibration and other environmental testing where long term reliability is the prime concern.

Unfortunately, it has become evident over the years that the development of *generic* test procedures characterized by MIL-SPECS and having the purpose of providing 'operational reliability' or 'mission integrity' has led in many instances to high rejection rates and higher cost through overdesign. This, in turn, has led to *custom* testing as a way to insure better products at lower cost. This is achieved by the development of alternate methodologies for the development of test specifications; the application of such methodologies, however, requires that vendors have good knowledge of the requirements and be able to employ to full advantage the advanced analysis/measurement techniques required.

Methodologies for the Development of DOD Test Specifications

Over the years, qualification and reliability tests have been conducted in both field and laboratory simulations, in either case the attempt being that of duplicating the anticipated operational environments. Sometimes field simulations alone can give a reasonable representation, especially when there is a substantial lack of knowledge about the significant environmental parameters. Such field simulations are, however, usually quite expensive and therefore the trend has been more and more toward the development of improved laboratory simulations. To provide simulations that include test procedures that are even more representative of the anticipated operational requirement than are those of, say, MIL-STD-810 depends upon an improved data base. This in turn requires the careful acquisition and analysis of field data under representative operational procedures and the development of new laboratory test criteria from those data. This step is one of considerable complexity and requires considerable engineering judgment. The following examples are intended to demonstrate the evolutionary nature of improved MIL-STDs and customized qualification testing.

Early vibration qualification tests for most hardware were based on swept sine, and sine dwell tests whose specifications could be developed from MIL-STD 810. However, as one might expect, this type of test was particularly severe on systems having significant resonances, and failures occurred. If it was suspected that the true environment was less severe than the one specified (as was often the case), one was faced with acquisition of field data and development of a suitable alternate test. An example of such a procedure occurred during qualification of the M200 Rocket Launcher for service on helicopter airframes. [4] It was first necessary to acquire flight vibration data for these units, which also required the development of a mission profile. Analog taped flight vibration data at anticipated critical locations were then acquired for various maneuvers of this profile. Analysis of these data led to two important conclusions:

- (1) data for some maneuvers were quite stationary (i.e., levels and frequency content were constant with time), while for others, such as turns and dives, the data were quite nonstationary, as shown in Figure 1

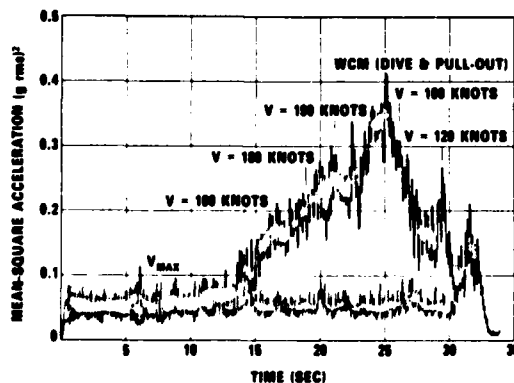


Fig. 1 — Mean-square accelerations from AH-1G flight tests, vertical axis

- (2) time averaged power spectra were a useful way of analyzing the data, again as shown typically in Figure 2.

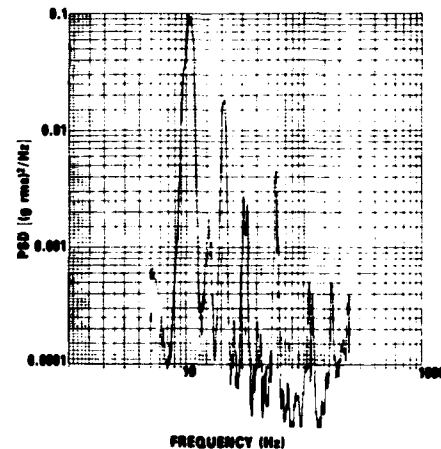
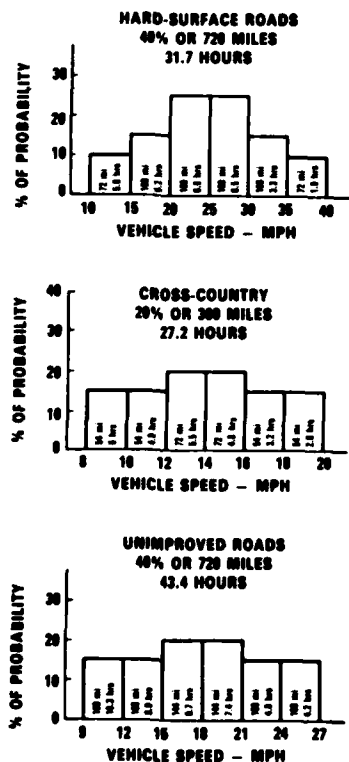


Fig. 2 — PSD plot of data from accelerometer No. 5, instrumentation (code A)

This data showed that vibrational energy was dominantly applied at the rotor passage frequency (11 Hz in this case) and several of its harmonics. Results of this type led to sine dwell tests applied only at these frequencies, rather than at resonances of the specimen, and time duration of the dwells was made commensurate with the mission profile and a specified number of missions. Ultimately, this work resulted in changes to recommended procedures for qualification testing of helicopter external stores when MILSTD-810B was revised to MIL-STD-810C; however, even these new procedures appear to be still too conservative for more recent lightweight store designs, and so the program has remained one of active development.

Another similar example, but for a ground vehicle vibration test specification development, was conducted for the LANCE missile. [5,6] This specification included heating and cooling as well as vibration tests. Originally, a swept sine test was developed to represent the typical lifetime operational environment, but the vibration levels were complicated by the different environments caused by mode of transportation, terrain, speed, etc. (Figure 3), and which resulted in early failures. Subsequently, the test was modified several times and ultimately, a swept narrow band random test was developed which was shown to be more representative of the field environment. Based on additional field test data, a completely different test was developed which included broad band random and a swept sine applied simultaneously. The swept sine component represented energy input from the vehicle track and varied with speed. Examples of power spectra from two different carrier modes on a gravel road are shown in Figure 4 for a given part of the service life. Similar data were acquired for truck and aircraft environments. These spectra were then used as a criterion for a laboratory time-accelerated test. An example of a comparison of scaled field spectrum and laboratory spectrum for one axis and terrain condition is shown in Figure 5. Test durations were again tailored to the corresponding service life.

The foregoing two examples show how environmental tests have developed in considerable complexity, but at the same time provide a more representative simulation. Such programs are costly, but can be justified for widely used systems. In order to develop further information on vibration environments, other fundamental studies have also been performed [7] in which a model hardware specimen (MHS) was instrumented to measure vibration, and was tested in several helicopter and ground vehicle environments. The specimen represented an arbitrary hardware item (an assemblage of beams) with natural vibrational modes randomly oriented in space and frequency. Figure 6 shows some typical results of vibration levels felt by each beam with the MHS secured in a M35 Truck which has run over a ground vehicle course; the strong character of nonstationarity of the data is again evident. A vibration test representing this environment was developed by matching power spectra for individual parts of the course, as shown in Figure 7. Again, the trend to additional complexity in the tests is evident; however, a more exact simulation is achieved.



PROBABILITY DISTRIBUTION OF VEHICLE MILEAGE AND TIME

SUMMARY:
 HARD-SURFACED ROADS - 720 MILES - 31.7 HOURS
 UNIMPROVED ROADS - 720 MILES - 43.4 HOURS
 CROSS-COUNTRY - 300 MILES - 27.2 HOURS
TOTAL 1000 MILES
FOR 102.3 HOURS

Fig. 3 - Probability distribution of vehicle speeds

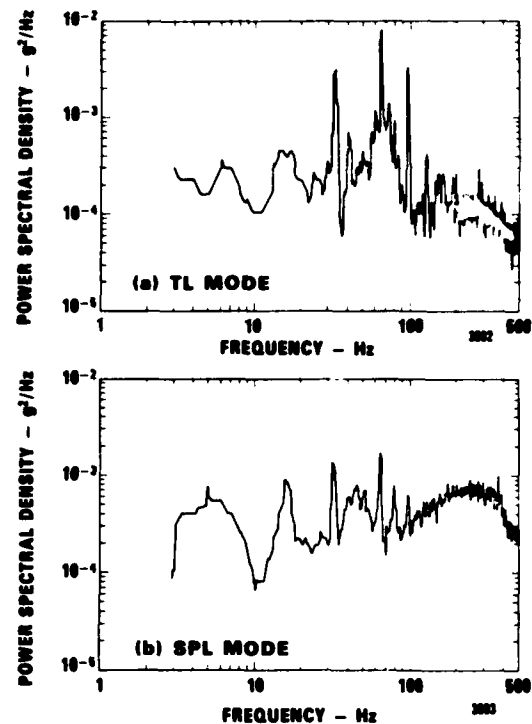


Fig. 4 - Power Spectral Density of Yuma Field Test Data - Gravel Terrain, 10 MPH, Aft Bulkhead, Vertical Axis

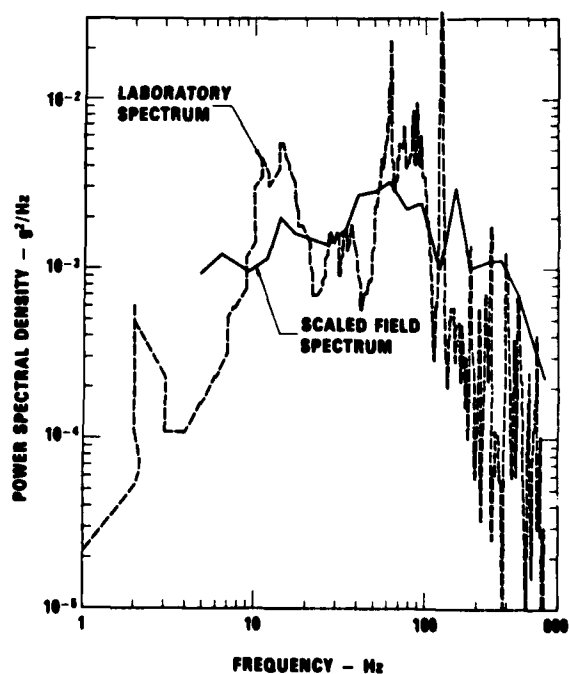


Fig. 5 - Comparison of scaled field spectrum with laboratory duplicate for VSL testing - gravel terrain, AFT bulkhead, vertical axis

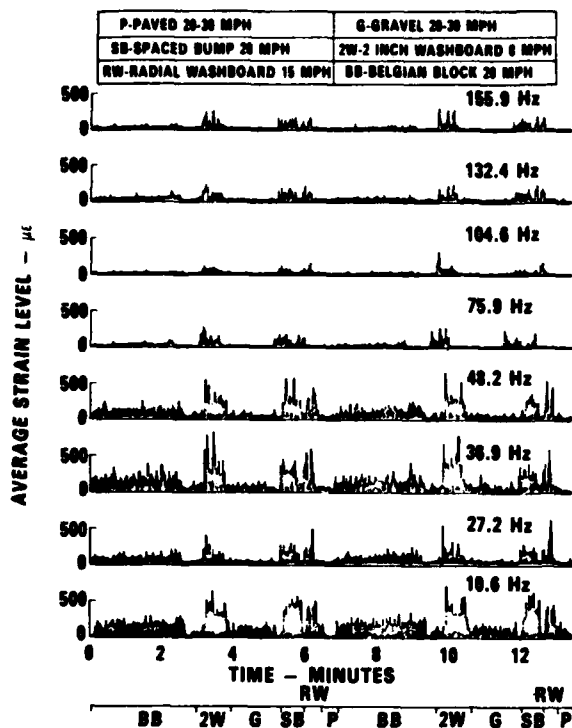


Fig. 6 — Average Strain Level Variation with Time Run No. 2A MHS Secured in Aft Cargo Area M35 Truck — Field Data

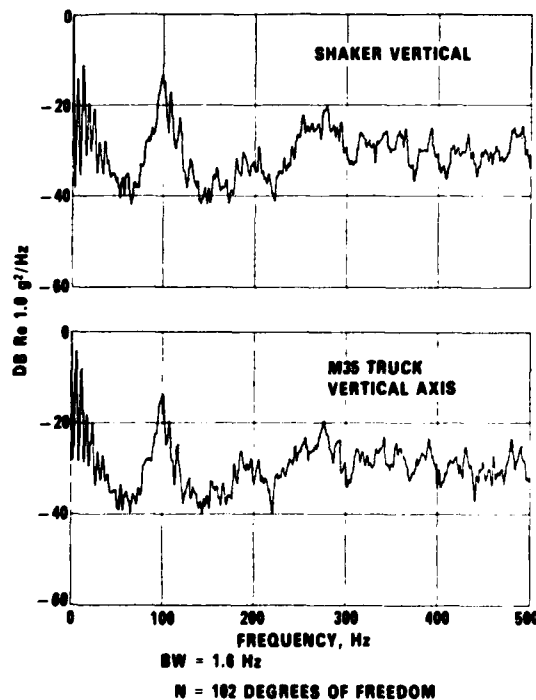


Fig. 7 — PSD of M35 truck on 2-inch washboard

There has also been considerable attention given to the development of better laboratory systems for producing reliability tests. For some time, there has been an interest in the Army Test Methodology program to develop a vibration system capable of producing vibration along several axes simultaneously, as is actually experienced by field hardware. Initially, the exact nature of the requirement for the multi-axis shaker was unknown, so a typical radio specimen was instrumented and flown in a helicopter under an appropriate operational plan. [8] Throughout these flights, excitation vibration analog tape data was acquired at three points on the radio face (where it was attached to the instrument panel), and response data was acquired at one point on the back of the radio. From the input-output data, a mathematical model of the radio was developed using power spectra and cross spectra. The mathematical model was then used to predict radio responses for several different types of physical representation of the excitation. An example of some result comparisons is shown in Figure 8. It was found that a triaxial system (three simultaneous independent orthogonal axes) for the shaker was most feasible. [9]

This development of a triaxial shaker system led to a concurrent program which was aimed at acquiring reliability

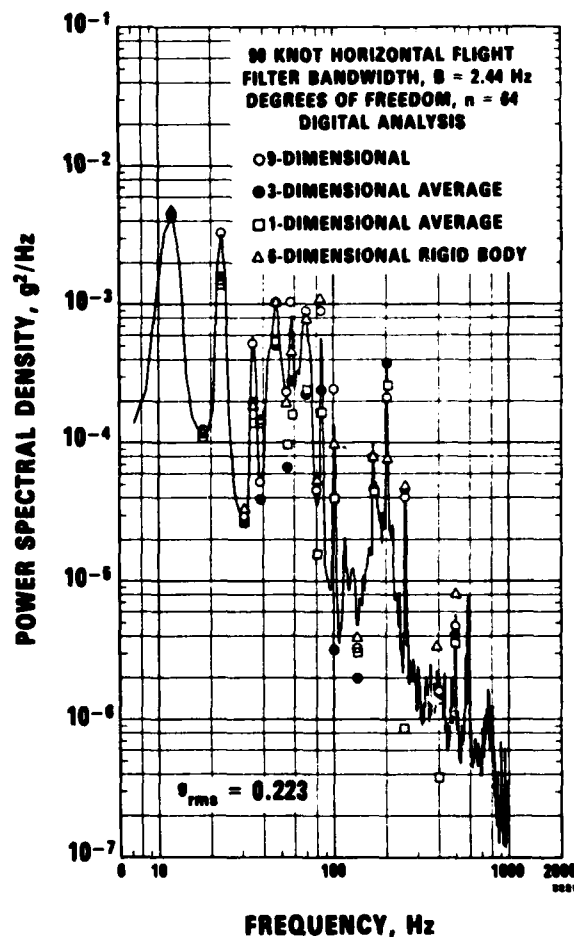
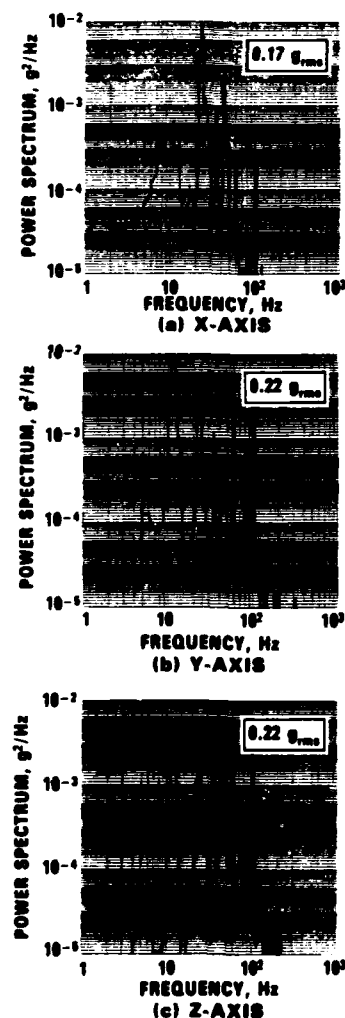


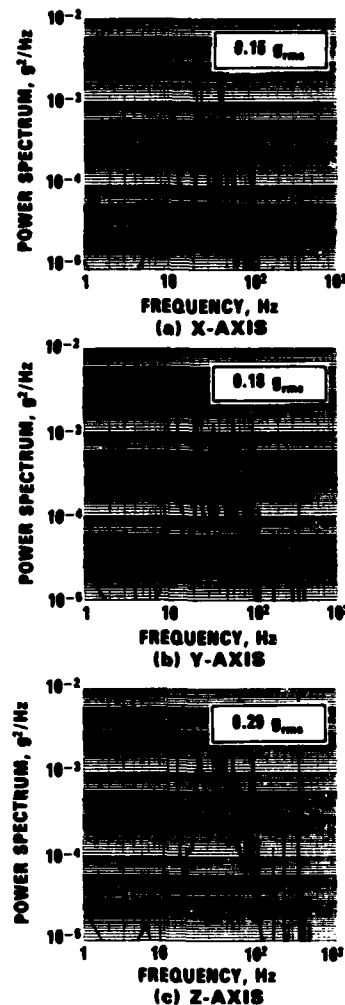
Fig. 8 — Longitudinal response amplitude (Y_{41}) and simulations for OH 58A helicopter

data to compare the effectiveness of several different types of reliability environments. [10,11] Five different types of reliability tests were applied to five different sets of five radios. Each test included operation of the radios and some form of simulated environment. Vibration data were acquired during flight, and this sequence was repeated many times for flight tests on the Sample Set V radios. This data was also used to develop tests for the Uniaxial (set II) and Triaxial (Set IV) radios. Figures 9 and 10, respectively, show samples of field and laboratory triaxial data. Of course, matching of time averaged power spectra for different parts of the operational sequence was used as the vibration test criteria. In addition, one group of five radios (Set III) was subject to the AGREE test specified in the B-version of MIL-STD-781, and one group (Set I) was subject only to bench tests, where only electrical operation was simulated. It was found that humidity



STRAIGHT LEVEL MINIMUM CRUISE
EFFECTIVE FILTER BANDWIDTH = 2.0 Hz
DEGREES OF FREEDOM = 120
SAMPLE LENGTH = 64 SEC

Fig. 9 — Acceleration power spectra from flight triaxial data



STRAIGHT LEVEL MINIMUM CRUISE
EFFECTIVE FILTER BANDWIDTH = 2.0 Hz
DEGREES OF FREEDOM = 120
SAMPLE LENGTH = 64 SEC

Fig. 10 — Acceleration power spectra from laboratory triaxial data

and nonuniformity of personnel operations had a large influence in the results, while results for the vibration tests remained inconclusive. The prohibitive cost and time for field testing is the driving force for continuing efforts along the lines of laboratory simulation just described.

QUALIFICATION TESTING FOR THE NUCLEAR POWER INDUSTRY

Background

Recommended procedures for seismic qualification of nuclear plant equipment and components have undergone a rapid development over the last several years. Although the general guidelines have remained relatively intact, the detailed

procedures have changed significantly. These changes result largely from reactions to individual problems that have arisen spontaneously in the various test laboratories during actual qualification tests; unfortunately, the details are often buried in company proprietary test reports, and have rarely been published for general evaluation. A major problem for seismic qualification testing is that there is no operational data base!

This lack of data base information further aggravates difficulties arising from the fact that many organizations are involved in the total qualification process. [12] The vendor issues a contract for testing of a specific hardware item, with given test specifications, to a chosen test laboratory. The specifications are written by the A&E firm to whom the vendor is a supplier. In turn, the A&E firm must satisfy its contractual requirements with the utility company whose plant it is constructing; and, finally, the utility must satisfy licensing requirements of the NRC. One of the few unifying aspects of this qualification process has been that many interested members of these various organizations have served on the IEEE committees that have actively developed the guidelines for qualification. The NRC has, in turn, published standards which either approve or supplement these guidelines. Unfortunately, the result of this somewhat convoluted process is that there has been very little published research evidence to support the test procedures that have evolved.

General guidelines for the conduct of seismic qualification tests are specified by the NRC in Standard Review Plans. [13,14] These guidelines require considerable supplemental explanation and, therefore, rely on standards written by committees of the IEEE. For example, IEEE 323 [15] is a standard* which addresses general environmental requirements, while IEEE 344 [16] is a more detailed guideline for seismic qualification of electrical equipment. It is further supplemented by NRC Reg. Guide 1.100 [17], which recognizes the use of IEEE 344 for qualification of both electrical and mechanical components. Such documents are further supplemented by various other standards that apply to more specific equipment such as Valve Operators. [18]

Although there has been little published hard data on developments in seismic qualification, several review papers have appeared. [19,20] These were followed by a further review [21] of research needs, which was based on observations during various seismic qualification tests. One research program, that was based on experimental data throughout, and which sought out and identified specific problem areas, recommended approaches for their solution and developed new concepts for handling the qualification process, has also been reported [22].

Test Methods and the Response Spectrum Anomaly

The following discussion is directed toward identifying some of the problem areas presently occurring in seismic qualification testing. The case to be reviewed involves an electrical network control cabinet [22], although the results are applicable to both electrical and mechanical equipment, in general, and to qualification by analysis as well as by test.

A typical electrical cabinet was subjected to a variety of seismic tests that are currently recognized by IEEE 344-1975, and furthermore, by Reg. Guide 1.100. The objective was to develop data from which the responses to various tests could be compared. Figure 11 illustrates the cabinet and instrumentation locations, the latter involving three triaxial

accelerometers and three strain gage channels to measure excitation and response data for the various tests. In preliminary tests, the cabinet natural modes were determined by resonance searches when mounted to the floor and when mounted on a biaxial seismic simulator. Figure 12 shows several of the prominent floor-mounted modes below 35 Hz. Typical transfer functions for the simulator-mounted searches are shown in Figure 13 from which it can be seen that some differences in frequencies occurred for the two different mounting methods. Procedures for handling these differences during qualification tests have evolved as a consequence of this data.

The cabinet was subjected to a series of qualification tests, including biaxial independent and biaxial dependent tests for typical *ground level* specifications. Both random and earthquake signal sources were used to develop the drive signals for the simulator. Further, another series of tests, for *floor level* specification, was also imposed that included biaxial independent, uniaxial, sine beat, and sine dwell excitations. Both random and earthquake signal sources were again utilized to produce a typical floor level test. Figure 14 shows time histories for a typical biaxial independent random ground level test run while corresponding required response spectra (RRS) and test response spectra (TRS) are shown in Figure 15. These response spectra demonstrate a typical, and very important, problem; both Figure 15a and 15b show an excessive test zero period acceleration (ZPA) compared with the required value. This problem has been discussed at length in References 20, 21, 22, and appears to indicate over-conservatism in the test, resulting from a mismatch of the response spectra. This discrepancy may be a consequence of an insufficient designation of tolerances required to achieve the proper ZPA, or can often occur because, indeed, no time history can be generated that will match the RRS entirely! In any event, the effects of this "apparent" overconservatism on test results needs to be evaluated.

Data from the individual runs during the various tests were correlated in terms of peak measured response (\bar{a}_3) as a function of peak response (\bar{a}_1) predicted from the response spectrum. That is,

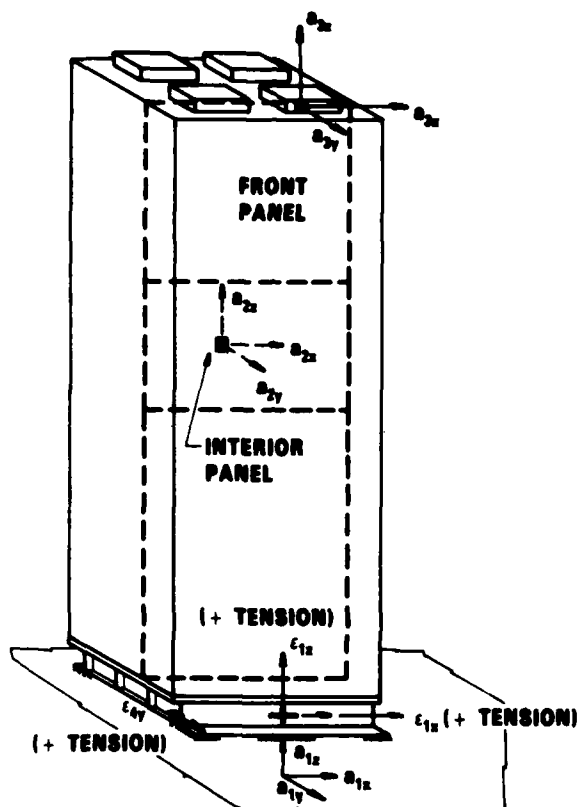
$$\bar{a}_3^* = 2\beta_r |H_{31}(\omega_r)| \bar{a}_1$$

where H_{31} is a transfer function and β_r is modal damping. Examples of typical results are shown in Figure 16. This type of correlation indicates that reasonable agreement exists between measured responses and those predicted by shock spectrum analysis. The principal discrepancy seemed to result from nonlinearity of the transfer functions for the various modes. A second type of correlation was developed in terms of average RMS response (\bar{a}_3) as a function of average RMS excitation (\bar{a}_1). That is,

$$\bar{a}_3 = A_{31} \bar{a}_1$$

where A_{31} is a constant. Correlations of this type are applications of the equations developed for a general structural system. [23] This also recognizes the RMS value as a useful measure of intensity, as has also been pointed out in Reference 24. Examples of some of the results are presented in Figure 17. In general, it can be seen that less scatter of data occurs for data of a given type of test run. Further, each test run having similar sustained damage potential falls on a corresponding curve, which helps point to the development of a parameter which describes an all-around damage severity of a given type of test. [25]

*An updated version of this standard is NUREG 0588.



TAPE RECORDER CHANNEL ASSIGNMENT

CHANNEL	OSCILLO- GRAPH	TAPE
1	a_{2x}	a_{2x}
2	a_{2y}	a_{1H}
3	a_{2x}	a_{2y}
4	a_{2x}	a_{1T}
5	a_{2y}	a_{2x}
6	a_{2x}	a_{1z}
7	ϵ_{1x}	a_{2x}
8	ϵ_{1y}	ϵ_{1x}
9	ϵ_{1x}	a_{2y}
10	a_{1x}	ϵ_{1x}
11	a_{1y}	a_{2x}
12	a_{1z}	ϵ_{1y}
13	—	X_{CH}
14	—	X_{CZ}

CONTROL ACCELERATION, a_{1x} , a_{1y} , a_{1z}

COMMAND DISPLACEMENT, X_{CH} , X_{CZ}

Fig. 11 — Positions of instrumentation

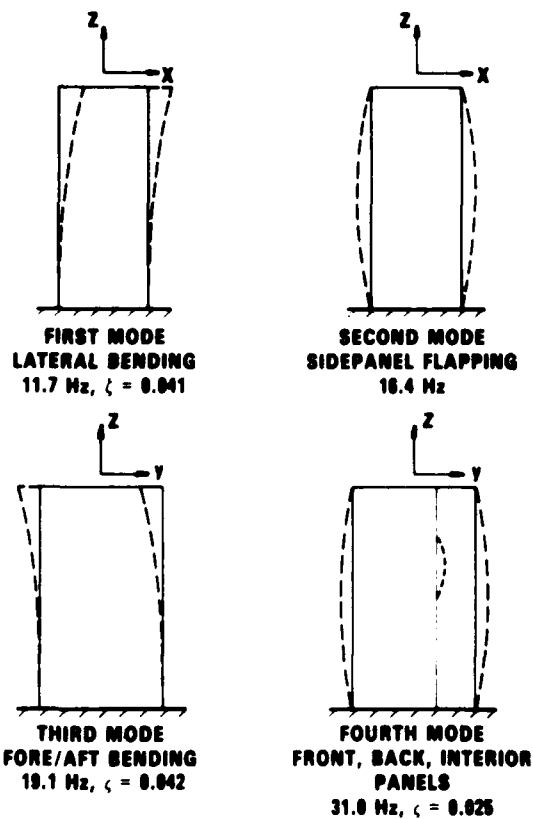


Fig. 12 — Cabinet natural modes below 35 Hz

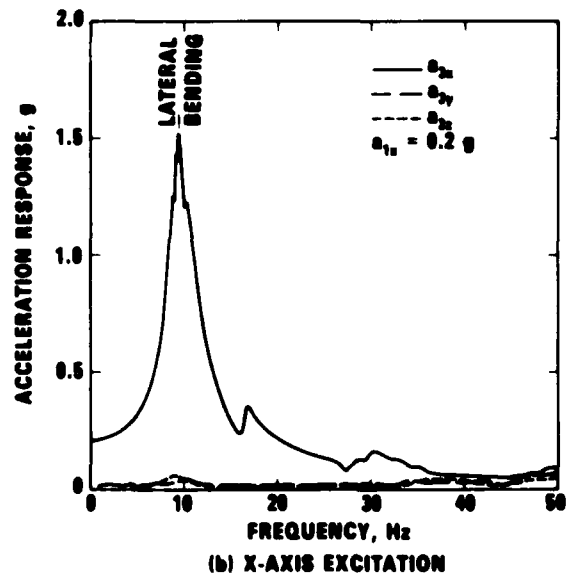
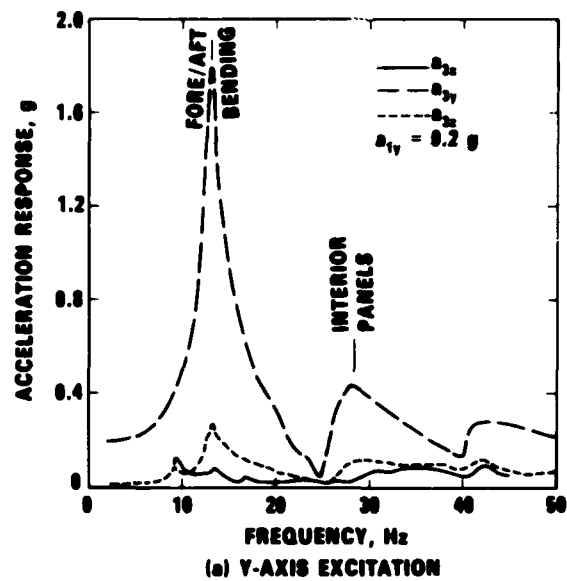


Fig. 13 — Top acceleration responses for simulator-mounted sweep test

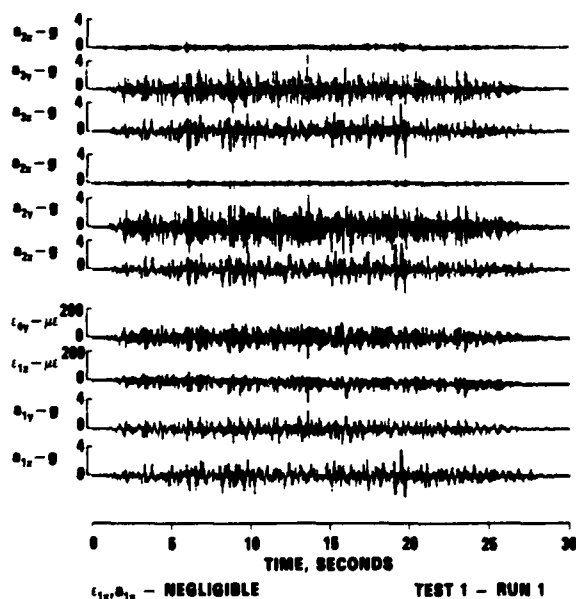


Fig. 14 - Responses for biaxial independent random ground level test, YZ-excitation

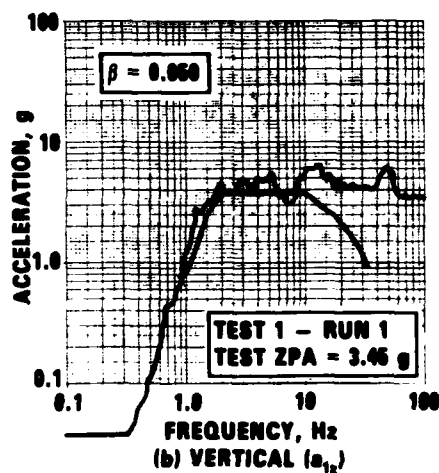
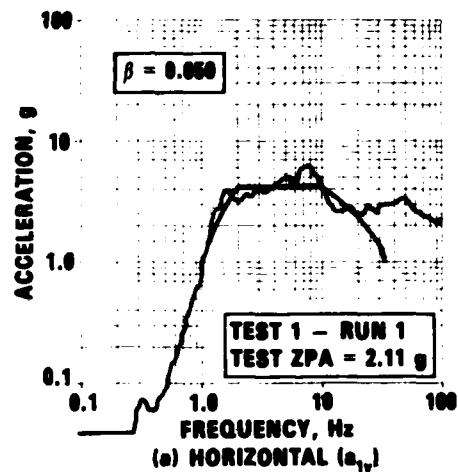


Fig. 15 - Response spectra for biaxial independent random ground level test, YZ-excitation

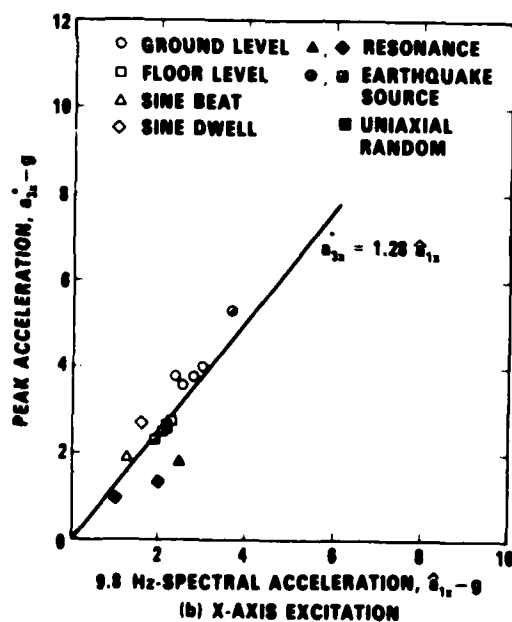
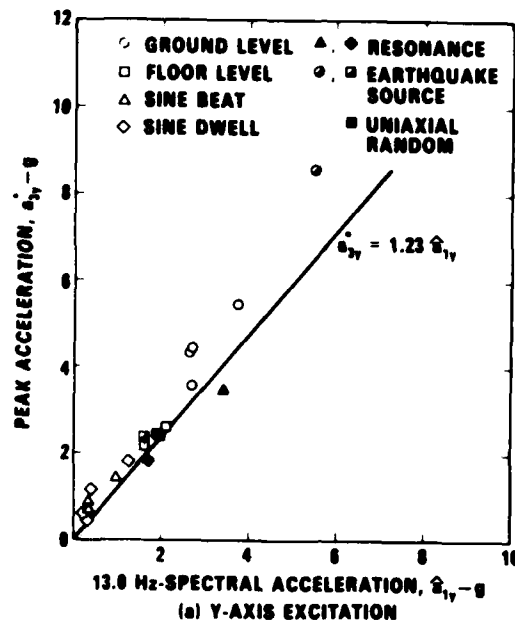


Fig. 16 — Peak acceleration responses at cabinet top

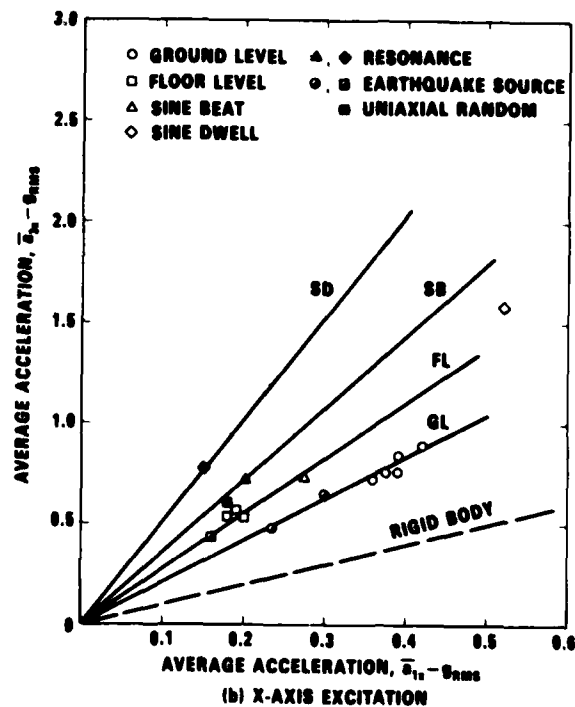
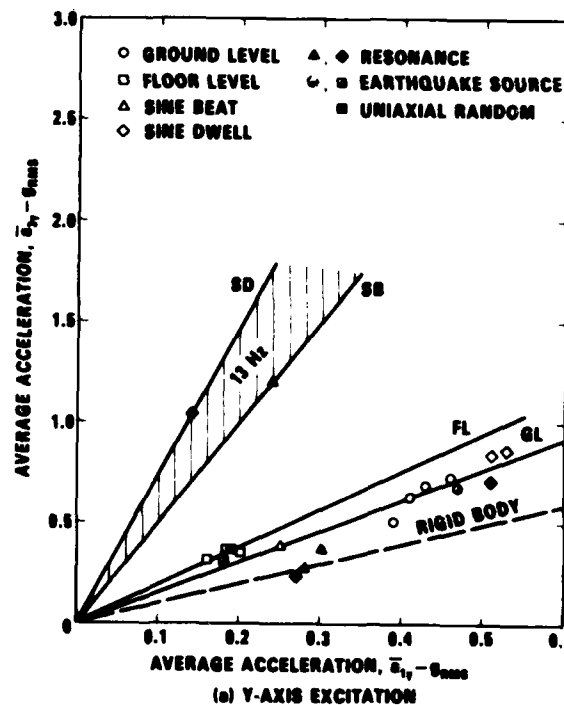


Fig. 17 — Time-average acceleration responses at cabinet top

A very important anomaly which affects the criterion for matching or enveloping a response spectrum has recently been delineated [22]: it appears that enveloping of a response spectrum *does not guarantee* that all modes of structure will be excited properly during some tests.

Figure 18a shows the RRS and matching TRS that was used for one run on the electrical cabinet. This run involved a ground level test in which motion was developed from a random noise generator and a ± 3 dB tolerance was allowed in the matching below 20 Hz. Note that this tolerance was slightly exceeded at about 7.5 Hz. Nevertheless, the TRS envelops the RRS at all frequencies above 3.4 Hz. Note also that the test ZPA exceeds that required by a factor of 3 so that this would appear to be a severe *overtest*; however, further investigation will show that this, in fact, represented an *undertest*.

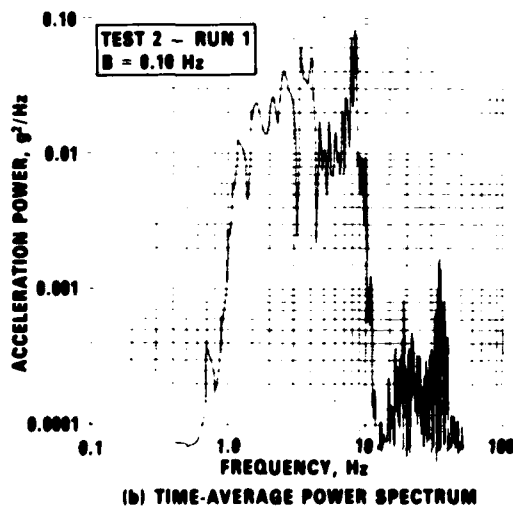
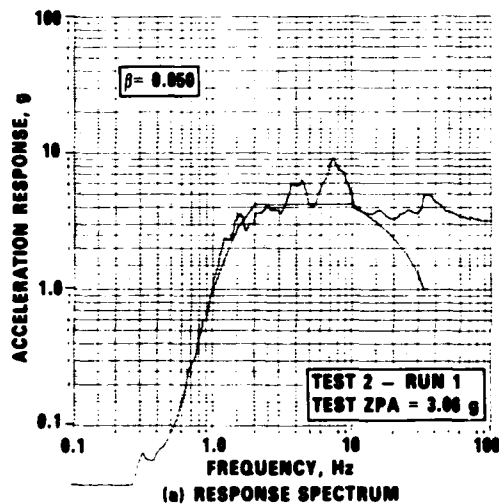


Fig. 18 - Parameters which describe ground acceleration (a_{1y}), YZ-excitation

The possibility of an undertest was suspected when a time-average power spectrum of the excitation was computed, with the results shown in Figure 18b. It is immediately apparent that there is essentially no energy in the input 13 Hz, where from Figure 13a, it can be seen that the first fore/aft bending mode of the cabinet occurred. On the other hand, the RRS indicates that energy input and amplification should occur at this frequency. Thus, a direct contradiction has occurred. This can further be realized by looking at the data in Figure 19, which is based on the response acceleration at the cabinet top. Although the input energy peak at 7.5 Hz is amplified, again, there is no resonance at this frequency; in fact, there is no amplified peak in the response spectrum at 13 Hz, where a resonance is known to occur. This is further evidenced in Figure 19b, where the response power spectrum shows no prominent energy in the response at 13 Hz.

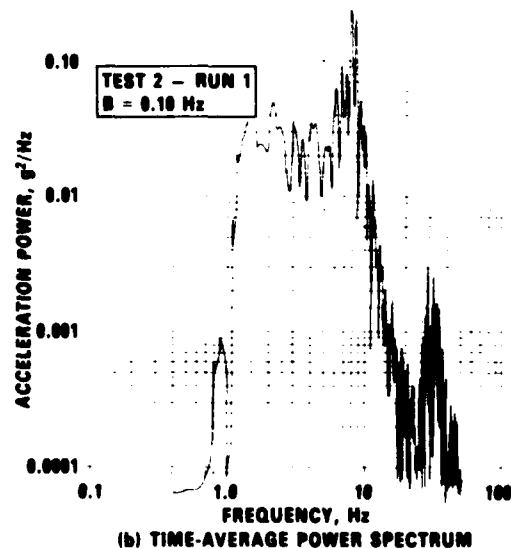
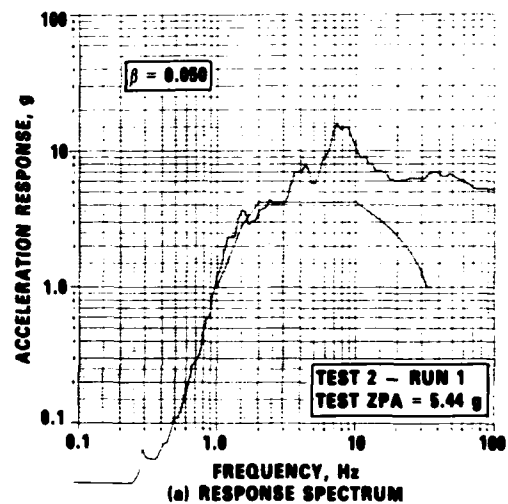


Fig. 19 - Parameters which describe cabinet top response acceleration (a_{3y}), YZ-excitation

In view of the above excitation response spectrum data (Figure 18a) alone, it would appear that a proper test has been conducted; and, in fact, that a severe overtest has been employed. On the other hand, the additional data and the power spectra in particular indicate that something is awry with the test, and an undertest has occurred. It must be emphasized that there is nothing special or peculiar about the time history used for this test run. In fact, similar results were found to be present for all ground level tests that were utilized for signals generated from both random and earthquake sources. It is immediately obvious that this type of anomaly can affect most of the qualification tests that are performed today.

Other Questions and Problems

It is important to mention the current revision efforts of the IEEE 344 Committee, as a way of outlining some of the other questions and problems that are evident. Generally, these deal with both analytical and testing areas of qualification.

There are several aspects of basic accuracy in enveloping an RRS with a TRS. The matter of margin deals with how much conservatism is inherent in an RRS even before a TRS is attempted. There is also a move toward making spectral damping values more uniform. Tolerances associated with enveloping are also being considered because these have a very pronounced effect on the costs of tests.

Adequacy of simulated earthquake waveforms is of concern. In both analysis by time history and in testing some form of earthquake representation is generated; there needs to be more evaluation of the potential methods of generating the appropriate time histories. Associated with this is the addition of motion from other dynamic sources (i.e., valve closure, etc.). How can these additional effects be properly added to those of an earthquake?

Spectrum intensity or damage severity is a very important concept. It is especially necessary to allow comparison of the effects of one type of test (or assumed analytical load) with that of another. It is especially important for SQRT efforts in evaluating prior qualification of operating plants. This also leads to the question of in-situ testing.

Generic and type testing procedures need to be clarified more in detail. In particular, how effective is combined test and analysis for qualifying a series of valves of different sizes?

Several areas of qualification by analysis are being considered for revision. As an example, should some form of partial experimental verification be included in all analyses? Is this appropriate for qualification of multiple cabinet combinations?

Various questions remain with regard to line-mounted equipment. Should torsional effects of valves on attached pipes be included? Are narrow band random motion tests more representative than the large amplitude sine sweep tests now in use?

SOME ADDITIONAL DISTINCTIONS AND PROBLEMS

Interactive Environmental Testing

In general, environmental testing in the DOD area is performed prior to vibration, acoustic, and shock testing, and usually in that sequence. The purposes of the environmental tests are to "age" the test item prior to subjecting it to dynamics environments and to insure the ability of the test item to survive the specified environments. Environmental testing in the nuclear power plant area, however, involves subjecting the test item to the specified conditions both pre- and post-vibrations testing. The purpose of the pre-vibration exposure is again aging, while that of the post-vibration exposure is to demonstrate that the test item can remain functional under postulated abnormal plant operating conditions occurring after a "worst case" seismic event.

The sequence and type of environmental tests performed under DOD philosophies varies widely with both the intended use and location of the test item; i.e., sheltered or non-sheltered equipment, location within an aircraft, missile, ground vehicle, etc., and whether the equipment is classified as mechanical, electrical, armament, etc. In contrast, environmental tests for nuclear service have a fixed sequence regardless of the intended location of the test item; the test parameters are, however, a function of test item location and are specific as to both a given plant and location within that plant.

The variety and sequence of environmental tests generally to be performed for DOD and nuclear service are shown in Figure 20. The DOD tests include a group of temperature and

<u>DOD</u>		<u>NUCLEAR</u>
		PRE VIBRATION TESTS
LOW PRESSURE (ALTITUDE)	}	TEMPERATURE PRESSURE
HIGH TEMPERATURE		
TEMPERATURE SHOCK		
TEMPERATURE-ALTITUDE		THERMAL AGING OPERATIONAL AGING RADIATION AGING
SOLAR RADIATION (SUNSHINE)	}	WEATHERING
RAIN		
HUMIDITY		
FUNGUS		
SALT FOG		
DUST (FINE SAND)		
EXPLOSIVE ATMOSPHERE	}	EXTREME ENVIRONMENT
LEAKAGE (IMMERSION)		
ACCELERATION		
		VIBRATION TESTS
		POST VIBRATION TESTS
ACOUSTICAL NOISE		ENVIRONMENTAL EXTREMES: MILD ENVIRONMENT SEVERE ENVIRONMENT-LOCA MAIN STEAM LINE BREAK
SHOCK		
TEMPERATURE-HUMIDITY-ALTITUDE		
GUNFIRE VIBRATION		

Fig. 20 — Comparison of Interactive environmental tests for DOD and nuclear related component qualification tests

pressure extremes, a group which can be said to be related to weathering or outdoor environments, and a group of other specialized conditions; all of these precede the group of tests characterizing dynamic environments. The nuclear environmental tests are intended to produce long term aging characteristic of a 40-year service life and primarily in controlled indoor environments. Extreme condition testing is then conducted after the dynamic testing to simulate abnormal operating conditions in the plant.

Frequency Range

Vibration testing typical of DOD requirements involves frequency ranges representative of the environment produced by vehicles such as fixed and rotary wing aircraft, ground vehicles, and ships. The frequency ranges to be used in vibration testing are specified in a few standards (MIL-STD 810C, MIL-STD 167, Ships) and are of the order 10^{-1} to 10^3 Hz.

On the other hand, nuclear related vibration testing is relatively more complex because the frequencies depend heavily not only on the seismic event itself (1-35 Hz), but on the attenuation or amplification of the dynamic environment provided by the response of the building structure in which the equipment is located. Other dynamic events, such as the activation of steam relief valves, response of pipelines to internal flow conditions, etc., may therefore extend the frequency range of interest up to the order of 10^2 Hz. There are no general standards available to provide guidance in nuclear qualification testing, and therefore test conditions are defined by the many different A/E firms responsible for plant design. There are very wide differences resulting from site specific considerations and even from differences in engineering judgment as to what constitutes conservatism. After-the-fact evaluation and judgment as to the adequacy of the testing procedures greatly aggravates the cost of component qualification.

Equalization and Control in Dynamic Testing

Probably the oldest vibration test procedure adopted either by the DOD or the nuclear industry is the sinusoidal test. While this general test method is quite useful for determining system characteristics such as resonant frequencies and damping, its use as a generic qualification procedure is limited and often unsatisfactory because it generally results in highly overdesigned equipment. A similar generic test developed specifically for the nuclear industry is called the RIM (Required Input Motion) test. This test specifies a dwell (or beat) at the equipment resonant frequency at a base g level equal to the maximum expected peak in the earthquake transient, i.e., a dwell at the ZPA level. Unfortunately, even for the lightest weight equipment, this test is so demanding of the test facilities that it is rarely attempted.

An alternative form of dynamic testing involves the application of a specified transient (shock) or continuous random waveform time histories (PSD) to linear systems. There are stand-alone digital based equalization and control systems readily available that can reproduce these inputs on electromagnetic exciters which are linear with respect to acceleration control. On the other hand, electrohydraulic actuators which are nonlinear with respect to acceleration control (linear with respect to displacement control) often require

iterative procedures in addition to the FFT and inverse transform algorithms employed in linear control systems. There are several digital control system techniques now developed for shock spectrum enveloping. [26]

Vibration test levels representative of operational DOD environments are often now specified in terms of an acceleration power spectrum (recall that the PSD spectrum is the time average rms acceleration levels taken from stationary random response time histories). The response spectrum for earthquake simulation, on the other hand, is the peak response of a series of single degree-of-freedom oscillators to a nonstationary random time history input. During the strong portion of an earthquake event, a duration of approximately 15 seconds, the time history is for the most part stationary. Using these facts, trends are underway in the nuclear industry to employ a mapping between the two spectrum representations. [27] This would allow methods for correcting an elevated spectrum for known levels of overttest and combining response spectrum on an energy basis. The nuclear industry is historically response spectrum oriented; however, there are studies in progress to supplement the specifications with corresponding strong motion PSD spectra.

It is rather interesting to consider where in the DOD and aerospace areas the power/response spectrum specification would be appropriate as well. One might consider those portions of a maneuver spectrum where a nonstationary vibration response would occur, for example, during a transition from one maneuver to another or during deployment of weaponry from a flight vehicle. The importance of such considerations stems from the fact that in a PSD spectrum the expected peak acceleration to overall rms level is usually about 3.0 while values on the order of 5 to 7 can actually be experienced in a nonstationary input such as in the earthquake event.

ACKNOWLEDGMENTS

I wish to express my gratitude to my colleagues R. L. Bessey, J. C. Simonis, and J. F. Unruh for several interesting discussions, and especially to D. D. Kana on whose work this paper is mostly based.

REFERENCES

1. Pusey, H. C., "Shock and Vibration — An Essential Technology," *National Defense*, Sept.-Oct. 1975, pp. 124-126.
2. *Environmental Test Methods*, MIL-STD-810C, Department of Defense, Washington, D.C.
3. *Reliability Design Qualification and Production Acceptance Tests: Exponential Distribution*, MIL-STD-781C, Department of Defense, Washington, D.C., 21 October 1977.
4. Storey, B. M., Kana, D. D., and Cox, P. A., "Evaluation Program of the Vibration Environment of Armament Systems Externally Mounted to Army Helicopters," Rpt. No. RT-TR-69-34, U.S. Army Missile Command, Redstone Arsenal, Alabama, December 1969.

5. Crosswhite, B. L., Kana, D. D., and Cox, P. A., "Vibration Testing of the LANCE Missile System-Part I, Engineering Development and Contractor Qualification Tests," Project No. DA-1X222251D231, U.S. Army Missile Command, Redstone Arsenal, Alabama, November 1972.
6. Crosswhite, B. L., Kana, D. D., Cox, P. A., and Scruggs, M. S., "Vibration Testing of the LANCE Missile System-Part II, Engineering Tests/Service Tests," Project No. DA-1X222251D231, U.S. Army Missile Command, Redstone Arsenal, Alabama, August 1973.
7. Kana, D. D., and Scheidt, D. C., "Fatigue Damage Equivalence of Field and Simulated Vibrational Environments," Final Report, Contract No. DAAD05-74-C-0729, Southwest Research Institute, San Antonio, Texas, November 1974.
8. Kana, D. D., Huzar, S., and Bessey, R. L., "Simulation of the Vibrational Environment Affecting Reliability of Avionics Equipment Onboard U.S. Army Helicopters," Final Report, Contract No. DAAD05-70-G-0271, Southwest Research Institute, San Antonio, Texas, 1 May 1971.
9. Edgington, F.M., "Development of a Simultaneous Three-Axis Vibration System," TECOM Project 7-CO-RD5-WS1-081, U.S.A. White Sands Missile Range, New Mexico, December 1976.
10. Kana, D. D., "A Comparison of Reliability Tests for Avionics Equipment Onboard U.S. Army Helicopters," Final Report, Contract No. DAAD05-72-C-0228, Southwest Research Institute, San Antonio, Texas, April 1975.
11. Kana, D. D., and Dunn, B. H., "A Comparison of Field and Laboratory Reliability Tests for Helicopter Radio Equipment," Final Report, Contract No. DAAD05-76-C-0769, Southwest Research Institute, San Antonio, Texas, June 1977.
12. Hadjian, A. H., Jan, H. W., and Linderman, R. B., "The Seismic Environment for Nuclear Power Plant Components - An Interface Problem," ASME Paper No. 75-DE-53, American Society of Mechanical Engineers, New York.
13. U.S. NRC Standard Review Plan, Section 3.9.2, "Dynamic Testing and Analysis of Mechanical Systems and Components," U.S. NRC NUREG 75/087, November 24, 1975.
14. U.S. NRC Standard Review Plan, Section 3.10, "Seismic Qualification of Category I Instrumentation and Electrical Equipment," Revision 1, U.S. NRC NUREG 75/087.
15. IEEE Std. 323-1974, "IEEE Standard for Qualifying Class 1E Equipment for Nuclear Power Generating Stations," 1974, Institute of Electrical and Electronics Engineers.
16. "IEEE Recommended Practices for Seismic Qualification of Class 1E Equipment for Nuclear Power Generating Stations," Standard 344-1975, The Institute of Electrical and Electronics Engineers, Inc., New York, January 31, 1975.
17. U.S. NRC Regulatory Guide 1.100, "Seismic Qualification of Electrical Equipment for Nuclear Power Plants," Revision 1, August 1977.
18. "Draft American Standard, IEEE Trial Use Guide for Type Test of Class 1E Electric Valve Operations for Nuclear Power Generating Stations," Standard IEEE 382, Draft 3, Rev. 6, The Institute of Electrical and Electronics Engineers, New York, November 1978.
19. Skreiner, K. M., and Test, L. D., "A Review of Seismic Qualification Standards for Electrical Equipment," *Journal of Environmental Sciences*, May/June 1975, pp. 13-17.
20. Skreiner, K. M., Fitzgerald, E. M., and Test, L. D., "Seismic Qualification of Class 1E Equipment Today," *Journal of Environmental Sciences*, January/February 1978, pp. 19-23.
21. Bessey, R. L., and Kana, D. D., "Some Research Needs for Improved Seismic Qualification Tests of Electrical and Mechanical Equipment," Paper JP/2, *Structural Mechanics in Reactor Technology Conference - IV*, San Francisco, California, August 1977.
22. Kana, D. D., "Seismic Qualification Tests of Nuclear Plant Components - Damage Severity Factor Concept," *Nuclear Engineering and Design*, 59, pp. 155-170, 1980.
23. Singh, M. P., and Chu, S. L., "Stochastic Considerations in Seismic Analysis of Structures," *Earthquake Engineering and Structural Dynamics*, Vol. 4 (1976), pp. 295-307.
24. *Earthquake Engineering*, edited by R. L. Wiegel, Ch. 4, Prentice-Hall Inc., New Jersey, 1970.
25. Kana, D. D., "Consideration of a Unified Single-Parameter Measure of Fragility," *Proceedings of Seminar on Extreme Load Design of Nuclear Power Plant Facilities*, Berlin, Vol. I, pp. 117-120, August 1979.
26. Unruh, J. F., "Digital Control of a Shaker to a Specified Shock Spectrum," 52nd Shock and Vibration Symposium, New Orleans, October 27-29, 1981.
27. Unruh, J. F., and Kana, D. D., "An Iterative Procedure for the Generation of Consistent Power/Response Spectra," *Nuclear Engineering and Design*, 66, 1981 (in press).

REQUIRED DEVELOPMENTS IN STRUCTURAL DYNAMICS

Ben K. Wada
Jet Propulsion Laboratory
Pasadena, California

INTRODUCTION

First, you have to understand my background so when I cover the topics that require developments in structural dynamics, you know from what viewpoint I am approaching it.

I developed much of the information from my association with NASA for the past 20 years; I spent the last 15 years participating in discussions on structural dynamics needs of NASA. About four or five years ago, NASA Headquarters formed a team comprised of various members from the NASA Centers, and we visited many organizations in an attempt to find out what industry felt were some of the pressing needs in the area of structural dynamics. We visited a representative number of military aircraft, commercial transport aircraft, helicopter, and aircraft engine organizations. We obtained a broad perspective of the needs from industry.

As expected, each particular type of industry had certain unique requirements. However, rather than to cover the unique requirements and needs of the various industries, I decided to cover subjects which would interest the broad majority of the people here, not specific interests to individual companies. I will talk about what I feel are some of the current and future needs of the vast engineering community from an engineering point of view.

In order to project the future requirements, I tried to determine what some of the key developments were in the structural dynamics area in the past 15 to 20 years which significantly affected the engineers. There were only about two, three or possibly four areas where I feel significant developments have occurred, and where the engineers can use the output by-products. They were really determined, not by new developments in the area of applied mechanics, but by developments in other fields which allow the use of some of the information we already had.

At the risk of contradiction I will name those two or three developments; and again, this is strictly my opinion. One was the finite element method which came out 20 years ago, and it was linked to the development of computers which aided the engineers. Another development which might fall in that category is the modal component synthesis. With the development of computers you suddenly had a massive number of modes which had to be truncated in order to obtain solutions in a reasonable time. I think the third area is in the area of testing using the Fast Fourier Transform packages which allow you to extract the mode shapes and the natural frequencies from test data. I am trying to project the future developments that might exist in other fields, and how

we can take advantage of those to develop new areas of structural dynamics which would be contributory.

The other thing that I noticed was that, generally, many of the developments were conceived by theoreticians. The programmers develop programs, the experimentalists develop experimental techniques, and the educators instruct students. When completed, they have looked at it from their own perspective, and not from the engineer's point of view. Frequently the engineers are forced to use the products that these individuals developed. Today the developments are so expensive, like the development of the NASTRAN program, for example, that it is very difficult to start over or to reformat the resulting product. It is becoming very expensive, not only from the point of view of the total dollars spent, but also from the length of time it requires to develop some of these tools. We estimate anywhere from one hundred to five hundred million dollars per year being spent on structural dynamics at the current time. Many commercial firms who sell computer time estimate anywhere from 30%-50% of their total revenues come from structural dynamics or structures-type analyses, so a lot of money is involved. Also, the software is frequently fixed, again, because of the tremendous investment. There are many organizations, including JPL, that are not in a position to maintain their own software programs because of the expense. So, we rely on commercial firms which have a wide base of users to help support the maintenance of some of these programs; this is a trend toward better control of their tools.

Many companies indicated difficulty in obtaining correct solutions. An engineer must have a good idea of the finite element method, to be able to take a blueprint and properly model, to eliminate numerical round-off and convergence errors. Many companies are finding that they have a very difficult time finding people whose answers they would believe. In fact, many companies said, "Yeah, we have one or two guys that we trust to get the right answers." They might have 12 others who are just developing numbers, but that is understandable. We have structural dynamicists who know about D-map statements and the like, but they have very little feeling for what a structure is.

In the future, the feeling is that getting correct answers will be one of the key items. In fact, if you look at one of the new requirements, nonlinear analysis will be very significant, the reason being they are beginning to push the technology areas and the structures are beginning to interact more with their environment. Consequently, many more nonlinear influences tend to be significant. This is not a situation where

you can just add mass to keep it linear. For example, they are trying to increase engine performance with higher speeds and lighter blades, which enhanced the flutter problems in the blades. Even today the problem in nonlinear analyses is how do you know when you have converged on the right answer? Often, the only criteria we use is, if the answer looks right, we must have converged. I think many other organizations will have the same problem unless they have something to guide their answers.

One of the questions we asked four or five years ago at NASA Headquarters was, "What will the new software package be in the future?" The general feeling is that it is too expensive. They will possibly have to get multi-governmental sponsorship, if it will be sponsored by the government, and that will be very difficult, I think. I have a feeling that there will be another tool, but I do not know what it will be. And again, new requirements such as large space structures and nonlinear analyses will be very important.

CURRENT DEFICIENCIES

I will concentrate on only a few of the current areas of structural dynamics requiring additional effort. One is to correctly calculate mode shapes and natural frequencies for complex structures. With massive stacks of computer output, it is not a matter of "Where do people sit these days, it is where to put the computer output." With the quantity of data (not necessarily information), it is very difficult for analysts to use their physical intuition to validate the answers. They do not have access to the information in the concise form to allow them to use their physical intuition.

I think the engineers have lost much of the control of the analysis because they are using complex "canned" programs that many of the engineers do not understand in sufficient depth to easily modify the output to concisely obtained data to help establish validity of the results. Every experienced engineer has an approach to condense data and to evaluate the information to establish validity, which is not documented and thus not transferred to the inexperienced. Somehow part of the information should be incorporated into a computer program so other engineers can use it to validate the results.

One example of condensing data which are already in existing programs is to calculate the kinetic energy distribution in the mode shapes. Mode shapes per se are vector quantities while kinetic energy is really a scalar quantity. You can combine them. You can subdivide a system into as small a number of divisions as desired. A user can obtain a good insight of the character of a mode shape from its kinetic energy distribution by reducing the quantity of data and properly selecting a subdivision.

To help illustrate my discussion, I will use the results of a modal test of the Viking propulsion system which was performed about eight years ago. Figure 1 depicts the test setup which predominately consisted of two large, partially filled tanks held together by a series of structural members. Table I illustrates how the first two mode shapes were described with a very few numbers which represents the percentage of the total kinetic energy per mode.

Another method to reduce data is to calculate strain energy distribution of a mode shape (scalar quantity which

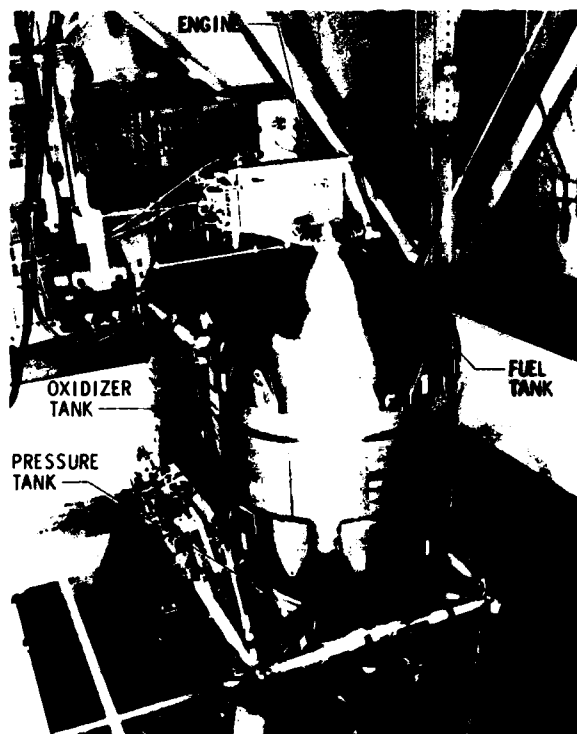


Fig. 1 — Original propulsion system model

can be algebraically added). The data provide information on the highly stressed areas of a structure for a particular mode, and provide insight on structure elements whose stiffness characteristics strongly influence the mode. If interested in changing stiffness to influence the mode, you must not concentrate on structure areas which necessarily have large displacements. For example, in the first mode of a cantilever beam, it is the base that has the highest strain energy and lowest displacement, whereas the tip has the largest displacement and smallest strain energy.

Inertial reactions at the base of a structure of various mode shapes allows you to calculate all of the lateral, axial or torsional modes which affect the interface loads. This information can provide valuable insight as to the proper subset of modes selected for a response analyses. One shouldn't arbitrarily select the number of lowest frequency modes which can be handled by a program. Table II illustrates effective weight evaluation.

Some of the valuable checks to help validate the results should be easily available to the engineer from a computer program. One is the rigid body motion. For each mode shape, a prescribed rigid body motion at its restraint will indicate ill-conditioning. As an example, if a unit motion results in motion of all nodes $> .99$, the mode shapes are sufficiently accurate to use in modal combination analyses, whereas values $< .99$ may result in ill-conditioning. The situation can be corrected by modifying the matrices to force near unity translation or modifying the mathematical model or using more accuracy in the computation.

In order to provide condensed data for the engineers, the computer programs must be adaptable to give each the information desired. This should include the option for an engineer to select the subdivision for kinetic energy and strain energy distribution and to quickly allow other information

necessary to help validate the results. The computer program can also be a repository of various methods and techniques used by engineers to check the results for the use of the inexperienced.

The next topic is correlation of math models with test data. Analysts use sophisticated methods to develop very complex mathematical models, and test engineers develop advanced test techniques. To some degree the test results and analysis never correlate. Often the goal is to update a math model to match the test data. At that point many organizations recognize a problem. "How do you update a gigantic math model to match the test data?" They go to all that trouble to obtain a sophisticated math model and test data, and very often techniques to update the math model to match the test data are not available. In an attempt to match the first and second modes, the other modes diverge. I think this situation has occurred on most programs. We made a few trial runs to attempt to update the math model and soon realized it was a long, hopeless problem to accomplish the task in a timely manner because the procedures were not automated. It was usually an engineer attempting to guess at the required changes. You have a model in the computer so let the computer help in updating math models to match the test results. Some work has been done. Several organizations, including JPL, have worked in this area, but I do not think we have the solution. I have some examples to illustrate this which I will discuss later. Another companion question is the criteria for correlation. There is almost no work in this area. We made an attempt to address the question at JPL several years ago, but we have not pursued it, not because it was not interesting, but because it was a tough problem. The tough problem is, "How close does a math model have to be to test data?" Should the frequencies be within 10% or 5%? The answer is not that simple. What will you use that model for? If it is for a forced response solution, what is the nature of the forcing function? If it is a transient-type forcing function,

Table I — Kinetic Energy Distribution, % of Total Kinetic Energy

MASS POINT AND DIRECTION	TEST	ORIGINAL ANALYSIS	MODEL A	MODEL B	TEST	ORIGINAL ANALYSIS	MODEL A	MODEL B
MODE 1					MODE 2			
OXIDIZER TANK	X				23.6	34.0	46.0	37.3
	Y	76.8	68.2	74.6	73.8			
	Z				50.1	35.1	18.7	27.8
FUEL TANK	X				13.8	16.7	21.3	18.0
	Y	18.0	24.3	18.5	19.1			
	Z				0.7	2.2	1.8	2.8

Table II — Effective Weight Comparison, % of Total Weight and Inertia

DIRECTION	TEST	ORIGINAL ANALYSIS	MODEL A	MODEL B	TEST	ORIGINAL ANALYSIS	MODEL A	MODEL B
MODE 1					MODE 2			
w_x					31.6	44.7	60.7	48.5
w_y	83.3	84.3	83.0	82.2	1.2	1.0	0	0
w_z	0	0.2	0.5	0.5	27.2	15.5	7.3	10.5
i_x	95.0	96.0	96.5	96.6	0	0.3	0	0
i_y					80.3	92.1	95.1	94.7
i_z	17.4	11.9	16.1	16.2				

then the correlation criteria differs from the criteria for a sinusoidal input. For instance, damping might be a significant factor. In one case it is important, and in other cases it is not. Is it for calculating accelerations? Is it for calculating internal member loads for structural design purposes? Those are two very distinct objectives. Are they to be used for control purposes? So again, depending upon how the data are used, the criteria for correlation will differ. In our work, we took a very simple case. We stated that we wanted the accelerations to within 10%, and we also stated that the forcing function was impulsive in nature. Then we were able to arrive at the correlation between the math model and the test data we needed to achieve accurate answers. I think there is very little serious research going on in this whole correlation criteria issue. I think engineers are always faced with that problem and they use either engineering guesses, or they proceed by default because they don't have an alternative.

Table III illustrates some of the efforts we tried to update the math model of the same propulsion system shown in Figure 1 to match test data. Again, of the same propulsion system. We grouped them into different groups of elements called them ABCDEFG. We analytically perturbed these elements by as much as 40%. Once we had the analytically perturbed structure, we attempted to use the math model updating procedure to converge to the original answers. Table IV shows the original frequencies and mode shapes

on the math model. Then we used iteration procedures which did allow convergence of the perturbed model to the original answers. So in a research sense, we found that if you used analytically perturbed models, many procedures developed by various investigators do converge to the original answers.

Table V illustrates the convergence when we tried the same procedure on real test data. We tried perturbing the math model in two ways to converge upon the test frequencies. In Model A we perturbed the stiffness elements, and once we did the best we could after changing the stiffness elements, we perturbed the mass elements. In Model B, we first perturbed the mass elements, then we perturbed the stiffness elements. We found that many of the procedures to update a math model with real test data do not work. I think the situation is that a math model doesn't contain the information needed to converge on the test data, or there are nonsystematic errors in the test data which aren't present in mathematically simulated test data.

The next logical significant area requiring effort is to establish a criteria for "goodness" of the correlation between analysis and test. Very little work has been performed in this area. An example of a simple criteria is shown in Table V. For mode 1, the difference between the test frequency and the original and updated math models are shown in parenthesis as (0.58), (0.55) and (-0.47) which indicates an improvement. An overall comparison for the first ten modes is shown at the bottom of Table V and it is the root-sum-square of the difference. They are 7.29 Hz, 3.52 Hz and 3.62 Hz which indicates an overall improvement. We tried many ways of establishing the criteria in addition to root sum of the squares which included absolute values, and weighted values. Then we realized that the values of direct interest to us were not frequencies but dynamic loads which are used to establish design loads. Comparing the root-sum-square of the modal force coefficients of two typical elements (Table VI), the errors increased as the difference in frequencies were decreased. The criteria for "goodness" of correlation has not been established and most likely is dependent on the unique requirements of the particular problem.

Table III — Perturbed Analytical Model Member Grouping

GROUP	DESCRIPTION	PERTURBATION
A	SIDE BIPODS, 4 MEMBERS SUPPORTING THE TANKS IN A VERTICAL PLANE	+40%
B	TOP BIPODS, 4 MEMBERS SUPPORTING THE TANKS IN A HORIZONTAL PLANE	-30%
C	3-HOLE TANK TABS, 4 SUPERELEMENTS THAT FORM THE LINK BETWEEN THE SIDE BIPODS AND THE RIGID TANK	+30%
D	TOP SIAMESE TANK TABS, 2 SUPERELEMENTS CONNECTING THE TWO TANKS AT THE TOP	-20%
E	BOTTOM SIAMESE TANK TABS, 2 SUPERELEMENTS CONNECTING THE TWO PLANES AT THE BOTTOM	+40%
F	PRESSURANT TANK ROUND MEMBERS, 3 MEMBERS SUPPORTING THE PRESSURANT TANK	+30%
G	PRESSURANT CONTROL ASSEMBLY (PCA) SUPPORT STRUTS, 4 MEMBERS SUPPORTING THE PCA	+40%

Table IV — Frequency Convergence of Perturbed Analytical Model

MODE NO.	ORIGINAL MODEL FREQUENCY, Hz	PERTURBED MODEL FREQUENCY, Hz	ITERATION				
			1st, Hz	2nd, Hz	3rd, Hz	4th, Hz	5th, Hz
1	12.37	13.49	11.87	12.34	12.36	12.37	12.37
2	15.85	16.34	15.07	15.83	15.85	15.86	15.85
3	19.37	20.29	18.51	19.34	19.37	19.38	19.37
4	26.49	26.25	26.49	27.15	26.24	26.48	26.49
5	27.90	28.30	27.50	28.13	27.95	27.91	27.90
6	34.19	34.29	34.08	34.26	34.17	34.20	34.19
7	42.06	42.64	41.66	42.09	42.09	42.08	42.06
8	47.69	49.43	45.10	47.49	47.62	47.97	47.69
9	52.39	52.61	51.56	52.49	52.48	52.41	52.39
10	52.51	54.21	52.41	52.65	52.65	52.50	52.51
11	60.47	61.94	58.65	60.34	60.30	60.52	60.47
12	60.96	64.23	59.48	61.21	61.26	61.05	60.96

*CONSIDERED AS THE TEST DATA TO WHICH THE PERTURBED MODEL IS TO CONVERGE.

Table V — Comparison of Test Frequencies to the Original and the Improved Models

MODE NO.	TEST FREQUENCY, Hz	ORIGINAL MODEL FREQUENCY, Hz	MODEL A FREQUENCY, Hz	MODEL B FREQUENCY, Hz
1	12.95	12.37 (0.58)*	13.50 (-0.55)	13.42 (-0.47)
2	17.66	15.85 (1.81)	17.59 (0.07)	17.28 (0.38)
3	20.80	19.37 (1.43)	20.67 (0.13)	20.98 (-0.18)
4	22.97	26.49 (-3.52)	22.94 (0.03)	22.97 (0.00)
5	28.33	27.90 (0.43)	28.35 (-0.02)	28.34 (-0.01)
6	32.76	34.19 (-1.43)	32.74 (0.02)	32.76 (0.00)
7	42.80	42.06 (0.74)	42.85 (-0.05)	42.85 (-0.05)
8	50.67	47.69 (2.98)	50.32 (0.35)	50.48 (0.19)
9	50.40	52.39 (-1.99)	52.73 (-1.56)	52.40 (-2.00)
12	65.38	60.96 (4.42)	62.28 (3.10)	62.43 (2.95)
RSS OF DIFFERENCE				
ALL 10 MODES		7.29	3.52	3.62
FIRST 6 MODES		4.50	0.57	0.63

*THE VALUES IN PARENTHESES REFER TO THE DIFFERENCE TEST FREQUENCY LESS MODEL FREQUENCY.

Table VI — Force Coefficients, Newtons

MEMBER NO.	TEST vs ANALYSIS	MODE NO.					RSS
		1	2	3	4	5	
4	TEST	-2527.5	343.0	-1183.7	-237.1	-194.4	
	ORIGINAL ANALYSIS	-2548.4	502.2	-1055.6	-491.5	-186.4	327
	MODEL A	-2977.8	768.4	-535.5	-321.2	-437.1	932
	MODEL B	-2930.6	689.4	-896.8	-307.2	-324.9	622
3	TEST	-297.1	-387.4	379.4	402.6	327.8	
	ORIGINAL ANALYSIS	-328.3	-488.0	323.4	552.0	433.7	219
	MODEL A	-303.7	-619.8	77.0	345.2	543.1	442
	MODEL B	-332.0	-629.1	187.1	354.5	486.5	352

For the lack of time, I will briefly touch upon other areas. The next topic is modal synthesis. There are computer programs, like NASTRAN, one can use for modal synthesis. One of the problems is that in order to use the modal synthesis technique, unlike the finite element method, engineering judgement must be used, and it is very easy to make undetectable errors. The correct displacement functions must be selected; if you add erroneous displacement functions, they may unduly constrain a structure which can't be easily detected. If you include dependent modes, the matrices become singular; there are many engineering errors that can be made that go undetected. I believe that very few engineers have sufficient insight to the analysis process to get good solutions using modal synthesis. Many of the "learned" process and check procedures should be incorporated as part of a computer program to document the experience.

Another topic is the accuracy of the response calculations. Difficulty exists in approximately calculating the least upper bound of the loads within the structure subjected to a dynamic forcing function. This situation exists in attempting to evaluate spacecraft loads from the launch vehicle (or Shuttle) as the dynamic characteristics of the spacecraft are modified.

Another very important problem requiring work is the "inverse" problem of determining the forcing function from the response data. Although the mathematics of the solution are not difficult and the "inverse" solution has been shown to be valid on mathematically simulated cases, the procedure has not resulted in satisfactory answers using real flight or test data. I think the primary reason for failure is that the frequencies and impedances of the math model did not adequately represent the real structure.

FUTURE

At JPL we ask, "What are the trends?" We are looking at this, and we are trying to determine where we should do our research, and in what areas we should invest some of our research funds. One trend is toward distributed computing. We feel computing is going toward the small mini computers spread throughout various facilities, and the big central computing facilities are beginning to disappear. One of the activities at JPL is to develop a VLSI for finite element computation in conjunction with parallel processing using our own large integrated circuit design and fabrication facility. The objective is to increase the speed and accuracy for computation to prepare for the future needs. Again, the hardware costs are decreasing, and software costs are increasing, both for its development and its maintenance. We cannot afford to maintain NASTRAN; we need experienced programmers

that will always be available. So in essence, we are going to computer centers to buy our NASTRAN, ANSYS, and other programs because it is just too expensive for us to develop computing capability and maintain the software. What is the next NASTRAN? Nobody knows, but I think more sophisticated tools will be required. The problems will be more complex and there will be many more analysts attempting to solve these very complex problems. The lack of engineers today to obtain solutions to complex problems will be enhanced in the future years.

One of the future requirements will be much more reliance on analysis than there is today. One reason is testing is extremely expensive and becoming more complex. Structures that interact more with their environment will be more prominent in the future because of the trend toward higher performance or a high area to density ratio. Nonlinearities will become more significant to the design resulting in test difficulties because of the difficulty in separating the cause and the effect. Large space structures will be another problem because they cannot be tested on earth. Six years ago JPL worked on a solar sail concept for propulsion. The concept was to build a 0.35 square mile 1/10 mil Kapton sail and use the solar pressure for propulsion. One reason the concept was eventually eliminated is that the dynamic analysis performed without a system test was not adequate to commit the solar sail for a mission. A system test couldn't be performed on earth. Thus I foresee requirements for higher confidence analyses of large complex structures, test verified subsystems which are mathematically integrated into a larger structure, requirements that are insensitive to structural characteristics of the characteristics.

I see a large number of problems and a number of different hardware and software tools available to the engineer for solving them. The engineers will select the appropriate set of tools to solve a problem with the help of a control activity to increase efficiency and accuracy. Preliminary efforts to evaluate the cost is under study at Duke University to simulate the cost of parallel processing computation versus serial processing computation for user defined problems. Other objectives are to establish the cost advantage of parallel processing and to evaluate the potential cost savings of numerical algorithms developed specifically for parallel processing. An example may be the introduction of the relaxation method of solving a series of linear equations.

We feel that artificial intelligence techniques, or some way of feeding back information to provide solution guidance to the engineers about their proposed solution technique, or methods to help assure accuracy of the results, must be provided with the analyses tools to solve the more complex problems with a larger arsenal of solution tools.

We have helped develop a program by which an engineer can interactively try different displacement functions to describe a finite element to help establish the impact of the assumption.

In summary, I tried to cover briefly what I feel the current problems are in structural dynamics from an engineer's point of view. Using history as a guide, major future contributions in structural dynamics will be closely related to developments in allied fields. We must provide the engineers with added tools and proper information with adequate feedback and flexibility to allow use of good engineering judgement and intuition. Engineering judgement will still be vital to obtaining answers in the future.

DISCUSSION

Mr. Himelblau (Rockwell International Corp.): You mentioned two of the more serious problems that we currently face; one is the accuracy in response calculations and the second, as you call it, is the inverse problem of determining loads from response. But the real key is the lack of information on damping, and I think this has been an issue that has not been faced in the last 20 years or more with possibly one exception. It appears to me on the basis of all of the future trend prognostications that I've seen, including your own, that that issue is still going to remain unfaced. I'd like your reaction.

Mr. Wada: I know how Harry feels. My feeling is that it is very difficult to predict damping beforehand. You can do all the analysis you want, but from everything I have seen damping is governed by factors such as joint slippage that can't be predicted. So, even if you did a million degrees of freedom finite element analysis to predict damping you will not get a better answer. I think it is the sort of situation where unless you actually build a damping device where you

want to know a prescribed value and properly put it into the design, you will have a very difficult time predicting it. Yes, it is important, but I feel there is little that can be done except to use good engineering judgment plus past experience to guess at some of the numbers.

Mr. Himelblau: Then why are we spending literally millions of dollars to develop computer codes to determine mode parameters, with one exception, and why don't we put any research money into the one factor that we recognize is one of the major deficiencies?

Mr. Wada: I don't give out the money, but when you spend money, you are looking for the return on the investment. If I look at damping, the return of research is very small or zero.

Mr. Himelblau: How large was the investment that you gave for that return?

Mr. Wada: It doesn't matter. If the return is zero, I don't think you should invest any money, but that is a personal feeling. There are specific special purpose dampers, and there are many organizations that provide them. But I think you are asking for research to predict modal damping, and we tried it. We tested riveted and bolted joints, and we found their damping was a function of manufacturing and a function of amplitude. There are so many variables that we couldn't even determine a trend. If you plot damping versus design, it is just like a big shotgun blast, and the general feeling was that it is so manufacturing-dependent that research in that area just didn't seem to make any sense.

Mr. Himelblau: So, you are saying that if we really can't get a handle on it, we should just try to ignore it.

Mr. Wada: No. No. No. You can't ignore it. You have to use your engineering judgement.

EFFECT OF SEALS ON ROTOR SYSTEMS

David P. Fleming
NASA Lewis Research Center
Cleveland, Ohio 44135

Seals can exert large forces on rotors. As an example, in turbopump ring seals film stiffness as high as 90 MN/m (500 000 lb/in) have been calculated. This stiffness is comparable to the stiffness of rotor support bearings; thus seals can play an important part in supporting and stabilizing rotor systems. This paper reviews the work that has been done to determine forces generated in ring seals. Working formulas are presented for seal stiffness and damping, and geometries to maximize stiffness are discussed. An example is described where a change in seal design stabilized a previously unstable rotor.

INTRODUCTION

Ring seals have received considerable study over the past dozen years. The principal reason for this attention is the increasing importance of seals in affecting the dynamic response of machinery. Large forces can be generated between shafts and seals; these forces can be useful in supporting and stabilizing rotating machinery. Conversely, improperly designed seals can promote instability.

Figure 1 illustrates a ring seal. This seal has the appearance of a journal bearing, so it is not surprising that bearing-like forces can be generated. Seals typically have larger clearances than bearings; thus hydrodynamically generated forces would be lower. (Stiffness, which equals force/displacement, changes as the inverse cube of clearance for laminar flow. Stiffness is frequently used rather than force to characterize a seal or bearing.) However, the pressure drop across a seal yields a hydrostatic force which varies directly with the pressure drop. This force can be quite large in high-pressure machinery; for example, the interstage seals of the Space Shuttle fuel pump, with a pressure drop of 140 bars (2000 psi) has a calculated stiffness of 38 MN/m (220 000 lb/in.) [1].

The purpose of this paper is to review the development of force determination in ring seals, and to present the latest, most accurate methods of calculating seal forces. Additionally, seal geometries to maximize generated forces will be discussed. An example of seal effect on rotordynamic behavior will also be presented.

SYMBOLS

A	defined by Eq. (22)
a	defined by Eq. (23)
B	seal damping coefficient
\bar{B}	dimensionless damping, $\frac{BC}{L^2 D \sqrt{\rho_0 \rho}}$
\tilde{B}	dimensionless damping, $\frac{BC}{L^2 D \sqrt{\gamma \rho_0 \rho_0}}$
C	radial clearance of concentric seal
\bar{C}	dimensionless damping, $\bar{B} \sqrt{\frac{8}{n + 2\sigma}}$
D	seal diameter
E	defined by Eq. (21)
F	seal radial force
G	seal inertia coefficient
h	local seal clearance
K	seal stiffness
\bar{K}	dimensionless stiffness, $\frac{KC}{\rho_0 L D}$

L	seal length
M	leakage flow
p	pressure
q	Rw/U
R	seal radius
Re	Reynolds number, $2C\rho U/\mu$
Re_0	"sonic" Reynolds number, $2C\sqrt{\gamma p_0 \rho_0}/\mu_0$
u	local fluid velocity
U	u for centered seal
V	swirl velocity
W	swirl ratio V/Rw
x,y	transverse coordinates
z	axial coordinate
α	seal taper half-angle
γ	specific heat ratio
ϵ	eccentricity ratio e/c
η	total entrance loss factor $1 + \xi$
λ	friction factor
μ	fluid viscosity
ξ	entrance loss factor
ρ	fluid density
σ	dimensionless seal length $\lambda L/C$
ω	angular velocity

Subscripts:

0	upstream stagnation region
1	seal entrance
2	seal exit

ANALYTICAL PRINCIPLES

In the earliest analyses numerous simplifying assumptions were made. Later work removed some of these assumptions. In order to aid in understanding how a high-pressure seal operates, it is useful to go through the most elementary analysis. For this analysis the list of assumptions is, of course, the longest and reads

1. The sealed fluid is incompressible.
 2. Effects of rotation are neglected.
 3. Fluid flow is one-dimensional in the axial direction, that is, any circumferential flow is neglected.
 4. The eccentricity is small compared with the seal concentric clearance.
 5. The fluid friction factor is constant throughout the seal.
 6. All flow is steady state.
 7. Entrance losses can be accounted for by a suitable choice of loss coefficient.
 8. There is no pressure recovery at the seal exit.
- The analysis begins with the continuity and momentum equations. These are given in [2] and for invariance with time are

$$h \frac{du}{dz} = 0 \quad (1)$$

$$-\frac{1}{\rho} \frac{dp}{dz} = \lambda \frac{u^2}{h} + u \frac{du}{dz} \quad (2)$$

The boundary conditions are

$$p = p_0 - \eta \rho u^2 / 2 \quad \text{at } z = 0 \quad (3)$$

$$p = 0 \quad \text{at } z = L \quad (4)$$

where η is the total entrance loss factor. It is the sum of the pressure drop, $\rho u^2 / 2$, that occurs due to Bernoulli's principle, and the pressure drop due to the developing velocity profile in the fluid. The value of η is 1.65 for laminar flow [3] and drops to near 1 for highly turbulent flow [4]

The solution to Eq. (1) is

$$u = \text{constant} \quad (5)$$

and to Eq. (2)

$$p = p(z = 0) - \frac{\lambda z \rho u^2}{h} \quad (6)$$

Applying the boundary conditions,

$$p_0 = \rho u^2 \left(\frac{\eta}{2} + \frac{\lambda L}{h} \right) \quad (7)$$

$$p = p_0 (L - z) \left/ \left(\frac{\eta h}{2\lambda} + L \right) \right. \quad (8)$$

The total restoring force on the seal can be found by integrating the restoring component of pressure over the seal area

$$F = -R \int_0^{2\pi} \int_0^L p \cos \theta \, dz \, d\theta \quad (9)$$

The local clearance h is given by

$$h = C(1 + \epsilon \cos \theta) \quad (10)$$

Invoking the small eccentricity assumption ($\epsilon \ll 1$), and substituting Eqs. (8) and (10) in (9),

$$F = \pi \lambda R p_0 L^2 n C \epsilon / (nC + 2\lambda L)^2 \quad (11)$$

or, defining a dimensionless stiffness \bar{K}

$$\bar{K} = \frac{F}{\epsilon p_0 L^2} = \frac{\pi n \sigma}{2(n + 2\sigma)^2} \quad (12)$$

where

$$\sigma = \lambda L / C \quad (13)$$

Having derived this simple expression for seal stiffness, we can use it and the seal model to gain some understanding of how the seal develops its stiffness. Figure 2 shows the fluid pressure in the concentric seal as a function of axial distance. After an initial abrupt drop (due to the Bernoulli effect and entrance loss, Eq. (3)), the pressure drops linearly to zero at the exit. The clearance and fluid velocity are uniform around the circumference.

Now consider what happens when the seal is moved to the side, Fig. 3. The clearance varies around the circumference according to Eq. (10). On the high-clearance side, the fluid can move faster than before, and, conversely, on the low-clearance side it has to go slower. The entrance pressure drop depends on the fluid velocity, so there's a greater initial drop on the high-clearance side. On both sides, the pressure must drop to zero at the seal exit. Thus the pressure profiles look like those depicted in Fig. 3. The pressure is generally higher on the low-clearance side, and this results in a force that tries to center the seal.

Figure 4 is a plot of the dimensionless seal stiffness, \bar{K} , versus the parameter σ which may be thought of as a dimensionless seal length. The entrance loss factor was chosen as $n = 1.1$, which is a value representative of turbulent flow. For low values of σ (i.e., short seals) stiffness rises with seal length. A peak is reached, and then stiffness drops as length increases. This phenomenon may be explained as follows: for very short seals, the entrance effect is the dominant pressure drop mechanism, that is, the seal behaves somewhat as an orifice. With wall friction playing such a small part, the pressure profile does not change much with seal eccentricity (see Fig. 5) and thus the stiffness is low. Conversely, for long seals wall friction causes the bulk of the

pressure drop and again the pressure profile changes little with eccentricity. Thus the greatest stiffness occurs when the pressure drop due to entrance effects is comparable to that due to wall friction. This is similar to the situation in externally pressurized bearings, where for maximum stiffness the restrictor pressure drop equals the film pressure drop. To carry the analogy further, one could say that the seal entrance is analogous to the restrictor in a pressurized bearing.

A SHORT HISTORY OF ANALYTICAL DEVELOPMENT

The foundations of seal force analysis were laid by Henry Black and coworkers [5,6,7]. In keeping with the assumptions listed above, Black's analyses are one-dimensional. Essentially, Black looks at flow in a duct with a wall which moves transversely; thus the flow is unsteady. The results consist of coefficients for stiffness, damping, and inertia, such that the force on the seal is given by

$$F = Kx + B\dot{x} + G\ddot{x} \quad (14)$$

In [6], shaft rotation is accounted for by assuming that the entire flow field rotates at one-half the shaft speed. The fluid equations are solved in a coordinate system which also rotates at half shaft speed (with fluid being assumed to flow axially in the rotating system). A coordinate transformation then yields an expression for forces on the shaft in the x and y directions

$$\begin{bmatrix} F_x \\ F_y \end{bmatrix} = - \begin{bmatrix} K - \frac{1}{4} G\omega^2 & \frac{1}{2} B\omega \\ -\frac{1}{2} B\omega & K - \frac{1}{4} G\omega^2 \end{bmatrix} \begin{bmatrix} x \\ y \end{bmatrix} - \begin{bmatrix} B & G\omega \\ -G\omega & B \end{bmatrix} \begin{bmatrix} \dot{x} \\ \dot{y} \end{bmatrix} - \begin{bmatrix} G & 0 \\ 0 & G \end{bmatrix} \begin{bmatrix} \ddot{x} \\ \ddot{y} \end{bmatrix} \quad (15)$$

K , B , and G are the same as those for the nonrotating case. Black did, however, modify the friction factor to account for the additional fluid velocity due to rotation. For turbulent flow

$$\lambda = 0.079 \left(\frac{2\rho UC}{\mu} \right)^{-1/4} \left[1 + \left(\frac{7}{16} \frac{R\omega}{U} \right)^2 \right]^{3/8} \quad (16)$$

This form was suggested by Yamada [8]. It may be noted that the mean flow velocity U is not known *a priori*; it must be found through iterative solutions of Eqs. (7) and (16). In [7], the circumferential variation of friction factor is accounted for; this results in a substantial increase in the direct stiffness coefficient K_{xx} (Fig. 6) but relatively small changes in the damping and inertia coefficients, compared with the constant friction factor

solution. As Fig. 6 shows, the rotational velocity affects the results; stiffness rises as rotational speed increases and, as shown in [7], damping decreases.

The works cited up to now have all used a small eccentricity analysis and presented results for small perturbations about a centered seal position. Allaire, Lee, and Gunter [2] extended the analysis to obtain results for a perturbation about a finite eccentricity position. They employed numerical integration to obtain stiffness, damping, and total load capacity for various seal eccentricities. In another departure from earlier analyses, the authors of [2] neglected the time variation of fluid velocity in the governing equations. This change simplifies the solution procedure but inevitably introduces some inaccuracy in the calculated damping coefficient (the stiffness is unaffected). In [1] this inaccuracy was found to be no more than 16 percent, with the simplified solution overestimating the damping.

The results of the finite eccentricity calculations showed that, in general, seal stiffness and damping are not much affected by eccentricity (Figs. 7 and 8). The exception is the damping in the direction of displacement, where, as would be expected, the damping coefficient increases considerably as the seal journal approaches the side wall. Seal rotation was not considered in [2].

Effect of inlet swirl. - As noted above, Black [6] accounted for seal rotation by assuming that the fluid circumferential velocity is one-half of the shaft speed throughout the seal. Actually, the fluid velocity only approaches this limit asymptotically as it proceeds through the seal. In applications such as centrifugal pump interstage seals, the fluid may enter the seal with little or no rotational velocity. Furthermore, if the seal length is short, fluid rotational speed may differ appreciably from the half-shaft-speed asymptotic value even at the seal exit. Thus seal dynamic properties are likely to vary with the amount of inlet swirl present. The effect of inlet swirl has been investigated in two papers, one by Black, Allaire, and Barrett [9] and one by Childs [10]. The analysis in [10] is the more comprehensive, as it solves the short-bearing turbulent lubrication equations of Hirs [11,12]. Since several of the assumptions listed in the Analysis section need no longer be made, it is worthwhile to list those assumptions still required by [10].

1. The sealed fluid is incompressible.

2. Pressure-induced circumferential flow is neglected (the "short bearing" approximation [13]).

3. The eccentricity is small compared with the seal concentric clearance.

4. Entrance losses can be accounted for by a loss coefficient.

5. There is no pressure recovery at the seal exit. Childs results [10] for direct and cross-coupled stiffness and damping are given for turbulent flow by

$$\begin{aligned} K_{xx} = K_{yy} = & \frac{\pi \sigma}{n + 2\sigma} \left\{ 1.25E - \frac{1}{\sigma} \left(L \frac{q}{D} \right)^2 \left\{ \frac{1 + 6E}{12} \right. \right. \\ & \left. \left. + \frac{2W_1 - 1}{a} \left[\left(E + \frac{1}{a^2} \right) (1 - e^{-a}) - \left(\frac{1}{2} + \frac{1}{a} \right) e^{-a} \right] \right\} \right\} \end{aligned} \quad (17)$$

$$\begin{aligned} K_{xy} = -K_{yx} = & \frac{\pi \sigma L q}{D(n + 2\sigma)} \left\{ \frac{E}{\sigma} + \frac{A}{12} (1 + 6E) \right. \\ & \left. + \frac{2W_1 - 1}{a} \left\{ AE + \left(\frac{1}{\sigma} - \frac{A}{a} \right) \left[(1 - e^{-a}) \left(E + \frac{1}{2} + \frac{1}{a} \right) - 1 \right] \right\} \right\} \end{aligned} \quad (18)$$

$$B_{xx} = B_{yy} = \frac{\pi \sigma}{\sqrt{2}(n + 2\sigma)} \left[\frac{E}{\sigma} + \frac{A}{12} (1 + 6E) \right] \quad (19)$$

$$\begin{aligned} B_{xy} = -B_{yx} = & \frac{\sqrt{2} \pi L q}{D \sqrt{n + 2\sigma}} \left\{ \frac{1 + 6E}{12} \right. \\ & \left. + \frac{2W_1 - 1}{2a} \left[(1 - e^{-a}) \left(E + \frac{1}{2} + \frac{1}{a} \right) - \frac{1}{2} - \frac{e^{-a}}{a} \right] \right\} \end{aligned} \quad (20)$$

$$E = \frac{n}{2(n + B\sigma)} \quad (21)$$

$$A = 1 + \frac{3}{q^2 + 4} \quad (22)$$

$$a = \sigma \left(1 + \frac{0.75 q^2}{q^2 + 4} \right) \quad (23)$$

Also, q is defined as the ratio of journal rotational speed to mean axial velocity,

$$q = \frac{R\omega}{U} \quad (24)$$

The initial swirl ratio W_1 is the ratio of circumferential fluid velocity at the seal entrance to the journal speed.

$$W_1 = \frac{V_1}{R\omega} \quad (25)$$

The swirl ratio approaches 1/2 as the fluid proceeds through the seal; $W_1=1/2$ implies the half-journal speed assumption of Black and Jenssen [6].

While the expressions above appear complicated, they can be programmed on a pocket calculator or digital computer in a straightforward manner. Figure 9 shows the results of the calculations. The seal used for these calculations has a length to diameter ratio of 1/2; the circumferential journal speed is 1/2 that of the mean axial fluid velocity.

As expected, preswirl has a stronger effect for small values of σ , the dimensionless seal length. The larger the initial value of circumferential fluid velocity, the smaller is the direct stiffness and the larger the cross-coupled stiffness and damping, while direct damping is completely unaffected. Cross-coupled stiffness is usually viewed as promoting instability. Small values of preswirl reduce K_{xy} and thus would appear to be stabilizing. The authors of [9] point out that negative preswirl - the fluid revolving opposite the direction of shaft motion - can result in negative K_{xy} and thus counteract whirl-producing forces elsewhere on the shaft.

State of the art. - This term is used with some misgivings, as ring seals continue to receive intensive study and new publications appear frequently.

Equations (17) to (20) presented above appear to be the most comprehensive available to calculate seal stiffness and damping, requiring the fewest simplifying assumptions and presenting results in explicit form. Results are limited to small displacements from the centered position, but, as shown in [2], seal stiffness and damping are largely insensitive to seal eccentricity. The source of Eqs. (17) to (20), [10], also presents expressions for inertia coefficients, but these are usually of minor importance.

Recently two authors have investigated seals of finite length (thereby eliminating the short seal assumption). In [14] the turbulent Reynolds equation was solved numerically for finite eccentricity ratios, using the finite element method. Childs, in [15], starts with Hirs' bulk flow equations [11,12], transforms them to ordinary differential equations by small eccentricity assumptions, and integrates numerically. Both references report that the short seal solution overestimates the seal coefficients with the error increasing for longer (L/D) seals.

In this connection, Black and Jenssen [6] proposed correction factors for finite length seals based on an approximate analysis. The results of [14] and [15] indicate that these factors result in overcorrection. A more accurate formula would seem to be

$$\left\{ \begin{matrix} K \\ B \end{matrix} \right\}_{\text{finite}} = \left\{ \begin{matrix} K \\ B \end{matrix} \right\}_{\text{short}} \frac{1}{1 + 0.6 \left(\frac{L}{D} \right)^2}$$

EXPERIMENTAL CORRELATION

Experimental data, particularly dynamic data, are very sparse. Black and Jenssen show results of experiments in [6] and [7] for axial Reynolds numbers up to 20 000 and rotational Reynolds numbers (based on half journal speed) up to 14 000. Both unidirectional and rotating load (due to unbalance) tests were run. In both papers, agreement between analysis and experiment is shown as close, although the analysis of [7] employed the local friction factor effect while that of [6] did not. Childs and Dressman [16] have presented preliminary results which show that measured direct stiffness is generally a good deal higher than predicted by [10] (to 90 percent) while direct damping is much lower than predicted.

OPTIMUM GEOMETRIES

Thus far it has been tacitly assumed that the seal clearance is constant in the axial direction; in other words the seal has a straight bore. From physical reasoning it is easy to see that the direct stiffness would be higher if the clearance at the fluid exit were less than at the entrance. In [17] Fleming calculated stiffness for seals with stepped and tapered bores (Fig. 10) and determined optimum geometries to maximize either the stiffness K or the ratio of stiffness to leakage K/M . This was followed with calculations for damping in tapered bore seals [1]. Figure 11 shows that substantial increases in stiffness are possible with an optimum taper configuration. The stiffness increase is obtained with only a moderate leakage penalty. The inlet-to-outlet clearance ratio for the maximum K/M seal is nearly constant over the entire range of dimensionless seal lengths (σ) shown in Fig. 11 having a mean value of 1.9. Direct damping is lower in tapered seals as shown in Fig. 12. This is principally because of the tapered seals larger average clearance (tapered and straight bore seals are compared using the minimum clearance in the seal). More recently Childs extended his solution of Hirs' lubrication equations to tapered bore seals [18]. His results agree qualitatively with those of [1] and [17]. Childs considers variable inlet swirl and rotational effects within the constraint of the short bearing approximation; thus greater accuracy would be expected.

SEALS FOR COMPRESSIBLE FLUIDS

The flow of a compressible fluid (most commonly a gas) differs from that of an incompressible fluid in that changes in pressure are accompanied by changes in pressure and temperature. For flow through a seal - usually approximated as adiabatic - as the pressure drops along the flow path the density and

temperature also drop, and the velocity increases. Except for the special case of a converging-diverging channel, the maximum fluid speed is limited by the speed of sound. Thus for some ratio of upstream to downstream pressure the flow will become choked and hence unaffected by further decreases in downstream pressure.

Fluid compressibility has a large effect on the forces generated in seals. Stiffness and damping coefficients are calculated for both straight bore and tapered-bore seals in [4] and [19]. All of the assumptions listed in the analysis section apply, except, of course, that compressibility is allowed; the fluid is assumed to be a perfect gas. Figure 13 shows stiffness of straight seals and optimum tapered seals for choked flow. The abscissa is the seal clearance-to-length ratio C_2/L times a Reynolds number Re_0 formed using the speed of sound for conditions upstream of the seal.

$$Re_0 = 2C\sqrt{\rho_0 p_0}/\mu_0$$

The curves on the left are for laminar flow. The nearly horizontal curves on the right are for turbulent flow; there is a separate curve for each value of C_2/L . The left end of the curves for turbulent flow corresponds to a Reynolds number in the seal passage of 3000; this is generally considered the lowest value for which one can be assured of turbulent flow. A Reynolds number of 2300 is usually taken as the upper limit for laminar flow. Points where $Re = 2300$ are shown for various C_2/L values on the laminar flow curves.

The surprising feature of the results is the negative stiffness predicted for low values of C_2/L . This is analogous to the lockup phenomenon observed in pressurized gas-lubricated bearings. Negative stiffness could cause rapid failure of floating ring seals and would rarely be beneficial even for rigidly mounted seals. Tapered seal stiffness is always positive and generally much higher than straight seal stiffness. The optimum clearance ratio is near 1.9 for most conditions, as it is for incompressible fluids.

Damping is shown in Fig. 14. As for stiffness, laminar flow curves are on the left and turbulent-flow curves (a separate one for each C_2/L) are on the right. Again, as for incompressible fluids, damping is lower for tapered seals. Damping is minimized for clearance-to-length ratios of 0.002-0.005 and is higher for ratios outside this range.

Experimental data are again sparse. Hendricks [20] obtained pressure measurements along the length of straight and tapered bore seals in the concentric and fully eccentric positions. Because of the small number of pressure taps he did not attempt to determine a net force generated by the seal; however, he estimated that the overall stiffness of the

tapered seal was no higher than that of the straight seal. Physical reasoning leads one to question this conclusion.

In work by Burcham and Diamond [21] the tapered bore seal was far superior to an alternative seal, a Rayleigh lift pad design. Both were floating ring seals, and the objective was to determine the endurance of the seals while maintaining satisfactory leakage control (i.e., minimizing wear). No internal pressure measurements or force measurements were made. In this type of test, the seal having a higher stiffness (higher centering force) can better minimize the rubs which cause wear. The investigators noted that there was less seal wear when sealed pressure was higher. This is in agreement with the analysis, which shows that a higher sealed pressure produces higher seal stiffness.

SEAL EFFECT ON ROTOR DYNAMICS

When significant forces (or equivalently, stiffnesses) are generated by seals, the effect on the shaft-rotor system is the same as if a bearing of that stiffness were placed on the shaft. Consequently, changes in dynamic response can be expected as a function of seal stiffness.

An example of seal forces being exploited to favorably influence rotor dynamic response is the high pressure fuel pump for the space shuttle main engine. The rotor of this pump is shown schematically in Fig. 15. Three centrifugal pump stages are driven by a two-stage axial turbine. The rotor is supported on two duplex ball bearings. Ring seals are used between pump stages. Originally, these seals were of serrated design (Fig. 16) to deliberately reduce the forces produced, as it was believed the cross-coupled stiffness would promote instability. In fact, other exciting forces produced a subsynchronous instability which began as the pump speed passed twice the first critical speed. Various modifications were tried to eliminate the instability. There was little success until the serrated seals were replaced with smooth-bore seals [22]. With this change the pump could be run to full speed without exhibiting signs of instability. The conclusion drawn was that the higher direct stiffness of the smooth seals was largely responsible for the stabilization and that the benefit of higher direct stiffness overshadowed the deleterious effect of the higher cross-coupled stiffness. The effect of higher-stiffness seals can be quantified in one respect by determining the effect on resonances. This is shown in Fig. 17 where resonant frequency is plotted as a function of interstage seal stiffness for a rotative speed of 37 000 rpm, the normal operating speed. The stiffness of the original serrated seals is not known precisely; however seal stiffness has little effect on resonant frequency for low values of stiffness. The first and second resonances are 9500 and 19 800 cpm,

respectively. When the serrated seals are replaced by smooth-bore seals, the resonances have risen to 13 500 and 23 000 cpm. Further increases occur if optimum tapered-bore seals, described earlier, are used. The two resonances then are 16 000 and 28 000 cpm. These frequencies are 70 and 40 percent higher, respectively, than the resonant frequencies with the original serrated seals.

CONCLUDING REMARKS

Significant forces can be generated by ring seals; film stiffnesses as high as 90 MN/m (500000 lb/in.) have been calculated for turbopump ring seals. These forces have been effectively utilized to support and stabilize shaft-rotor systems. This paper has presented a summary of work that has been done to determine forces generated in ring seals. Both compressible and incompressible fluids were considered; working formulas were presented to calculate seal stiffness and damping. Seal geometries to maximize stiffness were described. An example showed the effect seals can have on the dynamic behavior of rotor systems; use of high-stiffness seals raised the rotor critical speeds by nearly 50 percent.

REFERENCES

1. David P. Fleming, "Damping in Tapered Annular Seals for an Incompressible Fluid." NASA TP-1646, 1980.
2. P. E. Allaire, C. C. Lee, and E. J. Gunter, "Dynamics of Short Eccentric Plain Seals with High Axial Reynolds Number." *J. Spacecraft*, Vol. 15, No. 6, Nov.-Dec. 1978, pp. 341-347.
3. D. P. Fleming and E. M. Sparrow, "Flow in the Hydrodynamic Entrance Region of Ducts of Arbitrary Cross Section." *J. Heat Transfer*, Vol. 91, Aug. 1969, pp. 345-354.
4. David P. Fleming, "Stiffness of Straight and Tapered Annular Gas Path Seals." *J. Lubrication Technology*, Vol. 101, No. 3, July 1979, pp. 349-355.
5. H. F. Black, "Effects of Hydraulic Forces in Annular Pressure Seals on the Vibration of Centrifugal Pump Rotors." *J. Mechanical Engineering Science*, Vol. 11, No. 2, 1969, pp. 206-213.
6. H. F. Black and D. N. Jenssen, "Dynamic Hybrid Bearing Characteristics of Annular Controlled Leakage Seals." *Proc. Inst. Mech. Engineers*, Vol. 184, Part 3N, 1969-1970, pp. 92-100.
7. H. F. Black and D. N. Jenssen, "Effects of High Pressure Ring Seals on Pump Rotor Vibrations." ASME Paper 71-WA/FE-38, Nov. 1971.
8. Yutaka Yamada, "Resistance of a Flow through an Annulus with an Inner Rotating Cylinder." *Bulletin of JSME*, Vol. 5, No. 18, 1962, pp. 302-310.
9. H. F. Black, P. E. Allaire, and L. E. Barrett, "Inlet Flow Swirl in Short Turbulent Annular Seal Dynamics." Presented at Ninth Int. Conf. on Fluid Sealing, BHRA Fluid Engineering, Leeuwenhorst, Netherlands, 1981.
10. D. W. Childs, "Dynamic Analysis of Turbulent Annular Seals Based on Hirs' Lubrication Equation." To be published in *J. Lubrication Technology*.
11. G. G. Hirs, "Fundamentals of a Bulk-Flow Theory for Turbulent Lubricant Films." Doctoral Thesis, Delft Univ. Technology, 1970.
12. G. G. Hirs, "A Bulk-Flow Theory for Turbulence in Lubricant Films." *J. Lubrication Technology*, Vol. 95, No. 2, April 1973, pp. 137-146.
13. George B. DuBois and Fred W. Ocvirk, "Analytical Deviation and Experimental Evaluation of Short-Bearing Approximation for Full Journal Bearings." NACA Rep. 1157, 1953.
14. Richard H. Schmaus, "Static and Dynamic Properties of Finite Length Turbulent Flow Annular Seals." MS Thesis, Univ. Virginia, 1981.
15. D. W. Childs, "Finite Length Solutions for Rotordynamic Coefficients of Turbulent Annular Seals." Submitted to *J. Lubrication Technology*.
16. Dara W. Childs, John B. Dressman, and S. Bart Childs, "Testing of Turbulent Seals for Rotordynamic Coefficients." Paper in Rotordynamic Instability Problems in High Performance Turbomachinery, NASA CP-2133, 1980, pp. 121-138.
17. D. P. Fleming, "High Stiffness Seals for Rotor Critical Speed Control." ASME Paper 77-DET-10, 1977.
18. D. W. Childs, "Convergent-Tapered Annular Seals: Analysis for Rotordynamic Coefficients." Symposium volume, Fluid/Structure Interactions in Turbomachinery, ASME Winter Annual Meeting, 1981, pp. 35-44.
19. David P. Fleming, "Damping in Ring Seals for Compressible Fluids." Paper in Rotordynamic Instability Problems in High Speed Turbomachinery, NASA CP-2133, 1980, pp. 169-188.

20. R. C. Hendricks, "Some Flow Characteristics of Conventional and Tapered High-Pressure-Drop Simulated Seals." ASLE Transactions, Vol. 24, No. 1, pp. 23-28, 1981.
21. R. E. Burcham and W. A. Diamond, "High-Pressure Hot-Gas Self-Acting Floating Ring Shaft Seal for Liquid Rocket Turbopumps." NASA CR-165392, 1980.
22. Matthew C. Ek, "Solving Subsynchronous Whirl in the High-Pressure Hydrogen Turbomachinery of the SSME." J. Spacecraft, vol. 17, no. 3, 1980, pp. 208-218.

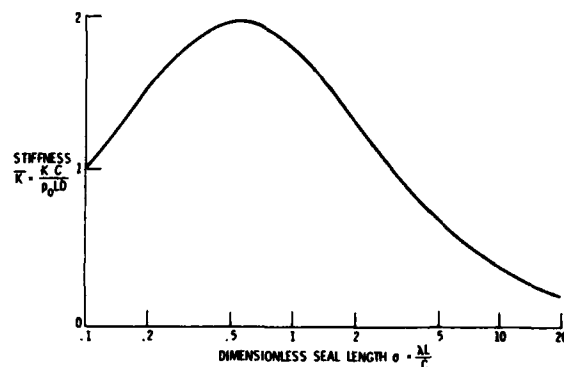


Figure 4 — Ring seal stiffness

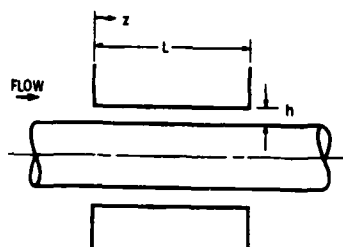


Figure 1 — Ring seal

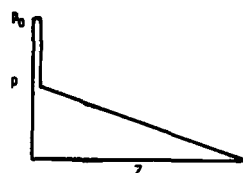


Figure 2 — Velocity and pressure profile in concentric seal

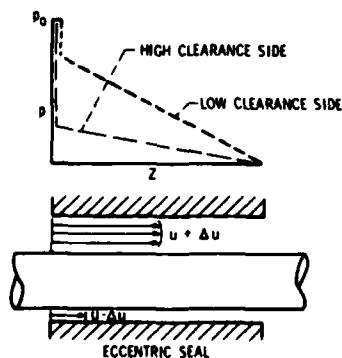
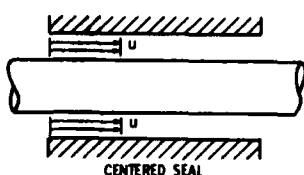


Figure 3 — Velocity and pressure profile in eccentric seal

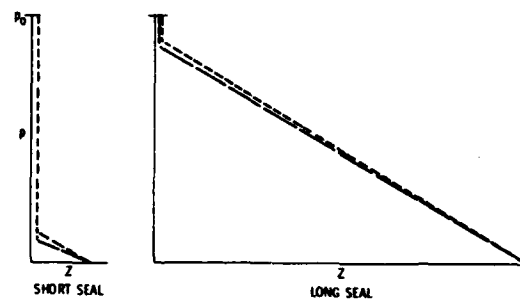


Figure 5 — Pressure profiles in short and long seals

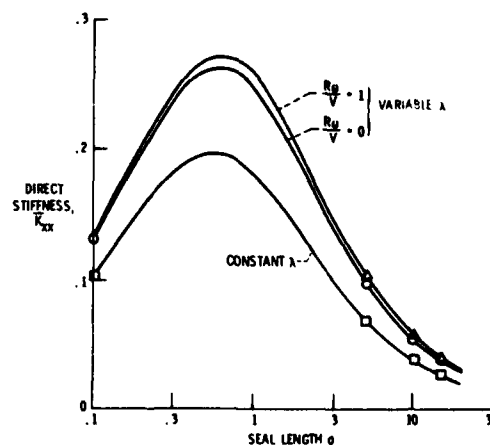


Figure 6 — Increase in stiffness due to effect of local Reynolds number on friction factor

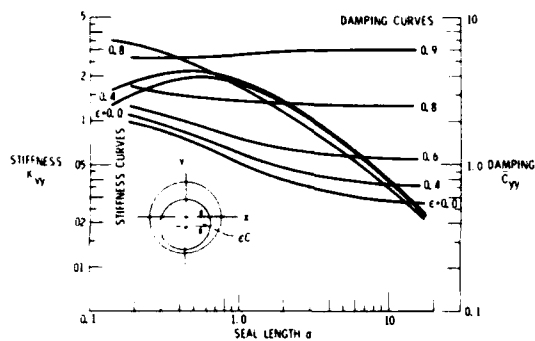


Figure 7 — Seal stiffness and damping in line with journal displacement (from [2])

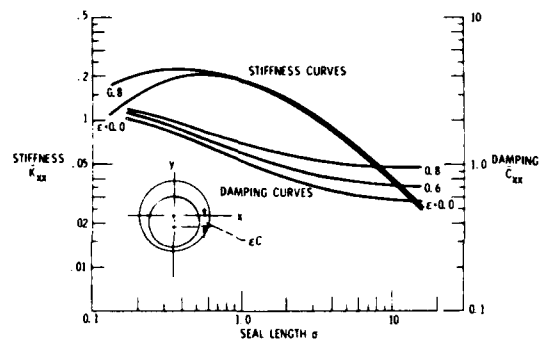
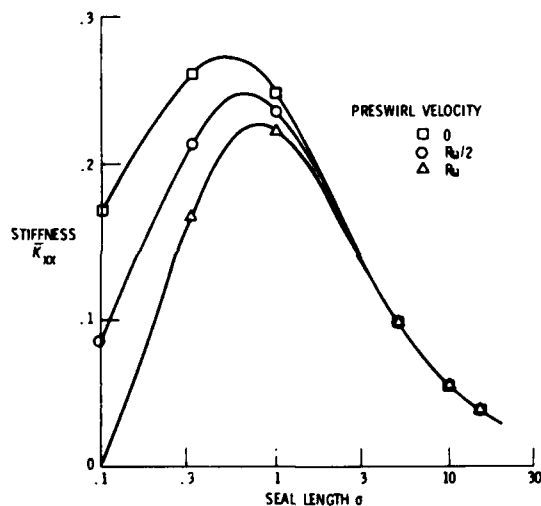
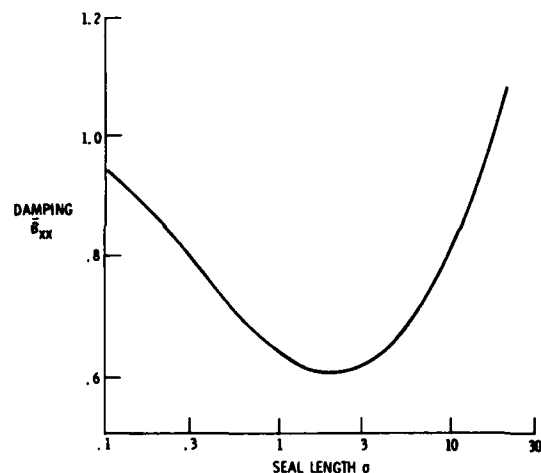


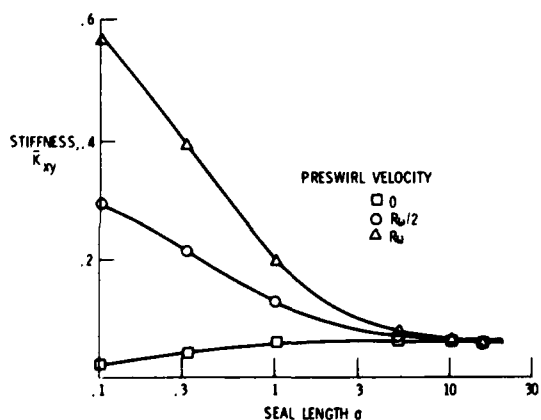
Figure 8 — Seal stiffness and damping normal to journal displacement (from [2])



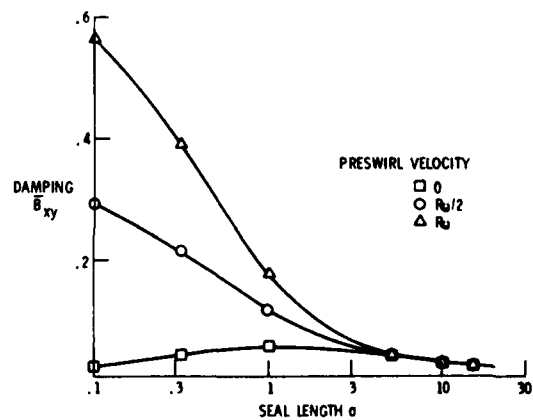
(a) Direct stiffness



(c) Direct damping (all preswirl values)



(b) Cross-coupled stiffness



(d) Cross-coupled damping

Figure 9 — Effect of preswirl on dynamic seal coefficients; $L/D = .05$, $R\omega/u_0 = .05$

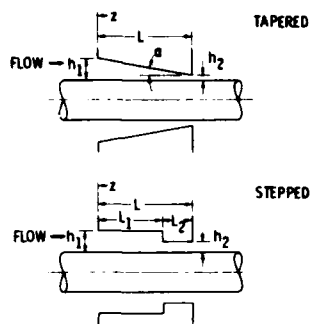


Figure 10 — Tapered and stepped annular seals

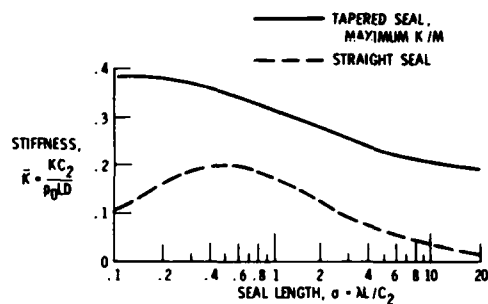


Figure 11 — Stiffness of tapered and straight seals

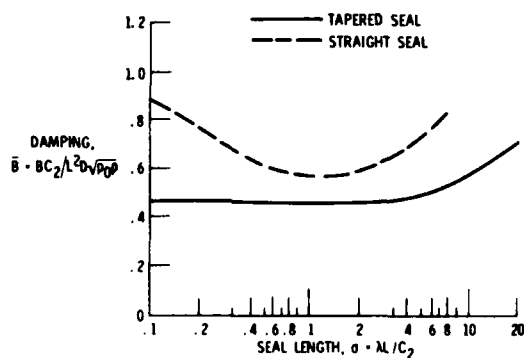


Figure 12 — Damping in tapered and straight seals

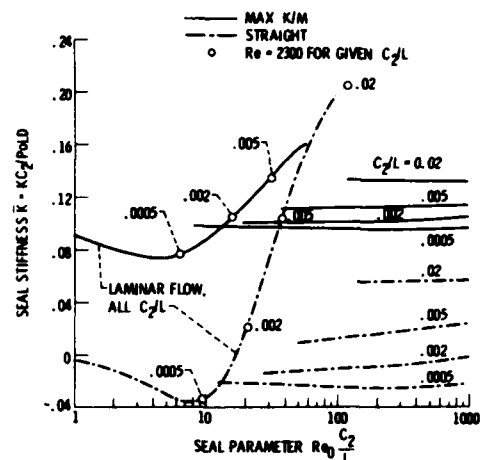


Figure 13 — Stiffness of straight and tapered seals; choked compressible flow

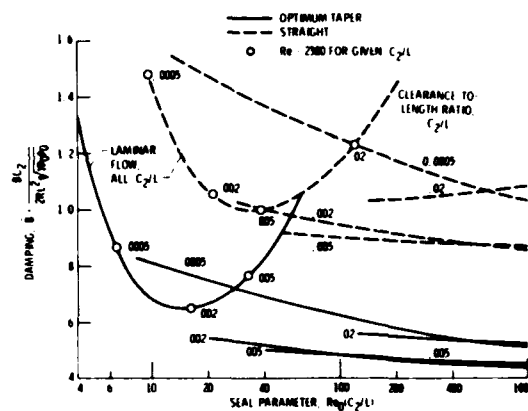


Figure 14 — Damping in ring seals; choked compressible flow

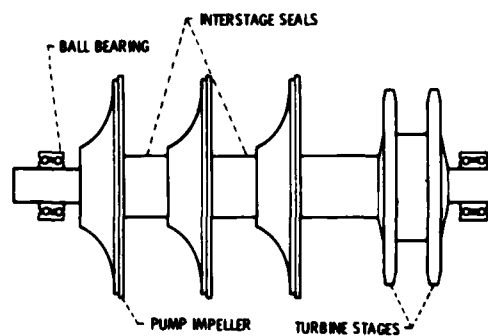


Figure 15 — Turbopump rotor

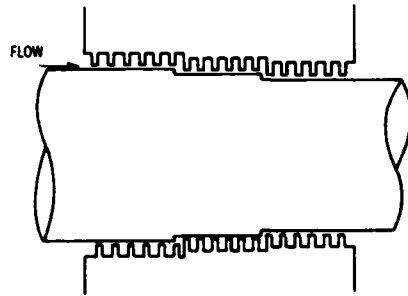


Figure 16 — Serrated seal

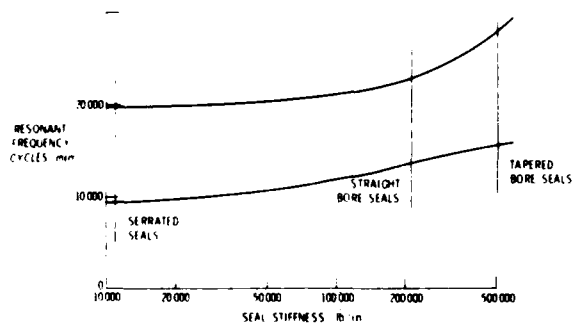


Figure 17 — Turbopump resonant frequencies at operating speed

MACHINERY VIBRATION EVALUATION TECHNIQUES

Ronald L. Eshleman
Vibration Institute
Clarendon Hills, Illinois

Direct frequency analysis of vibration signals is commonly used to evaluate the condition of machinery. This paper is concerned with this technique, its variations, and many other techniques available for machinery vibration evaluation. The techniques described and illustrated in this paper involve the time and frequency domains, orbital motions, transient tests, and parameter analyses -- either calculated or measured.

INTRODUCTION

The evaluation of machinery vibrations involves a knowledge of equipment design parameters, testing and/or computational techniques, and appropriate test equipment.

To conduct an effective analysis of a machine's problems it is essential to have a thorough knowledge of the equipment design characteristics, its installation state, and its environment. The forcing frequencies that result from equipment wear, faulty installation or manufacture, and design are required. The mass, elastic, damping characteristics that affect natural frequencies, mode shapes, instabilities, and thermal and structural response enable in-depth analyses. These parameters and conditions should be obtained prior to machine evaluation.

The development of sophisticated electronics, practical mathematical algorithms, and reliable transducers has provided the tools for machinery vibration analysis. In fact, the availability of machinery vibration evaluation parameters, techniques, and equipment raises machinery vibration analysis from an art to a science.

This paper is concerned with machinery vibration evaluation techniques. The techniques discussed in the paper are summarized in Table 1.

TIME DOMAIN ANALYSIS

Until recently wave analyzers and fast fourier transform computers were in such widespread use that diagnosticians tended to rely solely on the frequency domain (vibration amplitude vs frequency) for vibration analysis. However, valuable information can be obtained from the time domain (vibration amplitude vs time); fortunately, its advantages are becoming more widely recognized. Direct differential time measurement is given as a digital readout on some of the new analyzers and oscilloscopes. Such readouts allow accurate identification of the period of vibration events. In the discussion that follows, examples of both steady and transient vibrations are given to illustrate some of the uses of the time domain.

Vibration events that are either synchronous or nonsynchronous with speed can be observed and analyzed in the time domain. An example of a nonsynchronous vibration signal is a second harmonic of line frequency in an electric motor. It will move gradually with respect to the fundamental operating frequency of the motor in the time domain. Misalignment and other common mechanical problems are synchronous with shaft frequency. The nonsynchronous harmonic can be evidence of environmentally-induced vibration from adjacent equipment.

TABLE 1
Machinery Vibration Evaluation Techniques

Technique	Use	Description
Time Domain Analysis	parameter identification condition analysis fault diagnosis	amplitude vs time
Trend Analysis	condition analysis	amplitude vs extended time
Frequency Domain Analysis	parameter identification condition analysis fault diagnosis	amplitude vs frequency
Orbital Domain Analysis	condition analysis fault diagnosis	relative displacement of journal in X-Y coordinates
Transient Frequency Analysis		
Bode Plot	parameter identification	amplitude vs speed phase angle vs speed
Polar Plot	condition analysis	amplitude and phase vs speed
Cascade Plot	fault diagnosis	amplitude vs frequency at various speeds
Interference and Lund Diagrams	design analysis	frequency vs operating speed showing excitation and natural frequency interference -- damping given on Lund diagram
Critical Speed Map	design analysis	variation of critical speeds with shaft/bearing/foundation stiffness
Stability Map	design analysis	stability parameter vs eccentricity ratio -- logarithmic decrement vs rotor speed

The frequency of the spikes in a time domain measurement can be used to determine the number of cracked, chipped, or otherwise defective teeth on either a pinion or a gear. Figure 1 shows large spikes in a time domain measurement made on a gearbox with a broken tooth on the pinion.

$$f = \frac{N \times m}{60}$$

where: $f = \frac{1}{\tau}$ frequency of events, Hz

τ = measured period of events, sec

m = number of chipped or cracked teeth

N = speed of pinion or gear

The pinion speed was 207 RPM. The period of the impacts is

$$\tau = \frac{8.6 \text{ Div (meas. from fig.)} \times 0.2 \text{ sec/Div}}{6 \text{ cycles}}$$

$$\tau = 0.29 \text{ sec} \quad f = 3.45 \text{ cycles/sec}$$

$$m = \frac{60f}{N} = \frac{60 \times 3.45}{207} = 1.0$$



Figure 1. Seven Revolutions of a Jack Shaft Pinion.² time = 0.2 sec/div, amplitude = 0.5 volts/div

These calculations show that one tooth defect is present on the pinion.

Time domain measurements can also be used to determine natural frequency and damping from a bump or ringing test. Figure 2 shows the result of a bump test on piping. The decay of the vibration amplitude after the bump can be represented by the logarithmic decrement, which is a measure of system damping.

Bump tests have their limitations, however. The site at which the force is

applied must excite the appropriate natural frequency. In addition, in systems in which the natural frequencies vary with speed, the bump test is not useful. A bump test cannot be used to obtain natural frequencies of machines with hydrodynamic fluid-film bearings because the bearing stiffness varies with machine operating speed. The bode diagram (once per revolution vibration and phase angle) is a better means for determining critical speeds and thus natural frequencies. Machines with such large overhung disks as fans, impellers, and propellers have gyroscopic effects that alter apparent dynamic properties. If they are rung while not operating at speed, the natural frequencies obtained are incorrect because the gyroscopic effect stiffens the rotor and raises the natural frequency. Although rotors are often lifted out of machines and rung to obtain their natural frequencies, only the natural frequencies of the rotors are obtained -- not those of the system, and it is the system natural frequencies that are important. Pedestals, bearings, supporting foundations and even large overhung couplings can alter system natural frequencies and critical speeds.

Figure 2 shows that the natural period of the predominant vibration is 32 ms. From the time domain the natural frequency is thus

$$\tau = 0.032 \text{ sec}$$

$$f = \frac{1}{\tau} = 31.25 \text{ Hz}$$

This frequency can be verified by observing the frequency domain in Figure 2. The damping ratio (a measure of viscous damping) can be calculated from Figure 2.

$$\delta = \frac{1}{n} \ln \frac{x_0}{x_n}$$

δ = logarithmic decrement
 n = number of cycles of vibration
 x_0 = amplitude of vibration on the initial cycle
 x_n = amplitude of vibration on the nth cycle
 \ln = natural logarithm

$$\delta = \frac{2\pi \frac{c}{c_c}}{\sqrt{1 - \left(\frac{c}{c_c}\right)^2}} \quad \text{exact}$$

$$\delta = 2\pi \frac{c}{c_c} \quad \text{for } \frac{c}{c_c} < 0.5$$

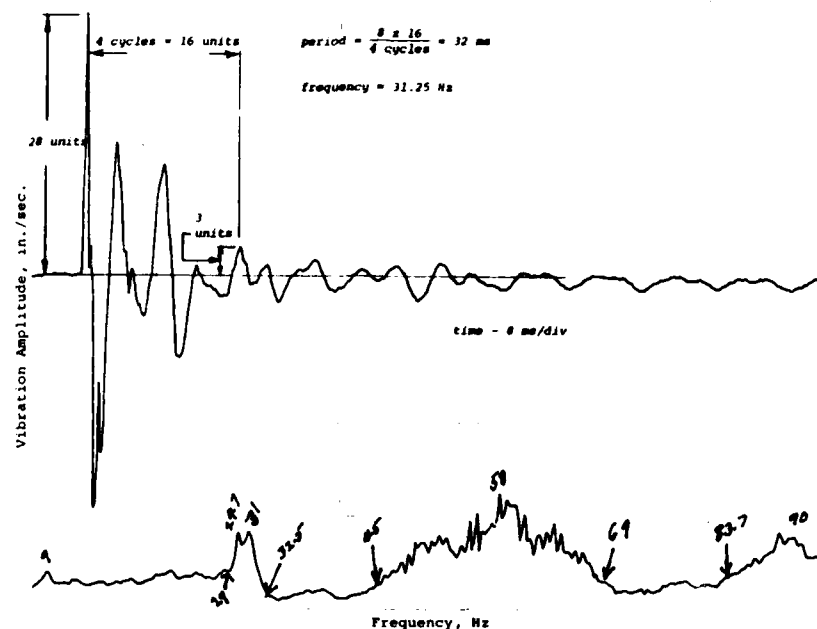


Figure 2. Bump Test on Line Shaft Turbine Piping
(courtesy of James I. Taylor)

δ = logarithmic decrement

$\frac{c}{c_c}$ = damping ratio

If $c/c_c = 1$, the system is critically damped and no vibration will occur. If $c/c_c = 0$, no damping is obtained. Some typical damping values are: rubber = 0.05, steel = 0.001, and fluid film bearings = 0.1 to 1.

The logarithmic decrement for the piping example shown in Figure 2 is

$$\delta = \frac{1}{4} \ln \frac{28}{3} = 2.33$$

$$\frac{c}{c_c} = \frac{\delta}{2\pi} = 0.37$$

The damping ratio of 0.37 indicates a moderately damped system that will be responsive to a forcing function.

TREND ANALYSIS

The trend display is an extended time display of a key measured parameter such as average, peak, or rms vibration velocity or acceleration, peak to peak displacement, temperature, or pressure. Trend data is obtained from monitoring and recording data at specific intervals

such as hours, days, weeks, or months. It can be continuously or periodically recorded. Information on time to failure is obtained by extrapolating the recorded data. Generalized techniques for extrapolation of data have not been developed due to the complexity of machines and their installations. Successful trending results from knowledge of the wear-vibration characteristics of specific machines. Figure 3 shows an example trending chart for the degradation of babbitt in a bearing undergoing electrical erosion.

FREQUENCY DOMAIN ANALYSIS

Frequency analysis techniques have provided a well used means for identification of vibration faults since the development of tunable analyzers with band pass filters. These techniques have been extended from direct single frequency identification to sum and difference frequency analysis as a result of the evaluation of real time analyzers with zoom or translator capability. The zoom feature provides the expansion of the frequency domain so that sidebands can be resolved.

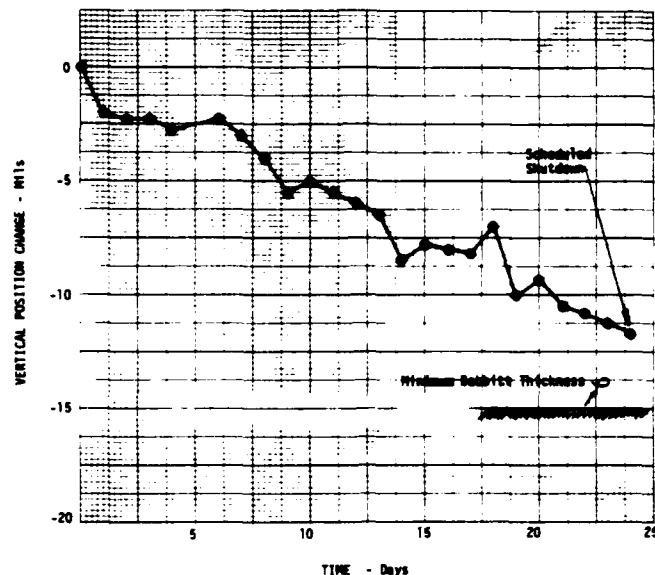


Figure 3. Trend Plot of Degradation in Babbitt Thickness Due to Electrical Erosion (After Eisenmann²)

Resonance Tests

Frequency analysis of structure and machine components where no continuous source of excitation is available can be made by ringing the component or system. The system natural frequencies are obtained using a swept frequency spectrum analyzer (excitation must be applied continuously) or a real time analyzer. Care must be exercised in ringing machines which have gyroscopic effects of large disks and fluid film bearings. These effects make machine natural frequencies a function of rotor speed. Natural frequencies obtained by ringing will be those of the stationary machine and not those of the operating machine.

Modal analysis of a structure can be obtained using a swept frequency spectrum analyzer or real time analyzer and a reference meter. The reference meter is used to ensure constant excitation application as the transducer is moved across the structure. The frequency analysis techniques to be discussed follow.

Direct Frequency Identification

- Single Frequency
- Single Frequency with Truncation
- Beats
- Multiple Frequency
- Pulses

Sum and Difference Frequency Identification

- Truncated Beats
- Truncated Multiple Frequency

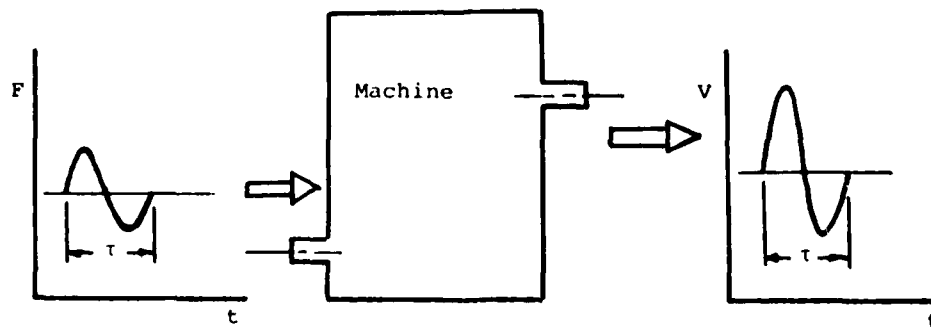


Figure 4. Vibration Response to Forcing Function in a Linear System

Direct Frequency Identification

Vibration analyses conducted to determine machine faults are concerned with the forces which cause wear, failure, and inferior performance. Unfortunately, these forces cannot be measured directly -- only vibration response. Fortunately, in a linear system (Figure 4) the frequency of the response is equal to the frequency of the force. Thus forcing frequencies can be identified directly -- particularly when a minimum number of frequencies are present. When the system stiffness becomes nonlinear truncation occurs and higher harmonics of the basic forcing frequency are present. This situation usually indicates the presence of a fault such as misalignment, looseness, or excessive loading. Figure 5 shows higher harmonics caused by excessive loading due to mass unbalance in a steam turbine operating near a piping resonance. The bearings are forced to operate in the nonlinear region yielding higher harmonics. When multiple frequencies

are present (Figure 6) which are not close in value, their frequencies will be given directly if the vibration sensor measures the sum of the two signals. If one signal modifies the amplitude of the other signal then sum and difference frequencies, not directly relatable to the forces, will be obtained (Figure 7).

The pump has four vanes on the impeller. This is a characteristic spectra of pump starvation. The fundamental is generated by unequal amounts of water in each vane (unbalance) and 54.4 Hz vane pass frequency is generated by the impeller vanes hitting the water.

Figure 8 shows schematically what happens when impulse type loadings are applied to machines. The impulse will excite a natural frequency of the system. When the defect becomes large, the natural frequency will be modulated (sidebands) with the repetition rate of the event.

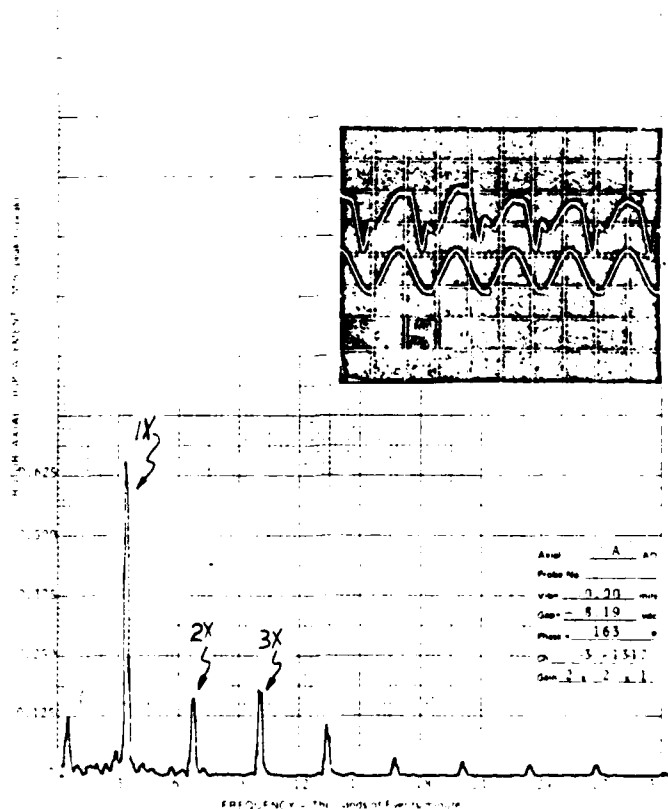


Figure 5. Vibration of an Unbalanced Steam Turbine Near a Piping Resonance

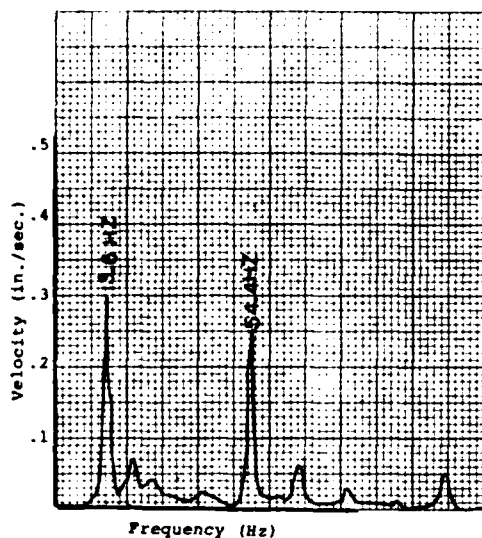


Figure 6. The Frequency Spectrum From a Large 800 RPM Pump (After Taylor³)

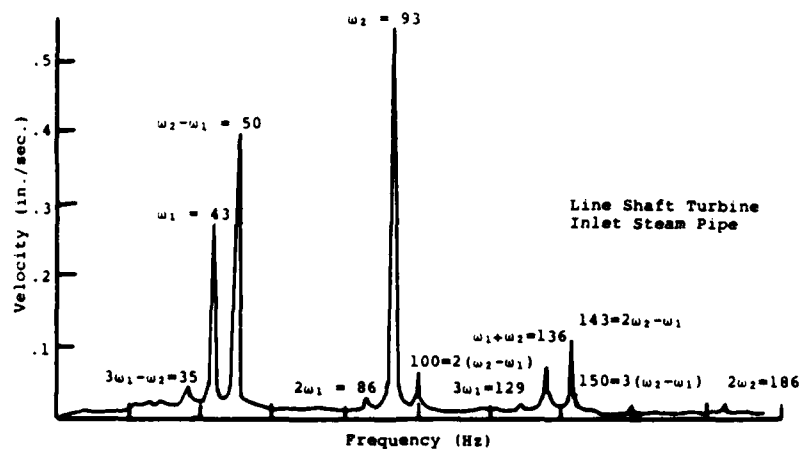


Figure 7. Frequency Domain Record of Line Shaft Turbine Piping Vibration (courtesy of James I. Taylor)

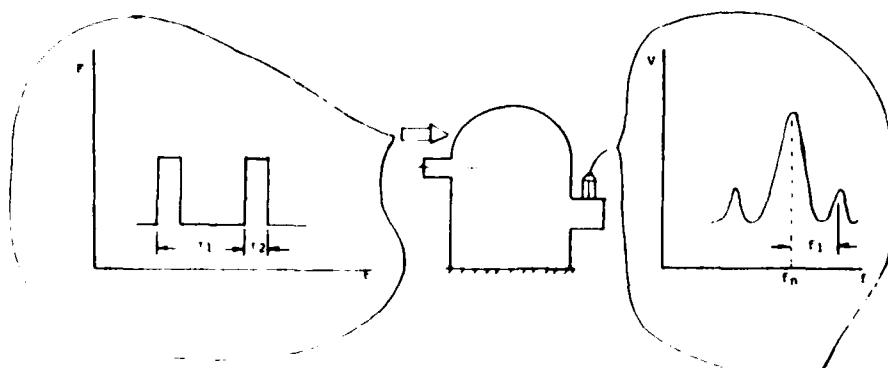


Figure 8. Response of Mechanical System to Impulse Type Excitation

Sum and Difference Frequency Identification

Increased complexity of rotating machinery and higher demands for speed and power have created more complex vibration problems. Vibration instrumentation provided through the development of electronics offers the practical capability to perform sophisticated frequency analyses of such complex vibration signals. This paper is concerned with machinery faults such as heavy loading, nonlinearities in stiffness, antifriction bearing and gear defects, oil whirl, rubs, trapped fluid, piping excitation, mass unbalance and torsional excitations which often can be related to measured sum and difference frequencies. A mechanism for the occurrence of these phenomena, first explained by Ehrich [4] who studied the interaction of mass unbalance and trapped fluid in a rotor, is described and related to practical machinery faults and their severity. Engineering judgments based on understanding of physical phenomena are still needed to provide the diagnosis and means of correction of these rotating machinery problems.

Mechanisms

The vibration response shown in Figure 9 is a truncated beat generated waveform. The beat phenomenon is a periodic pulsation in vibration amplitude due to the addition of the simultaneous response of equipment to two base excitation frequencies ω_1 and ω_2 .

$$v = a \sin \omega_1 t + a \sin \omega_2 t$$

where: v = vibration signal (volts)

a = amplitude of signal (volts)

ω_1 = frequency of component 1 (rad/sec)

ω_2 = frequency of component 2 (rad/sec)

t = time

If rearranged, this equation gives an apparent vibration signal at a mean frequency $(\omega_1 + \omega_2)/2$ and a pulsation in amplitude (amplitude modulation) at the difference frequency $(\omega_2 - \omega_1)$. Or the former equation can be written in the following form:

$$v = a \cos (\omega_2 - \omega_1)t \sin \frac{(\omega_2 + \omega_1)t}{2}$$

In order to obtain a number of sum and difference frequencies the beat waveform must be truncated as shown in

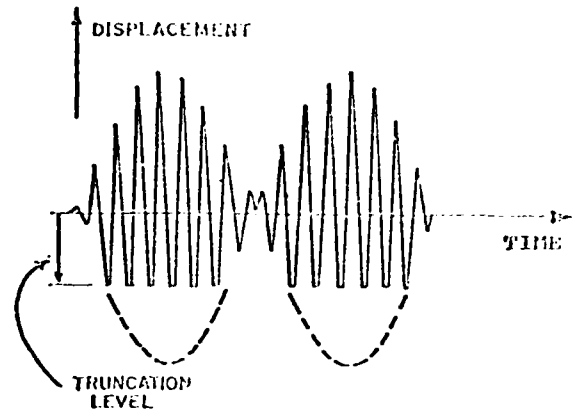


Figure 9. Hypothetical Vibration Response Exhibiting Beat Frequency

Figure 9. This truncation results from misalignment, looseness, and stiffness nonlinearities in many machines.

The truncated waveform is a periodic function of the beat frequency $(\omega_2 - \omega_1)$, thus it can be expressed as a series of harmonic functions using a Fourier series. Spectral analysis of this physical situation yields a number of discrete sum and difference frequencies depending on the exact shape of the vibration response. A mathematical analysis of this signal in the time domain was published by Ehrich [4]. The truncation of the "beat frequency" induces strong harmonics at sum and difference frequencies $(\omega_1 + \omega_2)$ and $(\omega_2 - \omega_1)$. Frequencies in the range of third harmonics -- $(2\omega_1 + \omega_2)$ and $(\omega_1 + 2\omega_2)$ -- are generated. In addition, the sum and difference frequency components are accompanied by side band frequency components separated by $(\omega_2 - \omega_1)$ from the center bands. Table 2 shows the pattern of frequency components which evolve from this analysis.

Figure 10 contains a schematic representation of the process of generation of sum and difference frequencies in rotating machinery. Excitations such as mass unbalance, antifriction bearing and gear defects, oil whirl, trapped fluid, and rubs cause rotor vibration at discrete frequencies on the rotor. Due to misalignment, looseness, and stiffness nonlinearities the stator vibration waveform caused by the rotor vibration is truncated. The truncated beat time domain signal yields sum and difference

TABLE 2
Pattern of Frequency Components in Truncated Beat
Frequency Wave Form (After Ehrich⁴)

Side Band Frequencies	Center Frequencies	Side Band Frequencies	Harmonic Zone No.
--	0	$(\omega_2 - \omega_1)$	0
$(2\omega_1 - \omega_2)$	ω_1	ω_2 $(2\omega_2 - \omega_1)$	1
$(3\omega_1 - \omega_2)$	$2\omega_1$	$(\omega_1 + \omega_2)$ $2\omega_2$ $(3\omega_2 - \omega_1)$	2
$(4\omega_1 - \omega_2)$	$3\omega_1$	$(2\omega_1 + \omega_2)$ $(\omega_1 + 2\omega_2)$ $3\omega_2$ $(4\omega_2 - \omega_1)$	3
		etc.	

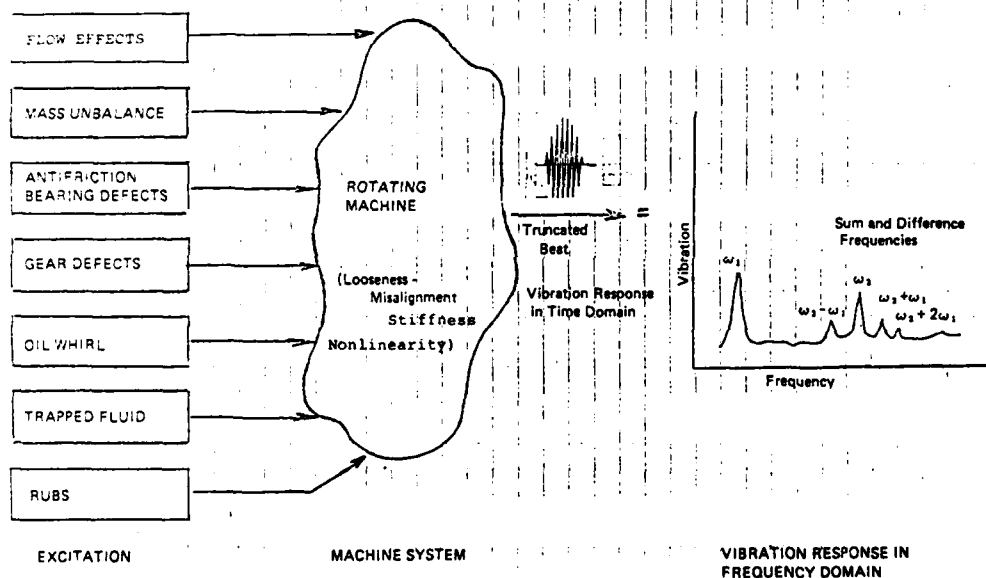


Figure 10. Rotating Machinery Fault Diagnosis Using Sum and Difference Frequencies (Eshleman⁵)

frequency.

ORBITAL ANALYSIS

The orbital plot, such as shown in Figure 11, shows the actual relative motion of the shaft. The presence of loops in the orbit indicates forward (internal) and reverse (external) whirl. Key phase markers show the once per revolution motion of the shaft. This allows the identification of the whirl

frequency. Figure 11 shows a comparison of the spectrum and time domain plots to the orbital plot for the exhaust shaft motion of a gas turbine.

TRANSIENT FREQUENCY ANALYSIS

Coast down and start up tests provide machinery vibration data at varied speeds. These data can be used for parameter identification, critical speeds, natural frequencies, and damping

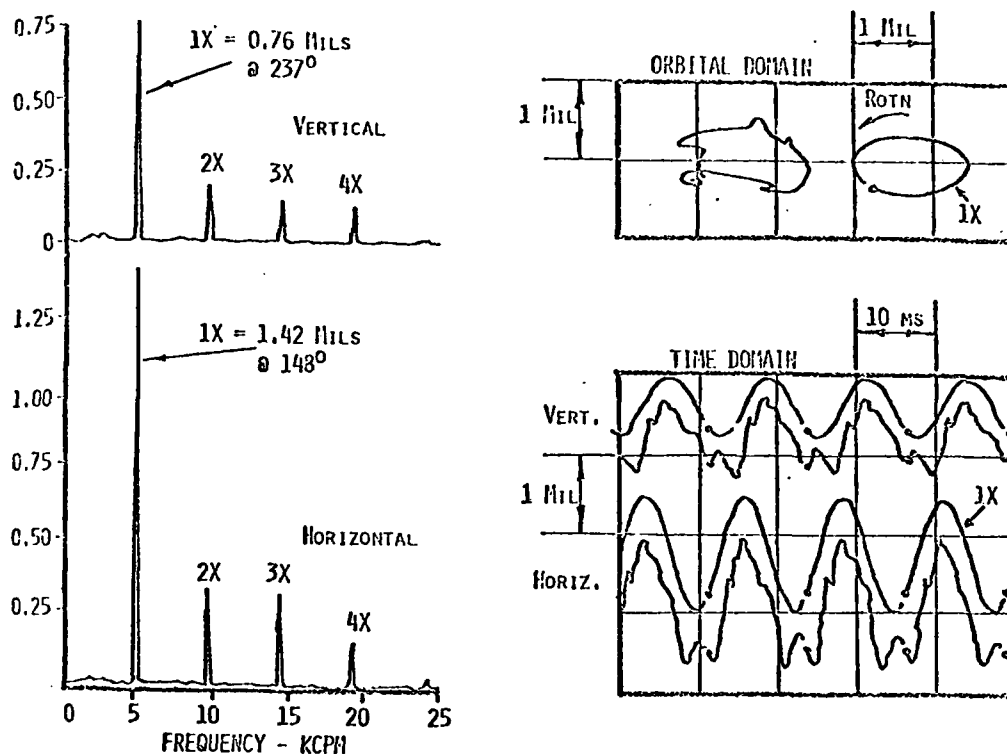


Figure 11. Exhaust Shaft Motion (After Eisenmann⁶)

constants. Vibration data are filtered using a synchronous tracking filter.

Polar/Bode Plots

The polar plot (Figure 12), also called a Nyquist diagram, is a plot of amplitude versus phase during machine start up. This plot is made by plotting the real and imaginary components of the vibration as speed increases. It shows the system resonances and critical speeds, as loops, more distinctly than the Bode plot (Figure 13). The Bode plot is the conventional plot of amplitude and phase versus speed during machine start up. These plots are used to determine machine critical speeds and structural resonances during start up and coast down. The mass unbalance is used as the excitation and the true machine characteristics are obtained. The polar plot can also be used for balancing.

Cascade Plot

A cascade plot (Figure 14) or vibration amplitude versus frequency

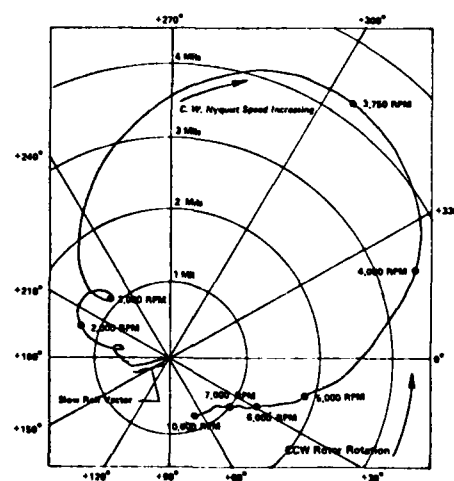


Figure 12. Polar Plot (After Eisenmann⁶)

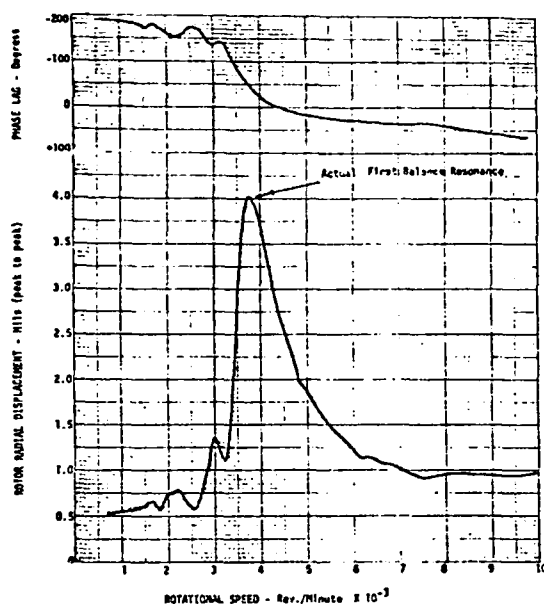


Figure 13. Continuous Bode Diagram of Rotor Displacement During Start Up (After Eisenmann⁶)

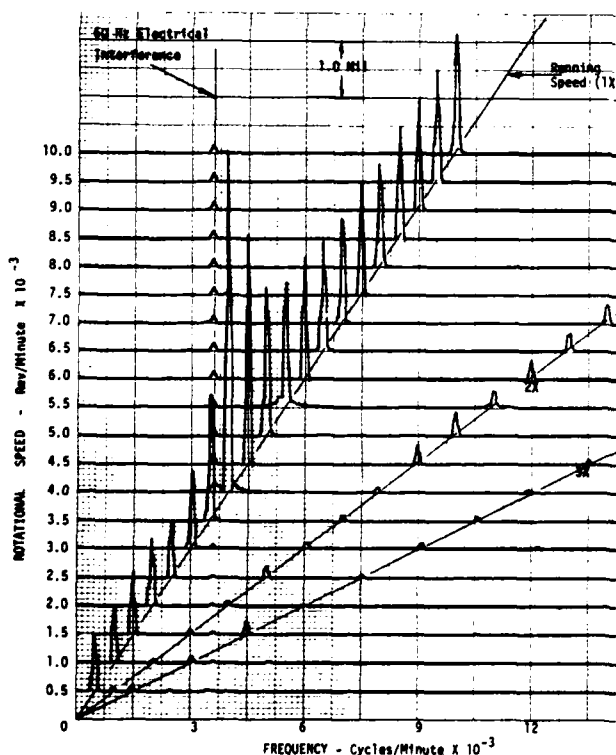


Figure 14. Cascade Spectrum Analysis of Rotor Displacement During Start Up (After Eisenmann⁶)

(spectrum analysis) for varied machine speeds is used for convenience in direct frequency identification. It allows tracking of each order of vibration through the machine speed range. Today this plot can be made on machine start up or coast down using a digital computer (for data storage and/or analysis), a spectrum analyzer, and tracking filters. Previously data were required to be obtained at individual steady operating speeds or by tape recording during transient conditions.

INTERFERENCE AND LUND DIAGRAMS

The interference diagram, which is a plot of excitation frequencies versus natural frequencies (Figure 15), is a good design and analysis tool. It shows the proximity of the excitations to the natural frequencies and thus identifies sources of potential problems (critical speeds and resonances). The Lund diagram, Figure 16, is more exact for this purpose because it shows the damping at

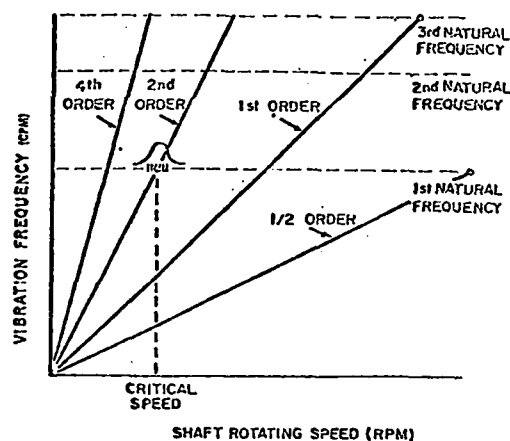


Figure 15. Interference Diagram for a Shafting System

each "interference". If the system is overdamped at the "interference", no vibration problem is expected. Thus only the strength of the excitation is unknown. The log decrement is identified at each speed. In this example of an 8 stage compressor the synchronous excitation from mass unbalance is identified by a dashed line. This chart shows that the natural frequencies of the system change with speed -- due to the fact that fluid film bearing stiffnesses change with speed. Four interferences shown on the chart show four possible critical speeds -- first mode with

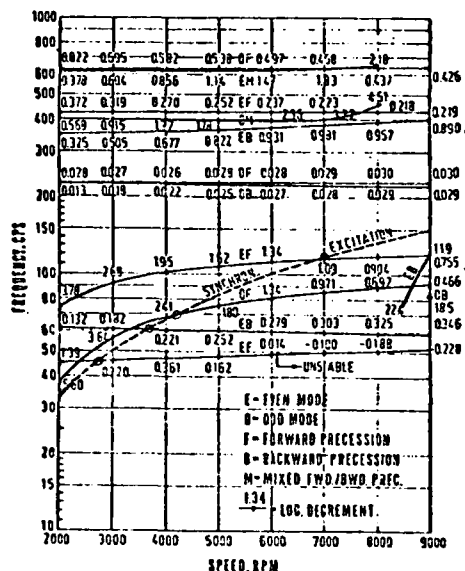


Figure 16. Damped Natural Frequencies of 8 Stage Compressor in Plain Cylindrical Journal Bearings (After Lund⁷)

forward precession at 2748 rpm ($\delta = .857$), first mode with backward precession at 3637 rpm ($\delta = 2.08$), second mode with forward precession at 4180 rpm ($\delta = 2.27$), and a third mode with forward precession at 6840 rpm ($\delta = 1.12$).

CRITICAL SPEED MAP

The critical speed map (Figure 17) is obtained from a computer program which determines the natural frequency of the machine system as a function of bearing/foundation stiffness and shaft size. This type plot is used to determine the effect of bearing and shaft stiffness on critical speeds. A machine chronically sensitive to mass unbalance may be operating near a critical speed. This type analysis gives information on critical speed changes through bearing alteration. Figure 17 shows how the bearing stiffnesses change with speed and the mode shapes at the various critical speeds.

STABILITY MAP

The plot (Figure 18) of stability parameter versus eccentricity ratio for a range of values of preload yields

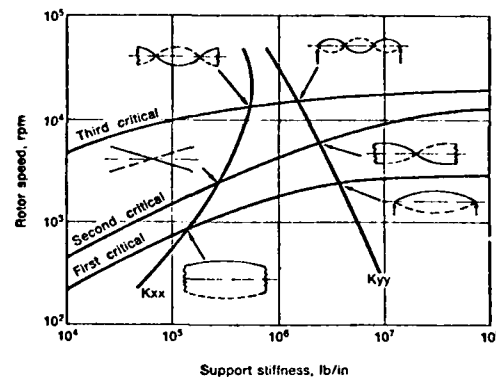


Figure 17. Rotor Mode Shapes for Varying Support Stiffnesses [8]

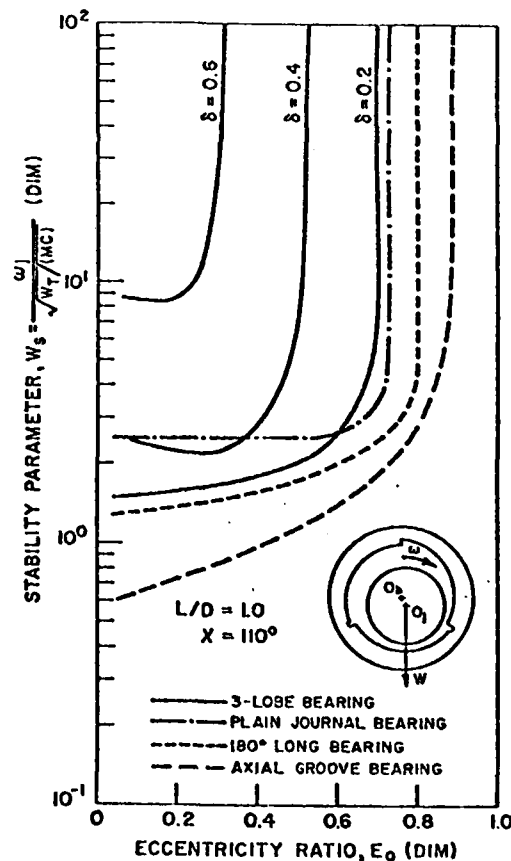


Figure 18. Stability of a Three-Lobed Bearing for Various Values of Preload (After Gunter⁹)

data on the zones of machine operation where stability problems might be encountered. This type analysis almost requires a map for each individual machine because it is dependent on bearing configuration and shaft flexibility. The plot shown in Figure 19 shows a stability map (logarithmic decrement vs rotor speed) for stiffness supports and cross coupled stiffnesses. A logarithmic decrement denotes instability. Note that the absence of negative cross coupling leads to a stable machine.

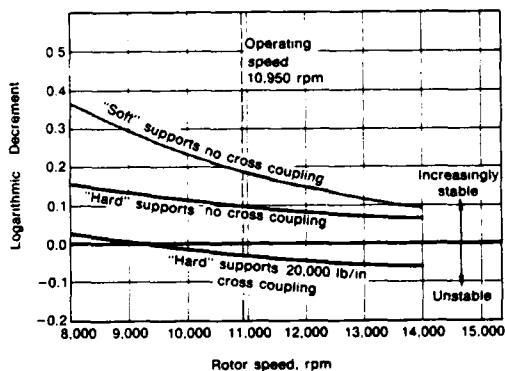


Figure 19. Stability Map for 8-Stage Centrifugal Compressor [8]

REFERENCES

1. Taylor, J.I., "Identification of Gear Defects by Vibration Analysis," Proceedings of Machinery Vibration Monitoring and Analysis Seminar, Vibration Institute, April 1979.
2. Eisenmann, R., "Data Presentation Techniques for Trend Analysis and Malfunction Diagnosis," Vibration Institute Machinery Vibration Monitoring and Analysis Seminar, February 1978.
3. Taylor, J.I., "Evaluation of Machinery Condition by Spectral Analysis," Proceedings of Machinery Vibration Monitoring and Analysis Seminar, Vibration Institute, April 1980.
4. Ehrich, F.F., "Sum and Difference Frequencies in Vibration of High Speed Rotating Machinery," J. Eng. Ind., Trans ASME, 94 (1) pp 181-184, Feb. 1972.
5. Eshleman, R.L., "The Role of Sum and Difference Frequencies in Rotating Machinery Fault Diagnosis," Proceedings of the Second International Conference on Vibrations in Rotating Machinery, Cambridge, UK, September, 1980, Mechanical Engineering Publications, Ltd., Bury St. Edmunds, Suffolk, UK, pp 145-149.
6. Eisenmann, R., "Shaft and Casing Motion of Large, Single Shaft, Industrial Gas Turbines," Proceedings of Machinery Vibration Monitoring and Analysis Seminar, Vibration Institute, April 1979.
7. Lund, J.W., "Stability and Damped Critical Speeds of a Flexible Rotor in Fluid Film Bearings," ASME Paper No. 73-DET-103, ASME Vibrations Conference, 1973.
8. Jackson, C. and Leader, M., "Rotor Critical Speed and Response Studies in Equipment Selection," Vibration Institute Machinery Vibration Monitoring and Analysis Seminar, April 1979.
9. Gunter, E.J., "Rotor-Bearing Stability," Proceedings of the First Turbomachinery Symposium, Texas A&M University, October 1972.

SHAFT VIBRATION MEASUREMENT AND ANALYSIS TECHNIQUES

Donald E. Bently, President
Bently Nevada Corporation
Minden, Nevada, USA

The use of electronic instrumentation for the measurement and analysis of rotating machinery has advanced greatly over the last fifteen years. Of the available vibration measurement transducers, the displacement proximity probe is most widely used on critical equipment. However, there are still some applications for the case-mounted transducers, velocity sensors, and accelerometers. For the purpose of machinery analysis, several hard copy data presentations are available. Data formats for steady-state machine conditions include oscilloscope time base waveforms and orbits and frequency spectra. For data from machines under transient conditions, the formats include Polar, Bode', cascade or waterfall plots, and change in average shaft centerline position.

The use of electronic instrumentation for measurement and analysis of rotating machinery has advanced greatly over the last fifteen years. In today's market, the old-time vibration measurement techniques using screwdrivers, balancing coins on edge, and using the human senses of sight, sound, and touch, are rarely used. Most critical machines have electronic sensors permanently installed with continuous readout and alarm (or shutdown) monitoring systems. Less critical machines may be observed with scanning-type microprocessors, or checked periodically with portable instrumentation.

Whenever a vibration measurement indicates a machine problem, a separate array of instrumentation is available to specially condition the vibration signal for analytical evaluation of the machine's dynamic behavior. In addition to vibration amplitude (which is the parameter measured by conventional monitoring systems), these special instruments evaluate vibration phase angle, frequency, time base waveforms, shaft orbits, and mode shapes. Machines can be analyzed in a steady-state (constant speed, load, pressure, flow, etc.) or transient condition (changing speed or other variables).

The end result of any data acquisition procedure on rotating machinery must involve the documentation of information processed by the instrumentation into various hard copy formats. It is this hard copy documentation that the mechanical engineer must use

to assess a machine's mechanical condition. *Data formats for steady-state measurements* include oscilloscope time base waveforms and orbits and vibration frequency spectra. Transient formats include Polar, Bode', and cascade or waterfall plots, and change in average shaft centerline radial position.

TRANSDUCER CONSIDERATIONS

Proper instrumentation must begin with the correct choice of measurement transducers. The three basic dynamic motion (vibration) transducers are the accelerometer, velocity transducer, and displacement proximity probe. Of these, the proximity probe can also be used for static (or average) position measurements. The choice of which transducer to use must be based on many factors. Among these are the characteristics related to electronic design such as physical environment, frequency response, engineering units of measurement, signal conditioning, and signal-to-noise ratio. However, a more important consideration is the desired type of measurement, from a mechanical standpoint, based on the behavior of the particular machine. There is a basic mechanical difference between transducer types, and this difference should be a primary factor in determining the choice of transducer. Accelerometers and velocity transducers measure machine housing motion with respect to free space (seismic or inertially referenced); proximity probes measure relative motion and position, typically shaft

relative to bearing or bearing housing.

The choice of transducer type usually depends on which part of the machine will provide the most reliable information for machine malfunction diagnosis, the shaft or the housing. The most frequently occurring malfunctions are shaft related. These include unbalance, external and internal preloads such as misalignment, axial thrust action, surge, cavitation, radial and axial rubs, thermally and mechanically bowed rotors, coupling problems, gear wear, self-excited mechanisms, lubrication loss, electrical problems in motors and generators, and cracked shafts, blades, and impellers. Generally, housing related malfunctions occur less frequently and include bearing support failure, excessive piping forces, housing and foundation resonances, insufficient foundation support, loose structural components, foundation material failure, and thermal warpage of the housing or baseplate. Most machine problems, therefore, are manifest as a change in shaft rather than housing motion.

Sometimes shaft-generated motion may be sufficiently transmitted for measurement on the housing. How much shaft motion energy is transmitted to the housing is a function of the mechanical impedance of the shaft/bearing/housing system. Mechanical impedance is determined by the system stiffness, damping and mass relationships of the rotor/support system. In some situations, both shaft motion relative to the housing and housing motion relative to free space may be significant. In these cases, a proximity probe and a seismic transducer should be used in the same plane of measurement.

If a machine is equipped with permanently installed monitor system, and if the transducers used for monitoring have been properly selected, then they should be suitable for analytical measurements also. However, the analysis of some machines and/or certain malfunctions may require different transducers in addition to those used with the monitor system. Transducers selected for a monitor system are intended to indicate the presence of only the most frequently occurring potential malfunctions. If this situation can be anticipated, it is much better to have the transducers permanently installed or at least have permanent provisions for installation on the machine. No transducer can provide meaningful data if the installation technique is questionable.

Displacement Proximity Probe

A proximity probe (Figure 1) measures relative motion displacement and is typically installed to measure shaft motion with reference to the bearing or bearing housing.

The typical frequency response is from zero Hz (dc) to 10 kHz, thus it measures static (or average) position as well as dynamic motion.

When mounted to observe the shaft radially, it measures both radial vibration and average shaft radial position relative to the journal bearing clearance; an axially installed probe measures axial vibration as well as axial shaft position with respect to the thrust bearing clearance. Proximity probes, when observing a once-per-turn shaft discontinuity, can also be used to measure shaft rotative speed and provide a reference for measuring vibration phase angle. A radial probe mounted some lateral distance away from the bearing can measure the amount of shaft bow or eccentricity at shaft slow roll speeds.

Since the most common machinery vibration problems are shaft related (unbalance, rubs, misalignment, etc.), shaft measurements are generally more reliable for overall machine protection monitoring systems or periodic machine measurements and provide more meaningful information for machine malfunction diagnosis. Many rotating machines, particularly those with fluid film bearings, generate much more shaft motion relative to the bearing or bearing housing than absolute bearing housing or machine casing motion.

The only major limitation when using proximity probes concerns the quality and nature of the shaft surface to be observed by the probe. Ideally, the probe should observe a surface equal in finish to the shaft bearing journal. Surface imperfections such as scratches, dents, rust, and out-of-roundness produce mechanical runout (Glitch) which appears as a noise component on the output signal of the Proximitor. In addition, the proximity transducer system is affected by changes in magnetic and conductive properties of the shaft surface material. "Spot magnetism", a concentrated magnetic field at one point on the shaft circumference, may produce a false signal output from the Proximitor (electrical runout). If surface conductive (resistivity) properties change significantly from one point on the shaft circumference to another, this may also cause electrical runout.

Such changes in surface resistivity may originate from metallurgical changes, surface hardness variations, heat treatments, certain grinding or finishing techniques, and plating or spray metalizing processes. Some shaft surface treatment techniques, such as burnishing, have been used effectively for the reduction of electrical runout.

Velocity Transducer

Velocity transducers (Figure 2) are of seismic design and are thus used to measure machine housing and structural vibration. The typical frequency response is from 15 Hz to 2 kHz. Velocity is also a function of frequency so the velocity transducer may tend to emphasize higher frequency motions and overlook lower frequency vibrations. For

lower frequency applications, integrating the velocity signal to displacement may help this situation. For measurements at very low frequencies, particular attention should be paid to the amplitude and phase errors of the transducer at the frequency of interest. Machine housings undergo vibration from structural excitations and resonances as well as shaft-transmitted motion. Many different frequencies may be present in the overall signal so that frequency measurement or spectrum presentations are often required for analysis.

If a particular machine exhibits significant housing motion which is transmitted from the shaft, then a velocity transducer may be useful for the measurement of overall machine vibration. It may be useful to integrate the velocity signal to displacement for this application. Also for this application, the velocity transducer is generally more suitable than an accelerometer, provided the vibration frequencies do not exceed its capabilities. The only major disadvantage is the mechanical (spring/mass/damper) construction of the transducer. Some deterioration can be expected over a period of time even during normal use, so a velocity transducer usually requires a calibration check more often than most types of accelerometers.

Accelerometer

Accelerometers (Figure 3) are inertially referenced transducers, and as such, measure absolute machine housing or structural motion relative to free space. The typical frequency response is from 5 Hz to 20 kHz and sometimes higher for special models. At first, this may seem like such a broad frequency range that an accelerometer could be used for all machine housing vibration applications. In fact, this is not the case because acceleration is a function of frequency squared, and at low frequencies of vibration the amplitudes of acceleration are very small. The amplitudes may be so small that the signal will be lost in the noise level of the transducer. For example, if a 900 rpm fan has a synchronous housing vibration of 5 mils peak-to-peak displacement, this yields about 0.05 g's zero-to-peak acceleration. At a typical accelerometer sensitivity of 100 mV/g zero-to-peak, the signal output amplitude would be only 5 millivolts zero-to-peak. However, at high frequencies, even low displacement amplitudes produce high acceleration amplitudes. Thus, accelerometers have some difficulty measuring low frequency motion, but are often best for very high frequency vibration. Therefore, it is difficult to apply accelerometers as the only transducer type used for overall evaluation of machine vibration characteristics.

Accelerometers can be used quite effectively for the exclusive measurement of high frequency vibrations. The measurement of most vibrations above 3 kHz require the use of

accelerometers. Also, because accelerometers have such a broad frequency response, it is usually necessary to use a filter(s) for meaningful vibration signal analysis. Frequency spectrum analysis is often mandatory when using accelerometers. Likewise, when used with a monitor system, filtering is sometimes required in the monitor.

Dual Probe

The dual probe (Figure 4) is a combination relative proximity probe and seismic velocity transducer mounted at the same radial and lateral location on a machine. Ideally, the seismic transducer is mounted to the same reference position on the machine structure as the relative proximity probe. In this installation, the seismic transducer measures vibration associated with the structure upon which the proximity probe is installed. The resulting information from this transducer arrangement consists of: (1) Shaft motion relative to the bearing housing, (2) Average radial shaft position relative to the bearing housing, (3) Absolute bearing housing motion and (4) Shaft absolute motion. The first two measurements are those normally associated with the use of a proximity probe transducer system. The third measurement is that which is normally associated with a velocity transducer system mounted on the bearing housing or probe support structure. The fourth measurement is obtained by electronic integration of the velocity signal to displacement, and a vectorial summation of the dynamic signals from the proximity probe and integrated velocity transducer. This vectorial summation consists of the shaft to bearing housing relative dynamic motion and the bearing absolute dynamic motion and yields a signal representative of the shaft absolute motion, or shaft dynamic motion with respect to free space.

The dual probe is somewhat analogous to the shaft rider transducer. A shaft rider consists of a mechanical rod which is placed in contact with the shaft member and is directly attached to a velocity transducer. The shaft rider provides a direct measurement of shaft motion with respect to free space, or shaft absolute vibration. The dual probe, however, is much more than a shaft rider. A shaft rider provides a measurement of shaft absolute motion only, whereas the dual probe provides this measurement in addition to the other three measurements listed above. Also, the shaft rider suffers from two mechanical systems, the shaft rider itself which must transmit shaft energy directly to the transducer, and the mechanical spring/mass/damper system associated with a velocity pickup. The Dual probe contains only one of these mechanical systems, that associated with the velocity transducer. For these reasons, the dual probe technique is replacing the shaft rider systems on most machines which require shaft absolute motion measurement.

Applications suitable for the use of a dual probe are those in which there is both significant shaft motion relative to the machine housing and machine housing motion relative to free space. On some machine designs, the majority of shaft dynamic motion is greatly attenuated by the time the energy reaches the machine housing. In this case, there will be significant shaft motion relative to the housing and very little housing motion relative to free space. In other machine configurations, the majority of shaft dynamic motion is transferred directly to the machine housing. In this case, there may be very little shaft motion relative to the housing and more significant housing motion relative to free space. The above two cases may be satisfactorily measured with a proximity probe in the first case, and a velocity transducer in the second case. However, some machine designs produce shaft dynamic motion and machine housing motion which are both significant in magnitude. For these situations, shaft relative, bearing housing absolute, and, therefore, shaft absolute motion should be measured. It is for these type of applications that the dual probe is intended.

A brief summary of the basic advantages and disadvantages of each of the three types of transducers is provided in Table I. The majority of these considerations relate to the electronic (or mechanical) design of the transducer itself. However, remember that the most important considerations when selecting a specific transducer type is what mechanical measurement is most desirable on the machine. To determine this, machine behavior must be evaluated (or estimated) in terms of shaft and housing vibrations under both normal operating and malfunction conditions.

TRANSIENT DATA

Typically, transient data is acquired during machine start-up or coastdown when rotor speed is changing as a function of time. Two of the data formats in this category, Polar and Bode' plots, display synchronous (1X) vibration amplitude and phase angle versus rotor speed. This information is available through the use of a once-per-revolution shaft reference (Keyphasor) probe. The transducer input signals can be from any one of the three types, but proximity probes provide the best data, since the measurement represents actual shaft dynamic motion.

The Bode' plot (Figure 5) is on an XYY' Cartesian format with one X variable (rotor speed) and two Y variables (amplitude and phase). The amplitude is determined using a synchronous tracking Digital Vector Filter, which measures amplitude at shaft rotative frequency (1X) only and discards all other frequencies. Since one of the basic rotor malfunctions, unbalance, produces vibration

at 1X, the Bode' plot is sometimes called an "unbalance response plot". The Bode' plot reveals information related to several fundamental rotating machinery characteristics. Among these are":

1. The overall response of the rotor to unbalance forces from zero rpm up to operating speed.
2. The extent of rotor bow by measuring amplitude and phase at slow roll speeds.
3. The definition of actual balance resonant frequency (critical speed) by determining the rotor speed at which an amplitude peak and phase shift occur.
4. The available system damping by measuring the height of the amplitude peak at resonance.

A similar XY plot can be made using the Digital Vector Filter in the direct or unfiltered mode. This plot represents amplitude of the overall composite (including all frequency components) vibration signal as a function of rpm. Comparing this to the Bode' plot will reveal the presence of any vibration frequency components which are not at shaft rotative speed.

The Polar plot (Figure 6), as the name implies, is on polar format and is obtained from the same data as the Bode' plot (rpm, 1X amplitude, and phase). The difference is that the Polar plot represents this information as vector quantities, which they are on the actual working machine. The distance from any point on the plot (length of vector) represents the vibration amplitude; the angular position of any point on the plot (direction of vector) represents the phase angle. The Polar plot reveals the same information listed above for the Bode' plot and, in addition, it provides:

1. A clearer picture of the changing vector response of a rotor through a resonant speed region. (Certainly, the approximate 180 degree phase shift is easier to see on Polar format.)
2. The effect of any slow roll vector, as from shaft bow, on the measured response (the slow roll vector can be easily subtracted from any point on the plot by graphical vector methods).
3. The presence of any structural resonances, which appear as inside loops on the plot.
4. The phase relationship of rotor response through two or more resonant speed regions.

STEADY-STATE DATA

Steady-state data is acquired when the machine is at constant operating conditions; i.e., constant rotor speed, flow, load, etc. Considering all transducer types, the vibration frequency spectrum is probably the most frequently used steady-state data presentation. This is an XY Cartesian display of vibration amplitude as a function of frequency. Since this format is widely known and published, an additional discussion will not be included here. Certainly, frequency of motion is one of the most revealing indicators of mechanical condition and the presence of specific malfunctions. However, for rotating machinery measurements, the shape of the vibration waveform and the dynamic path (orbit) of the shaft centerline can be equally informative.

A time base waveform display on an oscilloscope can reveal frequency modulations, which are not as easily seen on a spectrum display. When the scope display is enhanced by the addition of a Keyphasor pulse superimposed on the waveform, the display is even more informative. Exact frequency identification on a spectrum display is limited to the bandwidth of discrete filter segments. The scope with a Keyphasor input presents very directly the vibration frequency as compared to shaft rotative speed. Frequencies which are exactly at, exact multiples or integer fractions of rotative speed are represented by fixed position Keyphasor pulses on the waveform or orbit. Any other (nonsynchronous) frequencies will produce moving Keyphasor pulses.

Since an orbit is an exact representation of dynamic shaft centerline motion, this display can be very informative of mechanical condition and the presence of specific malfunctions. The shape of the orbit can indicate, for example, small or large motion

at shaft rotative speed with or without the presence of any unidirectional preloads, such as from misalignment. Shaft rotative speed motion from unbalance forces will be circular or slightly elliptical. With the addition of a preload, the orbit will become more elliptical.

Since the scope can be oriented to represent the true up and right (or down and left) directions on a machine, the orientation of the major and minor axes of the ellipse will determine the direction of the preload. If a rotor to stator rub is occurring, the exact location of the radial rub can be determined by the location of the rub indication on the orbit.

Figure 7 shows time base waveforms and orbits for a rotor undergoing oil whirl in a bearing. On both displays, the changing location of the Keyphasor dot indicates the presence of a nonsynchronous frequency component. It can also be seen that the direction of shaft centerline motion is in the same direction as shaft rotation. In fact, the oscilloscope is the only instrument which can reveal the direction of motion.

SUMMARY

Only a few of the many data presentations for rotating machinery have been presented here. A complete discussion of all the formats would require a complete text, not a brief technical paper. And then, the applicability of each format to the many varied machine types and for analysis of the many different mechanical malfunctions would require an additional text. However, with the proper application of vibration transducers and the availability of instrumentation for data display and documentation, rotating machinery analysis is rapidly evolving from an art to an engineering science.

TABLE I
EDDY-CURRENT PROXIMITY PROBES

Advantages	Disadvantages
<ol style="list-style-type: none"> 1. Measures directly the dynamic motion of the shaft, which is the source of vibration for the most common (frequently occurring) machine malfunctions, such as imbalance, misalignment, rubs, bearing instability, etc. 2. Measures average rotor position (relative to bearing or housing) within the bearing clearance, an important indicator of steady-state unidirectional preloads on the rotor, such as from misalignment, fluidic or aerodynamic influences, etc. 3. Ease of calibration; only static calibration required using spindle micrometer and digital voltmeter; since probes and extension cables themselves are not calibrated items, a spare probe and cable can be used with installed Proximity at the machine site (complete transducer system can remain installed on machine during calibration). 4. Same type of transducer can be used for axial thrust position, rotor eccentricity (bow), rotor speed, and phase angle (Keyphasor reference) measurements. 5. Measures directly in engineering units of displacement, the most meaningful units for evaluating overall machine response and vibration severity for the more common machine malfunctions. 6. Good signal-to-noise ratio; high level low impedance output, good for over 1,000 feet (300 meters) of transmission. 7. Measurement is via noncontact medium (proximity) so transducer will not influence vibratory motion of observed surface due to contact. 8. Broad frequency response, from zero Hz (dc or static position) to 10 kHz. 9. Solid-state for extended reliability (no moving parts). 10. Small in size and can therefore be installed in most machinery. 11. Upper temperature limit of 350°F (177°C) entirely adequate for most environments in and adjacent to bearing areas. 12. Modular system design with the least expensive part, the probe, only requiring occasional replacement (if inadvertently damaged). 	<ol style="list-style-type: none"> 1. Runout or Glitch (electrical and mechanical); dependent upon high quality shaft surface finish, free from scratches, rust, corrosion, etc., and localized (spot) magnetic fields. 2. Somewhat sensitive to various special shaft materials (metallurgical content); may require special calibration to specific material. 3. Requires external dc power source. 4. Can be difficult to install on some machine (bearing) designs. 5. Usually difficult to install quickly on a temporary basis; probes should be permanently installed even for periodic measurements. 6. Must be used in conjunction with a seismic transducer mounted on the bearing housing for machines with low mechanical impedance ratio (low impedance results from low case-to-rotor weight ratio and compliant bearing support structure); vectorial summation of the two signals yields shaft absolute (relative to free space) vibration measurement.

TABLE II

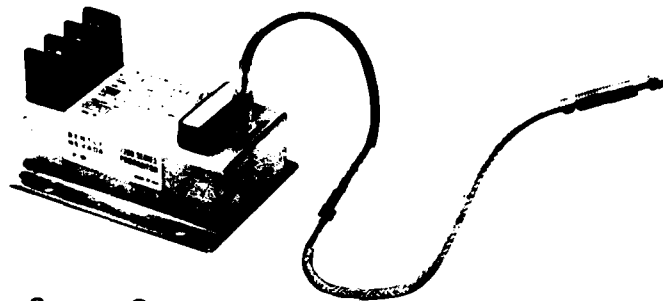
VELOCITY TRANSDUCERS

<u>Advantages</u>	<u>Disadvantages</u>
<ol style="list-style-type: none"> 1. Ease of installation in that it is mounted on external (housing) machine components. 2. Strong signal in the mid-frequency ranges (30 Hz to 1 kHz). 3. Self-generating, no external power source required. 4. Can measure shaft absolute (relative to free space) vibration when mounted to a shaft rider or "fishtail". 5. Adequate frequency response for overall evaluation of machines in the mid-speed range. 6. Can be temporarily installed with reasonable success using a magnetic base. 7. Some models are available for moderately high temperatures. 8. Velocity is relatively easy to integrate to displacement, which is a more meaningful engineering unit of measurement for overall evaluation of machinery vibration. 	<ol style="list-style-type: none"> 1. Provides only limited information about shaft dynamic motion (for overall evaluation of machine vibration), requires that the machine have low mechanical impedance. 2. Since mounting is on external machine components, measurement can be influenced by vibrations transmitted to the machine housing from the surrounding environment, e.g., piping, foundation, adjacent machinery, etc.; mounting location should be carefully selected so measurement will accurately reflect only vibration of the machine itself, with minimal outside influences. 3. Mechanical design (spring/mass/damper) dictates that performance will degrade somewhat over a period of time under normal use. 4. Unit construction means that any transducer fault requires replacement of complete transducer assembly. 5. Difficult calibration; requires removal from the machine and a shaker table. 6. Amplitude and phase errors introduced at low frequencies. 7. Cross axis sensitivity problems at high amplitudes. 8. Rather large and heavy.

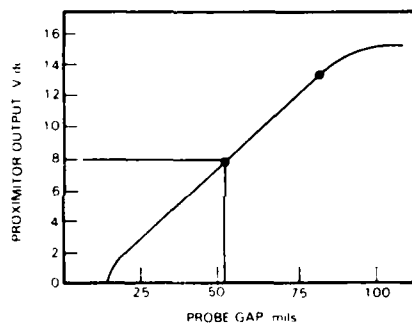
TABLE III

ACCELEROMETERS

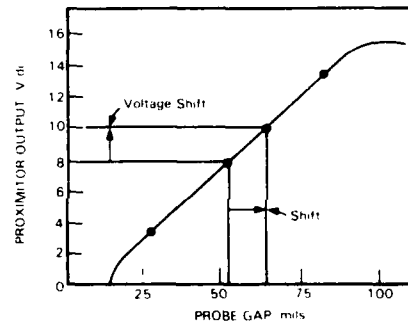
<u>Advantages</u>	<u>Disadvantages</u>
<ol style="list-style-type: none"> 1. Ease of installation in that it is mounted on external (housing) machine components. (However, refer to item 3 in the next column.) 2. Very useful for high frequency measurements above 5 kHz. 3. Effectively no moving parts for good reliability. 4. Some models available for high temperature applications. 5. Once certain maximum frequency and temperature limits are exceeded, an accelerometer becomes the only viable vibration transducer. 6. Relatively light weight. 	<ol style="list-style-type: none"> 1. Provides only limited information about shaft dynamic motion (for overall evaluation of machine vibration), requires that the machine have low mechanical impedance. 2. Since mounting is on external machine components, measurement can be influenced by vibrations transmitted to the machine housing from the surrounding environment, e.g., piping, foundation, adjacent machinery, etc.; mounting location should be carefully selected so measurement will accurately reflect only vibration of the machine itself, with minimal outside influences. 3. Susceptible to noise resulting from method of attachment or poor contact to machine housing; requires deliberate effort to achieve effective installation, difficult to succeed with temporary mounting, virtually impossible to hand-hold. 4. Unit construction means that any transducer fault requires replacement of complete transducer assembly. 5. Difficult calibration; requires removal from the machine and a shaker table. 6. Difficult to use for some low speed machines since low acceleration levels produce signals which are typically not far above noise floor. 7. Double integration to displacement for overall evaluation of machinery vibration is susceptible to noise problems. 8. Usually requires filtering in the monitor, and must be individually evaluated to specify filters for each machine case. 9. Requires external power source. 10. Somewhat sensitive to damage (requiring replacement) due to harsh impact (dropping on concrete, etc.), particularly in the nonsensitive axis.



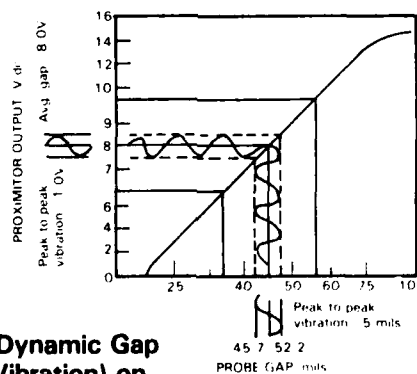
1a. System Components:
Proximitor, Extension Cable, Probe



1b. Typical Signal Output Characteristic of Proximitor



1c. Effect of Static Gap Change on Output



1d. Effect of Dynamic Gap Change (Vibration) on Output

Figure 1. Displacement Proximity Probe Transducer System

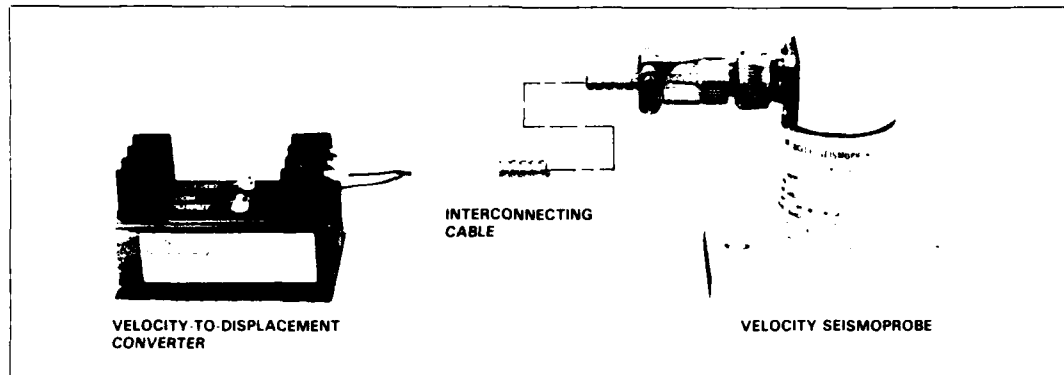


Figure 2. Velocity Transducer System

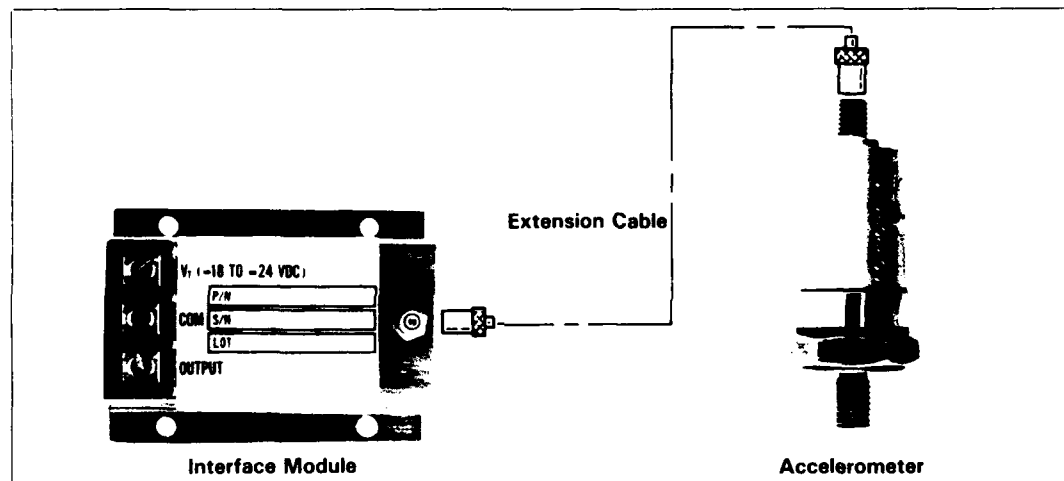


Figure 3. Accelerometer Transducer System

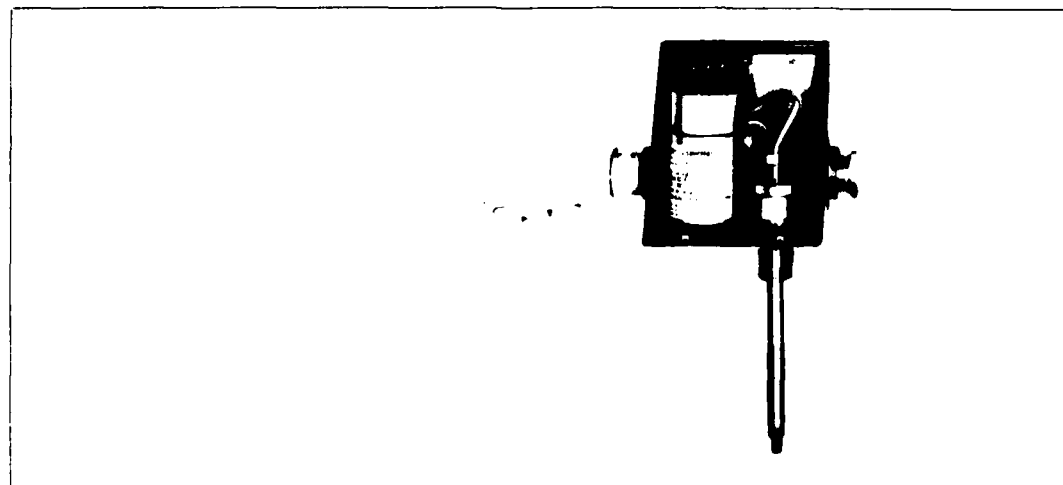
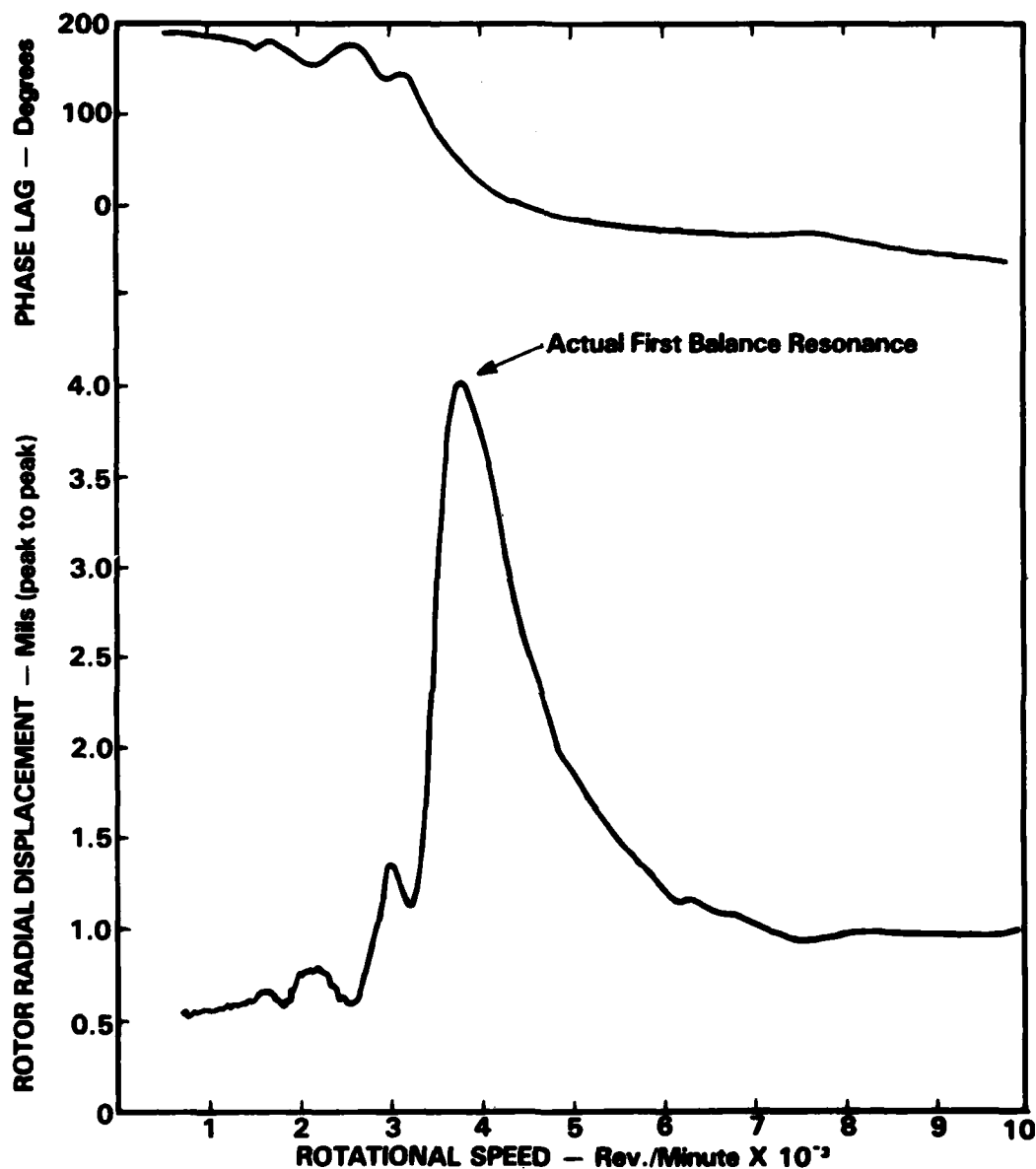


Figure 4. Dual Probe Transducer System



Bode Plot Showing:

- a. Resonant Frequency at ~ 3750 rpm
- b. Slow Roll Vector of 0.5 mils at 190°
- c. Available Damping Provides Amplification Factor of ~ 4
(4 mils at resonant peak + 1 mil at speed above resonance)

Figure 5

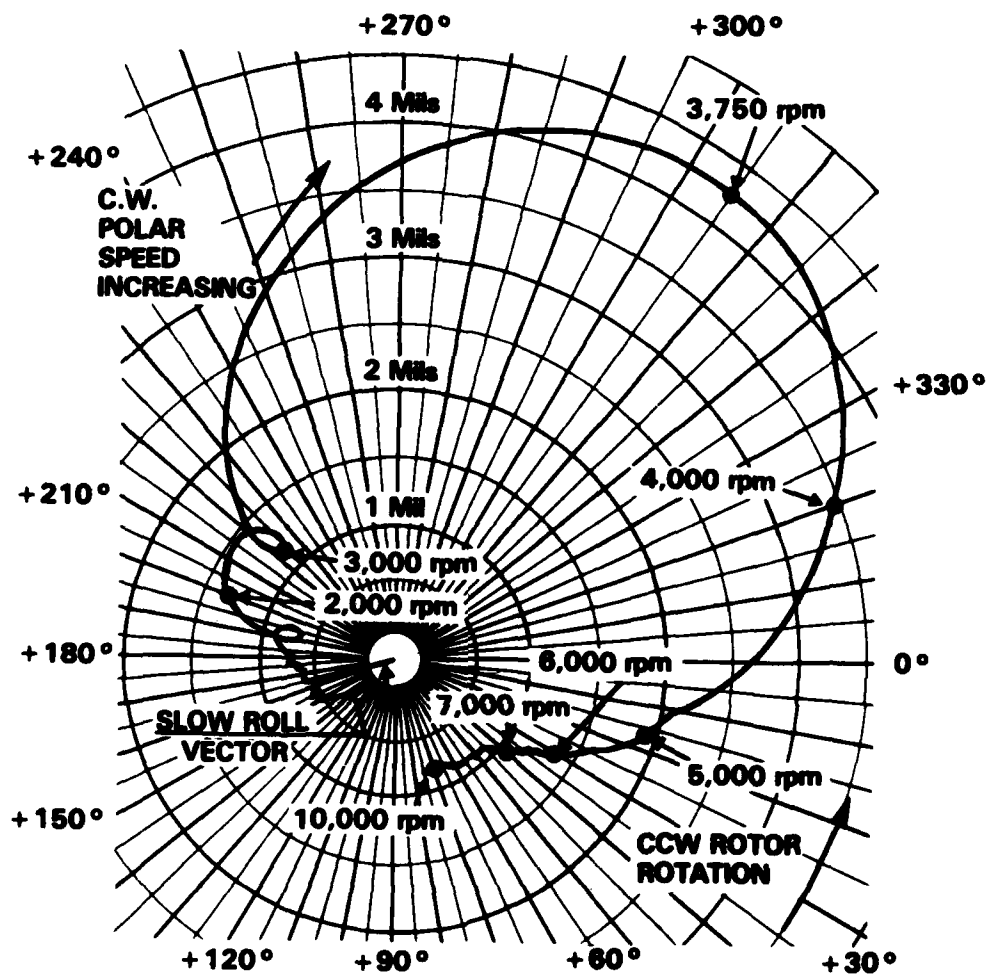


Figure 6. Polar Plot Showing:

- Resonant Frequency at 3750 rpm
- Slow Roll Vector of 0.5 mils at 165°
- 180° Phase Shift Through Resonance
- Phase Angle Lags (moves in opposite direction to shaft rotation) Through Resonance
- Minor Structural Resonances at 1500 rpm and 3000 rpm

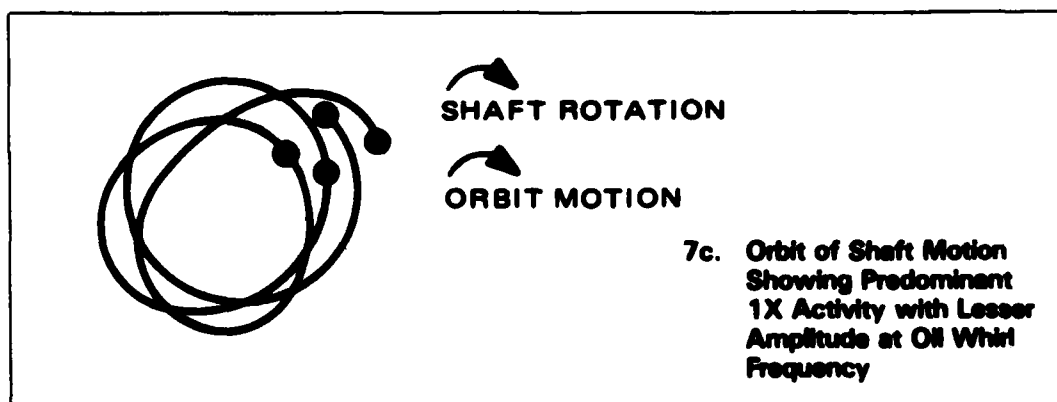
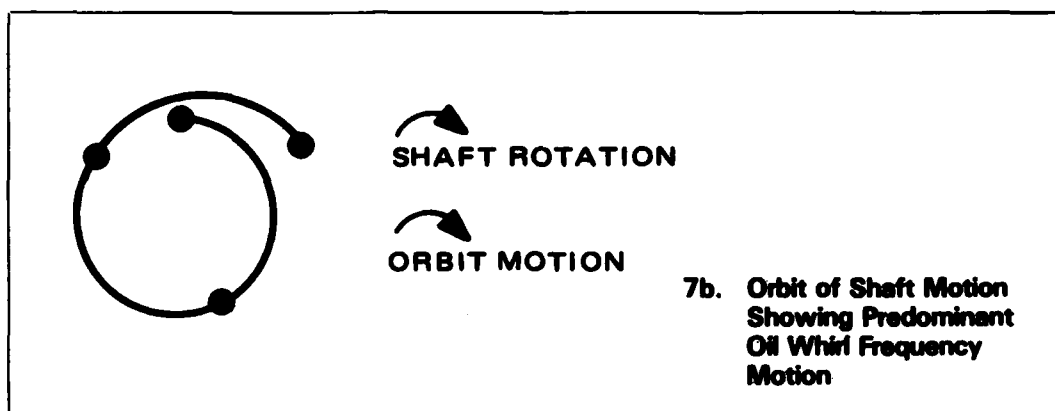
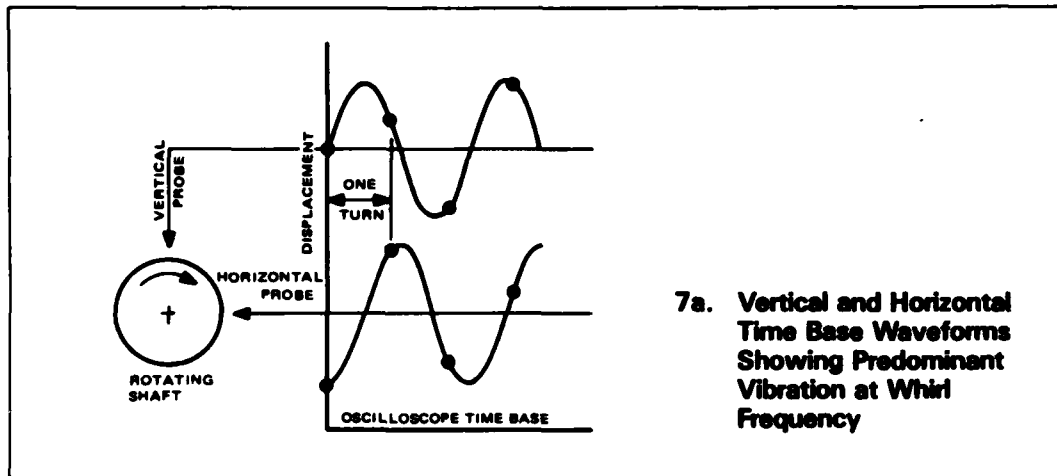


Figure 7. Oscilloscope Time Base and Orbit Display

ROTOR DYNAMICS AND MACHINERY VIBRATION

SPIN TEST VIBRATIONS OF PENDULOUSLY

SUPPORTED DISC/CYLINDER ROTORS

F. H. Wolff and A. J. Molnar
Westinghouse R&D Center
Pittsburgh, Pennsylvania

Forced vibration levels of disc and cylindrical shaped rotors as they are brought up to speed are calculated. The danger of spinning a pendulously supported rotor whose polar and diametral mass moments of inertia are nearly equal is analyzed and explained.

INTRODUCTION

To design pendulously supported high speed rotors, several vibration aspects must be considered - instabilities, unbalance vibrations, etc. Low frequency whirl instabilities caused by insufficient external (bearing) damping, shaft hysteresis, and looseness of mating rotor components must be avoided. Previous works [1,2] which addressed the instability problem demonstrate how to analyze a pendulously supported disc system to ensure a successful design.

A disc shaped rotor has the property that its ratio of polar moment of inertia (I_p) to moment of inertia about a diameter (I_d) is 2; i.e., $a = I_p/I_d = 2$. If external damping is sufficient, the unbalance vibration due to passing through the critical speeds as the disc is brought up to speed will be small. However for some specimens, the rotor configuration appears more like a cylinder than a disc; i.e., the ratio of inertias decreases. If $a = 1$ or $I_p = I_d$, the system will probably fail as it is brought up to speed. Previous failures have occurred, but have not been documented. The objective of this study was twofold: to explain the failure mechanism and to develop a program to calculate vibration amplitudes of proposed designs.

EQUATIONS OF MOTION FOR STEADY STATE UNBALANCE

Equations which describe the motion of a pendulously supported disc

have been derived in the literature [1,2,3]; however, for completeness they will be summarized. From Fig. 1A the beam deflection (η) and slope (θ) at the disc can be expressed as a function of unbalance force (P) and moment (M).

$$\eta = \alpha_{11} P + \alpha_{12} M \quad (1)$$

$$\theta = \alpha_{12} P + \alpha_{22} M$$

where the flexibility influence coefficients of a beam of length (L), with infinitely stiff end (λ), and rigidity (EI) are

$$\alpha_{11} = \frac{L^3}{3EI} + \frac{L^2\lambda}{EI} + \frac{L\lambda^2}{EI}$$

$$\alpha_{12} = \frac{L^2}{2EI} + \frac{L\lambda}{EI} \quad (L=L-\lambda)$$

$$\alpha_{22} = \frac{L}{EI}$$

The unbalance force and moment can be written as [1,2,3] functions of disc translation (r) and rotation (θ)

$$P = m \omega^2 r \quad (2)$$

and

$$M = -I_d \omega^2 \left(\frac{I_p}{I_d} \frac{\Omega}{\omega} - 1 \right) \theta \quad (3)$$

where m is the disc mass (lb sec²/in), ω is the whirl speed (rad/sec), Ω is

$$F = m \epsilon_1 \Omega^2 \sin \Omega t \quad (7)$$

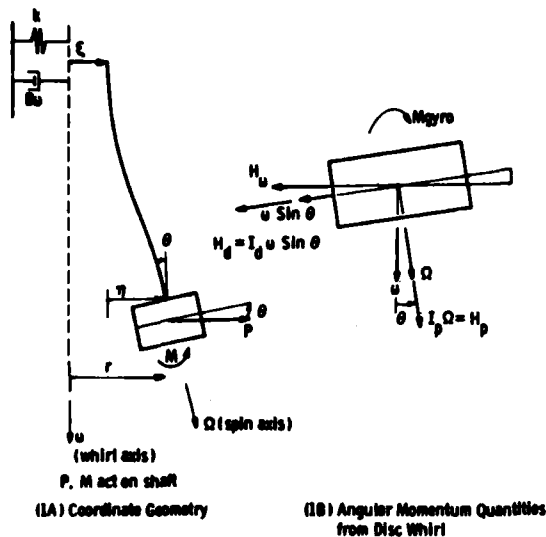


Fig. 1 - Dynamic model of spin test system (disc-shaft-bearing system)

the disc polar mass moment of inertia (in-lb-sec²), and I_d is the disc diametral mass moment of inertia (in-lb-sec²).

To find the damped steady state response of the disc mass unbalance, complex notation (-) is used. The bearing translation ($\bar{\xi}$) as a function of unbalance force is

$$\begin{aligned} \bar{\xi} &= \frac{\bar{P}}{k + iB\omega} \\ &= \frac{k}{k^2 + (B\omega)^2} \bar{P} - i \frac{B\omega}{k^2 + (B\omega)^2} \bar{P} \end{aligned} \quad (4)$$

where i is imaginary ($\sqrt{-1}$), k is the bearing stiffness (lb/in), and $b\omega$ is the bearing damping (lb/in). The total disc deflection (\bar{r}) is

$$\begin{aligned} \bar{r} &= \bar{\xi} + \bar{\eta} \\ &= \left\{ \frac{k}{k^2 + (B\omega)^2} + \alpha_{11} - i \frac{B\omega}{k^2 + (B\omega)^2} \right\} \bar{P} \quad (5) \\ &\quad + \{\alpha_{12}\} \bar{M} \end{aligned}$$

while the slope ($\bar{\theta}$) is

$$\bar{\theta} = \alpha_{12} \bar{P} + \alpha_{22} \bar{M} \quad (6)$$

Eccentricity (Fig. 2) of the disc center of mass gives a static unbalance force (F)

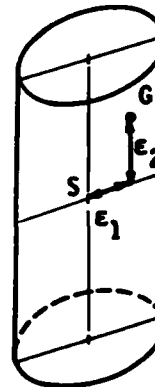


Fig. 2 - Eccentricity of mass center (G) from geometric center which creates force (F) and moment unbalance (T)

and a dynamic unbalance moment (T)

$$T = m \epsilon_1 \epsilon_2 \Omega^2 \sin \Omega t \quad (8)$$

due to centrifugal loads. Hence, the total unbalance force and moment are

$$\bar{P} = m \omega^2 \bar{r} + F \quad (9)$$

and

$$\bar{M} = -I_d \omega^2 (a \frac{\Omega}{\omega} - 1) \bar{\theta} + T \quad (10)$$

for $a = I_p/I_d$.

Combining equations (5) through (10) into matrix form gives

$$\begin{bmatrix} C_{11} & C_{12} \\ C_{21} & C_{22} \end{bmatrix} \begin{bmatrix} \bar{r} \\ \bar{\theta} \end{bmatrix} = \begin{bmatrix} D_{11} & \alpha_{12} \\ \alpha_{12} & \alpha_{22} \end{bmatrix} \begin{bmatrix} m \epsilon_1 \Omega^2 \sin \Omega t \\ m \epsilon_1 \epsilon_2 \Omega \sin \Omega t \end{bmatrix} \quad (11)$$

where

$$C_{11} = 1 - \left(\frac{k}{k^2 + (B\omega)^2} + \alpha_{11} \right) m \omega^2 + i \frac{B\omega}{k^2 + (B\omega)^2} m \omega^2$$

$$C_{12} = \alpha_{12} I_d \omega^2 \left(a \frac{\Omega}{\omega} - 1 \right)$$

$$C_{21} = -\alpha_{12} m \omega^2$$

$$C_{22} = 1 + \alpha_{22} I_d \omega^2 \left(a \frac{\Omega}{\omega} - 1 \right)$$

$$D_{11} = \frac{k}{k^2 + (B\omega)^2} + \alpha_{11} - i \frac{B\omega}{k^2 + (B\omega)^2}$$

For a synchronous whirl ($\Omega = \omega$), equation (11) reduces to

$$\begin{bmatrix} C_{11}^* & C_{12}^* \\ C_{21}^* & C_{22}^* \end{bmatrix} \begin{bmatrix} \bar{r} \\ \bar{\theta} \end{bmatrix} = \begin{bmatrix} D_{11}^* & \alpha_{12} \\ \alpha_{12} & \alpha_{22} \end{bmatrix} \begin{bmatrix} m \epsilon_1 \sin \Omega t \\ m \epsilon_1 \epsilon_2 \sin \Omega t \end{bmatrix} \quad (12)$$

where

$$C_{11}^* = \frac{1}{\Omega^2} - \left(\frac{k}{k^2 + (B\Omega)^2} + \alpha_{11} \right) m + i \frac{B\Omega}{k^2 + (B\Omega)^2} m$$

$$C_{12}^* = \alpha_{12} I_d (a-1)$$

$$C_{21}^* = -\alpha_{12} m$$

$$C_{22}^* = \frac{1}{\Omega^2} + \alpha_{22} I_d (a-1)$$

$$D_{11}^* = \frac{k}{k^2 + (B\Omega)^2} + \alpha_{11} - i \frac{B\Omega}{k^2 + (B\Omega)^2}$$

SECOND FORWARD WHIRL MODE

The pendulously supported rotor of Figure 1 has two forward whirl modes [1]: The lower forward whirl mode involves primarily disc translation (r) with a smaller angular rotation (θ) where both r and θ have the same sign; the second forward whirl mode involves translation with the larger rotation having opposite signs. Both modes (undamped) are found from the characteristic polynomial associated with the homogeneous form of equation (11).

Figure 3 shows the spin-forward whirl characteristics for a disc ($a = I_p/I_d = 2$) with the rotor system properties in Table 1. The lower mode frequency initially increases because of a gyroscopic effect then asymptotically approaches a maximum value, while the second mode frequency monotonically increases with running

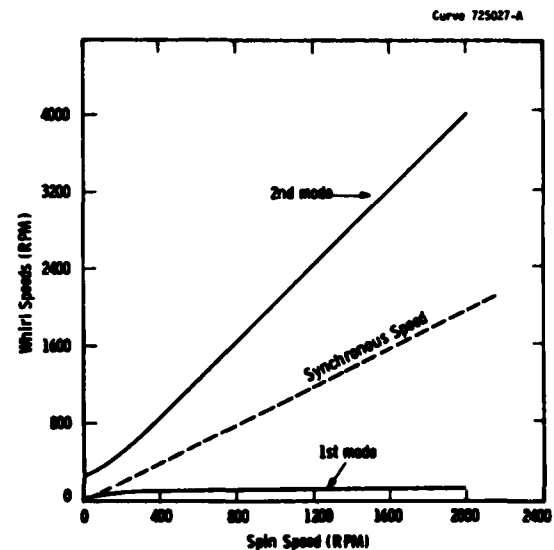


Fig. 3 - Forward whirl speeds for disc shaped ($a = I_p/I_d = 2$) specimen

speed (spin). The running speed dashed line (Figure 3) passes through the lower forward whirl mode but is always well below the second forward whirl mode. Because of the small unbalance forces at the lower speeds and bearing damping, the vibration levels while passing through the first critical are usually small.

With some effort most disc shaped ($a=2$) rotors can be designed so that vibration amplitudes are acceptable while the rotor is being brought up to speed. However, if the inertia ratio (a) differs substantially from 2, forced vibration of the second forward whirl mode could be serious. If the two inertias are equal ($a=1$), the second forward whirl mode speed and running speed (dashed line) nearly coincide (Figure 4). Furthermore, running speed and second forward whirl mode speed approach each other with increasing run speed. In effect, the system is forever running near resonance when $a=1$. It becomes apparent why earlier systems with this peculiarity have failed.

Figure 4 shows the second forward whirl modes for the rotor system of Table 1 with inertia ratios ranging from 0.25 to 2.0. For ratios less than 1.0 when the rotor resembles a cylinder rather than a disc, the running speed is above the second forward whirl mode speed for most of the run up. However, the second mode must be accelerated through which involves a resonant condition. On the contrary when the inertia

ratio is greater than 1.0, the second mode speed is always above running speed and they diverge with increasing run speed.

TABLE 1
Properties of Cylinder and Spin Test Rig

Modulus of Elasticity	E	30E+6	lb/in ²
Shaft Diameter		.75	in.
Shaft Length	l	20	in.
Stiff Length	λ	10	in.
Bearing Stiffness	k	2000	lb/in
Bearing Damping	B_w	2000	lb/in
Disc Weight	W	1200	lb
Polar Moment of Inertia	I_p	350.0*	lb-in-sec ²
Diametral Moment of Inertia	I_d	175.0	lb-in-sec ²

* for $a=2$

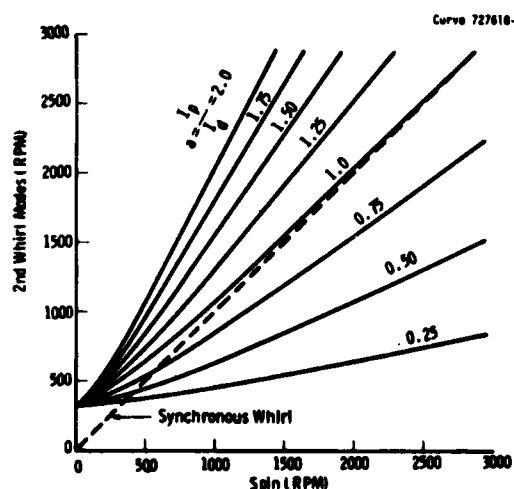


Fig. 4 - 2nd forward whirl modes of rotors with various inertia ratios ($.25 \leq a \leq 2.0$)

UNBALANCE VIBRATION OF THE SECOND FORWARD WHIRL MODE

To evaluate rotor designs the vibration response to mass imbalance should be determined using equation (12). The primary source of excitation of the second forward whirl mode would come from a moment (T) caused by a non-uniform mass distribution (ϵ_2) along

the spin axis in addition to an eccentricity (ϵ_1) of the mass center from the geometric center (Figure 2). The mass center eccentricity (ϵ_1) also causes a static unbalance force (F). Figures 5 and 6 show angular responses (θ) of the rotor as a function of inertia ratio for a 1 mil eccentricity of the mass center and an additional 10 mil moment unbalance. The angular displacement responses were divided by the static angular displacement ($m\epsilon_1\epsilon_2/I_d$) to produce amplification.

Figure 5 resonance curves show evidence of the second forward whirl mode being passed through when the inertia ratio is less than 1. Although bearing damping is only slightly effective in this mode (motion at the bearing is relatively small, $r/\theta \ll 1$), the peaks are very sensitive to the inertia ratio (a). For inertia ratios approaching unity, the vibration amplitudes increase both at the instant the second mode is passed through and at high speeds. With an inertia ratio of unity, the vibration level increases indefinitely with running speed because running speed approaches the second forward whirl mode speed. Even though the unbalance moment which is a function of the square of speed is smaller at lower speeds, there are regions at low speeds where an inertia ratio less than 1.0 can produce vibrations greater than those produced with a ratio of unity. For example, an inertia ratio of 0.8 gives a peak amplification of 35 near 700 rpm while the peak at 700 rpm with $a=1$ would only be 5 (Figure 5). However, for speeds above 900 rpm, the response for an inertia ratio of 0.8 would always be less than the response for $a=1.0$.

For inertia ratios greater than 1.0, the larger the ratio, the lower the vibration level over the entire speed range (Figure 6). Vibration levels are greatly reduced for only slight increases in inertia ratio; e.g., at 1900 rpm an increase in inertia ratio from 1.0 to 1.1 will reduce the vibration amplitude by a factor of 8.

EFFECTS OF BEARING DAMPING

Because of the small motion at the bearing in the second forward whirl mode, damping is only slightly effective in limiting vibration levels. For example, with an inertia ratio of unity at 1500 rpm (Figure 7), the amplification can only be reduced from 27.5 to 26.25 by doubling the amount of bearing damping (Table 1). For inertia ratios less than 1.0, an increase in damping

resulted in larger responses until running speed surpassed the second mode speed. For inertia ratios greater than 1.0, the difference in responses due to damping is hardly noticeable; e.g., at $a=1.1$, the heavier damped response is slightly smaller.

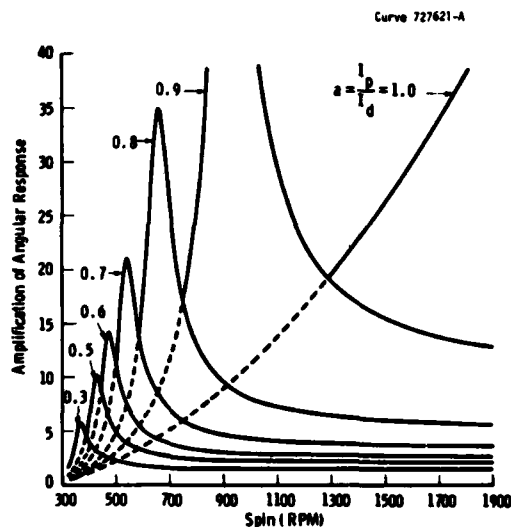


Fig. 5 - Angular displacements (amplification) of rotors with inertia ratios ≤ 1.0

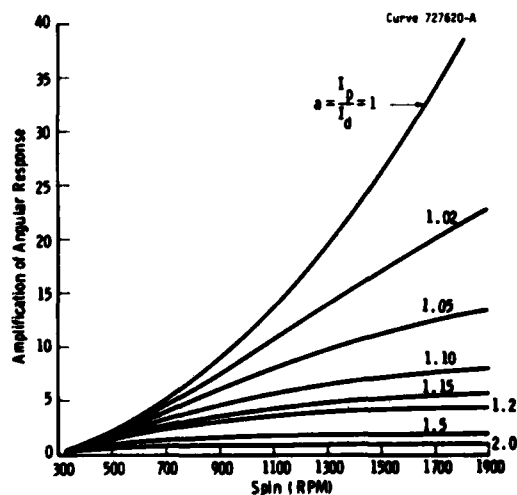


Fig. 6 - Angular displacements (amplification) of rotors with inertia ratios ≥ 1.0

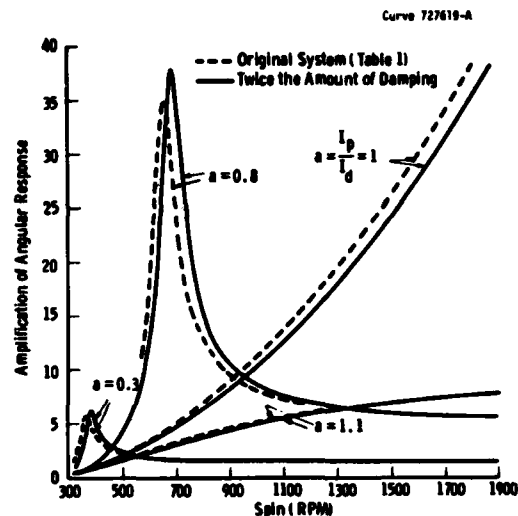


Fig. 7 - Effects of damping on the forced vibration of the 2nd forward whirl modes of rotors with various inertia ratios

CONCLUSIONS

Pendulously supported rotors with inertia ratios at or near unity must be avoided. If not, excessive unbalance vibrations of the second forward whirl mode can occur. The second mode speed asymptotically approaches running speed with increasing speed. Therefore, the unbalance vibration will increase indefinitely with running speed.

Angular rotation of the rotor which predominates in the second forward whirl mode is many times greater than motion at the bearing; accordingly, bearing damping has only a slight influence on vibration levels.

Inertia ratios above unity ($a > 1$) are preferred. Slight increases in the ratio produce significant reductions in the angular vibration amplitudes. When inertia ratios are less than unity ($a < 1$), the second forward whirl mode must be accelerated through. The smaller the inertia ratio, the smaller the buildup is as the critical speed is passed. Also, vibrations at high speed decrease with decreasing inertia ratios.

REFERENCES

1. W. T. Thomson, F. C. Younger, and H. S. Gordon, "Whirl Stability of the Pendulously Supported Flywheel System," J. of Applied Mechanics, Paper No. 77-APM-20, 1977.

2. F. H. Wolff, A. J. Molnar,
G. O. Sankey, and J. H. Bitzer,
"Lateral Instability During Spin
Tests of a Pendulously Supported
Disc," Shock and Vibration Bulletin,
No. 50, 1980.
3. J. P. Den Hartog, "Mechanical
Vibrations," 4th ed., McGraw-Hill
Book Co., New York, 1956.

MODAL ANALYSIS AS A TOOL IN THE EVALUATION
OF A TURBINE WHEEL FAILURE

Anthony L. Moffa
Franklin Research Center
Philadelphia, PA

Robert L. Leon
Franklin Research Center
Philadelphia, PA

Modal Analysis can be a viable tool in the investigation of turbine wheel failures. With the advent of the portable dual channel analyzer, and impact excitation techniques, modal data can be accurately and easily taken right at the plant site. Armed with this additional information, a better estimate of the actual failure mode can be made.

Following a turbine failure, the system is taken out of service, the failed parts are metalurgically analyzed, and the turbine is either repaired or replaced. It is during this often lengthy time period that modal testing can be performed and its evaluation used to aid in the failure analysis.

The following guidelines will be helpful in this endeavor.

- a. The modal test should be performed on the failed wheel, and on an unfailed spare or sister wheel if possible.
- b. The resulting mode shapes should be compared to the actual failure.
- c. A review of the system excitation sources should be made.
- d. An investigation of turbine running data for the possible detection of suspected modal frequencies should be performed.
- e. Finite element and fatigue life analyses should be conducted.
- f. All the above information should be reviewed before final conclusions are drawn.

This paper follows these guidelines, and illustrates by techniques, examples, and actual test data how modal analysis can play an important part in failure evaluation.

1. MODAL ANALYSIS TECHNIQUE

A standard impact modal technique is employed. First, one or two response accelerometers are applied to the structure. Just one will be used, the other serving only to insure that no potentially important modes are being missed. The structure is then impacted at several different points in orthogonal directions, and for each case, a frequency domain transfer function is determined relating the response to the force. The natural frequencies, mode shapes, and damping factors are determined from these transfer functions. Typically the modes are not widely spaced, and some curve fitting capability is required to properly isolate them. This capability is available in many of today's dual channel analyzers. Some also provide special windowing for the force and response waveforms, and in addition, many can display animated mode shapes viewed from any direction.

To illustrate the technique, we discuss the test of a failed control stage of the high pressure turbine shown in Figure 1. The wheel is composed of 36 blades, shrouded in groups of 3. The failure, which is shown, is such that 2 blades, the shroud and a section of the wheel failed completely. Two other blades were cracked at the blade root. These failures started from the exhaust side, and analysis of the completely failed sections was indicative of fatigue.

The frequency range of interest should include as a minimum up to twice nozzle or blade pass frequency relating to the failed stage.

For our example this frequency would be equal to 4320 Hz (36 blades x60x2).

Since the frequency range is broad, the modal test will reveal many natural resonances. In order to accurately describe these different modes, it is necessary to allow a minimum of 12 frequency points within 3 dB of the peak for each mode of interest. This procedure establishes the zoom ranges in which transfer function data is to be gathered.

In addition, sufficient impact points must be established on the structure so that accurate mode shapes can be determined. For blade modes, the size and construction of the blade will help determine the number of impact points. Blades should be impacted on both the immission (leading) edge and exhaust (trailing) edge in two orthogonal directions. If the blades are shrouded into groups, all the blades within each group should be impacted.

Wheel modes are identified by their node lines. In order to accurately find the nodal positions, a sufficient quantity of impact points need to be spaced circumferentially around the wheel. The number of impact points should be at least twice the maximum number of nodes to be detected. With this approach aliasing of mode shapes still occurs for wheel modes which have more nodal diameters than the maximum we are prepared to detect. To help overcome this problem each wheel mode must be identified in sequence. Figure #2 shows those impact points which were selected for our example.

With the use of an exponential response window in the dual channel analyzer, fewer averages are required, and usually good coherence can be obtained by impacting each point only three times. Transfer functions formed in this manner are not truly accurate since they contain added damping, however this is automatically taken into account by the analyzer later on in the determination of the modal parameters.

To save field time, it is desirable to pre-program the analyzer as much as possible prior to the test. The most time saving suggestion is to pre-model the wheel and blade system in the analyzer using the selected impact points. Changes to this program can be made in the field rather easily.

Once the data have been recorded, the analyzer will curve fit and analyze the transfer functions for each indicated natural frequency. Since all analyzers are memory limited, be sure to keep the number of modes to be reviewed within the capacity of the analyzer.

A typical frequency and damping table is shown in Table 1. Also, the analyzer develops a residue table for each mode. These residues define the mode shape and specify the full displacement positions in the animated display.

It is possible for a test of the nature just described to be completed within a 3 to 5 day period in the field. The next phase is to review the modal data in light of the available excitation sources and the actual failure mode.

2. EXCITATION SOURCES

The turbine system must be reviewed to determine which excitation frequencies could cause resonance of the various modes. All stages of the turbine should be reviewed since resonance of a mode at one stage can come from an excitation at another. The excitation sources for the example high pressure turbine are listed in Table 2.

3. MODE SHAPE COMPARISON TO FAILURE

All the mode shapes should be reviewed and identified as to their type. Some of the typical mode shapes for turbine wheels are listed in Table 3. After the mode shapes are determined they can be compared to the actual wheel failure. Table 4 lists the actual modes for our example, their frequencies, and possible excitation sources.

Figures 3 through 7 illustrate some of the mode shapes obtained from the analyzer. These plots form the basis for describing each mode. The figures shown identify a 4 node mode. (Mode #4 of Table 1). The location of the nodes can be accurately determined relative to a reference point on the wheel.

Figure 8 shows a comparison of Mode #4 to the actual failure. Figure 9 shows a comparison of Mode #5 to the actual failure. It is possible that either mode could have caused the failure assuming that the stresses at the node and antinode points were high enough such that if the mode were excited, fatigue could result over an extended time period. A finite element analysis of the rotor section can be conducted to help identify the maximum stress areas pertaining to each mode shape.

Both tolerances and environment can cause the modal frequencies and mode shapes to differ from those established by the test. Manufacturing tolerances can lead to variations between corresponding wheels on two different rotors. The difference depends upon the accuracy of construction and the material consistency. Usually, the shape and frequency differences for a given mode are small, but the position of the wheel node lines can be substantially different.

The operating environment can have a significant effect on the modal frequency, but a smaller effect on its shape. Modal frequencies vary with temperature due to modulus changes. Figure #10 illustrates the effect of temperature on frequency for three types of materials.

Additionally, centrifugal force tends to stiffen the wheel and the blades, and also

results in an increase in the modal frequency and a possible change in its mode shape. The increase in frequency depends on the mode shape, but typically blade modes are affected more than wheel modes.

It is important to estimate the effect of the above operational factors. In our example, if the wheel material is an ascoloy, we can anticipate a 9% reduction in the modal frequency if the wheel operates at 1000°F (see Figure 10). However, the effect of the centrifugal force on the wheel frequency is less, and can be neglected by comparison.

Applying the temperature effect to Modes 4 and 5, we found that these frequencies were reduced to 1854 and 1956 Hz respectively. We then compared these temperature compensated frequencies to the excitation sources and found that an excitation existed on the impulse wheel at 1920 Hz due to nozzle pass, and from the #6-#10 stages of the rotor due to blade pass. This 1920 Hz excitation source is very close to Mode #5 (1956 Hz).

4. MODE SHAPE EXCITATION AND ITS AMPLIFICATION

For a particular mode of vibration to cause fatigue failure it must be excited sufficiently to cause high amplitude cyclic stresses. In order for this to occur, it must have low damping, the natural frequency and driving frequency must be very close, and the forcing mechanism must be such as to be able to drive the mode effectively.

Thus, the mere proximity of a natural frequency to an excitation frequency is not automatically a problem. In our example for instance, the control stage nozzle passing frequency at 1920 Hz does not necessarily imply severe resonance of Modes 4 or 5.

First, it is important to know the damping ratios. Table 1 indicates damping ratios of 0.215% for Mode 4, and 0.107% for Mode 5. If excited right at their natural frequencies, these modes would exhibit very large amplification factors, Q , equal to 232 and 466 respectively. But Table 5 shows Q 's of 14.3 and 25 for the two modes when driven at the 1920 Hz nozzle passing frequency. Here, Mode 4 was assumed to have a temperature corrected natural frequency of 1854 Hz, and Mode 5 had a temperature corrected natural frequency of 1956 Hz.

Table 5 shows the effect on Q if these natural frequencies were only slightly different. Note how a small decrease in the natural frequency of Mode 5 from 1956 Hz to 1920 Hz would result in a nearly twenty-fold increase in amplification factor. Turning this around, if the natural frequency and excitation frequency are not extremely close, severe resonance probably will not occur. The fatigue stresses generated in the wheel are greatest when the excitation source and natural frequency are closest.

The final necessary ingredient for high amplitude resonance is an effective final forcing mechanism to excite the mode. One such possible mechanism results from the kick each blade receives as it passes each nozzle. A blade group sees the summation of this effect from all the blades in the group, and a wheel sees the total effect from all of its blades. In all of these cases, the nozzle passing frequency is the number of nozzles in the stage times rotational speed when evenly spaced nozzles fill the circumference. But when some nozzles are missing, or not on, as in a control stage, the true nozzle passing frequency is determined by the nozzle spacing. This can be seen by reviewing Figures 11 through 16. Figure 11 shows a simulated time plot of 32 evenly spaced nozzles in a 50 Hz turbine. Figure 12 shows the spectrum, with as expected a 1600 Hz nozzle passing frequency along with its harmonics. Figures 13 and 14 show the same two plots after the elimination of six nozzles, and Figures 15 and 16 after the elimination of fifteen nozzles. Note that in all cases, the 1600 Hz nozzle passing frequency along with its harmonics remains. The added sideband energy in the latter two cases is a result of the rotationally repeated amplitude modulation (on or off) pattern of the nozzles.

Nozzle passing frequency, or one of its harmonics, can usually excite a matching blade mode. But for wheel modes, which are subject to excitation by many nozzles at any one time, it is important to determine whether they might be effectively working against each other in this endeavor. If they are, it will be difficult to excite the mode.

In addition to nozzle passing frequency, blade passing frequency can be another source of excitation. Assume for the moment, only one nozzle. As each blade passes this nozzle, it receives a kick. Blade pass is obviously equal to the number of blades times rotational speed. Though each individual blade does not see this blade passing frequency, the wheel does. And in fact, the wheel sees the totality of all the blades passing all the nozzles. Thus blade passing frequency as well as nozzle passing frequency acts on the wheel. However the excitation frequencies from these two sources have a subtle difference.

To best understand this difference consider two simplistic cases. In the case of nozzle passing frequency, picture one blade on the wheel and many evenly spaced nozzles, while in the case of blade passing frequency, picture many blades and one nozzle. In the first case, the force at the nozzle passing frequency is acting on a point fixed in the wheel as the blade passes each nozzle. In the second case, the force at blade passing frequency is stationary, acting on the wheel at the fixed nozzle position. To a point fixed on the wheel, however, this excitation is rotating around at rotational speed. Since wheel modes are almost always fixed with respect to the rotating wheels

themselves, this latter condition causes blade passing excitation frequencies to differ from the natural frequencies of the wheel modes they excite. This concept is described in reference 1.

The conclusions of the referenced paper show that a given wheel mode can be excited by a stationary source at two specific excitation frequencies. These are dependent upon the wheel speed, natural frequency and mode shape according to the equation

$$F_e = F_n \pm N F_r \quad (1)$$

F_e = excitation frequency necessary to excite the mode

F_n = natural frequency of wheel mode

N = number of nodal diameters in the mode shape

F_r = wheel running speed

If we relate this to our example, the stationary blade passing frequencies necessary to excite modes 4 and 5 with the wheel rotation at 60 Hz would be as follows:

Mode	F_n Temperature Compensated	F_e (stationary)
4	1854 [2 nodal diameters]	1854 \pm (2) 60 = 1974 and 1734 Hz
5	1956 [3 nodal diameters]	1956 \pm (3) 60 = 2136 and 1776 Hz

If one compares the 2160 Hz blade passing frequency to the excitation frequencies Mode 5, which requires an excitation of 2136 Hz, could be resonantly excited with an amplification factor of approximately 48. In this case, the actual vibration frequency of the wheel, as sensed by a strain gage for instance, would be (2160 - 180) Hz or 1980 Hz.

Similar to the nozzle passing case, the multiplicity of nozzles results in additional cancellatory effects, and blade passing frequency may be able to excite only some of the above modes in an effective manner.

Steam flow noise can excite the free vibration modes of the blades and the wheel. Since the excitation is of a random nature, one cannot consider it to be a major source of failure. However, this effect may be useful in identifying natural frequencies during operation.

5. OPERATIONAL MEASUREMENTS AND ANALYSES

The question arises as to whether, in a sister turbine or following repair, resonance of any of the blade or wheel modes during operation can be detected by accelerometers mounted on the bearing caps of the turbine.

To answer this question, one must first look into how the resonant blade or wheel motion would translate into motion at the bearing caps. Any mode that would tend to either bend the shaft or move it axially should have some effect at the journal and thrust bearings respectively. Obviously, symmetric wheel modes fall into neither category, but actual modal testing shows that these modes are not always so symmetrical. For example, a 2 nodal diameter mode instead of its radii being separated by 90° might actually have separation angles of 105°, 84°, 96°, and 76°. This means that in one half of the vibrational cycle, more wheel mass is moving toward one end of the turbine, and it reverses in the other half cycle. This would result in both an axial and bending effect fixed with respect to the rotating wheel.

It is important to note that just non-symmetrical nozzle spacing can result in shaft bending, fixed with respect to the rotating system. Figure 17 shows a wheel with 48 blades and 6 unequally distributed nozzles. The blade pass frequency is equal to 48/rev while nozzle pass is 8/rev based on nozzle spacing (45° between nozzles).

As the wheel rotates through one revolution we sum the forces on one half the wheel and subtract this force from the summation on the other wheel half and we obtain an amplitude versus time wave form similar to Figure 18. The frequency spectrum of this waveform is shown in Figure 19. This is the frequency content of the wheel vibration due to bending through one shaft revolution. Note how only odd harmonics are generated. This is due to the mirror symmetrical nature of the waveform. Also note though the dominance of the 5, 7, and 9 per rev and the 47 and 49 per rev components, these surrounding the 6, 8 and 48 per rev frequencies one might have initially expected. The fact that all these order related components exist complicate the detection of any existing forced resonance.

Order related vibration components will exist on the bearing caps due to the presence of not only the vibration sources in the rotating and stationary planes but also other sources of excitation which effect the stationary plane.

In contrast to these discrete, order related components which result from resonance and forces at multiples of rotational speed, it is possible for the blades and wheels to ring at their free vibration natural frequencies in response to random steam flow noise.

These frequencies are not order related and they do not show up as discrete frequencies in a spectrum. This is true because they are randomly amplitude modulated in the analysis window, which results in a smeared sideband effect. Figure 20 shows this effect for the first bending natural frequency of a large fan rotor. This frequency, which exists slightly above running speed, is being excited by flow turbulence.

The same condition can and does exist in turbines. In order to identify it however, one must realize that any vibration, fixed along one direction in the rotating frame will appear to be translated by plus and minus rotational speed when viewed by a stationary sensor. This is discussed in detail in reference (2). The concept is illustrated in Figure 21. Here a 3 per rev vibration, fixed in a shaft, appear as 2 per rev and 4 per rev vibrations to a stationary proximity probe.

Figures 22 and 23 show the spectra of an actual free vibration mode fixed in the rotating system as sensed by an axial accelerometer at the thrust bearing. Here, both the untranslated and translated components appear; the former because the axial components are not translated by rotation, and the latter because the radial motion is coupled to axial motion by the support structure. Note from the two plots the advantage of using order analysis to pick up discrete order components even when speed is changing.

Order analysis might also enable one to determine true operational natural frequencies by spotting when an excitation order such as nozzle pass, which is normally above a given natural frequency, excites it on start up. In our example, Mode 4 at high temperature should be approximately 1854 Hz. The nozzle passing frequency (32/rev) goes through this frequency when the turbine is running at 3,476 rpm (57.93 Hz). If excitation of this mode occurs during startup, we can observe the 32/rev component during startup from an axial probe (31/rev and 33/rev from a radial probe), and look for sudden changes in magnitude and phase. By noting the exact turbine speed at which this occurs, one could more closely pinpoint the true operational natural frequency of the suspected mode.

Review of the accelerometer data as discussed above may be helpful in gaining a better understanding of the actual failure mode, but unfortunately due to the many order related frequency components that exist, this may not be conclusive in terms of detecting and defining a resonance condition during actual operation. However, FRC is developing a technique aimed at doing just that (3). This technique, which will not be discussed here, uses a stationary dynamic pressure transducer downstream of the suspect wheel and through complex signal enhancement procedures is capable of detecting and locating any blades vibrating

excessively in resonance.

6. FINITE ELEMENT ANALYSIS AND FATIGUE LIFE

If time and money permit, a finite element analysis can be performed which will identify the maximum stress points present in the disc for certain mode shapes. These points can be compared to the failed sections. In addition, the finite element analysis can be used with fatigue life data to establish modal amplitudes necessary to generate the stresses required to cause fatigue.

The stress levels that cause fatigue reduce as the operating temperature increases. These levels are reduced still further if coupled to a static tensile stress such as can be caused by centrifugal acceleration.

If we assume a certain mode to be the failure cause, by knowing the time of turbine operation we can establish the number of cycles of stress reversal which caused the fatigue failures. We can then relate this to an operating stress by referring to data relating stress, temperature, and the number of fatigue cycles.

This stress can then be input into the finite element analysis to determine the amplitudes of vibration necessary to generate the required fatigue stress.

7. CONCLUSIONS

- o Modal testing is practical in the field with proper pre-planning.
- o If there is a possibility that a turbine blade or wheel failure can be a result of resonant excitation of a natural mode, the modes of the failed system should be investigated.
- o Analysis of this type should include:
 - a. establishment of the mode shapes
 - b. comparison to the failure
 - c. investigation of excitation sources
 - d. identification of mode frequency changes due to environmental conditions
 - e. investigation of major stress areas and life expectancy
- o Analysis of running vibration data could show the existence of the suspected mode or modes, but it becomes a very difficult task to identify them. This is due to the existence of a vast amount of data which emanates both from rotating and stationary sources. The relationship which exists between a rotating vibration source and the identification of this source from a stationary plane makes the analyses even more complex.

REFERENCES:

1. Horner, J.E., MacBain, J.D., Stange, W.A., "Vibratory Response of a Rotating Disk Incorporating Image Derotation Techniques and Holographic Interferometry," Technical Report AFAPL-TR-78-62, September 1978.
2. Benko, G.B., "Notes on the Measurement of Vibrations on Rotating Systems," Vibrations In Hydraulic Pumps and Turbines, The Institution of Mechanical Engineers, Proceedings 1966-67, Vol. 181, Part 3A, pp. 50-54.
3. Leon, R.L. "A Doppler Technique For Detecting and Locating Excessively Vibrating Blades In A Running Turbine," Reliability, Stress Analysis and Failure Prevention Methods in Mechanical Design, Intl. Conf., Aug. 1980, ASME: 1980, pp. 59-66.

Typical Impulse Wheel

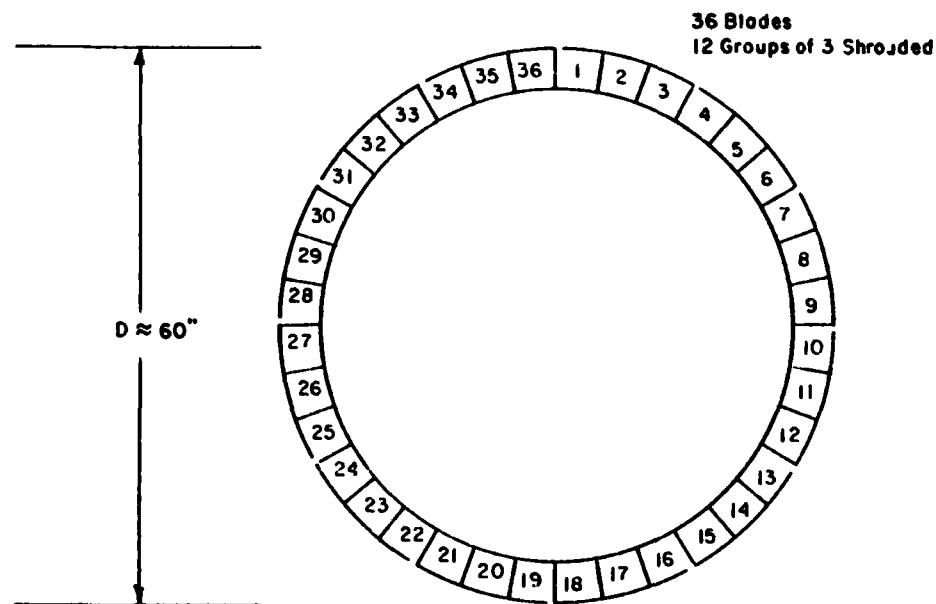


Figure 1

Modal Test Impact Points

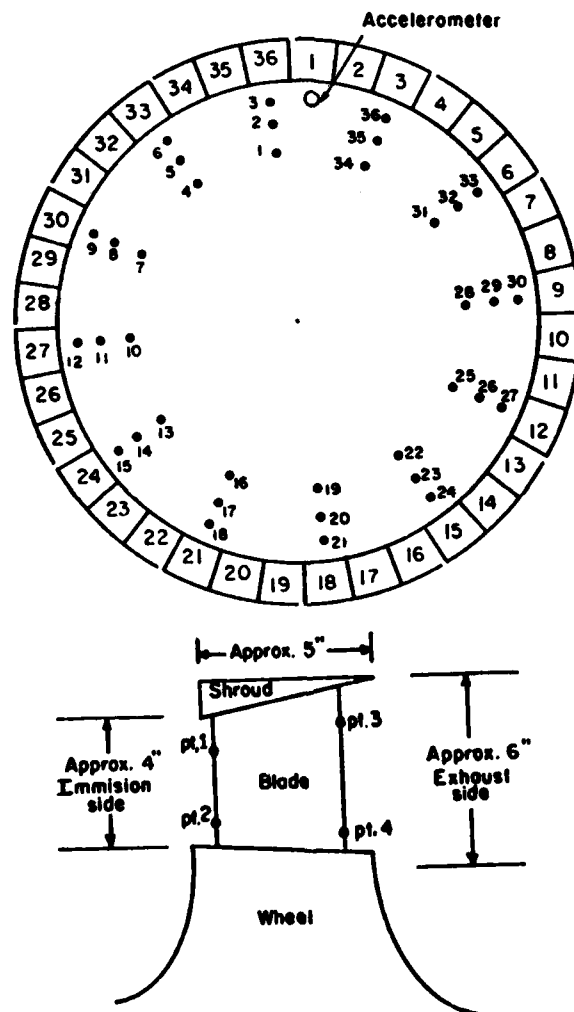
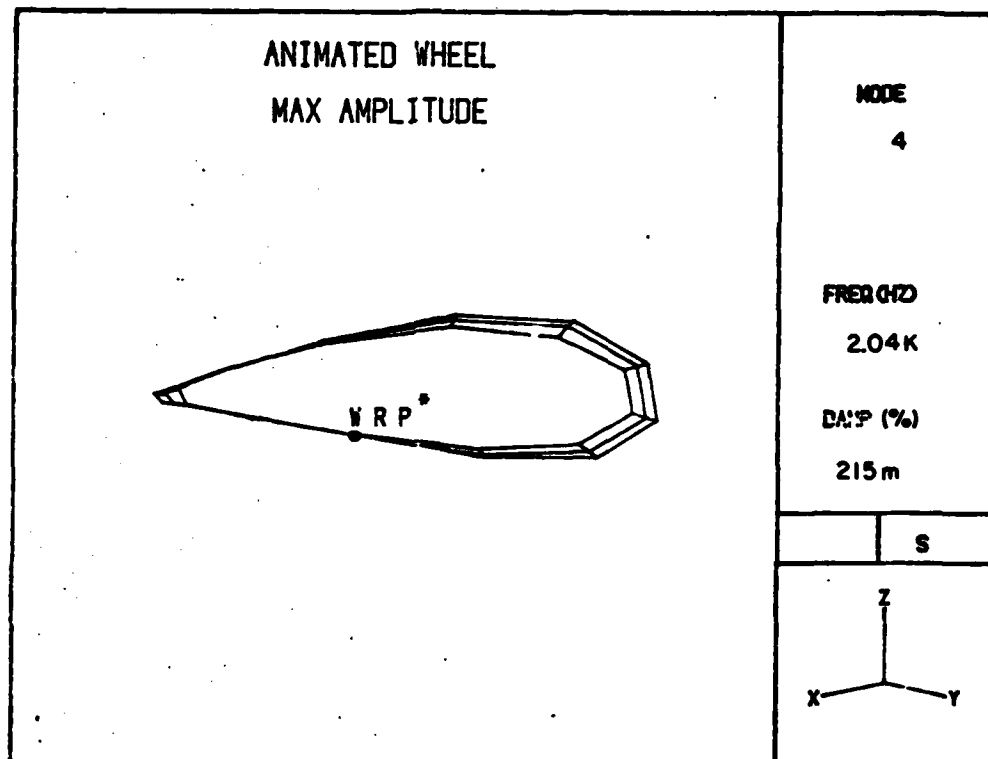
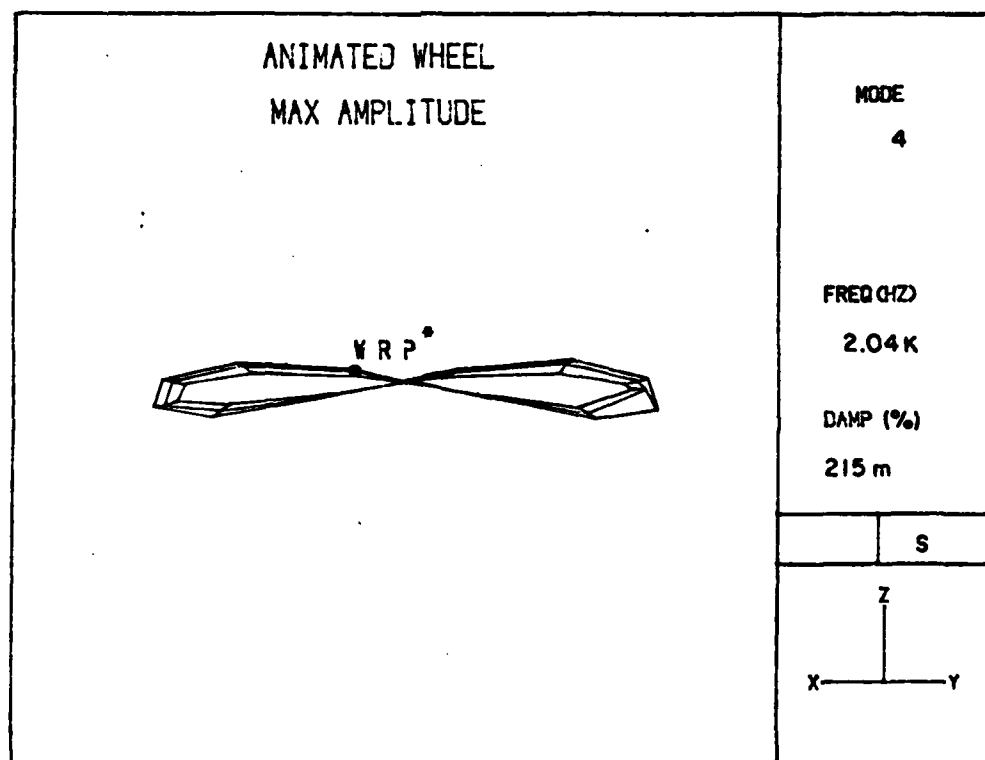


Figure 2



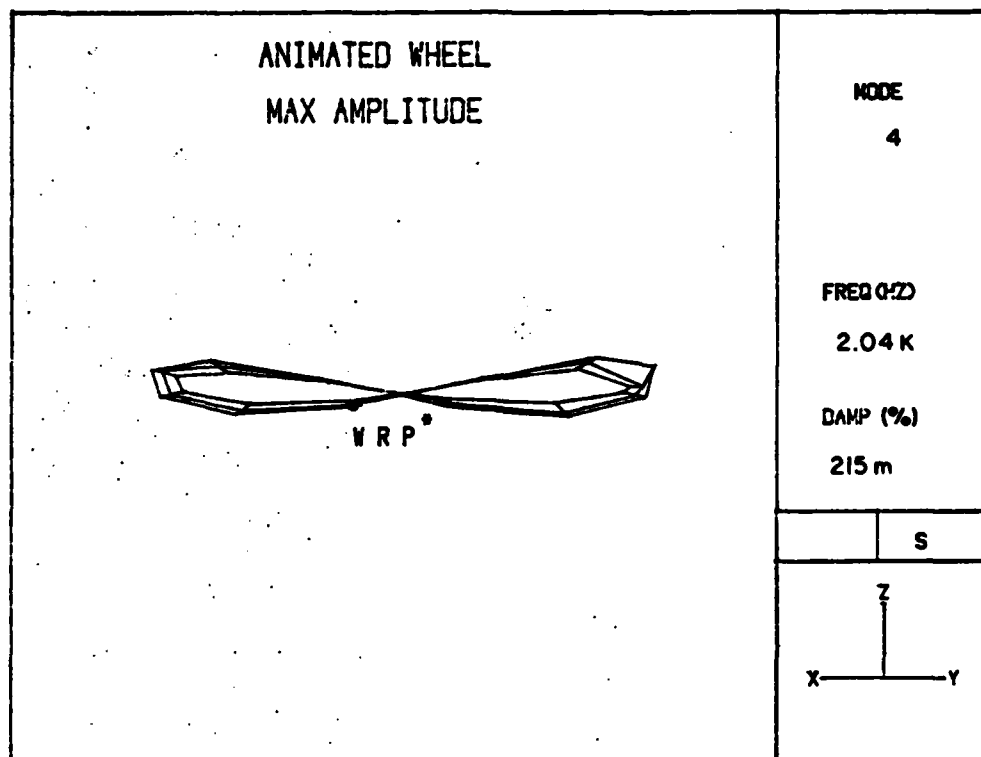
*: WHEEL REFERENCE POINT

Figure 3



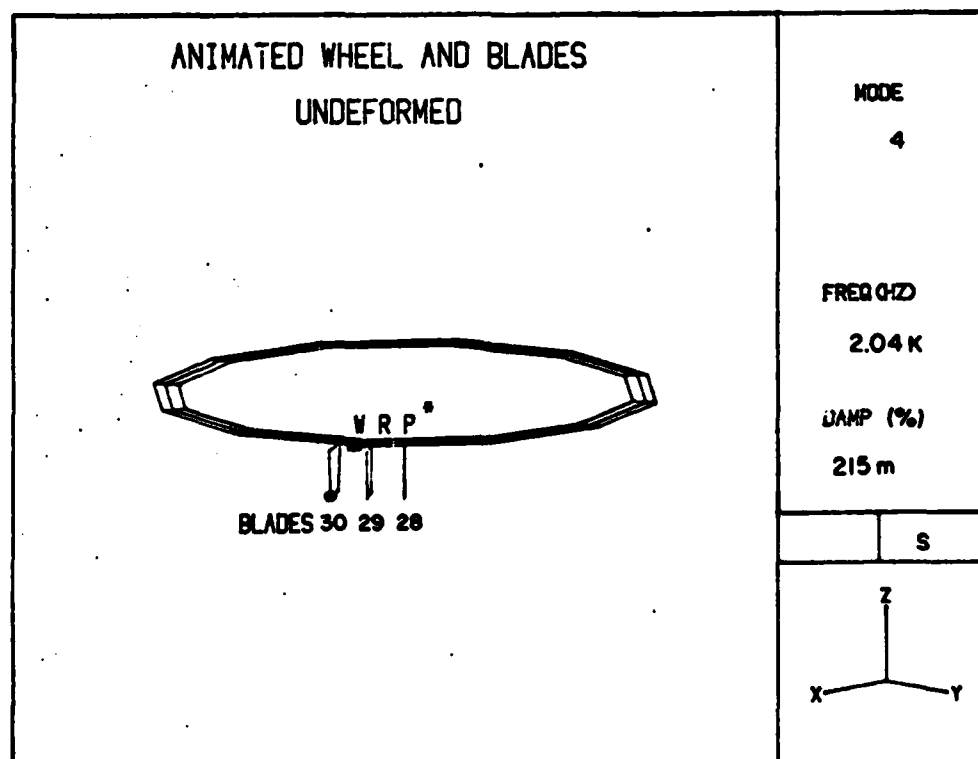
*: WHEEL REFERENCE POINT

Figure 4



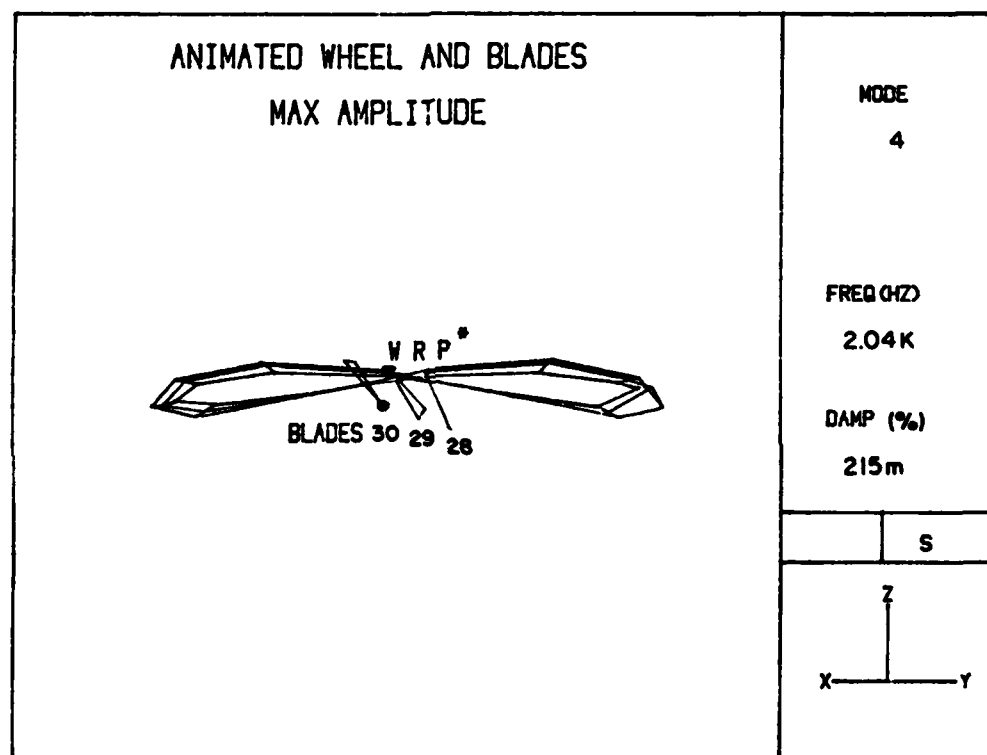
* WHEEL REFERENCE POINT

Figure 5



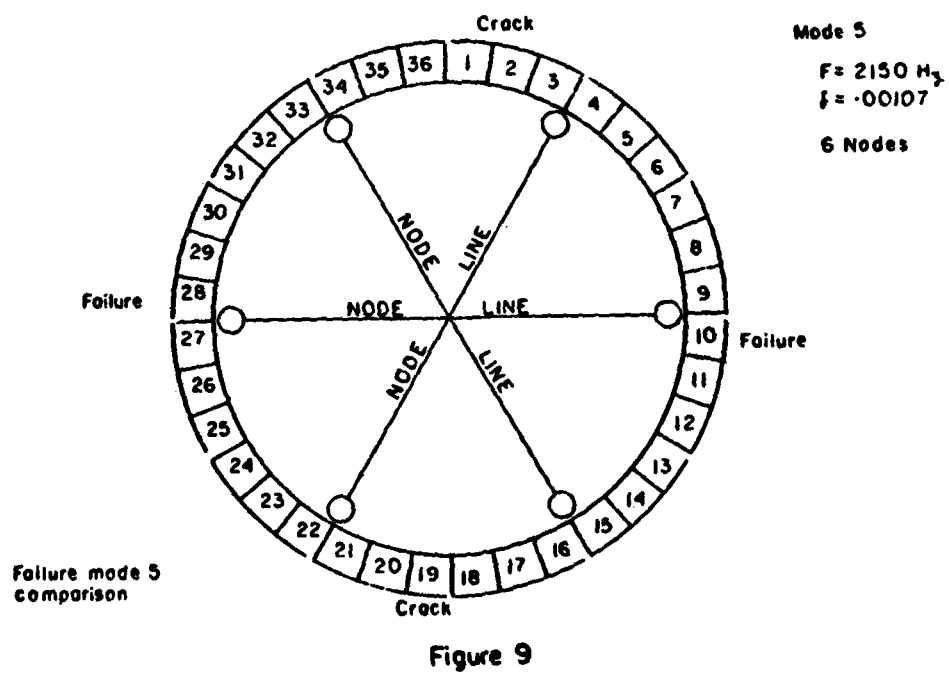
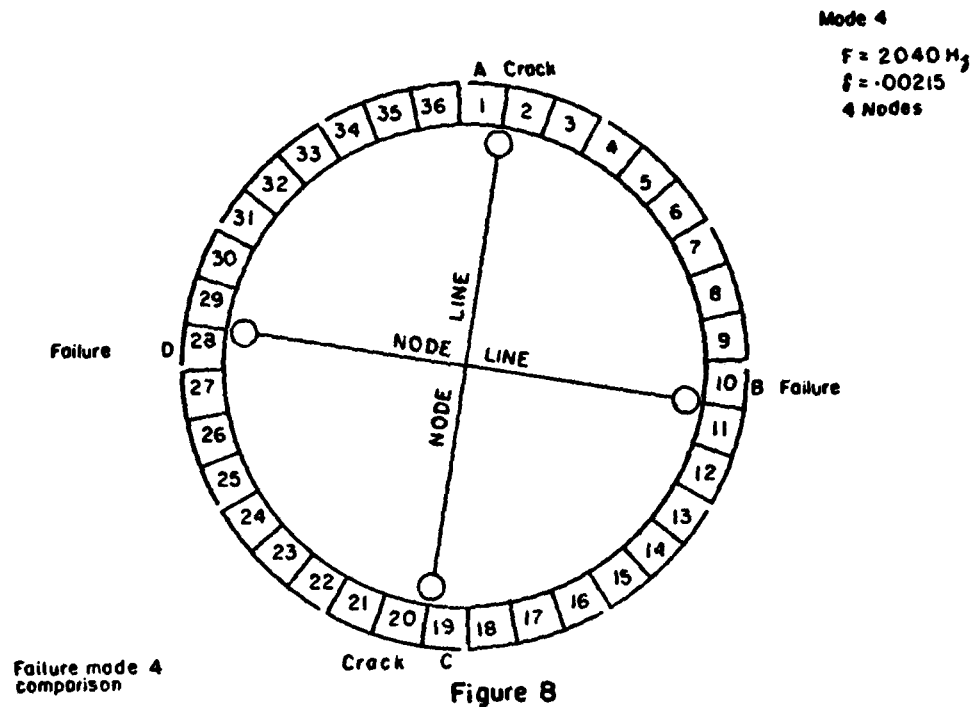
* WHEEL REFERENCE POINT

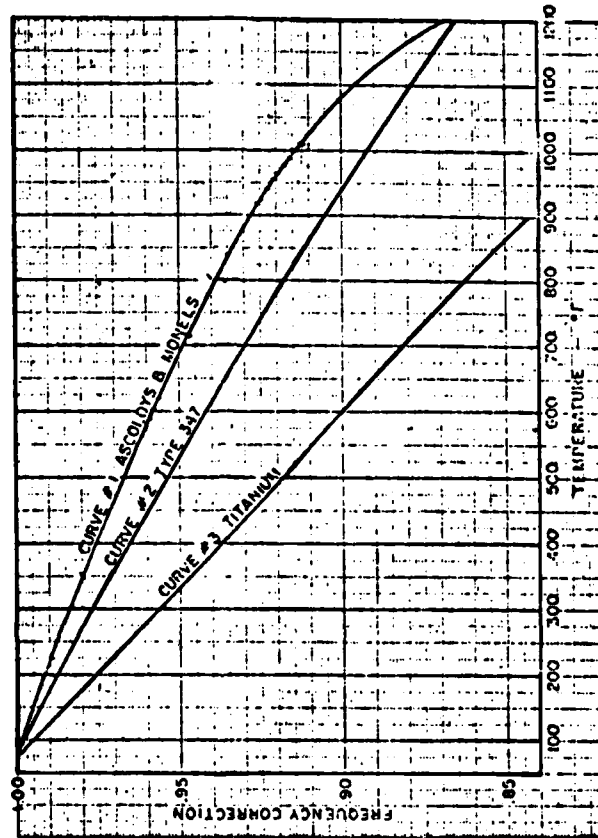
Figure 6



* WHEEL REFERENCE POINT

Figure 7





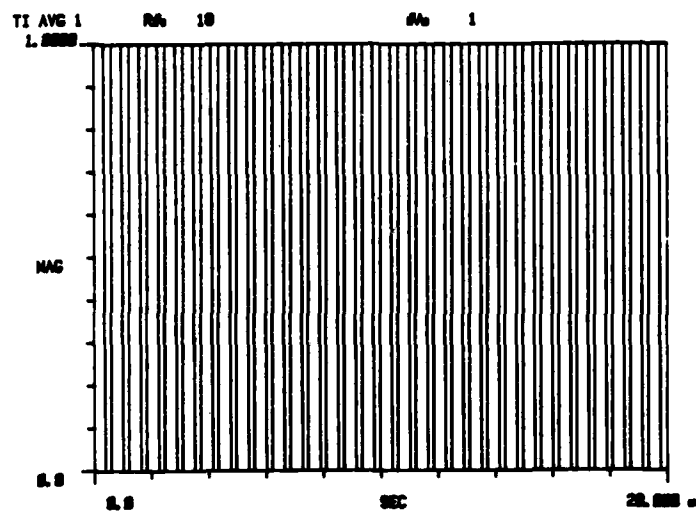
CURVE 1 AVG. OF DATA FOR B7B20A, B50A125C AND B50A125E
SATISFACTORY FOR MONELS - B14H2 AND B14H25 TO 500°F
REFERENCE FOR ASCOLOYS - H-9634148, 156 & 157
REFERENCE FOR MONELS - CH-9634035 & 038
CURVE 2 TYPE 347 STAINLESS - REFERENCE CH-8214683
CURVE 3 AVG. OF DATA FOR TITANIUM FORGINGS: COMMERCIAL PURE
Ti 100 A & Ti 150 A - REFERENCE - CH-9634077, 129, & 162
THESE CURVES ARE BASED ON CORRECTED RESULTS ISSUED BY R.F. BALDWIN
ON NOV. 11, 1952

(COPIED FROM KH-9318475)

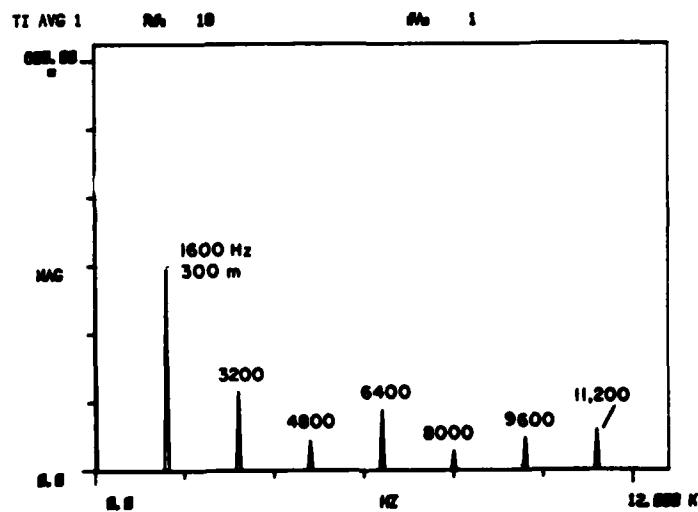
		VIBRATION FREQUENCY CORRECTION FOR TEMPERATURE EFFECT	
		MADE BY <i>General Electric</i> <i>March 26, 1955</i>	INSPECTED <i>March 26, 1955</i>
		GENERAL ELECTRIC	K-55378-27
REVISIONS		APPROVED BY <i>WOMMS</i>	SHEET 1 OF 2 CONT. ON SHEET -

TB

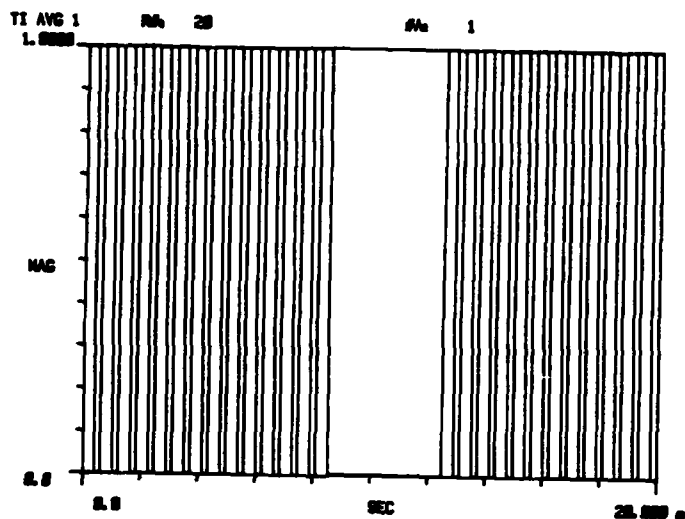
Figure 10



Time Window
32 pulse - Represents 32 nozzles
of impulse stage evenly spaced
Figure 11

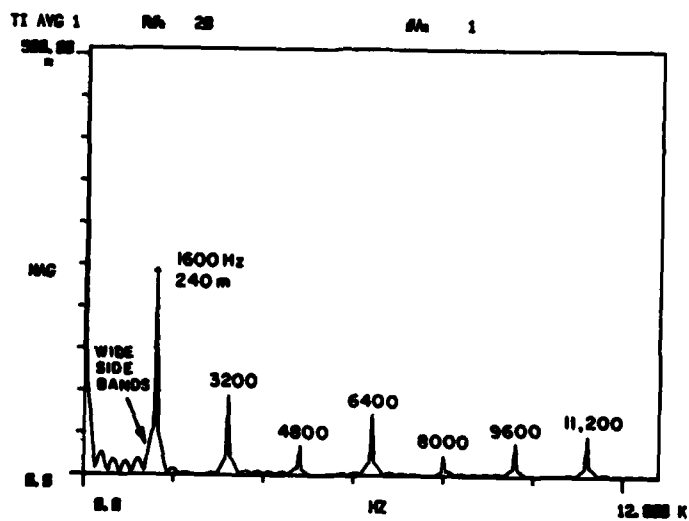


Frequency spectrum of Figure 11
Figure 12



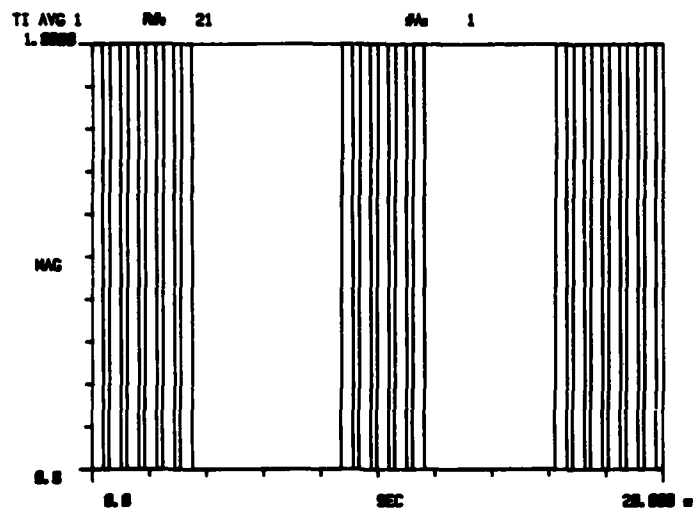
Time Window
Elimination of 6 nozzles around
Impulse stage

Figure 13



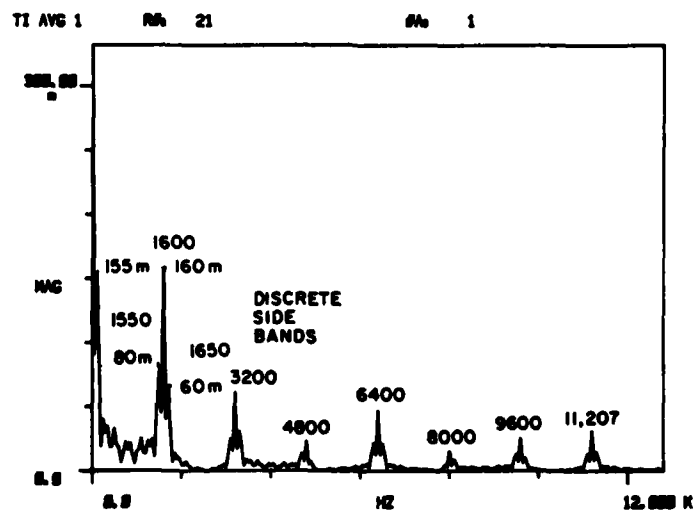
Frequency spectrum of Figure 13

Figure 14



Time Window
Elimination of 15 nozzles around
impulse stage

Figure 15



Frequency spectrum of Figure 15

Figure 16

Impulse Stage High Pressure Turbine

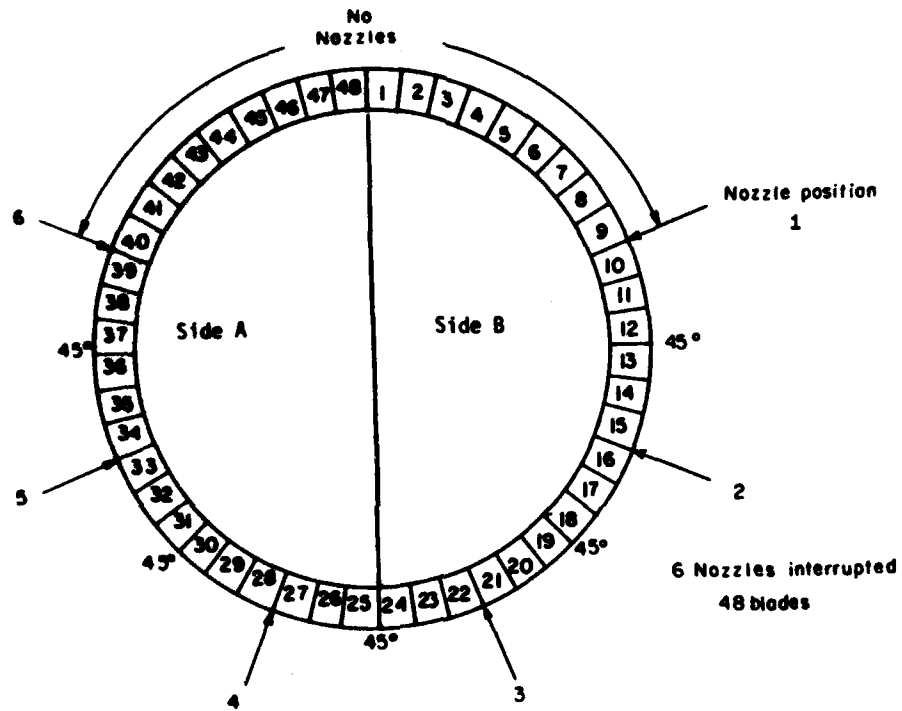
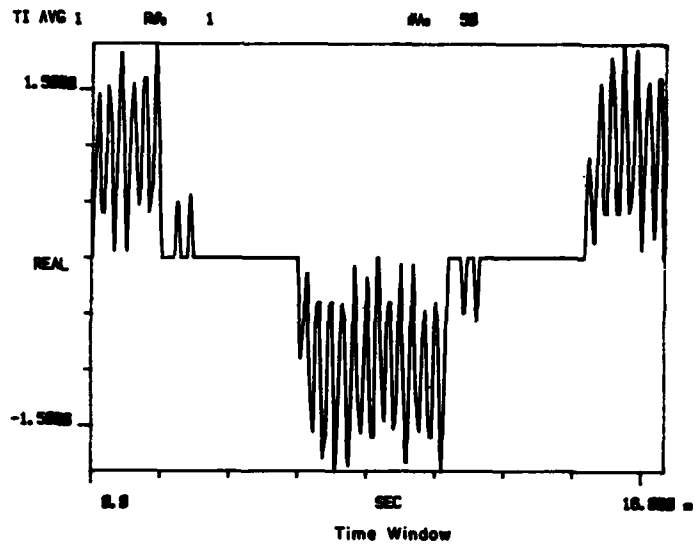


Figure 17



SIGNAL - Describes nozzle force DELTA between wheel halves as wheel rotates thru one revolution (See Figure 17)

Figure 18

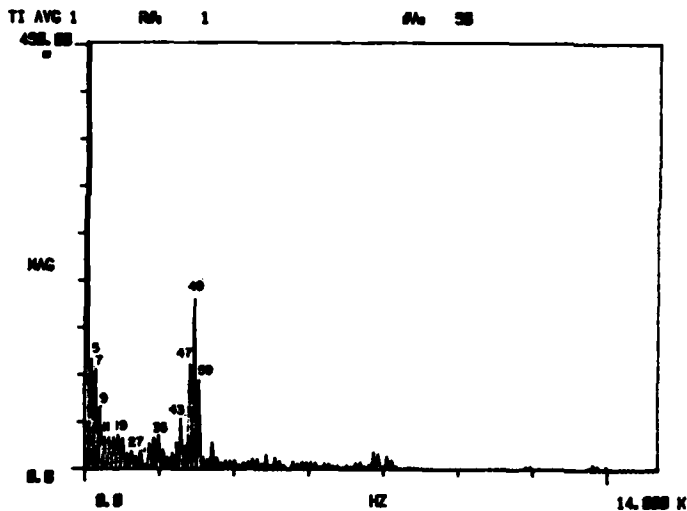
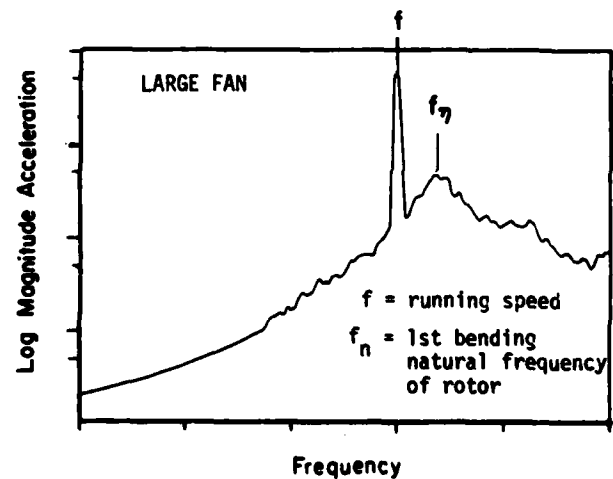


Figure 19

Figure 20 Auto. Spectrum - bearing cap vibration.



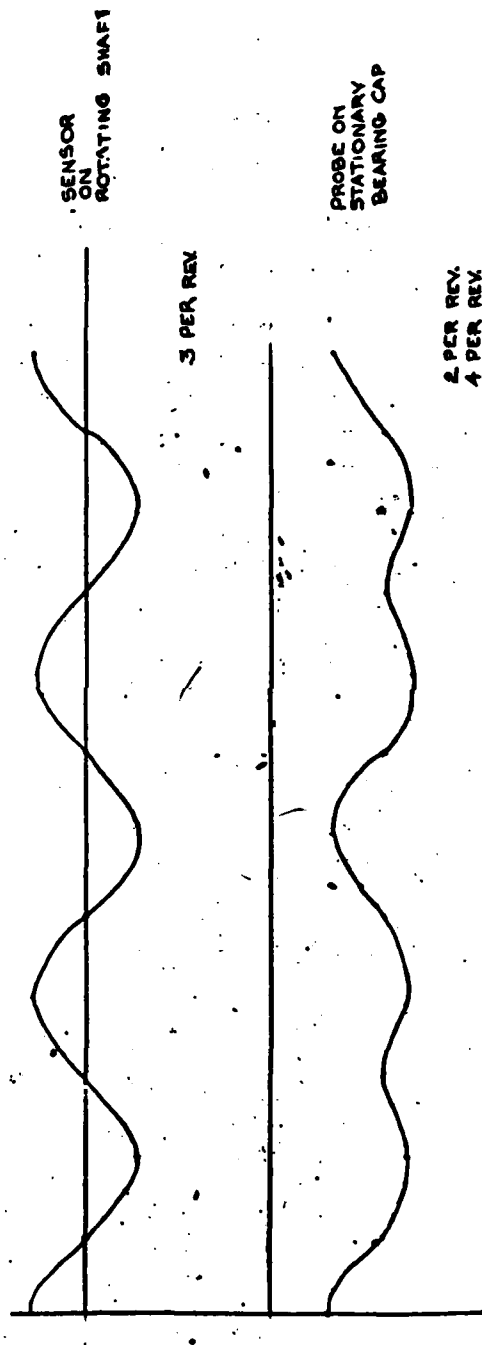
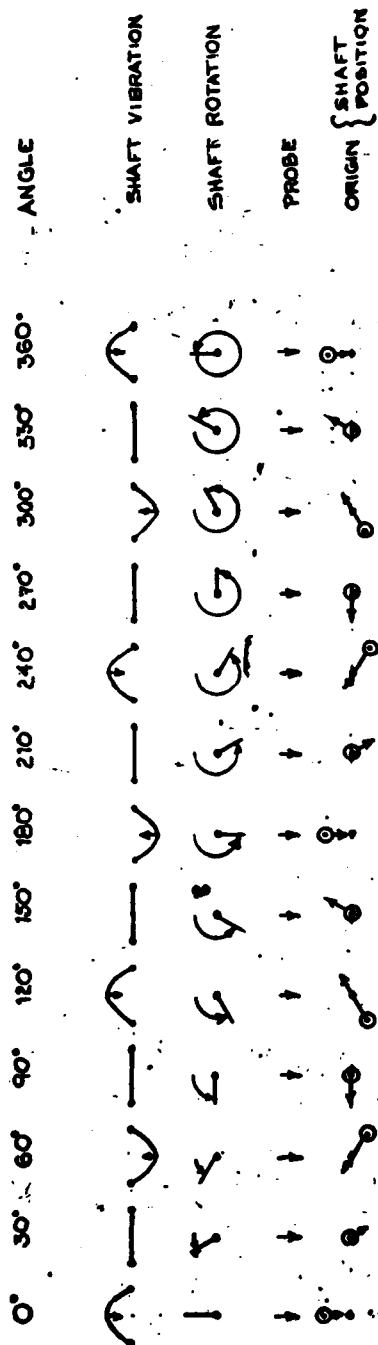


Figure 21 Vibration in Rotating Plane as viewed in Stationary Plane

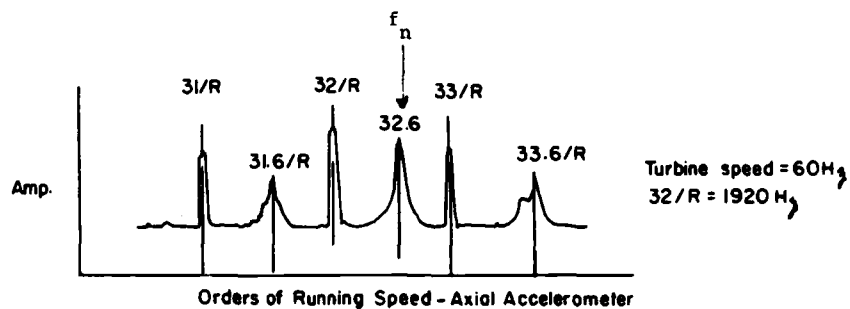


Figure 22

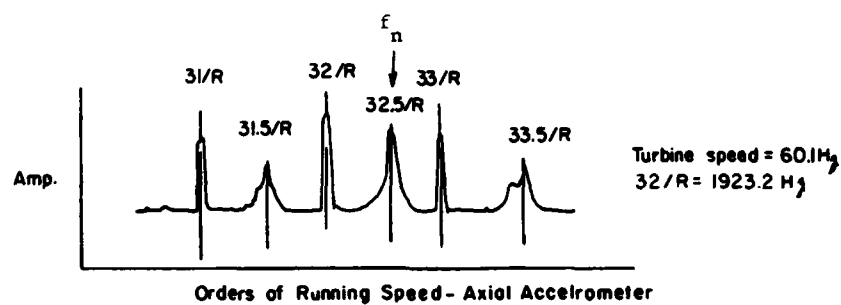


Figure 23

Table 1. Frequency and Damping Table From Analyzer

Mode No.	ω_n in (Hz)	ω_n in (R/S)	$= c/c_r$ %	$\sigma = \omega_n \delta$ in (Hz)	σ in (R/S)
1	202.7	1.274 K	1.71	3.466	21.78
2	461.8	2.902 K	1.85	8.543	53.68
3	1.205 K	7.571 K	542M	6.531	41.03
4	2.040 K	12.818 K	215.1M	4.386	27.56
5	2.150 K	13.509 K	107.2M	2.300	14.45
6	2.390 K	15.017 K	75.5M	1.804	11.33
7	2.84 K	17.844 K	172.2M	4.885	30.69
8	4.242 K	26.653 K	118.5M	5.005	31.44
9	4.75 K	29.845 K	40.5M	1.924	12.08

Table 2. Possible Excitation Sources in a Typical HP Turbine

<u>Turbine Construction</u>		[Rotational Speed = 60 Hz]	
<u>Impulse stage</u>	36 blades	<u>Impulse</u>	32 nozzles evenly spaced
<u>Stages 2 thru 5</u>	28 blades	<u>Rows 1 thru 4</u>	20 nozzles evenly spaced
<u>Stages 6 thru 10</u>	30 blades	<u>Rows 5 thru 9</u>	32 nozzles evenly spaced

Major Excitation Sources

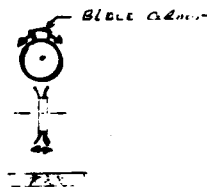
o <u>Nozzle Pass</u>	Impulse section	= $32/R \times 60 = 1920$ Hz	Sources existing in rotating plane
	Rows 1-4	= $20/R \times 60 = 1200$ Hz	
	Rows 5-9	= $32/R \times 60 = 1920$ Hz	
o <u>Blade Pass</u>	Impulse	= $36/R \times 60 = 2160$ Hz	Sources existing in stationary plane
	Stages 2-5	= $28/R \times 60 = 1680$ Hz	
	Stages 6-10	= $32/R \times 60 = 1920$ Hz	
o <u>Unbalance</u>		$1/R \times 60 = 60$ Hz - Rotating plane	
o <u>Misalignment</u>		$1 \text{ \& } 2/R \times 60 = 120$ Hz - Stationary plane	

Note: Additional sources exist such as sidebands of nozzle pass frequency caused by nozzle construction. These frequencies are usually discretely separated from nozzle pass by multiples of running speed.

Table 3. Typical Mode Shapes

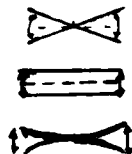
1. Blade Mode

- a. Circumferential
- b. Axial
- c. Twisting
- d. Combination



2. Disk Wheel Modes

- a. Stiff (Rocking)
- b. Stiff (Axial)
- c. Oil can
- d. Node



2



4



6



3. Combination Disk & Blade

Table 4 Actual Modes (Static) and Possible Excitation Sources

	(Hz)	Type of Mode	Possible Excitation Source
1	202.7	Blade (Circum)	3/Rev = 180 Hz
2	461.8	Blade (Axial)	8/Rev = 480 Hz
3	1205	Wheel	<u>Nozzlepass Rows</u> 1-4 (20/R) = 1200 Hz
4	2040	Wheel 4 node combination Blade Group	<u>Nozzlepass</u> Rows 5-9 (32/R) = 1920 Impulse (32/R) = 1920 <u>Blade Pass</u> Stg 6-10 = 1920 Hz
5	2150	Wheel Mode -6 node combination Blade Group	<u>Same as for Mode 4</u> Plus blade pass impulse = 36/R = 2150 Hz
6	2390	Wheel Multinode	<u>Blade Pass Impulse</u> 36/R = 2160 Hz
7	2840	Wheel Multinode	NA
8	4242	" "	NA
9	4750	" "	NA

Table 5. Amplification Factor Variance

Mode 4 Excitation Frequency = 1920 Hz

$$\omega_n = \text{Natural Frequency} = 2040 \text{ Hz, with temp. effect} = 1854 \text{ Hz}$$

Damping Ratio $\zeta = .00215$

Q = Amplification Factor

ω_n	Q	% ω/ω_n
1800	7.3	106.7
1840	11.2	104.3
1880	23.4	102.1
<u>1920</u>	<u>232.5</u>	<u>100</u>
1960	24.8	97.9
2000	12.5	96.0
<u>2040</u>	<u>9.1</u>	<u>94.0</u>
<u>1854</u>	<u>14.3</u>	<u>103.6</u>

Mode 5 Excitation Frequency = 1920 Hz

$$\omega_n = \text{Natural Frequency} = 2150 \text{ Hz, with temp effect} = 1956 \text{ Hz}$$

Damping Ratio $\zeta = .00107$

Q = Amplification Factor

ω_n	Q	% ω/ω_n
1850	13	103.8
1900	48	101.1
1950	32.2	98.5
2000	12.5	96
2050	8.5	94.5
2100	6.2	91.0
<u>1956</u>	<u>25</u>	<u>98.0</u>
<u>1920</u>	<u>466</u>	<u>100.0</u>

$$Q = \frac{1}{\sqrt{[1 - (\omega^2/\omega_n^2)]^2 + (2\zeta)(\omega/\omega_n)]^2}}$$

CONTRIBUTION TO THE DYNAMIC BEHAVIOUR OF FLEXIBLE MECHANISMS

E. Imam, J. Der Hagopian, M. Lalanne
Institut National des Sciences Appliquées
Laboratoire de Mécanique des Structures - E.R.A. C.N.R.S. 911
Villeurbanne, France

In high speed rotating mechanisms links cannot be taken as perfectly rigid. In this paper general expressions for kinetic and strain energies of deformable plane rotating mechanisms are presented. The differential equations of the system are obtained using finite element techniques. The number of degrees of freedom of the system is reduced by a modal method and the solution of the system is obtained from a closed form algorithm taking into account the motion periodicity.

A four bar system was tested. In order to reduce stresses and strains, damping has been introduced by a viscoelastic sandwich treatment. The agreement between experimental and theoretical results is satisfactory for both the damped and undamped system.

INTRODUCTION

Mechanisms are commonly used in machinery to drive a specific point along a given path. Until recently angular speeds were low and the motion could be well described by considering rigid links. To day due to the high speed achieved it is necessary to take into account link deformations. The analysis is then performed by introducing simultaneously kinematic, dynamic and elastic aspects of the behaviour (kinetic elasto-dynamics analysis (K.E.D.)).

For the last ten years various studies on K.E.D., generally restricted to mathematical aspects, have been performed. Using flexibility matrices Winfrey [1], [2], proposed a numerical method that uncouples rigid body motion and strains. Erdman and al. [3] studied a plane mechanism considering clamped-free or pinned-pinned beams. In [4] Imam and al. analyze the rate of change of frequency as a function of the position of the mechanism. Later [5], Imam and Sandor published a general analytical approach. In [6], [7] a modelisation using concentrated parameters has been proposed. This modelisation has been compared with experiments on a slider-crank mechanism [8] the connecting rod is elastic, the crank perfectly rigid and the agreement between experimental and predicted results is satisfactory. In [9] the authors have included the longitudinal motion in the analysis of the system presented in [8].

Song and Haug have recently presented

general equations for flexible mechanisms, [10]. In [11], [12], [13], Midha, Erdman, Frohrib have given equations for rotating systems and presented a general very efficient algorithm to solve differential systems with periodic coefficients and successfully applied this method to mechanisms. In [14], [15] Nath and Ghost have studied the steady state response of rotating mechanisms. Alexander and Lawrence [16], [17] and Sutherland [18] are, to our knowledge, amongst the first to have tested flexible rotating mechanisms.

In this paper a general approach of the dynamic behaviour of plane mechanism is presented. At first, kinetic and strain energies expressions of a beam rotating in a plane are given. Using the finite element technique, the various matrices are obtained. The Lagrange's equations are then applied to get the equations of motion of the systems. The solution of the equations is obtained by a combination of a modal method and of a closed form algorithm taking into account motion periodicity.

A four bar mechanism has been built and experimental and finite element results are in good agreement.

ANALYTICAL MODELLISATION

$R_0(OXY)$ is an absolute fixed coordinate system.

$R(Axy)$ is a coordinate system fixed to the undeformed rotating beam.

θ is the angular position of the beam, u and v are respectively longitudinal and bending displacements of a representative point, (Fig.1).

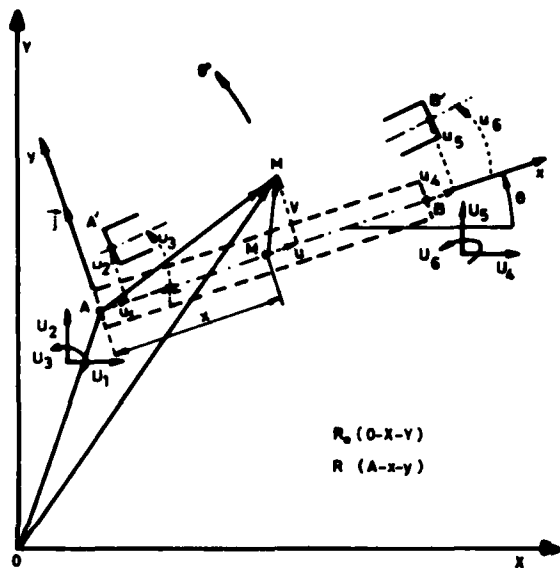


Fig.1 : Rotating beam element.

Kinetic energy

The cross section dimensions of the beam may be neglected in comparison of its length L , thus the velocity of a point of the cross section will be supposed to be equal to the velocity of the point M of the cross section situated on the beam axis.

The velocity \vec{V}_M of M will be expressed by its components in the rotating system.

$$\vec{OM}^R = \vec{OA}^R + \vec{AM}^R = (x_A + x + u)\vec{i} + (y_A + v)\vec{j} \quad (1)$$

The angular velocity vector of R is :

$$\vec{\omega}_{R/R_0}^R = \begin{bmatrix} 0 \\ 0 \\ \theta^\circ \end{bmatrix} \quad (2)$$

$$\text{with : } \theta^\circ = \frac{\partial \theta}{\partial t}$$

Then,

$$\begin{aligned} \vec{V}_{M/R_0}^R &= \frac{\partial \vec{OM}^R}{\partial t} \Big|_{R_0} = \dot{x}_M^o \vec{i} + \dot{y}_M^o \vec{j} \\ &= \begin{bmatrix} \dot{x}_A^o + \dot{u} \\ \dot{y}_A^o + \dot{v} \\ 0 \end{bmatrix} + \begin{bmatrix} 0 \\ 0 \\ \theta^\circ \end{bmatrix} \wedge \begin{bmatrix} x_A + x + u \\ y_A + v \\ 0 \end{bmatrix} \end{aligned} \quad (3)$$

Where

$$\dot{x}_M^o = \dot{x}_A^o + \dot{u} - \theta^\circ v - \theta^\circ y_A \quad (4)$$

$$\dot{y}_M^o = \dot{y}_A^o + x \theta^\circ + \dot{v} + \theta^\circ u + \theta^\circ x_A$$

The kinetic energy for the element T_e is :

$$\begin{aligned} T_e &= \frac{1}{2} \int_0^L V^2 dm \\ &= \frac{1}{2} \int_0^L \rho S (\dot{x}_M^{o2} + \dot{y}_M^{o2}) dx \end{aligned} \quad (5)$$

Substituting (4) in (5) gives the kinetic energy expression :

$$T_e = T_1 + T_2 + T_3 + T_4 + T_5 \quad (6)$$

with,

$$\begin{aligned} T_1 &= \frac{1}{2} \int_0^L \rho S (\dot{u}^2 + \dot{v}^2) dx \\ T_2 &= \frac{\theta^{o2}}{2} \int_0^L \rho S (u^2 + v^2) dx \\ T_3 &= \theta^\circ \int_0^L \rho S (u\dot{v} - v\dot{u}) dx \end{aligned} \quad (7)$$

$$T_4 = T_4^1 + T_4^2 + T_4^3 + T_4^4 + T_4^5 + T_4^6$$

$$\begin{aligned} T_5 &= \frac{1}{2} \int_0^L \rho S (\dot{x}_A^{o2} + (\dot{y}_A^o + x\theta^\circ)^2 + \theta^{o2}(y_A^2 + x_A^2) \\ &\quad - 2y_A\theta^\circ\dot{x}_A^o + 2\theta^\circ x_A(\dot{y}_A^o + x\theta^\circ)) dx \end{aligned}$$

and

$$\begin{aligned} T_4^1 &= \theta^\circ \int_0^L \rho S (y_A^o \dot{u} - x_A^o \dot{v}) dx \\ T_4^2 &= \theta^{o2} \int_0^L \rho S (x_A u + y_A v) dx \\ T_4^3 &= \theta^\circ \int_0^L \rho S (-y_A \dot{u}^o + x_A \dot{v}^o) dx \\ T_4^4 &= \theta^{o2} \int_0^L \rho S x u dx \\ T_4^5 &= x_A^o \int_0^L \rho S \dot{u}^o dx \end{aligned}$$

$$T_1^6 = \int_0^L \rho S (y_A^0 + x \theta^0) v^0 dx \quad (8)$$

Classical displacement functions are then used for the finite element modelisation :

$$u(x) = \begin{bmatrix} 1 - \frac{x}{L} ; \frac{x}{L} \end{bmatrix} \begin{bmatrix} u_1 \\ u_4 \end{bmatrix} = \phi_1(x) \cdot u_1 + \phi_4(x) \cdot u_4$$

$$v(x) = \begin{bmatrix} 1 - \frac{3x^2}{L^2} + \frac{2x^3}{L^3} ; x - \frac{2x^3}{L^3} + \frac{x^3}{L^2} ; \\ \frac{3x^2}{L^2} - \frac{2x^3}{L^3} ; -\frac{x^2}{L} + \frac{x^3}{L^2} \end{bmatrix} \begin{bmatrix} u_2 \\ u_3 \\ u_5 \\ u_6 \end{bmatrix} \quad (9)$$

$$= \phi_2(x)u_2 + \phi_3(x)u_3 + \phi_5(x)u_5 + \phi_6(x)u_6$$

From (9)

$$d = \begin{bmatrix} u \\ v \end{bmatrix} = N \delta \quad (10)$$

with

$$\delta = [u_1, u_2, u_3, u_4, u_5, u_6]^t \quad (11)$$

Then

$$T_1 = \frac{1}{2} \delta^0 t m \delta^0 \quad (12)$$

Where m is the classical mass matrix including longitudinal and bending motion [19].

$$T_2 = \frac{\theta^0 2}{2} \delta^t m \delta \quad (13)$$

$$T_3 = -\theta^0 \delta^0 t c_c \delta \quad (14)$$

Where c_c is the antisymmetric Coriolis matrix whose terms are zero except for :

$$c_{c12} = -c_{c21} = \frac{7\rho SL}{20} \quad c_{c42} = -c_{c24} = \frac{3\rho SL}{20}$$

$$c_{c13} = -c_{c31} = \frac{\rho SL^2}{20} \quad c_{c43} = -c_{c34} = -\frac{\rho SL^2}{15} \quad (15)$$

$$c_{c15} = -c_{c51} = \frac{3\rho SL}{20} \quad c_{c45} = -c_{c54} = \frac{7\rho SL}{20}$$

$$c_{c16} = -c_{c61} = -\frac{\rho SL^2}{30} \quad c_{c46} = -c_{c64} = -\frac{\rho SL^2}{20}$$

T_4 may be written

$$T_4 = -|F_1 + F_2 + F_4|^t \delta + |\bar{F}_3 + \bar{F}_5 + \bar{F}_6|^t \delta^0 \quad (16)$$

where $F_1, F_2, F_3, F_4, F_5, F_6$ are given in the appendix. T_5 is not taken into account because it only gives rigid body motion.

Strain energy

It is obtained from the classical expressions :

$$V_e = \frac{1}{2} \int_0^L EI \left(\frac{\partial^2 v}{\partial x^2} \right)^2 dx + \frac{1}{2} \int_0^L ES \left(\frac{\partial u}{\partial x} \right)^2 dx \quad (17)$$

Where EI, ES are respectively the bending and the longitudinal stiffnesses. With (9) and (10), (17) becomes :

$$V_e = \frac{1}{2} \delta^t k \delta \quad (18)$$

Where k is the classical stiffness matrix [19].

System equation

A convenient set of generalized independent coordinates U_1, \dots, U_6 is used and :

$$\delta = \begin{bmatrix} \lambda & \mu & 0 & 0 & 0 & 0 \\ -\mu & \lambda & 0 & 0 & 0 & 0 \\ 0 & 0 & 1 & 0 & 0 & 0 \\ 0 & 0 & 0 & \lambda & \mu & 0 \\ 0 & 0 & 0 & -\mu & \lambda & 0 \\ 0 & 0 & 0 & 0 & 0 & 1 \end{bmatrix} \begin{bmatrix} U_1 \\ U_2 \\ U_3 \\ U_4 \\ U_5 \\ U_6 \end{bmatrix} = B \cdot U \quad (19)$$

Where $\lambda = \cos \theta$, $\mu = \sin \theta$

Using (19) equations (12), (13), (14), (16), (18) become :

$$T_1 = \frac{1}{2} U^0 t B^t m B U^0 = \frac{1}{2} U^0 t M U^0 \quad (20)$$

$$T_2 = \frac{\theta^0 2}{2} U^t B^t m B U = \frac{\theta^0 2}{2} U^t M U \quad (21)$$

$$T_3 = -\theta^0 U^0 t B^t c_c B U = -\theta^0 U^0 t C_c U \quad (22)$$

$$T_4 = -|F_1 + F_2 + F_4|^t B U + |\bar{F}_3 + \bar{F}_5 + \bar{F}_6|^t B U^0 \quad (23)$$

$$V_e = \frac{1}{2} U^t B^t k B U = \frac{1}{2} U^t K U \quad (24)$$

Applying Lagrange's equations

$$\frac{d}{dt} \left| \frac{\partial T}{\partial \dot{q}_i} \right| - \frac{\partial T}{\partial q_i} + \frac{\partial V}{\partial q_i} - Q_i = 0 \quad (25)$$

Where q_i are generalized coordinates and Q_i are generalized forces (zero in this case) the contribution of an element can be easily obtained from (25), (20), (21), (22), (23), and (24).

It must be noted that as the transformation matrix B is a function of the angular position θ , which is itself a function of the time t , some of the matrices defined above are not constant.

The respective contribution of the previous expressions are :

$$\frac{d}{dt} \left[\frac{\partial T_1}{\partial \dot{U}^0} \right] - \frac{\partial T_1}{\partial U} = M \ddot{U}^0 + \frac{d}{dt} (M) \cdot U^0 \quad (26)$$

$$\frac{d}{dt} \left[\frac{\partial T_2}{\partial \dot{U}^0} \right] - \frac{\partial T_2}{\partial U} = - \theta^{02} M U \quad (27)$$

$$\begin{aligned} \frac{d}{dt} \left[\frac{\partial T_3}{\partial \dot{U}^0} \right] - \frac{\partial T_3}{\partial U} &= - 2 \theta^0 C_C U^0 - \theta^{00} C_C U \\ &- \theta^0 \frac{d}{dt} (C_C) U \end{aligned} \quad (28)$$

$$\begin{aligned} \frac{d}{dt} \left[\frac{\partial T_4}{\partial \dot{U}^0} \right] - \frac{\partial T_4}{\partial U} &= B^t |F_1 + F_2 + F_3 + F_4 + F_5 + F_6| \\ &+ \frac{d}{dt} (B)^t \cdot |\bar{F}_3 + \bar{F}_5 + \bar{F}_6| \end{aligned} \quad (29)$$

$$\frac{\partial V_e}{\partial U} = K U \quad (30)$$

where F_3, F_5, F_6 are also given in the appendix.

For the mechanism the set of equations is then :

$$\begin{aligned} M \ddot{q}^{00} + [C_C + M^0] \dot{q}^0 + [K + K_a + C_a + C_C^0] q \\ = F_I + F_{II} \end{aligned} \quad (31)$$

with

$$M = \Sigma M ; C_C = - \Sigma 2 \theta^0 C_C ;$$

$$K = \Sigma K ; K_a = - \Sigma \theta^{02} M$$

$$C_a = - \Sigma \theta^{00} C_C ; M^0 = \Sigma \frac{d}{dt} (M) ; \quad (32)$$

$$C_C^0 = - \Sigma \theta^0 \frac{d}{dt} (C_C)$$

$$F_I = \Sigma F, F_{II} = - \Sigma \frac{d}{dt} (B)^t |\bar{F}_3 + \bar{F}_5 + \bar{F}_6|$$

Solution of the equations

As all matrices and force vectors are functions of time, the differential system cannot be solved by a simple procedure. In fact a workable solution can be obtained by :

- neglecting the Coriolis influence (i.e. C_C and C_a) and the supplementary stiffness matrix K_a . This simplification is acceptable when, as in the application described below, medium speed are considered,

- using a numerical closed form algorithm which is very efficient to get the periodic response of a system with variable periodic characteristics [13]. The basic idea is to divide the period of the motion in short intervals during which system characteristics may be taken as constant. Then, displacement and velocity are obtained and their values at the end

of each short interval are the initial conditions of the next interval. The procedure is continued until the end of the period at which time, displacement and velocity, are the same as those at the beginning of the procedure. It was assumed in this study that the modal solutions are in phase which is not necessarily always the case.

As the closed form algorithm assumes that, the matrices are constant in the intervals, matrices M^0, C_C^0, F_{II} may be neglected. A viscous damping matrix C has been introduced to take into account the damping of the system and the following equations have been solved :

$$M \ddot{q}^{00} + C \dot{q}^0 + K q = F_I \quad (33)$$

The method has been applied to (33) in which the degrees of freedom have been reduced to two by the modal method.

FOUR BAR MECHANISM

The mechanism built is presented in Fig.2 and its schematisation in Fig.3.

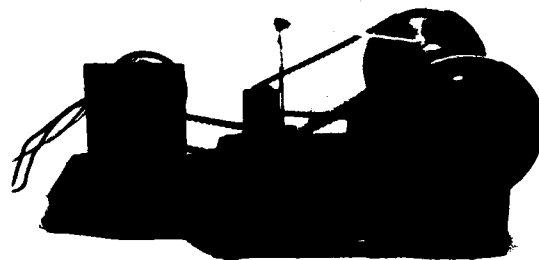


Fig.2 : Mechanism

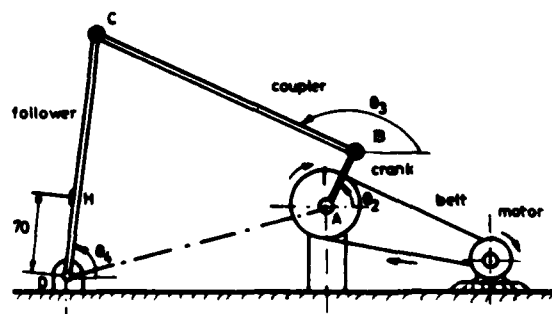


Fig.3 : Four bar mechanism schematisation.

It is made of duralumin whose characteristics are :

$$\rho = 2810 \text{ kg/m}^3 ; \quad E = 7,91.10^{10} \text{ N/m}^2$$

The dimensions of the beams are :

DC : L, length = 0.2 m ; l, width = 0.025 m ;
h, thickness = 0.003 m ; CB : L = 0.22 m ;
l = 0.025 m ; h = 0.003 m.

The beam BA has been made of two identical beams to ensure planar motion. Characteristics of the equivalent beam are :

L = 0.09 m ; l = 0.02 m ; h = 0.003 m

Mechanism at rest

In a first step the mechanism was tested and calculated for different values of the crank angle θ_2 . The system was modelled by 13 elements (AB : 3, BC : 5, CD : 5). In Fig.4 the variation of the five first frequencies versus θ_2 are presented. The agreement between theory and experiment is seen to be satisfactory further the first two frequencies are observed to be the most sensitive.

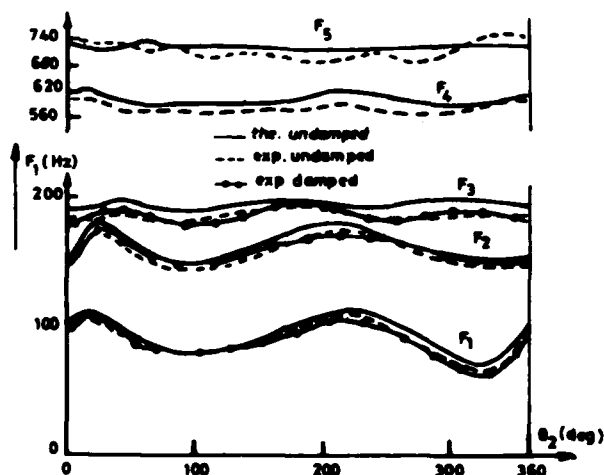


Fig.4 : Frequencies versus angular position θ_2

Experiments have also been run at rest with the mechanism damped by a viscoelastic sandwich treatment consisting of a 3 M composite (0.1 mm glue, 0.2 mm duralumin) glued on the both sides of both crank and follower. Resonance frequencies were measured and it was noted that F_1, F_2, F_3 were very close to the corresponding values of the undamped mechanism (Fig.4). The influence of the added material on mass and stiffness is therefore neglected. The first three equivalent modal damping factors of the system $\zeta_1, \zeta_2, \zeta_3$ have been measured in order to appreciate the damping of the structure when it rotates Fig.5. They have been obtained from a -3 db bandwidth measurement.

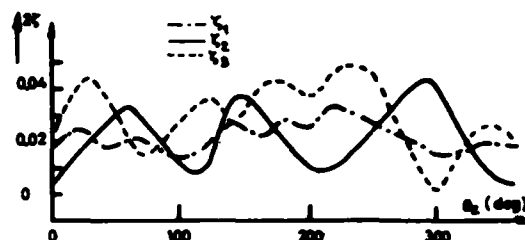


Fig.5 : Modal viscous damping coefficient versus θ_2 .

Mechanism in rotation

Mechanism deformations were measured using strain gages mounted on the links. Signals given by one of the follower gages (Fig.3) for three speeds (500, 550, 600 rpm) are presented Fig.6-11 for both the damped and undamped case. Strains are given as a function of the crank angle θ_2 . The agreement between experiment and theory is satisfactory. For the damped mechanism the agreement is not as good, as the equivalent viscous damping measured at rest underestimates the damping value at speed, probably because of friction at the connecting points.

CONCLUSION-SUGGESTIONS

General expressions for kinetic and strain energies of deformable plane rotating mechanisms have been presented. Using simplifying assumptions the finite element technique and a numerical closed formal algorithm have been used and the agreement between experiment and theory for a four bar mechanism is satisfactory. It has been observed that the introduction of viscoelastic material could significantly reduce vibration amplitudes.

In high speed applications the entire set of expressions (31) which include periodic coefficients in some of the matrices should be taken into account. Clearly this problem is of a different order of magnitude. Further the entire energy dissipation problem is still to be solved.

APPENDIX

$$F_1 = \frac{\rho SL}{2} \begin{vmatrix} -\theta^0 y_A^0 \\ \theta^0 x_A^0 \\ \frac{L}{6} \theta^0 x_A^0 \\ -\theta^0 y_A^0 \\ \theta^0 x_A^0 \\ -\frac{L}{6} \theta^0 x_A^0 \end{vmatrix} \quad F_2 = -\frac{\rho SL}{2} \begin{vmatrix} \theta^{02} x_A \\ \theta^{02} y_A \\ \frac{L}{6} \theta^{02} y_A \\ \theta^{02} x_A \\ \theta^{02} y_A \\ -\frac{L}{6} \theta^{02} y_A \end{vmatrix}$$

$$F_3 = \frac{d}{dt} |\bar{F}_3| = \frac{\rho SL}{2} \begin{vmatrix} -\theta^{\circ} y_A^{\circ} - \theta^{\circ\circ} y_A \\ \theta^{\circ} x_A^{\circ} + \theta^{\circ\circ} x_A \\ \frac{L}{6} (\theta^{\circ} x_A^{\circ} + \theta^{\circ\circ} x_A) \\ -\theta^{\circ} y_A^{\circ} - \theta^{\circ\circ} y_A \\ \theta^{\circ} x_A^{\circ} + \theta^{\circ\circ} x_A \\ -\frac{L}{6} (\theta^{\circ} x_A^{\circ} + \theta^{\circ\circ} x_A) \end{vmatrix}$$

$$F_4 = -\rho SL \begin{vmatrix} \frac{L}{6} \theta^{\circ 2} \\ 0 \\ 0 \\ \frac{L}{3} \theta^{\circ 2} \\ 0 \\ 0 \end{vmatrix} \quad F_5 = \frac{d}{dt} |\bar{F}_5| = \frac{\rho SL}{2} \begin{vmatrix} x_A^{\circ\circ} \\ 0 \\ 0 \\ x_A^{\circ\circ} \\ 0 \\ 0 \end{vmatrix}$$

$$F_6 = \frac{d}{dt} |\bar{F}_6| = \frac{\rho SL}{2} \begin{vmatrix} 0 \\ y_A^{\circ\circ} + \frac{3L}{10} \theta^{\circ\circ} \\ \frac{L}{6} y_A^{\circ\circ} + \frac{L^2}{15} \theta^{\circ\circ} \\ 0 \\ y_A^{\circ\circ} + \frac{7L}{10} \theta^{\circ\circ} \\ -\frac{L}{6} y_A^{\circ\circ} - \frac{L^2}{10} \theta^{\circ\circ} \end{vmatrix}$$

REFERENCES

- 1 - R.C. WINFREY, "Elastic link mechanism dynamics," J. Eng. Ind., Trans. ASME, pp 268-272 (1971).
- 2 - R.C. WINFREY, "Dynamic analysis of elastic link mechanism by reduction of coordinates," J. Eng. Ind., Trans. A.S.M.E., pp 577-582 (1972).
- 3 - A.G. ERDMAN, G.N. SANDOR, R.G. OAKLBERG, "A general method for kineto-elastodynamic analysis and synthesis of mechanisms," J. Eng. Ind., Trans. ASME, pp 1193-1205 (1972).
- 4 - I. IMAM, G.N. SANDOR, S.N. KRAMER, "Deflection and stress analysis in high speed planar mechanisms with elastic links," J. Eng. Ind., Trans. ASME, pp 541-548 (1973).
- 5 - I. IMAM, G.N. SANDOR, "High speed mechanism design - A general analytical approach," J. Eng. Ind., Trans. ASME, pp 609-628 (1975).
- 6 - J.P. SADLER, G.N. SANDOR, "A lumped parameter approach to vibration and stress analysis of elastic linkages," J. Eng. Ind., Trans. ASME, pp 549-557 (1973).
- 7 - J.P. SADLER, G.N. SANDOR, "Nonlinear vibration analysis of elastic four-bar linkage," J. Eng. Ind., Trans. ASME, pp 411-419 (1974).
- 8 - E.P. GOLEBIEWSKI, J.P. SADLER, "Analytical and experimental investigation of elastic slider crank mechanism," J. Eng. Ind., Trans. ASME, pp 1266-1271 (1976).
- 9 - S.C. CHU, K.C. PAN, "Dynamic response of high speed slider crank mechanism with an elastic connecting rod," J. Eng. Ind., Trans. ASME, pp 542-550 (1975).
- 10 - J.O. SONG, E.J. HAUG, "Dynamic analysis of planar flexible mechanisms," Comp. Met. App. Mech. Eng., pp 359-381 (1980).
- 11 - A. MIDHA, A.G. ERDMAN, D.A. FROHRIB, "An approximate method for the dynamic analysis of elastic linkage," J. Eng. Ind., Trans. ASME, pp 504-609 (1977).
- 12 - A. MIDHA, A.G. ERDMAN, D.A. FROHRIB, "Finite element approach to mathematical modelling of high speed elastic linkage," Mech. Mach. Th., pp 603-618 (1978).
- 13 - A. MIDHA, A.G. ERDMAN, D.A. FROHRIB, "A closed form numerical algorithm for the periodic response of high speed elastic linkage," J. Eng. Ind., Trans. ASME, pp 154-162 (1979).
- 14 - P.K. NATH, A. GHOST, "Kineto-elastodynamic analysis of mechanisms by finite element method," Mech. Mach. Th., pp 179-197 (1980).
- 15 - P.K. NATH, A. GHOST, "Steady state response of mechanisms with elastic links by finite element methods," Mech. Mach. Th., pp 199-211 (1980).
- 16 - R.M. ALEXANDER, K.L. LAWRENCE, "An experimental investigation of the dynamic response of an elastic mechanism," J. Eng. Ind., Trans. ASME, pp 268-274 (1974).
- 17 - R.M. ALEXANDER, K.L. LAWRENCE, "Experimentally determined dynamic strains in an elastic mechanism," J. Eng. Ind., Trans. ASME, pp 791-794 (1975).
- 18 - G.H. SUTHERLAND, "Analytical and experimental investigation of high speed elastic membered linkage," J. Eng. Ind., Trans. ASME, pp 542-550 (1975).
- 19 - J.S. PRZEMIENIECKI, "Theory of matrix structural analysis, Mc Graw Hill, 1968.
- 20 - E. IMAM, "Contribution à l'étude dynamique des mécanismes déformables," Dr. Ing. Thesis (1981).

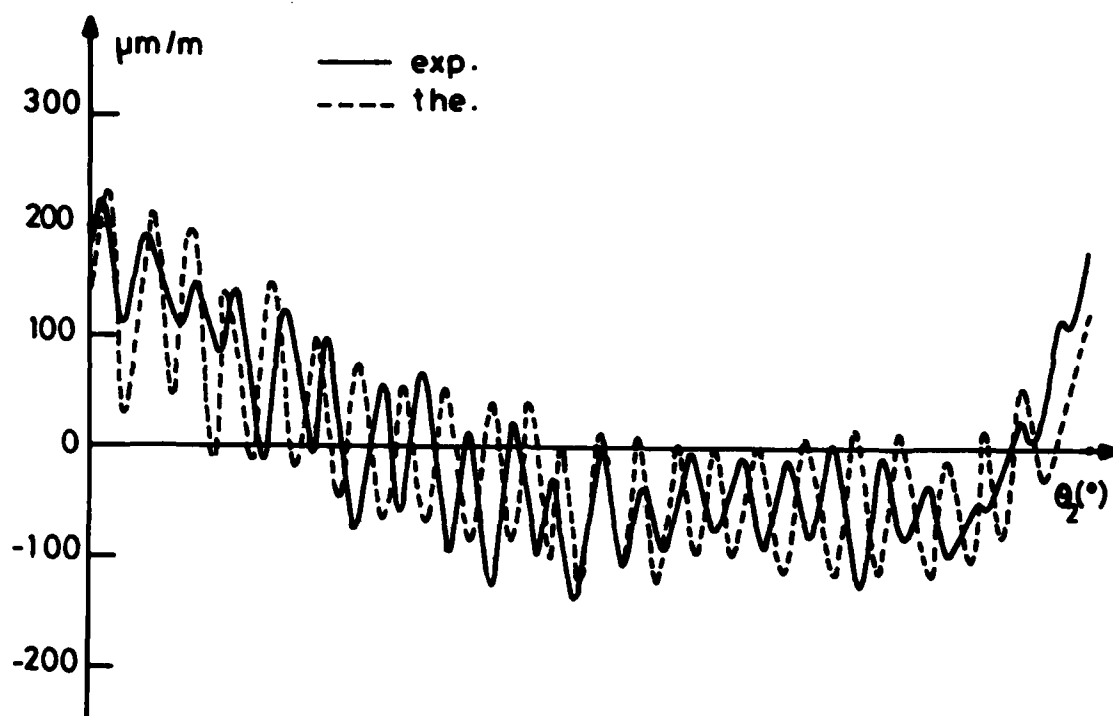


Fig.6 : Strains versus θ_2 at 500 rpm (undamped mechanism).

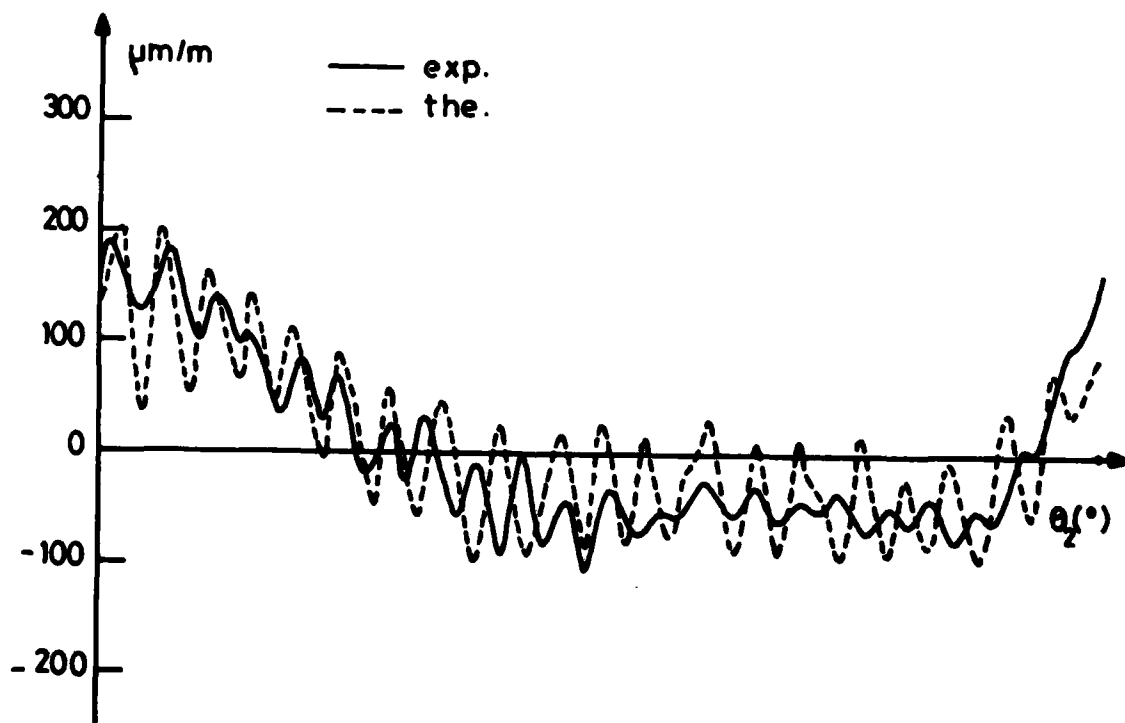


Fig.7 : Strains versus θ_2 at 500 rpm (damped mechanism).

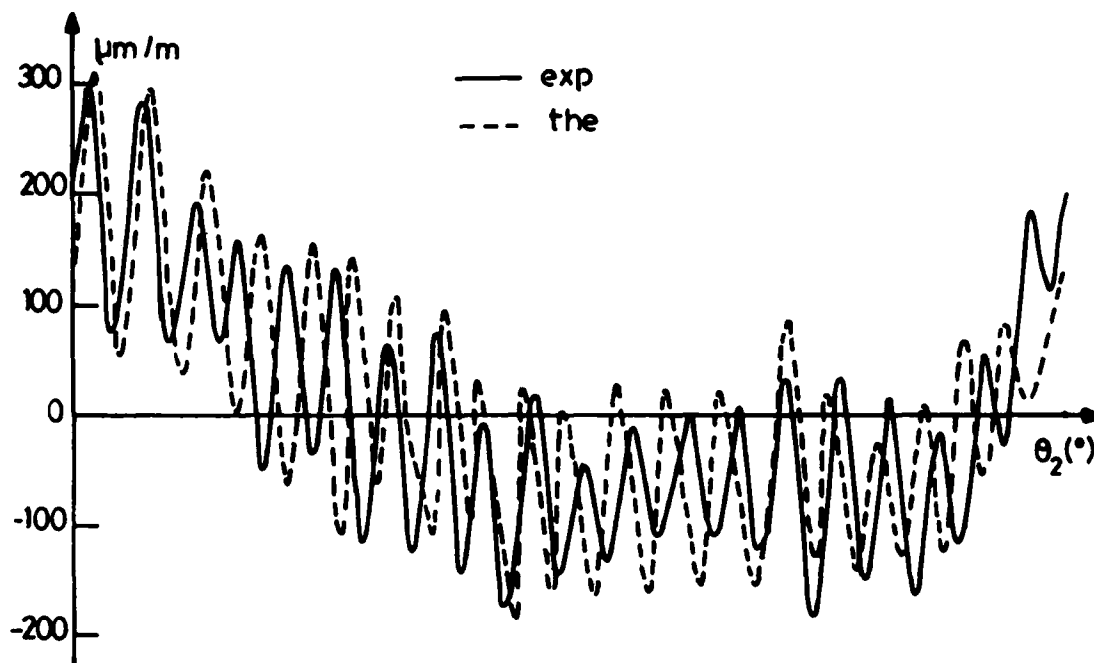


Fig.8 : Strains versus θ_2 at 550 rpm (undamped mechanism).

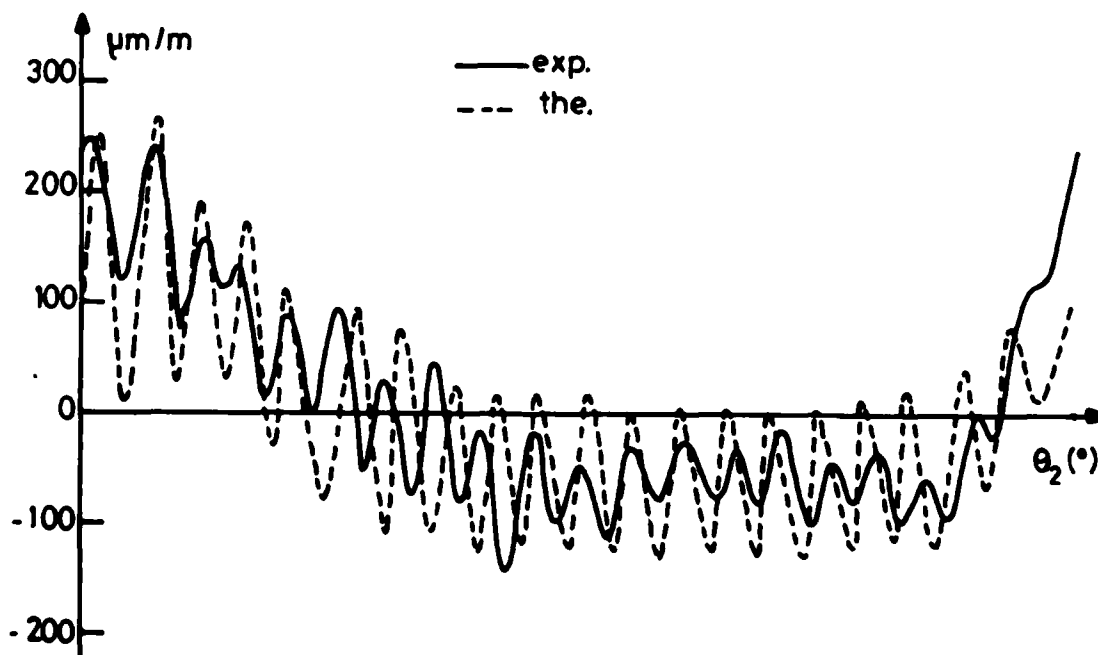


Fig.9 : Strains versus θ_2 at 550 rpm (damped mechanism).

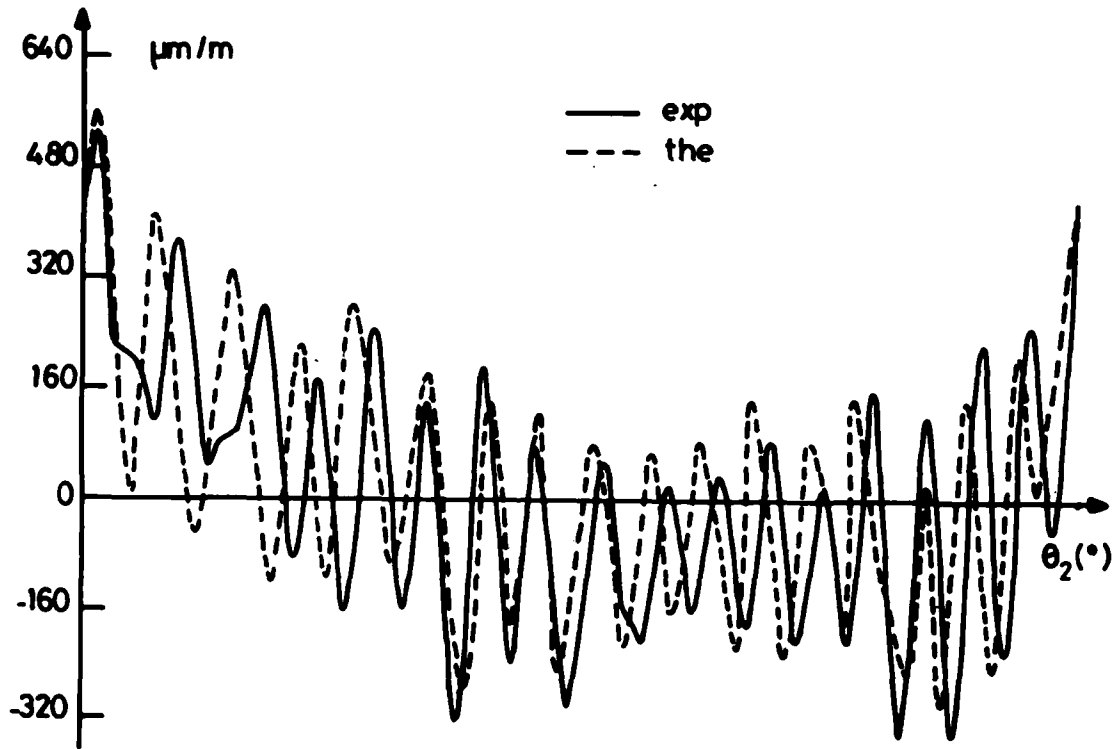


Fig.10 : Strains versus θ_2 at 600 rpm (undamped mechanism).

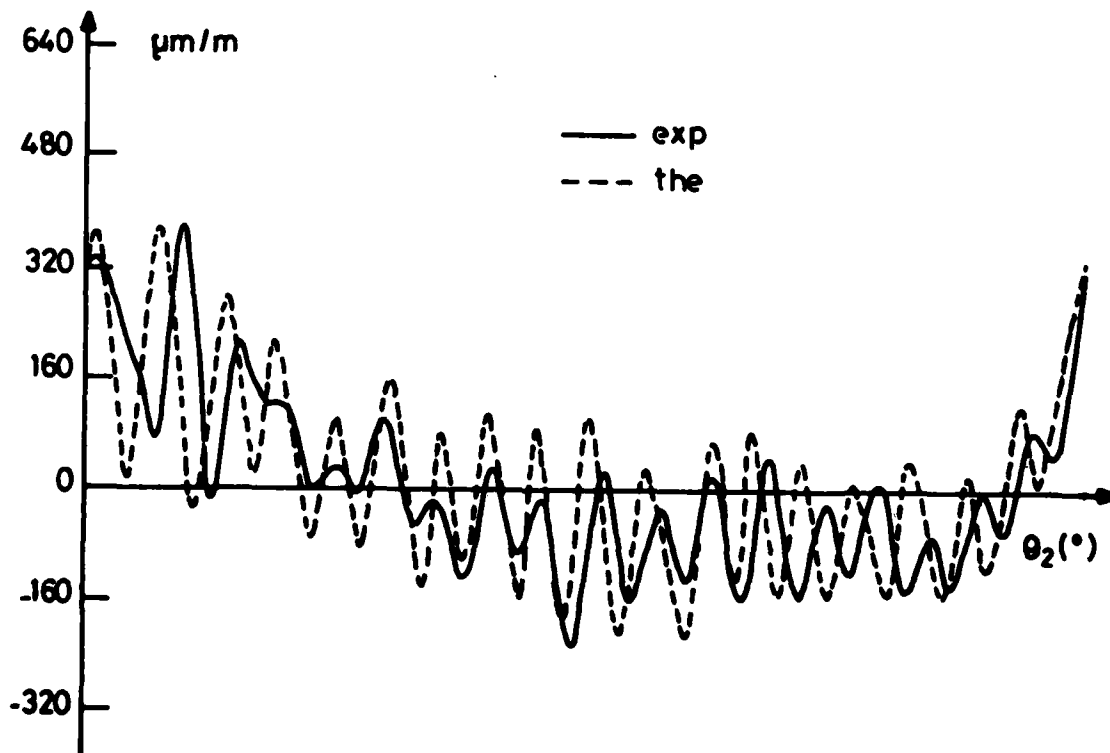


Fig.11 : Strains versus θ_2 at 600 rpm (damped mechanism).

SELF-EXCITED VIBRATION OF A NONLINEAR
SYSTEM WITH RANDOM PARAMETERS

Raouf A. Ibrahim
Assistant Professor
Department of Mechanical Engineering
Texas Tech University
Lubbock, Texas 79409

This paper deals with the dynamic behavior of a nonlinear single degree-of-freedom system with negative linear damping and subjected to broad band random excitations. The system response is analyzed by using two different approaches: the Stratonovich stochastic averaging method, and the Itô stochastic calculus together with the Gaussian closure. Closed-form solutions of the stationary responses are obtained. It is shown that the two methods provide solutions which bifurcate from two different points for all the cases considered except at one point where the parametric excitations and the nonlinear restoring force are removed. It is concluded in this analysis that the Gaussian closure may be regarded as a linearization technique.

The nontrivial stationary response suggests that the system can achieve a stable limit cycle provided a positive nonlinear damping is included. Unlike the Gaussian approximation, the influence of the nonlinear restoring force is not manifested in the averaging method results.

1. INTRODUCTION

Simultaneous occurrence of self-excited and random parametric vibrations may be encountered in several structural systems, such as machine tools and water-lubricated bearings. These types of vibrations are not desirable and may endanger the safe operation and reliability of mechanical systems. It is the purpose of this paper to investigate the dynamic response and stability of such structural systems.

The dynamic behavior of nonlinear systems, including sources of self-excited vibrations, is investigated in depth by Tondl [1]. In two other monographs, Tondl examined the deterministic problems of interaction of self-excited vibra-

tion with forced vibration [2] and with parametric vibration [3]. In these studies, it was shown that the inclusion of nonlinear damping force causes the system to reach a limit cycle for which the stability "in the large" was the main concern of these studies. It was also indicated that for systems with a nonlinear restoring force, the response is manifested in the phase plane as an unstable limit cycle which separates the regions of the domains of attraction. The domains of attraction are those boundaries between the regions of initial conditions leading to different steady state solutions.

In most cases, however, the actual time variation in damping or in stiffness parameters is not periodic. In order to obtain a more realistic description of the behavior

of such systems, these parametric excitations should be modeled by random processes. In an effort towards that regard, several investigators considered a number of problems pertaining to parametric and autoparametric systems under stochastic excitations (see, for example, the two review articles [4,5]). Recently, the author has investigated the random parametric excitation of a nonlinear single degree-of-freedom system with positive linear damping [6,7]. The statistical moment equations of the system response were obtained by using two approaches: the Fokker-Planck equation [6] and the Itô stochastic calculus [7]. The two approaches led to the same set of moment equations, which were found to form an infinite hierarchy set. A number of truncation schemes have been used in the past as closure approximation for this type of equations. These schemes are usually based on the assumption that the probability distribution of the response is "nearly" Gaussian. With this assumption, higher order moments are related to lower order moments through one of the schemes discussed in reference [5]. These approximate methods have no rigorous mathematical basis, but satisfactory results have been obtained [4]. On the other hand, the methods may lead to invalid solutions which do not preserve moments properties [6], or they may not depict the proper nonlinear behavior of the system [8,9]. Ariaratnam [9] has shown that the stationary response of a nonlinear system bifurcates from a point different from the one obtained by the Gaussian closure.

In this paper the stationary response of a nonlinear system containing a source of self-excited vibration, and subjected to wide band random parametric excitations is analyzed. Two analytical approaches will be considered: the Stratonovich stochastic averaging, and the Itô stochastic calculus together with the Gaussian closure of the moment equations of the system response. Comparison of the results obtained from the two methods reveals a number of differences in addition to those found by Ariaratnam [9]. It is found that the moment equations derived by the averaging method do not involve the effects of the nonlinear restoring force, although the moment equations become identical if one removes that force from the system equation. With the inclusion of a positive nonlinear damping force, the

system is found to be capable of achieving a stable limit cycle.

2. STOCHASTIC DIFFERENTIAL EQUATIONS OF THE SYSTEM

The dynamic behavior of a nonlinear single degree-of-freedom system as described in the introduction can be modeled by the dimensionless differential equation:

$$\ddot{X} - [2\zeta - \beta X^2 + W_1(\tau)]\dot{X} + [1 + \gamma X^2 - W_2(\tau)]X = 0 \quad (1)$$

where X is the displacement, ζ is the damping ratio of the negative damping force, β is the coefficient of positive nonlinear damping, and γ is the coefficient of the nonlinear stiffness. $W_1(\tau)$ and $W_2(\tau)$ are independent, "physical," broad band random processes describing the time variation in damping and stiffness coefficients, respectively. These parametric excitations are assumed to have zero means and stationary Gaussian distributions with smooth spectral densities D_1 and D_2 , such that their correlation time is very small compared with the time scale of the system oscillations.

The response parameters of the system (1) can be regarded as effectively Markovian if the two processes $W_1(\tau)$ and $W_2(\tau)$ are approximated as white noise processes in the physical sense interpreted by Gray and Caughey [10]. Accordingly, equation (1) may be written in the state vector form, with $X_1 = X$, and $\dot{X}_1 = X_2$:

$$\begin{aligned} \dot{X}_1 &= X_2 \\ \dot{X}_2 &= (2\zeta X_2 - X_1 - \beta X_1^2 X_2 - \gamma X_1^3) \\ &\quad + X_2 W_1(\tau) + X_1 W_2(\tau) \end{aligned} \quad (2)$$

It is customary to regard $W_1(\tau)$ and $W_2(\tau)$ as the "formal" derivatives of the Brownian motion processes as:

$$W_1(\tau) = \sigma_1 \frac{dB_1(\tau)}{d\tau}, \quad (3)$$

$$W_2(\tau) = \sigma_2 \frac{dB_2(\tau)}{d\tau}$$

where $dB_1(\tau)$ and $dB_2(\tau)$ are two independent Brownian motion processes with unit variance parameters, and σ_1^2 and σ_2^2 are the spectral densities

where $\sigma_1^2 = 2D_1$, and $\sigma_2^2 = 2D_2$. It is

assumed that $W_1(\tau)$ and $W_2(\tau)$ have zero cross correlation. It is convenient to rewrite equations (2) in terms of the differentials:

$$dX_1 = X_2 d\tau$$

$$dX_2 = (2\zeta X_2 - X_1 - \beta X_1^2 X_2 - \gamma X_1^3) d\tau \quad (4)$$

$$+ \sigma_1 X_2 dB_1(\tau) + \sigma_2 X_1 dB_2(\tau)$$

Since $W_1(\tau)$ and $W_2(\tau)$ represent the limiting case of smooth, wide-band processes, the system equations (4) should be interpreted as stochastic differential equations of Stratonovich type corresponding to the general form [11,12]:

$$dX_i = f_i(\underline{X}, \tau) d\tau \quad (5)$$

$$+ \sum_{j=1}^N G_{ij}(\underline{X}, \tau) dB_j(\tau),$$

$$i=1, 2, \dots, n$$

Equations (4) may in turn be transformed into stochastic equations of the Ito type:

$$dX_i = [f_i(\underline{X}, \tau) + \frac{1}{2} \sum_{k=1}^N \sum_{j=1}^N G_{kj} \frac{\partial G_{ij}}{\partial X_k}] d\tau + \sum_{j=1}^N G_{ij}(\underline{X}, \tau) dB_j(\tau) \quad (6)$$

Comparison of the system equations (4) with Itô's equation (6) reveals that, for the system considered, the Ito correction term, which is sometimes known as the Wong and Zakai correction term [13], is $\frac{1}{2} \sigma_1^2 X_2$. Such a correction term is

obtained when the random excitation appears as the coefficient of the next to highest derivative in the differential equation [14-16]. The Itô stochastic equations of the system may be written in the form:

$$dX_1 = X_2 d\tau$$

$$dX_2 = (2\zeta X_2 - X_1 + \frac{1}{2} \sigma_1^2 X_2 - \beta X_1^2 X_2 - \gamma X_1^3) d\tau + \sigma_1 X_2 dB_1(\tau) + \sigma_2 X_1 dB_2(\tau) \quad (7)$$

The stationary response of the system will be determined by considering equations (4) and (7).

3. STRATONOVICH AVERAGING APPROACH

In order to apply the Stratonovich averaging method, the system equations (4) are considered. The method requires the introduction of new variables describing the amplitude and the phase as:

$$X_1 = A \cos \theta,$$

$$X_2 = -A \sin \theta, \quad (8)$$

$$\theta = \tau + \psi(\tau)$$

Equations (4) become:

$$dA = (2\zeta A \sin \theta - \beta A^3 \cos^2 \theta \sin \theta - \gamma A^3 \cos^3 \theta) \sin \theta d\tau + \sigma_1 A \sin^2 \theta dB_1(\tau) - \sigma_2 A \sin \theta \cos \theta dB_2(\tau) \quad (9)$$

$$d\theta = (2\zeta \sin \theta - \beta A^2 \cos^2 \theta \sin \theta - \gamma A^2 \cos^3 \theta) \cos \theta d\tau + \sigma_1 \sin \theta \cos \theta dB_1(\tau) - \sigma_2 \cos^2 \theta dB_2(\tau)$$

A and θ may also be approximated by a vector-Markov process. Carrying out the stochastic averaging of Stratonovich [17] to equations (9), the following Itô equations are obtained:

$$dA = \left[\frac{1}{16}(5\sigma_1^2 + 3\sigma_2^2) + \zeta - \frac{\beta}{8}A^2 \right] A d\tau + \left(\frac{3}{8} \right)^{1/2} \sigma_1 A dB_1(\tau) - \left(\frac{1}{8} \right)^{1/2} \sigma_2 A dB_2(\tau) \quad (10)$$

$$d\theta = -(\beta - 3\gamma) \frac{A^2}{8} d\tau + \left(\frac{1}{8} \right)^{1/2} \sigma_1 A dB_1(\tau) - \left(\frac{3}{8} \right)^{1/2} \sigma_2 A dB_2(\tau)$$

Since the first equation in (10) is independent of the phase θ , the amplitude $A(\tau)$ constitutes a Markov diffusion process by itself [8,9]. The probability density function $p(A, \tau)$ should satisfy the Fokker-Planck equation:

$$\frac{\partial p}{\partial \tau} = \frac{\partial}{\partial A} \left[\left\{ \frac{1}{8}(5D_1 + 3D_2) + \zeta - \frac{\beta}{8}A^2 \right\} A p \right] + \frac{1}{8}(3D_1 + D_2) \frac{\partial^2}{\partial A^2} (A^2 p) \quad (11)$$

Here D_{12} is set to zero since it has been assumed that both random excitations are uncorrelated. It is not possible to obtain a closed-form analytical solution for the transition probability of equation (11). However, one can obtain a stationary solution by setting the left-hand side of equation (11) to zero, as:

$$p(A) = CA^{2n-1} \cdot e^{-DA^2} \quad (12)$$

where

$$C = \Gamma^{-1}(n) \left[\frac{\beta}{2(3D_1 + D_2)} \right]^n, \quad D = \frac{\beta}{2}(3D_1 + D_2)^{-1} \quad (13) \\ n = (D_1 + D_2 + 4\zeta) / (3D_1 + D_2)$$

The mean and mean square of the response amplitude A are:

$$E[A] = 2^{-n} \left[\frac{2\pi}{\beta} (3D_1 + D_2) \right]^{1/2} \Gamma(2n) / \Gamma^2(n) \quad (14)$$

$$E[A^2] = \frac{1}{\beta} (4\zeta + D_1 + D_2) \quad (15)$$

For the case $D_1=0$, the mean square (15) becomes identical to that obtained by Schmidt [8] and Ariaratnam [9] if ζ is replaced by $-\zeta$. For the purpose of comparison with the results of the next section, the differential equation of the second moment of $p(A)$ is derived from the Fokker-Planck equation (11) as:

$$\frac{d}{dt} E[A^2] = (2\zeta + 2D_1 + D_2) E[A^2] - \frac{\beta}{4} E[A^4] \quad (16)$$

It is seen that the above results are independent of γ . Figure (1) shows the mean and the root mean square of the amplitude A as function of the excitation spectral density of damping variation ($D_1/2\zeta$) with $D_2=0$. It is clear that these amplitude parameters are monotonically increasing with $D_1/2\zeta$. In terms of X_1 , the mean square of X_1 ,

$X_1, m = E[X_1^2]$, is illustrated in figures (2) and (3) by solid lines.

4. GAUSSIAN CLOSURE OF MOMENT EQUATIONS

4.1 Dynamic Moment Equations

A set of differential equations of the response joint moments of the probability density function $p(X, \tau)$ can be derived by using the method of stochastic calculus [12] which requires the introduction of the scalar-valued real function:

$$\phi = (X_1^k X_2^l) \quad (17)$$

and the joint moment of the system response of order $N=k+l$

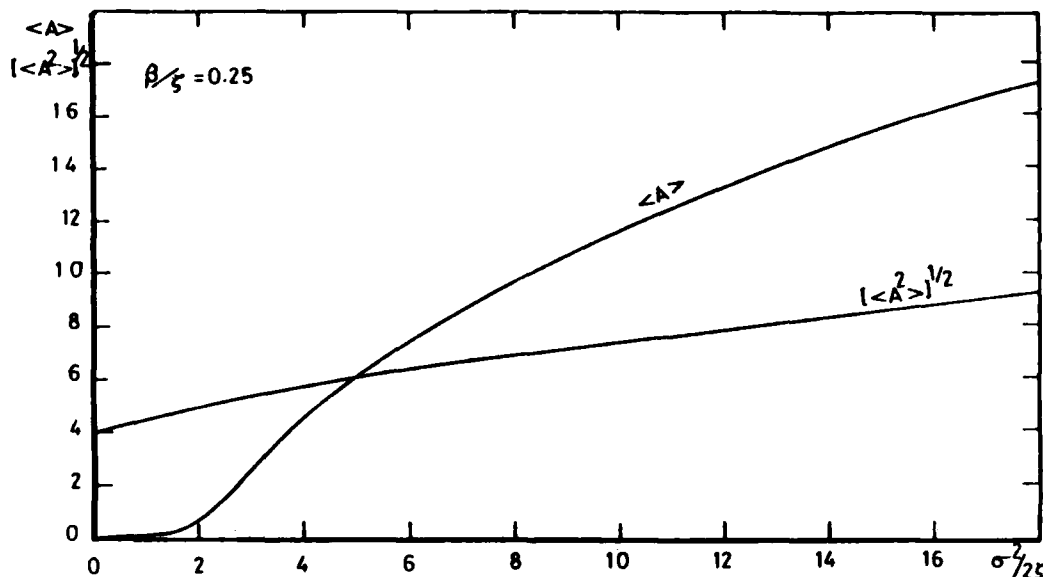


FIG (1) Mean and Root-Mean-Square of the Amplitude as Function of the Excitation Spectral Density According to Stratonovich Averaging Method

$$m_{k1} = E[X_1^k X_2^k] = E[\phi] \quad (18)$$

$$= \int_{-\infty}^{\infty} \int_{-\infty}^{\infty} X_1^k X_2^k p(\underline{X}, \tau) dX_1 dX_2$$

The two-dimensional process function ϕ possesses a stochastic differential, and according to the Ito theorem, $d\phi$ takes the form [12]:

$$d\phi = \left(\frac{\partial \phi}{\partial X_1} \right)^T \{dX_1\} \quad (19)$$

$$+ 1/2 \text{ Trace } [G][Q][G]^T \left[\frac{\partial^2 \phi}{\partial X_1 \partial X_j} \right] d\tau$$

$$\text{where } [Qd\tau] = E[\{dB_1\}\{dB_1\}^T]$$

Substituting the corresponding expressions of $[G]$, $[Qd\tau]$ from equations (7) into equation (19), then taking expectation and dividing both sides by $d\tau$ gives:

$$\dot{m}_{k1} = km_{k-1,l+1} + 2\lambda m_{k,l} - \lambda m_{k+1,l+1} \quad (20)$$

$$- \lambda \beta m_{k+2,l} - \lambda \gamma m_{k+3,l-1}$$

$$+ \lambda D_1 m_{k,l} + D\lambda(l-1)m_{k,l}$$

$$+ D_2 \lambda(l-1)m_{k+2,l-2}$$

Equation (20) represents a system of linear first order differential equations of the system moments response. Inspection of equation (20) shows that the inclusion of damping and stiffness nonlinearities causes the system (20) to form an infinite hierarchy of moment equations. This, of course, creates serious difficulties in determining the system response or stability criteria "in the large." In order to obtain solutions for a finite set of moments, equation (20) must be truncated. Most of the available closure schemes [5] assume Gaussian distribution of the response joint moments. This is valid for linear systems described by differential equations with constant coefficients. On the contrary, for linear systems under parametric excitations as well as nonlinear systems, it is known that the response is not Gaussian distributed if the excitation is Gaussian. However, for systems with very small nonlinearities, the joint distribution functions of the response may not deviate significantly from Gaussian form. The validity of such approximation must be examined by comparison with the exact solution or with experimental results. In this paper the first alternative will be followed.

4.2 Stationary Responses

The stationary responses of the system may be described adequately in terms of first and second moments because higher moments have no physical meaning and the physical interpretation of higher moments stability would be difficult. The first moment equation can be written directly from equation (20) by setting $k=1$, $l=0$, and $k=0$, $l=1$:

$$\dot{m}_{10} = m_{01} \quad (21)$$

$$\dot{m}_{01} = 2\zeta m_{01} - m_{10} - \delta m_{21} - \gamma m_{30} + D_1 m_{01}$$

Similarly, the second order moment equations are:

$$\begin{aligned} \dot{m}_{11} &= m_{02} + 2\zeta m_{11} - m_{20} - \delta m_{31} \\ &\quad - \gamma m_{40} + D_1 m_{11} \\ \dot{m}_{20} &= 2m_{11} \end{aligned} \quad (22)$$

$$\begin{aligned} \dot{m}_{02} &= 4\zeta m_{02} - 2m_{11} - 2\delta m_{22} + 4D_1 m_{02} \\ &\quad + 2D_2 m_{20} - 2\gamma m_{31} \end{aligned}$$

The stationary solutions of equations (21) and (22) may be obtained by setting the left-hand side of these equations to zero. The first equation in (21) and the second equation in (22) give:

$$m_{01} = m_{11} = 0 \quad (23)$$

This result indicates that the displacement and velocity of the system are uncorrelated. To complete the solution, the third and fourth order moments in equations (21) and (22) will be replaced by first and second order moments by using the cumulant truncation scheme [5]. This process will result in the following algebraic equations:

$$\begin{aligned} m_{10}(1+3\gamma m_{20}-2\gamma m_{10}^2) &= 0 \\ m_{02}-m_{20}-3\gamma m_{20}^2+2\gamma m_{10}^4 &= 0 \quad (24) \\ 2\zeta m_{02}-\delta m_{20}m_{02}+2D_1 m_{02}+D_2 m_{20} &= 0 \end{aligned}$$

Three possible solutions of (24) will be examined.

4.2.1 Null Solution

It is seen that equation (24) are satisfied by the trivial solution:

$$m_{10} = m_{20} = m_{02} = 0 \quad (25)$$

This solution describes the equilibrium position of the system and can be obtained from the linear theory. The stability "in the small" in terms of first and second moments can be determined by employing the Routh-Hurwitz criteria. Introducing small perturbations δk_i to the null solution, the following stability criteria are obtained:

i. Stability of the first moments can be determined by examining the associated characteristic equation:

$$\lambda^2 - (2\zeta + D_1)\lambda + 1 = 0 \quad (26)$$

Equation (26) indicates that the system is unstable in the mean.

ii. Stability of the second moments can also be obtained from the characteristic equation:

$$\begin{aligned} \lambda^3 - (6\zeta + 5D_1)\lambda^2 + 4(\zeta^2 + 3\zeta D_1 + D_1^2 + 1)\lambda \\ - 4(2\zeta + D_2 + 2D_1) = 0 \end{aligned} \quad (27)$$

It is obvious that the system is unstable in the mean square.

4.2.2 Zero Mean Solution

Equations (24) give the following semi-trivial solution:

$$\begin{aligned} m_{10} &= 0, \quad m_{11} = 0 \\ m_{20} &= \frac{\zeta}{\delta} \left(1 - \frac{\delta}{6\gamma\zeta} + \frac{D_1}{\zeta} \right. \\ &\quad \left. + \left[\left(1 + \frac{\delta}{6\gamma\zeta} + \frac{D_1}{\zeta} \right)^2 + \frac{\delta D_2}{3\gamma\zeta} \right]^{1/2} \right) \end{aligned} \quad (28)$$

$$m_{02} = m_{20}(1+3\gamma m_{20})$$

The dependence of the mean square of the displacement m_{20} upon the excitation parameter $D_2/2\zeta$ is shown by the dotted curves in figures (2) and (3), for the two values of $D_1/2\zeta = 0, 2$, and for three values of $\gamma = 0.01, 0.05$ and 0.1 . It is seen

that m_{20} is diminishing as the nonlinear restoring force parameter is increasing. The influence of the nonlinear parameters γ and β are examined separately:

i. For $\gamma = 0$ and $\beta \neq 0$, the solution of (24) becomes:

$$m_{20} = m_{02} = \frac{1}{\beta}(2\zeta + 2D_1 + D_2) \quad (29)$$

This solution is represented by the dotted straight lines in figures (2) and (3).

ii. For $\beta = 0$ and $\gamma \neq 0$ equations (24) give the solution:

$$m_{20} = -\frac{(2\zeta + 2D_1 + D_2)}{6\gamma(\zeta + D_1)}, \quad (30)$$

$$m_{02} = m_{20}(1 + 3\gamma m_{20})$$

This solution is invalid since it gives negative mean squares. The invalidity of this solution may be attributed to a number of sources; these could be the inaccuracy incurred by using the Gaussian closure scheme, or the system may not be able to reach a stationary response. This point will be discussed in detail in section 5.

The stability "in the large" of the mean squares can be examined in the neighborhood of the stationary solution (28). Introducing small perturbations δ_{ki} to that solution as:

$$m_{ki} = m_{ki}^0 + \delta_{ki} e^{\lambda t} \quad (31)$$

$$\lambda^3 + b_2 \lambda^2 + b_1 \lambda + b_0 = 0 \quad (32)$$

where

$$b_2 = 5\beta m_{20}^0 - 6\zeta - 5D_1$$

$$b_1 = 2(2\zeta + 2D_1 - \beta m_{20}^0)(2\zeta + D_1 - 3\beta m_{20}^0) + 2(2 + 7\gamma m_{20}^0) \quad (33)$$

$$b_0 = 4[\beta m_{02}^0 + (1 + 6\gamma m_{20}^0)$$

$$(\beta m_{20}^0 - 2\zeta - 2D_1) - D_2]$$

Inspecting the coefficients b_i for particular values of the solution (28) yields positive values. Furthermore, the minor determinants of the Routh-Hurwitz array are found positive. This result indicates that the solution (28) is stable "in the large." It also suggests the existence of a stable limit cycle provided the system possesses a positive nonlinear damping. This result confirms Tondl's findings for a similar deterministic system [3].

4.2.3 Nonzero Mean Displacement Solution

For the case of $m_{10} \neq 0$, equations (24) indicate that M_{10} is coupled with the second moments. The solution of these coupled equations is:

$$m_{10} = \left[\frac{1}{2\gamma}(1 + 3\gamma m_{20}) \right]^{1/2} \quad (34)$$

$$m_{02} = -\frac{1}{2}\left(\frac{1}{\gamma} + 4m_{20} + 3\gamma m_{20}^2\right)$$

and m_{20} is given by the solution of the cubic equation:

$$m_{20}^3 + \frac{2}{3}\frac{2}{\gamma} - \frac{3}{\beta}(D_1 + \zeta)m_{20}^2 + \frac{1}{3}\left[\frac{1}{\gamma} + \frac{2}{\beta\gamma}(D_2 - 4\zeta - 4D_1)\right]m_{20} - \frac{2}{3\beta\gamma}(D_1 + \zeta) = 0 \quad (35)$$

It is clear that this solution violates the moments properties since it gives negative mean squares. It is also noticed from equations (24) that the coupling between the first and second order moments depends on the presence of the nonlinear restoring force.

5. DISCUSSION OF RESULTS AND CONCLUSIONS

Figures (2) and (3) illustrate the stationary mean square response of the displacement m_{20} as obtained by the averaging method (solid lines) and the Gaussian approximation scheme (dotted curves). Comparison of the results of the two approaches can be carried out by dropping the nonlinear stiffness term γX^3 from the system

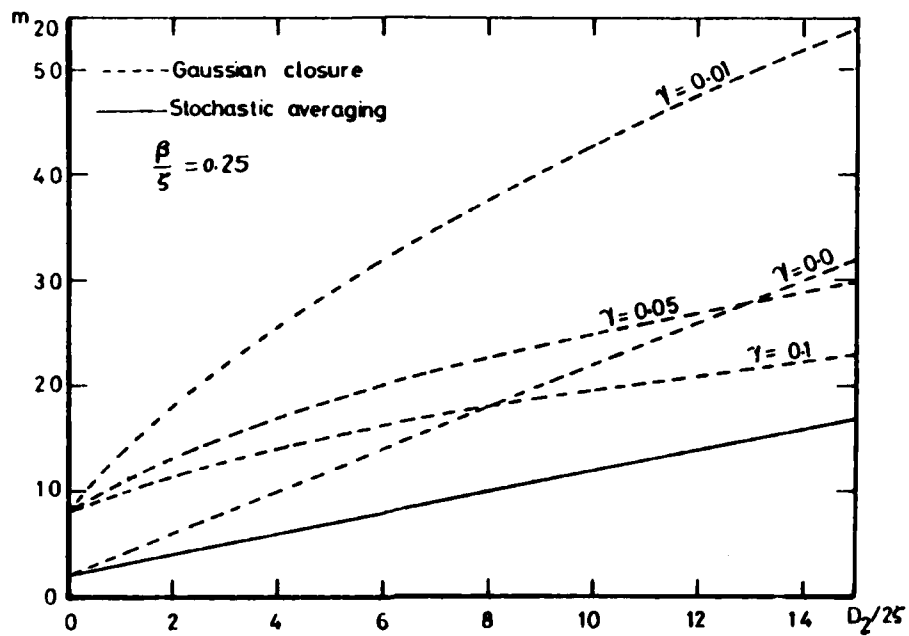


FIG (2) Displacement Mean-square Response ($D_1/2\zeta = 0$)

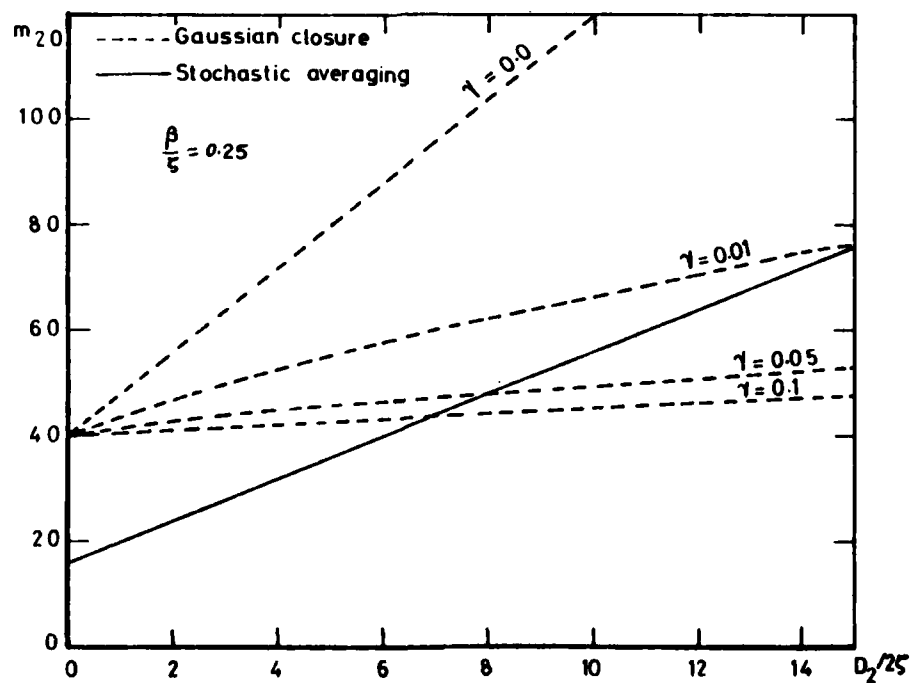


FIG (3) Displacement Mean-square Response ($D_1/2\zeta = 2$)

equation (1). It is seen that the two methods give different results, except at one point $D_2/2\zeta=D_1/2\zeta=0$, shown in figure (2). The mean square m_{20} of the Gaussian approximation is almost twice the result of the averaging process. This difference may be due to mainly the closure approximation of replacing higher order moments by first and second moments. A similar situation was first noticed by Ariaratnam [8,9]. Previous studies [18,19] of linear systems, with positive linear damping and excited parametrically by the white noise $W_2(\tau)$, have shown that such systems are stable in the mean square if the condition $D_2/2\zeta < 1$ is met. On the other hand, when the same system includes a nonlinear damping force, the averaging leads to the condition $D_2/2\zeta < 2$, [9], while the Gaussian approximation gives a result identical to that of the linear theory [6]. The Gaussian closure can then be regarded as a linearization procedure of the nonlinear system. Therefore, one may conclude that the closure techniques based on Gaussian distribution of the response may annihilate the inherent dynamic characteristics of certain nonlinear systems, especially those under parametric excitations. However, these approximations have shown to be very powerful tools for other types of nonlinear systems under random forced excitations [20,21]. The main features of the dynamic behavior of a nonlinear system with autparametric coupling [21], examined by using the Gaussian approximation, were confirmed by Schmidt [8] who investigated a similar system by employing the averaging method. To the author's knowledge, the discrepancy resulting in using the Gaussian closure techniques has to date been found to occur in problems with parametric excitations. In that regard, it is recommended that a nonGaussian closure of the type outlined by Crandall [22], or by Robson [23], be considered since the resulting relations between the response moments are dependent upon the system nonlinear coefficients. Notice that the Gaussian closure gives truncated relations as $m_{N+1}=F(m_N, m_{N-1}, \dots, m_1)$, while the nonGaussian closure leads to relations of the type $m_{N+1} = F(\gamma, \beta, m_N, \dots)$.

As a consequent result of the moment truncation, and because of the

properties of the parametric excitations, the Gaussian approximation leads to zero means of the response. On the other hand, the averaging method gives a finite value for the mean amplitude response, equation (14), although the result would agree with the Gaussian closure if one considered the mean $m_{10} = E[\text{Acos}\theta]$. It is also seen that the result obtained by the averaging method is independent of γ . In connection with the effect of γ alone, the averaging method fails to give a closed form solution and the Gaussian approximation gives invalid results. Stability study of the stationary response, as obtained by the Gaussian closure, shows that the inclusion of a positive nonlinear damping is essential to guarantee a stable limit cycle; otherwise, the system is unstable "in the large."

The author strongly recommends experimental investigations to establish the validity of the analytical results presented in this paper.

REFERENCES

1. Tondl, A., Self-Excited Vibration, National Research Institute for Machine Design, Bechovice, Prague, Monograph No. 9, 1970.
2. Tondl, A., On the Interaction Between Self-Excited and Forced Vibrations, National Research Institute for Machine Design, Bechovice, Prague, Monograph No. 20, 1976.
3. Tondl, A., On the Interaction Between Self-Excited and Parametric Vibrations, National Research Institute for Machine Design, Bechovice, Prague, Monograph No. 25, 1978.
4. Ibrahim, R. A. and Roberts, J. W., "Parametric Vibration, Part V: Stochastic Problems," The Shock and Vibration Digest, Vol. 10, No. 5, 1978, pp. 17-38.
5. Ibrahim, R. A., "Parametric Vibration, Part VI: Stochastic Problems(2)," The Shock and Vibration Digest, Vol. 13, No. 9, 1981.

6. Ibrahim, R. A., "Stationary Response of a Randomly Parametric Excited Nonlinear System," Journal of Applied Mechanics, Trans. ASME, Series E, Vol. 45, No. 4, 1978, pp. 910-916.
7. Ibrahim, R. A. and Roberts, J. W., "Broad-Band Random Parametric Excitation of a Nonlinear System," Proceedings of the VIIIth International Conference on Nonlinear Oscillations, Prague, 1978, pp. 355-360.
8. Schmidt, G., "Probability Densities of Parametrically Excited Random Vibrations," in Stochastic Problems in Dynamics, Editor B. L. Clarkson, Pitman, London, 1977, pp. 197-213.
9. Ariaratnam, S. T., "Bifurcation in Nonlinear Stochastic Systems," in New Approaches to Nonlinear Problems in Dynamics, Editor P. J. Holmes, SIAM, Philadelphia, 1980, p. 470-474.
10. Gray, A. H. and Caughey, T. K., "A Controversy in Problems Involving Random Parametric Excitation," Journal of Mathematics and Physics, Vol. 44, No. 3, 1965, pp. 288-296.
11. Arnold, L., Stochastic Differential Equations: Theory and Application, John Wiley & Sons, New York, 1974.
12. Jazwiniski, A. H., Stochastic Processes and Filtering Theory, Academic Press, New York, 1980.
13. Wong, E. and Zakai, M., "On the Relation Between Ordinary and Stochastic Differential Equations," International Journal of Engineering Science, Vol. 3, 1965, pp. 213-229.
14. Mitchell, R. P. and Kozin, F., "Sample Stability of Second Order Linear Differential Equations with Wide Band Noise Coefficients," SIAM Journal of Applied Mathematics, Vol. 27, No. 4, 1974, pp. 571-605.
15. Ariaratnam, S. T. and Tam, D. S. F., "Random Vibration and Stability of a Linear Parametrically Excited Oscillator," Zeitschrift fur Angewandte Mathematik und Mechanik, Vol. 59, 1979, pp. 79-84.
16. Lin, Y. K., Fujimori, Y., and Ariaratnam, S. T., "Rotor Blade Stability in Turbulent Flows-Part I," American Institute of Aeronautics and Astronautics Journal, Vol. 17, No. 6, 1979, pp. 545-552.
17. Stratonovich, R. L., Topics in the Theory of Random Noise, Vol. II, Gordon and Breach, New York, 1967.
18. Ariaratnam, S. T., "Dynamic Stability of a Column under Random Loading," Proceedings of the International Conference on Dynamic Stability of Structure, 1965, Editor G. Herman, Pergamon Press, 1967, pp. 255-265.
19. Mitchell, R. P. and Kozin, F., "Stability of a Simply Supported Rod Subjected to a Random Longitudinal Force," NASA-CR-98016, 1968.
20. Newland, D. E., "Energy Sharing in Random Vibration of Nonlinearly Coupled Modes," Journal of the Institute of Mathematics and Applications, Vol. 1, No. 3, 1965, pp. 199-207.
21. Ibrahim, R. A. and Roberts, J. W., "Broad Band Random Excitation of a Two-Degree-of-Freedom System with Autoparametric Coupling," Journal of Sound and Vibration, Vol. 44, No. 3, 1976, pp. 335-348.
22. Crandall, S. H., "NonGaussian Closure for Random Vibration of Nonlinear Oscillators," International Journal of Nonlinear Mechanics, Vol. 15, 1980, pp. 303-313.
23. Robson, J. D., "A Simplified Quasi-Gaussian Random Process Model Based on Nonlinearity," Journal of Sound and Vibration, Vol. 76, No. 2, 1981, pp. 169-177.